THE UNIVERSITY
of LIVERPOOL

Designing and Utilising an *in vitro* Model to Investigate Cellular Pathways Involved in Idiopathic Pulmonary Fibrosis and Connective Tissue Disease Associated Interstitial Lung Disease

Thesis submitted in accordance with the requirements of the University of Liverpool for the degree of Doctor in Philosophy

by

Dr Caroline Victoria Cotton

November 2018

Abstract

Designing and Utilising an *in vitro* Model to Investigate Cellular Pathways Involved in Idiopathic Pulmonary Fibrosis (IPF) and Connective Tissue Disease Associated Interstitial Lung Disease (CTD-ILD)

ILD represents a heterogeneous spectrum of diseases caused by excessive deposition of extracellular matrix (ECM) into the interstitial space leading to distortion of the lung architecture and impairment of gas exchange. In this thesis the design of an *in vitro* model is described to test the pathways involved in the fibrotic response. The model was first tested on fibroblast and epithelial cell lines, two cell types that are implicated as key players in pulmonary fibrosis, treating cells with the pro-inflammatory cytokine Transforming Growth Factor-β (TGF-β), ensuring that this model was reliable and reproducible.

Once a model had been established, it was utilised by treating cells with plasma from patients with IPF and Systemic Sclerosis Associated ILD (SSc-ILD). This was to assess whether treatment with plasma from patients with fibrotic lung disease would induce any changes in these cell lines. When cells were treated with plasma there were no changes in gene expression of the MRC5 fibroblasts but there was an increase in proliferation of the fibroblast cells when treated with IPF patient plasma. When the A549 epithelial cells were treated with plasma from patients with IPF, there was a significant reduction in *COL3A1* and *FN-EDA*. This was associated with a significant downregulation of *N-cadherin*. These changes are not those expected in EMT. Conversely treatment of the same cell line with SSc-ILD plasma led to a significant increase in gene expression of *COL3A1* and *FN-EDA*.

Finally, this model was adapted to imitate the constant movement of the lungs by stretching the cells *in vitro*. Stretch alone caused no significant differences in any of the genes associated with fibrosis in either cell type. However, when used alongside TGF-β treatment there was an attenuation of the fibrotic response in *COL1A1*, *FN-EDA* and *CCN2* in the fibroblasts and *COL1A1* and *Slug* in the epithelial cells.

In conclusion, this thesis has produced a novel way to explore some of the key pathways involved in fibrosis and the changes that plasma treatment induces on cell lines.

Acknowledgements

It is a pleasure to thank my primary supervisors Professor Robert Cooper and Professor George Bou-Gharios for their constant support, encouragement, knowledge and expertise. They have been fantastic mentors and their dedication throughout the last four years have made this thesis possible.

I would like to thank Mr Paul New, Study Co-ordinator for the UK-Biomarkers in Interstitial Lung Disease Study. This work would not be possible without his continued efforts and hard work for ongoing recruitment to the study. I would also like to thank Dr Lisa Spencer and Dr Janine Lamb for their guidance and support, as well as the Centre for Integrated Research into Musculoskeletal Ageing (CIMA) for funding the first year of this project. I am also grateful to the collaborators on the UK-BILD study, including the consultants and research nurses at the 38 centres, who recruited the patients into the study to allow this research to go ahead. As well as massive thanks to the patients and healthy volunteers for their involvement for the research to occur.

I am obliged to my numerous colleagues in the laboratory. I could not possibly mention all the people who have helped throughout this work, with their hints and tips for improving my scientific methodology or just keeping me sane when things didn't work. I would also like to thank my NHS colleagues for their help and career support.

Last but not least I would like to thank my family and friends for their help and advice throughout.

Contents

Abbreviations

ADAMTS	A disintegrin and metalloproteinase with thrombospondin motifs
AIP	Acute Interstitial Pneumonia
AIP	Acute Interstitial Pneumonia
ANA	Antinuclear Antibody
Anti-CCP	Anti-cyclic citrullinated peptide
Anti-MDA5	Anti-melanoma differentiation-associated gene 5 antibody
APS	Ammonium Persulphate
ASS	Antisynthetase Syndrome
ATS	American Thoracic Society
BMPs	Bone Morphogenetic Proteins
BSA	Bovine Serum Albumin
CADM	Clinically Amyopathic Dermatomyositis
CCN1, Cyr61	Cysteine-Rich Protein 61
CCN2, CTGF	Connective Tissue Growth Factor
CCN3, NOV	Nephroblastoma Overexpressed Gene
CCN4, WISP-1	WNT1-Inducible Signalling Protein
CCN5, WISP2	WNT2-Inducible Signalling Protein
CIGMR	Centre for Integrated Genomic Medical Research
CK	Creatine Kinase
COL1A1	Collagen 1 alpha 1
COL3A1	Collagen 3 alpha 1
COP	Cryptogenic Organising Pneumonia
CTD	Connective Tissue Disease
dcSSc	Diffuse Cutaneous Systemic Sclerosis
DEPC	Diethylpyrocarbonate
DIP	Desquamative Interstitial Pneumonia
DM	Dermatomyositis
DMSO	Dimethyl sulphoxide
DNA	Deoxyribonucleic Acid
dNTP	Deoxyribonucleotide Triphosphate
ECM	Extracellular matrix
ELISA	Enzyme-Linked Immunosorbent Assay
EMT	Epithlial-Mesenchymal Transition
Endo-MT	Endothelial Mesenchymal Transition
ERS	European Respiratory Society
ESR	Erythrocyte sedimentation rate
FBS	Fetal Bovine Serum
FGF	Fibroblast Growth Factor
FN	Fibronectin
FN-EDA	Fibronectin extra type III domain A
FN-EDB	Fibronectin extra type III domain B
FVC	Forced Vital Capacity
HAQ	Health Assessment Questionnaire
HRCT	High Resolution Computed Tomography

HRP	Horse Radish Peroxidase
HSPG	Heparin Sulphate Proteoglycan
IBM	Inclusion-Body Myositis
IIM	Idiopathic Inflammatory Myopathies
IIP	Idiopathic Interstitial Pneumonia
ILD	Interstitial Lung Disease
IPF	Idiopathic Pulmonary Fibrosis
ISA	ILD-Specific Antibody
JDM	Juvenile Dermatomyositis
LAM	Lymphangioleiomyomatosis
LAP	Latency-Associated Protein
LCH	Langerhans Cell Histiocytosis
lcSSc	Limited Cutaneous Systemic Sclerosis
LIP	Lymphoid Interstitial Pneumonia
LTBP	Latent-TGF-β-Binding Protein
MAA	Myositis Associated Antibody
MCTD	Mixed Connective Tissue Disease
MDT	Multidisciplinary Team
MEM	Minimum Essential Medium
MMP	Matrix Metalloproteinase
MRTB	Myositis Research Tissue Bank
MRTF	Myocardin Related Transcription Factor
MSA	Myositis Specific Antibody
NBF	Neutral Buffered Formalin
NCBI	National Centre for Biotechnology Information
NSIP	Non-Specific Interstitial Pneumonia
PAH	Pulmonary Arterial Hypertension
PBS	Phosphate Buffered Saline
PBST	Phosphate Buffered Saline with Tween
PCNA	Proliferating Cell Nuclear Antigen
PDGF	Platelet Derived Growth Factor
PDGFR	Platelet Derived Growth Factor Receptor
PFT	Pulmonary Function Test
PI3K	Phosphatidylinositol-3-Kinase
PM	Polymyositis
qPCR	Quantitative Polymerase Chain Reaction
RA	Rheumatoid Arthritis
RB-ILD	Respiratory Bronchiolitis-Associated Interstitial Lung Disease
REC	Research Ethics Committee
RNA	Ribonucleic Acid
SARA	Smad Anchor Receptor Activation
SDS	Sodium Dodecyl Sulphate
SDS-PAGE	Sodium Dodecyl Sulphate-Polyacrylamide Gel Electrophoresis
SLE	Systemic Lupus Erythematosus
SLRP	Small Leucine-Rich Proteoglycan
Slug	Snail Family Transcriptional Repressor 2, SNAI2
Snail	Snail Family Transcriptional Repressor 1, SNAI1
SRF	Serum Response Factor

SSc	Systemic Sclerosis
ssSSc	Systemic Sclerosis sine scleroderma
TBS	Tris Buffered Saline
TBST	Tris Buffered Saline with Tween
TCA	Trichloroacetic acid
TEMED	Tetramethylethylenediamine
TGF-β	Transforming Growth Factor-β
TIMPs	Tissue Inhibitor of Metalloproteinases
UCTD	Undifferentiated Connective Tissue Disease
UIP	Usual Interstitial Pneumonia
UK-BILD	United Kingdom - Biomarkers in Interstitial Lung Disease
VEGF	Vascular Endothelial Growth Factor
ZEB	Zinc-Finger-E-Box-Binding
α-SMA	α-Smooth Muscle Actin

1 Introduction

1.1 Lung Anatomy and Physiology

The lungs are the organs responsible for gaseous exchange in the body, functioning to oxygenate blood and therefore intricately linked to the cardiovascular system.

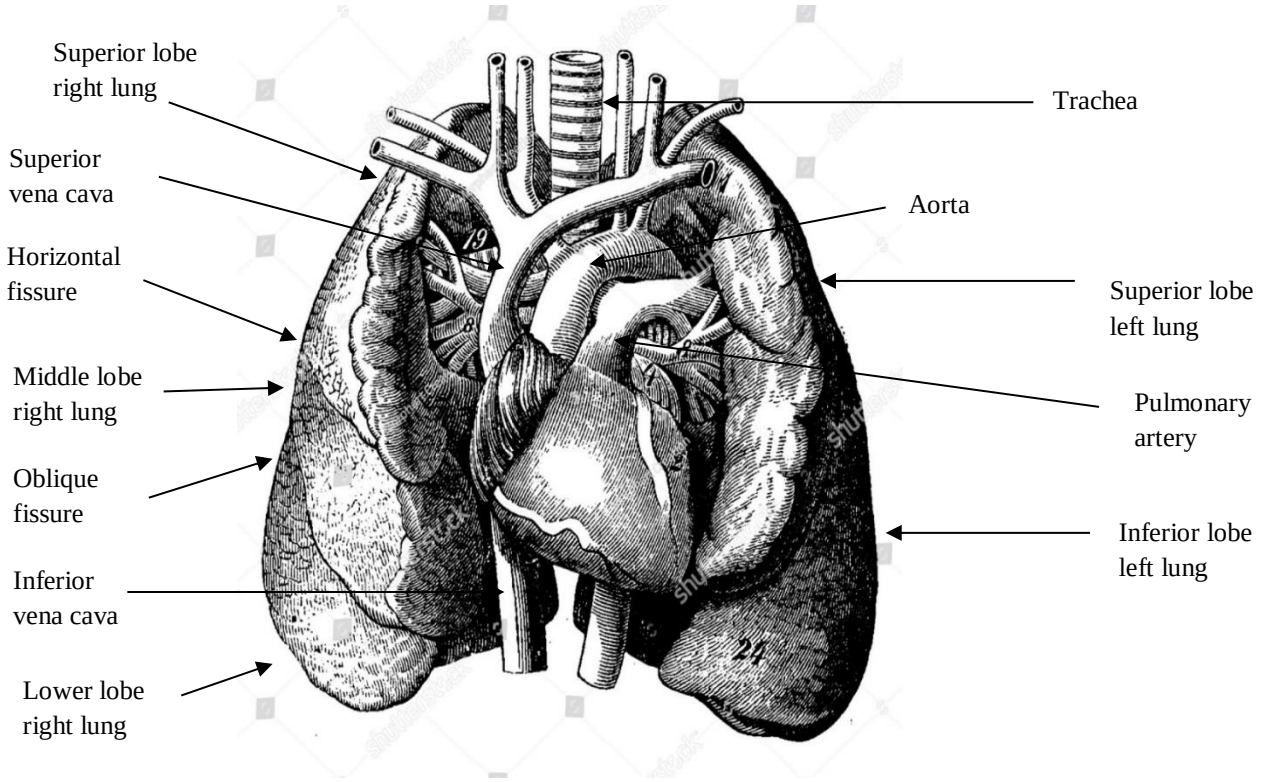

Figure 1-1 Diagram of the lung anatomy. This figure shows the right lung is split into three lobes (upper, middle and lower) and the left lung is split into two lobes (upper and lower). There is branching of the airways, with the central trachea splitting into the right and left main bronchus, and dividing into the smaller bronchi and bronchioles. It is highly vascularised to allow efficient gas exchange. Image courtesy of shuttershack.

Deoxygenated blood is carried to the lungs from the pulmonary artery which arises from the right side of the heart. Once oxygenated, this returns to the left atrium of the heart via four pulmonary veins where it passes to the left ventricle to be pumped through the aorta and then circulates around the body (1).

During breathing the diaphragm, innervated by the phrenic nerve, contracts and flattens. At rest, the diaphragm contracts just small amounts but during exercise it can contract much further allowing for much deeper inspiration. The external intercostal muscles also contract, moving the ribs forwards and upwards, increasing the size of the chest cavity further (2). This reduces the pressure in the thoracic cavity thus drawing air through the mouth and down the trachea, which divides into the right and left main bronchi. These divide into smaller bronchi and bronchioles that continue to divide into smaller and smaller branches until they end in the terminal airways, called alveoli.

The alveoli have thinly lined walls and a vast network of capillaries to allow gaseous diffusion to occur efficiently. This allows for easy gas exchange with diffusion of oxygen into the blood and carbon dioxide back into the lungs to be exhaled. The walls of the alveoli mainly consist of flattened type I alveolar epithelial cells. Type II alveolar epithelial cells are interspersed between them and act to secrete surfactant, a fluid which lowers the surface tension within the alveoli, allowing them to open easily (2). Pulmonary macrophages act as resident phagocytes, having an immunological role.

Between the alveolar epithelium and the capillary endothelial layer is the pulmonary interstitium. This contains fibroblastic cells which secrete extracellular matrix (ECM) providing structure for the lungs.

1.2 Definition and Classification of Interstitial Lung Disease (ILD)

ILD is an encompassing term used to describe any process damaging the pulmonary parenchymal tissues. There is excessive deposition of ECM in the interstitial space, as described in Figure 1-2, which leads to distortion of the lung architecture and impairment of gas exchange. Clinically, patients with ILD usually present with a dry cough and increasing dyspnoea. If treatment is not commenced, or treatment is commenced but is non-therapeutic, the disease can progress, eventually leading to respiratory insufficiency and death.

Figure 1-2 gives a basic pictorial description of the pulmonary parenchyma, with the epithelial cell layer and endothelial cell layer being separated by the two basement membranes and the pulmonary interstitium. In ILD, there is increased production and deposition of ECM in the pulmonary interstitium, increasing the distance that gasses need to transfuse across for oxygenation of the blood.

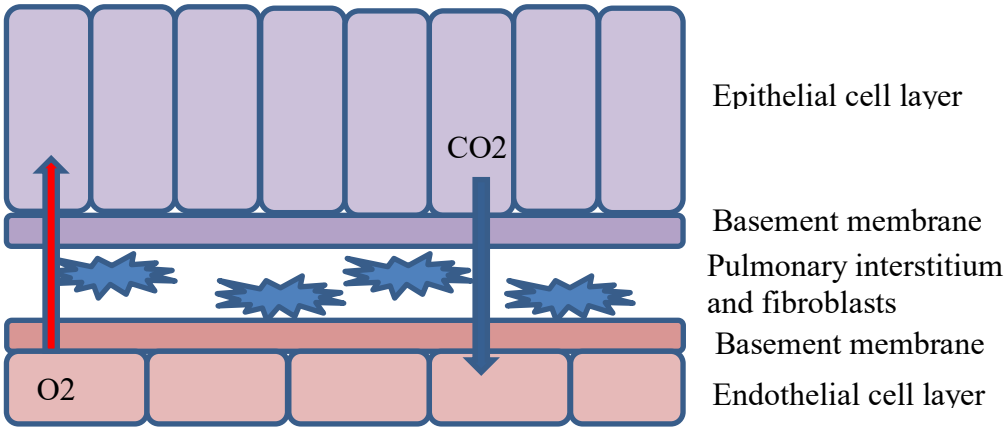

Figure 1-2 Diagram of the pulmonary parenchyma. The above diagram depicts the epithelial cell layer that comprises the alveolar sacs. Gaseous exchange occurs across these layers, with diffusion of oxygen from the lungs through the pulmonary interstitium and the endothelial cell layer to be absorbed by red blood cells. Usually the layers for diffusion are very thin, making this process incredibly efficient. If excess matrix is secreted into the interstitial space, the layers that gases need to diffuse across thicken making gas exchange less efficient. It also distorts the architecture of the lung and results in increased breathlessness for the patient.

1.3 The Clinical Considerations of Interstitial Lung Disease (ILD)

It is important to note that not all ILDs are the same. The ILD spectrum is a heterogeneous group of conditions (over 200) caused by inflammation and fibrosis of the lung. Recent literature has attempted to subgroup and categorise the ILD cases as represented in Figure 1-3 (3). However, the largest group in this classification is the idiopathic group, which are not linked by pathological mechanisms. The idiopathic and Connective Tissue Disease (CTD)-associated groups will be discussed in more detail below.

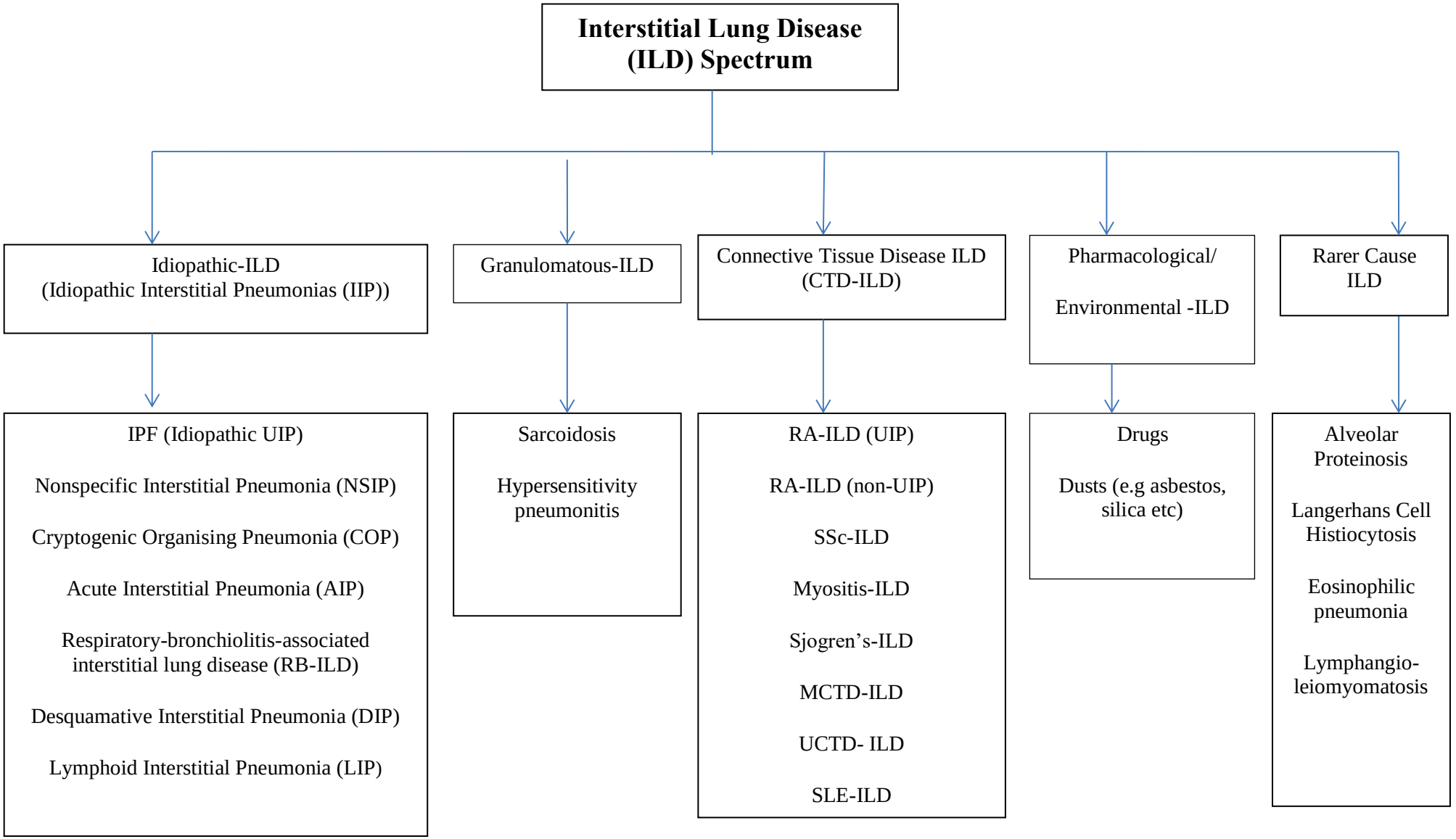

Figure 1-3 A classification of ILD into groups and subgroups. Given the large number of individual lung diseases that the term ILD encompasses this thesis focuses on the idiopathic and CTD-ILD subgroups. Reference adapted from Ryerson CJ, Collard HR. Update on the diagnosis and classification of ILD. Curr Opin Pulm Med 2013; 19: 453-9.

1.3.1 Diagnosing ILD

Subgrouping patients with ILD requires consideration of the patient's history and clinical examination findings. The treating chest physician would be assessing for a clear occupational or environmental exposure such as asbestosis or subtle features of an underlying CTD. In some cases, a precipitating cause is not found or is not immediately apparent and the patient is given an idiopathic subgroup label. The term "idiopathic" describes any disease or condition in which the underlying cause is unknown. Investigations for patients with ILD include pulmonary function tests (PFTs), which often show a restrictive pattern and reduced gas transfer, High Resolution Computed Tomography (HRCT) and, if required, a lung biopsy. In many cases a lung biopsy is not performed as it carries a relatively high mortality for a diagnostic procedure (cited as 3.6% in one meta-analysis) (4) and patients may be too frail or have lung function that is too poor for the procedure to occur safely.

1.3.2 HRCT Appearances in ILD

Difficulties acquiring lung tissue to diagnose ILD have meant that HRCT is an important tool in diagnosing and classifying ILD. There are a number of distinct radiological patterns recognised. Usual Interstitial Pneumonia (UIP) is characterised by a reticular pattern with honeycombing and a relative lack of ground glass change. It predominantly affects the bases of the lungs. Lobar volume loss and distortion of the lung architecture may often be seen in advanced disease (5). This pattern is a classic feature of IPF but can also be seen in a number of CTDs particularly rheumatoid arthritis (RA) and occasionally in systemic sclerosis (SSc) (6, 7). The Non-Specific Interstitial Pneumonia (NSIP) pattern is characterised by ground-glass attenuation typically present at the periphery and the bases of the lungs. Patients may be further sub-grouped into those with predominantly fibrotic changes (fibrotic NSIP) and those with inflammatory change and more ground-glass attenuation (cellular NSIP). This may occur without an identifiable underlying cause and makes

up one of the idiopathic subgroups (7). It is also the most commonly seen pattern in SSc, occurring in 80% of patients, as well as occurring in other CTDs such as myositis-associated ILD (8, 9). Ground-glass shadowing is suggestive of inflammatory change and suggests a potentially reversible pathology that may respond to immunosuppressive treatment. However, work in SSc shows that this appearance also represents fine intra-lobular fibrosis with inconsistent improvements with immunosuppressive treatment (10, 11).

Organising Pneumonia is another recognised HRCT pattern. In idiopathic disease it is called Cryptogenic Organising Pneumonia (COP), however, it is also a recognised pattern occurring in a number of CTDs, including myositis-associated ILD (9). It is characterised by patchy bilateral consolidation and tends to respond well to steroids and immunosuppression whether or not an underlying CTD is discovered.

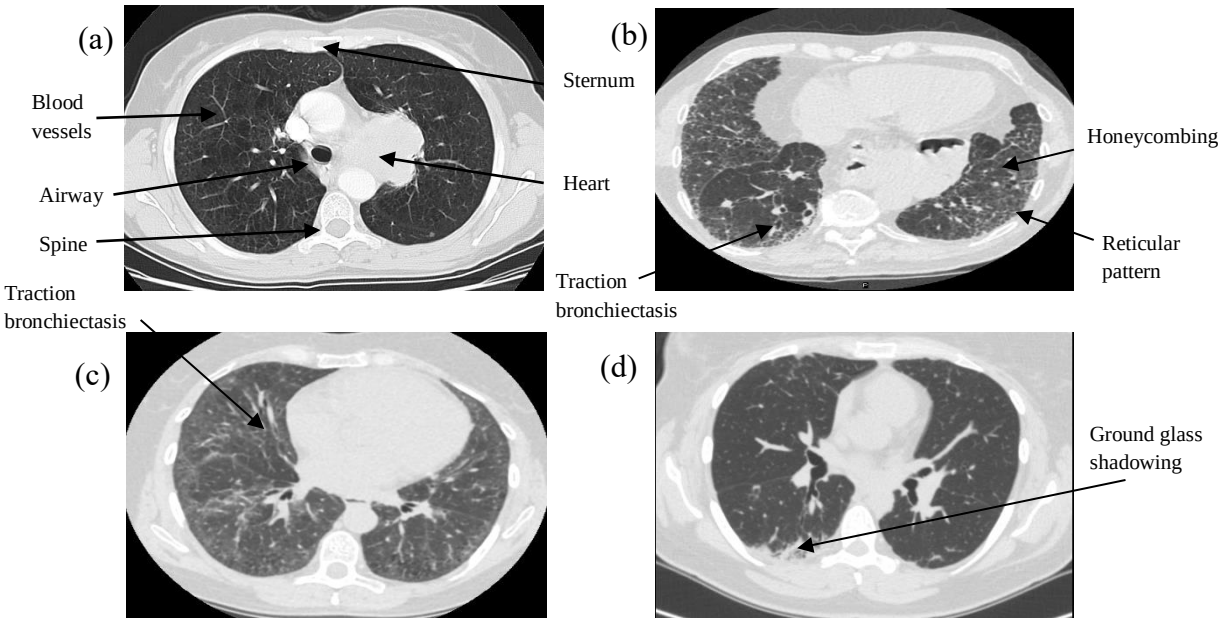

Figure 1-4 HRCT appearances in ILD. (a) Normal lung appearance. (b) Typical pattern of Usual Interstitial Pneumonia (UIP) with a reticular pattern and honeycombing predominantly affecting the bases and periphery of the lung. (c) A representative example of a Non-Specific Interstitial Pneumonia (NSIP) pattern. This shows ground-glass shadowing with reticular opacity typically affecting the periphery and bases of the lungs. (d) Typical HRCT pattern with organising pneumonia and evidence of patchy bilateral consolidation.

Although HRCT is recognised as a useful tool in the diagnosis and management of ILD there are a number of limitations with the technology. As discussed above, patterns do not indicate a particular diagnosis but give a differential of possible causes (eg, a UIP pattern can occur in idiopathic disease, multiple CTDs and asbestosis). Identifying patterns can be difficult because two or more typical characteristics may be present in one HRCT scan (e.g. honeycombing with extensive ground-glass shadowing) and there is recognised inter-observer variation even between specialist radiologists (5, 12). HRCT is also associated with a large radiation dose for patients making frequent follow-up scans more difficult. This suggests that although HRCT is valuable it is not infallible, and therefore other biomarkers in ILD would be helpful to secure a correct diagnosis, allow for monitoring of the disease and give clues regarding the underlying pathogenesis of the disorder.

1.3.3 Idiopathic Pulmonary Fibrosis (IPF)

IPF is defined as a specific form of chronic, progressive fibrosing interstitial pneumonia, with fibrosis limited to the lungs (11). It tends to affect older males and the prevalence is higher in smokers (13). It is the most common form of idiopathic ILD which is progressive and lethal, with death occurring within a median time of 3 years from diagnosis (14). It was historically treated with high-dose steroids and immunosuppression in the form of azathioprine, although trials have shown this did not improve mortality (15). It therefore suggests that inflammation does not have a significant role in this disease. Newer antifibrotic drugs, such as Pirfenidone and Nintedinib, are now available and may have a role in slowing progression of the disease (16-18). Given the different therapeutic options available in ILD it is imperative that a correct diagnosis is made in every case to ensure that patients receive the correct treatment.

IPF is characterised by a UIP pattern on HRCT. According to American Thoracic Society / European Respiratory Society (ATS / ERS) criteria published in 2011 (11), IPF should be diagnosed in a multi-disciplinary setting and patients must meet the following criteria;

(a) Exclusion of any other cause of ILD.
(b) The presence of a UIP pattern on HRCT.
(c) **Or** specific combinations of HRCT appearances and / or the presence of surgical lung biopsy findings that are discussed in a multidisciplinary team (MDT) setting.

To diagnose "definite IPF", the patient can have a UIP pattern on HRCT which has been shown to be diagnostically accurate for IPF, particularly when made by a specialist ILD centre (19). If patients have a HRCT appearance that lacks honeycombing and appears like fibrotic NSIP then ideally a surgical lung biopsy should be performed. If this shows features consistent with UIP the patient is diagnosed with definite IPF. Unfortunately, given that surgical lung biopsy is an invasive procedure with a substantial morbidity associated with it and that many

patients are elderly with poor lung function at presentation, surgical lung biopsy can only be performed in a small number of patients. However, patients may be diagnosed with "probable IPF" if they are older in age group and after MDT discussion (11).

1.3.4 ILD as a complication of CTD

As can be seen in Figure 1-3, ILD is a common complication of many CTDs including systemic sclerosis (SSc), rheumatoid arthritis (RA) and the idiopathic inflammatory myopathies (IIM), polymyositis (PM) and dermatomyositis (DM). Whereas morbidity and mortality from CTD complications other than ILD appear to be improving with therapeutic advances, this is not so with ILD, which remains a significant clinical problem (20). These conditions have a number of clinical features and hallmark characteristics discussed in detail below.

1.3.4.1 Idiopathic Inflammatory Myopathies (IIM)

IIM can be subdivided into several distinct groups, the most common of which include PM, DM, inclusion-body myositis (IBM), myositis-CTD overlap and juvenile dermatomyositis (JDM). They have in common the presence of moderate to severe muscle weakness and muscle inflammation (21).

IIMs have a strong association with ILD. Like many of the other CTDs, the IIM are associated with the presence of autoantibodies and these can predict the likelihood of developing ILD. This will be discussed in detail in section 1.3.4.4. ILD can present prior to the onset of muscle symptoms or late during the course of the disease. ILD is an important manifestation of the disease and its presence has a major impact on mortality (22). IIM-ILD can present with a variety of HRCT appearances including NSIP, organising pneumonia or UIP (23). However, myositis-associated ILD tends to respond well to immunosuppression (24).

1.3.4.2 Systemic Sclerosis (SSc)

SSc is characterised by a generalised vascular abnormality and fibroblast dysfunction leading to extensive fibrosis of the skin and internal organs (25). Women are much more frequently affected than men (26). Many organs can be affected including the skin, gastrointestinal tract and kidneys (26). In the lungs, SSc is associated with pulmonary arterial hypertension (PAH) and the development of ILD. The prevalence of ILD in SSc is estimated between 25-90%, depending upon the definition of ILD used (27, 28). Pulmonary complications are the leading cause of mortality in SSc, with pulmonary fibrosis being responsible for 20-30% of deaths (20, 29).

SSc can be broadly classified into three subsets; (a) Diffuse cutaneous systemic sclerosis (dcSSc), associated with skin thickening above the elbows and severe fibrosis of multiple internal organs. It has a higher prevalence of severe ILD. (b) Limited cutaneous systemic sclerosis (lcSSc) associated with skin thickening limited to the hands, face, feet and forearms. These patients tend to suffer with isolated PAH but less severe ILD. (c) Systemic sclerosis sine scleroderma (ssSSc), where patients experience internal organ involvement without skin thickening (30). This subset is more difficult to diagnose given the lack of overt clinical signs.

1.3.4.3 Rheumatoid Arthritis (RA)

RA is a chronic, systemic inflammatory disease primarily affecting the joints. It affects around 1% of the population and is a leading cause of disability. However, the disease can affect a number of extra-articular sites including the eyes and lungs. ILD, identified on HRCT, occurs in roughly 20% of patients with RA (31). Risk factors for its development include older age, raised erythrocyte sedimentation rate (ESR) and higher Health Assessment Questionnaire (HAQ) score, a score rated by patients which gives an idea of the amount of disability suffered due to the condition (32). The presence of anti-CCP antibodies is also an independent risk factor for developing ILD (33). Interestingly, in RA-ILD there is a higher prevalence of UIP pattern disease unlike in other CTDs where the pattern is much less prevalent. In

RA-ILD the UIP pattern is associated with a much poorer survival (3.2 years) than those with other HRCT patterns (6.6 years) (6). The UIP pattern and poor survival is much more similar to IPF than other CTDs and it does not appear to respond to immunosuppression. Trials are currently being undertaken to assess if RA-ILD will respond to Pirfenidone and Nintedinib, drugs used to slow fibrotic progression in IPF.

1.3.4.4 Autoantibodies

CTDs are characterised by the presence of circulating autoantibodies. These can act as biomarkers and give a good prediction for the phenotypic features of disease that a patient may exhibit. In myositis there are a growing number of myositis-specific and myositis-associated autoantibodies (MSA/MAA) that are detectable. Several MSA strongly associated with ILD include the antisynthetase autoantibodies. These target one of several amino-acyl-transfer RNA synthetases (Table 1-1). MSA are usually mutually exclusive. The presence of one of these antibodies is associated with the antisynthetase syndrome (ASS) characterised by the presence of myositis, ILD, Raynaud's phenomenon, mechanic's hands, fever and an inflammatory arthritis. The most common antibody in this group is anti-Jo-1. This autoantibody is directed against histidyl-tRNA synthetase and is routinely detectable in clinical practice. The other antisynthetase antibodies are much rarer and the ability to test for them is usually only available in specialised centres.

Interestingly, certain antisynthetase antibodies are more strongly associated with ILD than with myositis. Roughly 70% of patients with anti-Jo-1 antibody will develop ILD (22). However, in the case of anti-PL-7 or anti-PL-12 almost 100% of patients will develop ILD, and often in the absence of myositis (34, 35). This could be described as an "amyopathic" form of disease, where patients have features such as rash or ILD but lack muscle involvement. These antibodies could be better described as "CTD-ILD specific" autoantibodies, or "ILD-specific autoantibodies" (ISA), as myositis may be an absent feature.

When anti-Jo-1 levels are measured they correlate with creatine kinase (CK) levels as well as other measures of myositis activity. This suggests that anti-Jo-1 levels

could be a potential biomarker for disease activity. The possibility also arises that anti-Jo-1 antibodies are involved in the pathogenesis of disease and further work is needed to assess if this is the case (36).

The anti-melanoma differentiation-associated gene 5 antibody (anti-MDA5) is another MSA. This occurs in association with clinically amyopathic dermatomyositis (CADM) and is associated with a rapidly progressive and indeed fulminant ILD, particularly in patients of Japanese ethnicity. In Caucasian patients the antibody is associated with muscle involvement, in the presence of a typical DM skin rash and an ILD that, although often severe, tends to respond to immunosuppression (37).

Myositis Specific Antibody (MSA)	**Prevalence in Myositis**	**Clinical Associations**	**Likelihood of developing ILD**
Anti-synthetases and their target protein: - Jo-1 (histidyl)	15-20%	Associated with antisynthetase syndrome, and characterised by the presence of: - Myositis (PM or DM) - Arthritis - ILD - Raynaud's - Fevers - Mechanic's hands	~ 70% develop ILD (22)
- PL-12 (alanyl)	< 5%		~ 90% develop ILD, myositis often mild (35)
- PL-7 (threonyl)	< 5%		~90% develop ILD, often prior to myositis (34)
- Anti-KS (asparaginyl)	< 5%		~ 90% develop ILD, myositis rare (38)
- Anti-OJ (isoleucyl)	< 5%		Up to 100% develop ILD (39)
- Anti-EJ (glycyl)	<5%		Up to 100% develop ILD (40)
- Anti-Zo (phenylalanyl)	<1 %		ILD-associated (41)
- Anti-Ha (tyrosyl)	<1%		No literature
Anti-MDA5	7% (37)	Associated with clinically amyopathic DM (CADM) Rapidly progressive ILD, especially in Japanese and Chinese patients	50 - 70% develop rapidly progressive ILD in Japanese/Chinese ethnicity (42) ~ 50% in Caucasian (43)

Table 1-1 MSA and their association with ILD. Prevalence data has been adapted from reference below, with ILD data from the cited references in the table. Several antisynthetase antibodies are associated with ILD in the absence of myositis (44).

There are also several MSA that are not specified in Table 1-1 that are less frequently associated with ILD. These include anti-SRP, anti-Mi-2, anti-TIF1-gamma, anti-NXP2 and anti-SAE. They are associated with other features of the myositis disease spectrum including skin rash and malignancy.

1.3.4.5 Myositis Associated Autoantibodies (MAA)

MAA are antibodies that are associated with myositis but with features of overlap disorders, i.e. the patient may have sclerodactyly associated with SSc. Table 1-2 describes the association of MAA with ILD.

Myositis Associated Autoantibodies (MAA)	**Prevalence of Antibody**	**Disease Associations**	**Likelihood of developing ILD**
Anti-PM-Scl	Occurs in up to 17% of patients with overlap myositis (45) 3-6% of patients with SSc (46)	Associated with scleromyositis	~50% of patients will develop ILD (45, 47)
Anti-Ku (myositis)	Occurs in 13% of patients with overlap myositis (45)	Associated with myositis overlap syndrome	~30% of patients will develop ILD (45)
Anti-U1RNP	5 – 35% of patients presenting with SSc or overlap syndromes (46)	Associated with mixed connective tissue disease (MCTD)	~35% show HRCT abnormalities associated with ILD, ~20% classified as severe (48)
Anti-Ro-52/60	~40% of IIM patients have anti-Ro-52/60 alongside their MSA or MAA (47)	Frequently occur with an MSA, especially with the anti-syntheases, or with various MAAs.	~40% of patients develop ILD, however it is unlikely that these antibodies are responsible for the ILD risk, which is instead due to the MSA/MAA detected. (47)

Table 1-2 MAA and their association with ILD. Table is compiled from the cited references.

1.3.4.6 SSc-Specific Antibodies

SSc is also associated with a number of disease-specific autoantibodies. Like the IIM, the particular antibody that an SSc patient has can aid in predicting the subset of disease and the clinical phenotype that the patient exhibits. Table 1-3 gives a summary of the antibodies in SSc and their association with ILD.

SSc-associated antibody	**Prevalence of Antibody**	**Disease Associations**	**Likelihood of developing ILD**
Anti-topo-isomerase (Scl70)	~30% of SSc patients (49)	Diffuse SSc (50)	~ 60% of patients develop ILD (51)
Anti-Th/To	~5% of SSc patients (50)	Limited SSc (52)	~50% of patients develop ILD (53)
Anti-U3 RNP	~8% of patients with SSc (54)	Occurs in SSc. Associated with skeletal muscle involvement and PAH (55)	~40% of patients have ILD (55)
Anti-U11/U12 RNP	~3% of patients with SSc (56)	Occurs in SSc	~80% of patients develop ILD which is often severe (56)
Anti-RuvBL1/2	1-2% of SSc patients (57)	Associated with myositis overlap and diffuse skin thickening (57)	Over 50% of patients will develop ILD (57)
Anti-EIF2B	~1% of patients with SSc / SSc overlap (58)	Associated with SSc / SSc overlap syndrome	Up to 100% of patients will develop ILD (58)

Table 1-3 SSc-Associated Autoantibodies and their association with ILD. Table is compiled from cited references.

Anti-topoisomerase antibody is associated with dcSSc (59). It is associated with a higher frequency of lung fibrosis, with over 60% of patients who have the antibody developing ILD (51, 60, 61), and is an independent predictor for the development of ILD in SSc (51). Interestingly, a study that monitored anti-topoisomerase levels over time identified a sub-group of patients who became antibody negative over the course of the disease. They experienced less progressive ILD and had better survival rates than patients who remained antibody positive (62). This has led to further investigation to assess if the presence of autoantibodies has any mechanism in the pathogenesis of fibrosis. It is thought that antibodies may be involved in the activation of immune cells or may amplify the immune response and much work is being undertaken in this field to assess the exact pathway by which the disease process occurs and if antibodies have a direct pathogenic role (63).

1.3.5 Diagnostic Uncertainty in ILD

A thorough clinical history and examination will often enable clinicians to assign individual patients into the correct ILD diagnostic subgroup. For example, patients with a clear history of occupational exposure to asbestos or use of typical medications such as nitrofurantoin or amiodarone may be easy to classify. Other patients may have clear evidence of an underlying CTD on physical examination. Where subgroup diagnostic labelling remains difficult, diagnostic assignments should be undertaken by tertiary multidisciplinary teams (3). Occasionally, distinguishing between idiopathic and CTD-ILD subgroup cases may prove difficult, and several factors contribute to such difficulties:

- CTD symptoms and signs may be absent or subtle, so easily missed in a busy respiratory clinic. For example, in the antisynthetase syndrome the expected CTD features other than ILD (i.e. Raynaud's phenomenon, myositis, mechanic's hands, DM rash and inflammatory arthritis) may be absent at ILD onset (35). Furthermore ILD patients may only volunteer CTD symptoms if directly asked, and chest physicians may not enquire regarding subtle symptoms (64).

- CTD symptoms and signs other than ILD may never develop once the immunosuppression used to treat ILD has commenced.

- As previously discussed, the HRCT appearances in ILD cases labelled as idiopathic also occur in CTD-ILD (5). Thus, while HRCT is an important tool in ILD diagnosis, it may not always accurately distinguish between subgroups. There are various HRCT patterns in CTD-ILD that vary in frequency depending upon the underlying CTD. For example, SSc-ILD tends to present with an NSIP pattern (65). In contrast, RA-ILD has a much higher prevalence of a UIP pattern (6, 7).

- Not all investigations are available to the treating physician. For example, a large number of patients are precluded from undergoing a lung biopsy as they are too frail or do not have the respiratory reserve. Also, comprehensive serology is not available in every NHS hospital.

Assigning every individual ILD patient into the correct ILD diagnostic subgroup has become crucial based on recent mechanistic insights and drug developments. Treatment strategies now differ considerably between ILD subsets, so making a correct diagnosis is vitally important to ensure optimal treatment choices. For instance, patients with SSc-ILD will often respond to prednisolone and cyclophosphamide even if their HRCT shows a UIP pattern (66). However, if this pattern is associated with IPF steroids are harmful and so contra-indicated (Raghu, 2012). These differing treatment outcomes make it vital that a correct ILD subgroup diagnosis is achieved in every case. Accumulating research suggests that use of comprehensive CTD-serology is likely to represent a vital tool in this respect (67).

This serological classification has now been identified as having an important role in diagnosing and managing patients with ILD and has been included in the recently published ATS / ERS guidelines for the management of ILD (68). This guideline recognises that there is a "serological domain" required when diagnosing patients with idiopathic ILD and suggests the category "interstitial pneumonia with

autoimmune features" for patients who have certain features suggesting an autoimmune process but the patient does not meet criteria for a diagnostic label of a CTD.

This leads to the clinical question of whether patients who are diagnosed with IPF actually have an underlying CTD that can be disclosed by comprehensive serology. It is important to ascertain if patients are being misdiagnosed thereby receiving incorrect treatments. This quantification of diagnostic error in IPF has not been studied in a UK population previously. Previous studies have been performed but these have been in East Asian populations and have included all idiopathic ILD subgroups without distinguishing IPF. These are discussed in more detail in chapter 4 but suggest the diagnostic error may be between 6.6 – 38% in patients with idiopathic ILD (69, 70). The first part of this thesis assesses the level of diagnostic error within a UK population of patients diagnosed with IPF and what proportion actually have an underlying CTD when serum is analysed using immunoprecipitation. It is important that this work is undertaken prior to any mechanistic work to ensure that the IPF population being examined is as homogeneous as possible.

1.4 Mechanistic Research

As for any disease, the effectiveness of ILD therapies will be dictated by their specificity, i.e. how well they target the pathological mechanisms causing the parenchymal injury. A major stricture currently limiting the effectiveness of ILD treatments is that their underlying pathologies are so poorly understood. Gaining mechanistic insights would therefore clearly be of benefit.

A number of animal models of pulmonary fibrosis have been developed to try to better understand mechanisms of disease. As the underlying cause of ILD is unknown it is difficult to develop a model that directly mimics the disease process. One model of IPF uses inhaled bleomycin to induce a fibrotic response in rodents. This medication is used as a treatment for cancer in humans but has the side effect of

causing lung fibrosis. The inhaled drug causes an initial inflammatory response which can be measured in broncho-alveolar lavage (BAL) fluid. By day 14, this response subsides and an increase in production and deposition of collagen in the interstitial space occurs (71). The advantages of this model include a fibrotic process that targets the lungs without other systemic effects. It also produces a picture of pulmonary fibrosis with histology similar to that seen in IPF. Unfortunately, this model also has limitations as there appears to be an initial inflammatory response that has not been seen in patients with IPF. This model has been adapted by giving mice smaller, repetitive doses of bleomycin to represent the chronic injury thought to occur in IPF (72). Another established model, used to investigate the molecular pathways occurring in IPF, is to expose mice to doses of radiation. This appears to cause changes in the lungs similar to those occurring in IPF and has been used in several molecular studies described later in this chapter (73).

Genetic mouse models have also been developed that overexpress key molecules involved in fibrosis such as Transforming Growth Factor-β (TGF-β) (74). This is to better understand the pathways involved in the fibrotic process. Unfortunately, these models also have their drawbacks as genetic analyses in IPF have shown the condition is likely due to a complex interplay of multiple factors. However, certain genetic defects such as MUC5B increase susceptibility in individuals. Unfortunately, a perfect model with which to study ILD does not exist.

1.4.1 The Extracellular Matrix (ECM)

It is hypothesised that CTD-ILD is preceded by inflammation, which if suppressed appropriately may prevent parenchymal fibrosis and scarring (75). This does not apply in all ILD subtypes, as in IPF fibrosis does not appear to be preceded by inflammation. Irrespective of whether fibrosis is preceded by inflammation, fibrotic damage follows activation of the myofibroblast which leads to excessive amounts of ECM production in the interstitial space. The production of ECM is a dynamic process that is continually remodelled and the balance between production and

degradation is tightly regulated. The ECM has multiple versatile functions including binding to growth factor signalling molecules, influencing cell migration and it can also change a number of behaviours based on the stiffness of the underlying matrix (76). The ECM is made up of two main classes of macromolecules; proteoglycans and fibrous proteins including collagens, elastins and fibronectin (77). There are a number of different collagens in the body, however collagen type I and collagen type III are the most abundant in the ECM of the lung. Collagen type I is composed of two alpha 1 chains and one alpha 2 chain, which are the products of two genes *COL1A1* and *COL1A2*, located on chromosome 17 and 7 respectively. Each chain consists of 1050 amino acids. Once formed, these peptides are then transported into the rough endoplasmic reticulum where they are modified by a number of different reactions and then wound into a triple helix structure before being secreted into the extracellular space. Extracellular enzymes, the procollagen peptidases and a disintegrin and metalloproteinase with thrombospondin motifs (ADAMTS), remove the N-terminal and C-terminal propeptides at the end of the collagen molecule. This then allows them to polymerise in the extracellular space forming fibrillary structures (78). These undergo cross-linking catalysed by enzymes belonging to the lysyl oxidase family. There is evidence to suggest that it is these hydroxyallysine cross-links that lead to the irreversibility of fibrosis and prevent the degradation of collagen by members of the Matrix Metalloproteinase (MMP) family (79).

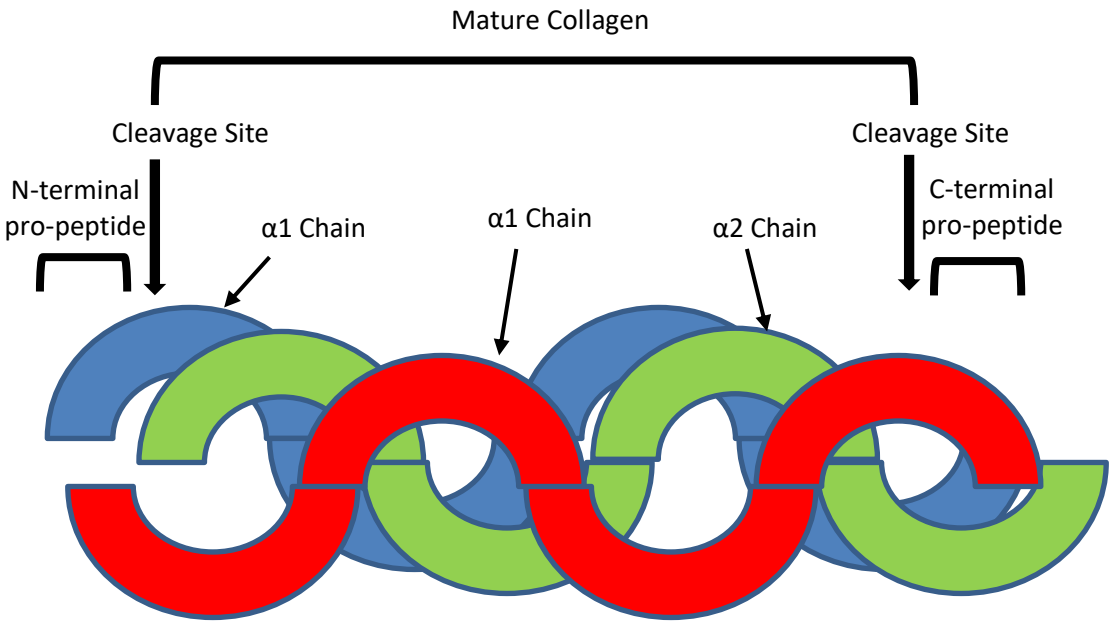

Figure 1-5 The collagen type 1 molecule. Collagen type 1 consists of two α 1 chains and one α 2 chain which are wound into a triple helix structure before being secreted into the extracellular space.

Fibronectin (FN) is a glycoprotein that is secreted into the ECM. It is produced by hepatocytes in a soluble form (called plasma fibronectin). It is also produced in an insoluble form by a number of cell types including mesenchymal and epithelial cells, where it constitutes part of the ECM and is termed cellular fibronectin. It has several functions but in the ECM acts as a cell adhesion molecule by joining to collagen. It can also act as a ligand for several integrin receptors. Despite being produced from a single gene it undergoes post-translational splicing and can exist as several isoforms, with at least 20 different subtypes recognised in humans (80). The insoluble form may be spliced into extra type III domains A and B (FN-EDA and FN-EDB respectively). FN-EDA appears to play a crucial role in the development of pulmonary fibrosis. Early work showed FN-EDA to be present in the fibroblastic foci in biopsy specimens from patients with IPF (81). Further work using a murine model showed that genetically modified mice, that are null for the FN-EDA splice variant, and then treated with intratracheal bleomycin fail to develop pulmonary

fibrosis 21 days after treatment. This was compared to wild-type mice who have significant fibrotic change (82). The surprising part of this paper was that this did not improve mortality in these mice, as FN-EDA null mice had a higher mortality rate due to a more severe and prolonged inflammatory response after bleomycin. They hypothesised this may be due to a lack of ability to activate TGF-β and its paradoxical anti-inflammatory properties. The same authors also cultured primary fibroblasts from patients with IPF undergoing lung biopsy and found that these patients also produced more α-Smooth Muscle Actin (α-SMA) and FN-EDA than control specimens from patients undergoing lung biopsies for non-fibrotic conditions (82). For these reasons the genes that are assessed later in this work include *COL1A1* and *COL3A1* as well as *FN-EDA*, a splice variant of the FN gene. These molecules appear to play a crucial role in the formation of the ECM as well as feedback mechanisms in propagating fibrosis.

The proteoglycan molecules also play an important role in the ECM. These are proteins that have glycosylated side chains. Several members are in the small leucine-rich proteoglycan family (SLRP) and include decorin, biglycan and fibromodulin. Others, for example versican, are much larger molecules. They can have an effect upon signalling molecules within the matrix such as fibroblast growth factor (FGF), platelet derived growth factor (PDGF) and vascular endothelial growth factor (VEGF) (83). At 14 days post-inhaled bleomycin in mice there was a significant increase in these proteoglycan molecules including versican, heparin sulphate proteoglycan (HSPG), biglycan and fibromodulin (84). Lung specimens from patients with IPF also show an increase in glycosaminoglycan proteins compared to those from healthy control subjects (85).

There are a number of molecules that interact to keep the balance between ECM formation and degradation tightly regulated, these are members of the Matrix Metalloproteinase (MMP) family and tissue inhibitor of metalloproteinases (TIMPs). MMPs are expressed by a number of different cell types including fibroblasts, epithelial and endothelial cells (86). The MMPs have been highly studied in IPF and other fibrotic diseases as they have a role in the degradation of collagen. This has yielded some very interesting results as many MMPs are upregulated in IPF which appears paradoxical. For example, MMP-3 mRNA and protein is increased in the lungs of people with IPF and mice that lack MMP-3 are

protected against fibrosis when they are administered intratracheal bleomycin (87). Similarly, MMP-7 null mice are also protected in this model (88). MMPs may have both antifibrotic and pro-fibrotic roles, depending on the cell type that secretes them or during the initiation or propagation of fibrosis. In the extracellular space, MMPs are tightly regulated by TIMPs, which bind to the active site of MMPs making them less active.

1.4.2 The Role of Transforming Growth Factor-beta (TGF-β) and Other Signalling Pathways in Pulmonary Fibrosis

There are a number of important cytokines that act upon the ECM, ensuring that homeostasis is maintained. The TGF-β superfamily consists of the TGF-βs, bone morphogenetic proteins (BMPs) and activins (89). There are 3 recognised isoforms of TGF-β referred to as TGF-β1, TGF-β2 and TGF-β3. The experiments performed in this thesis assessed the effects of TGF-β1 and this will be referred to when TGF-β is used unless specified. TGF-β has a critical role in inflammation, as discovered when TGF-β null mice were genetically produced. Some mice did survive to term, although there appeared to be considerable intrauterine loss as much fewer mice were born than expected. These mice grew normally for 2 weeks but died at 3-4 weeks due to an excessive inflammatory response in many organs including the heart and lungs (90). The TGF-β pathway, as shown in Figure 1-6 (91), is a well-recognised signalling pathway implicated in fibrosis. It also has effects on apoptosis, migration and EMT. TGF-β is secreted and held in a latent form by bonding with a latency-associated protein (LAP) and the latent-TGF-β-binding protein (LTBP) (92). It is activated by a variety of molecules including plasmin, MMP-2, MMP-9, thrombospondin-1 and integrins. Each appears to interact with LAP to form an active molecule. This then allows the dissociation of TGF-β, allowing it to bind to its receptor on the cell surface.

Activation of the Smad cascade is one way that TGF-β can act. This pathway is activated when the dissociated TGF-β binds to the TGF-β type II receptor on the cell surface. This leads to recruitment and phosphorylation of the TGF-β type I receptor. A Smad 2 / Smad 3 complex (also referred to as the R-Smad complex) is bound to the TGF-β type I receptor along with Smad anchor receptor activation (SARA). This in turn phosphorylates the R-Smad complex and it is released into the cytoplasm to form a complex with Smad 4. This permits the complex to enter the nucleus where it can bind to promoters and regulate gene transcription, as shown in Figure 1-6 (91). Smad 7 acts as an inhibitory Smad and blocks phosphorylation of the R-Smad complex, inhibiting signalling and consequently gene transcription (93).

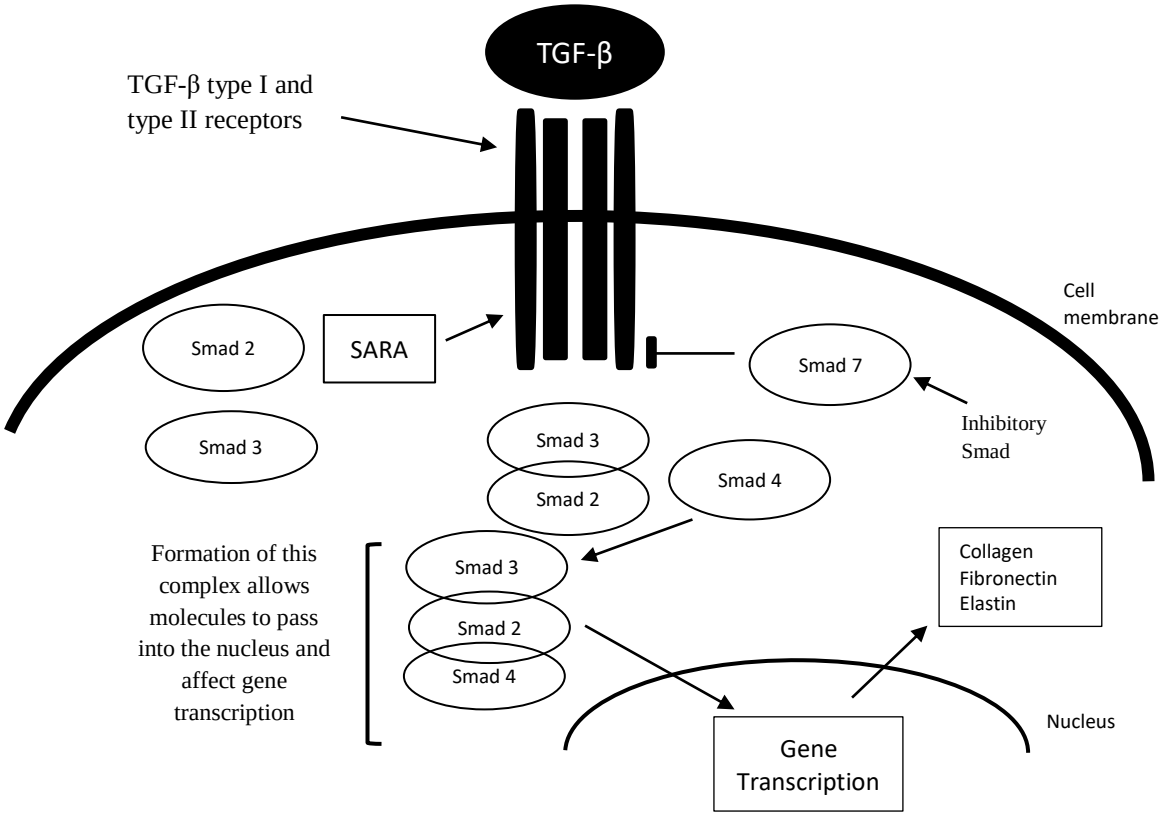

Figure 1-6 Summary of TGF-β signalling. The Smad pathway occurs when active TGF-β binds to the TGF-β type II receptor which recruits and phosphorylates the TGF-β type I receptor. Smad 2 and 3 are then phosphorylated and released, where they bind to Smad 4 and are able to enter the nucleus and cause gene transcription. TGF-β also has effects through non-canonical signalling.

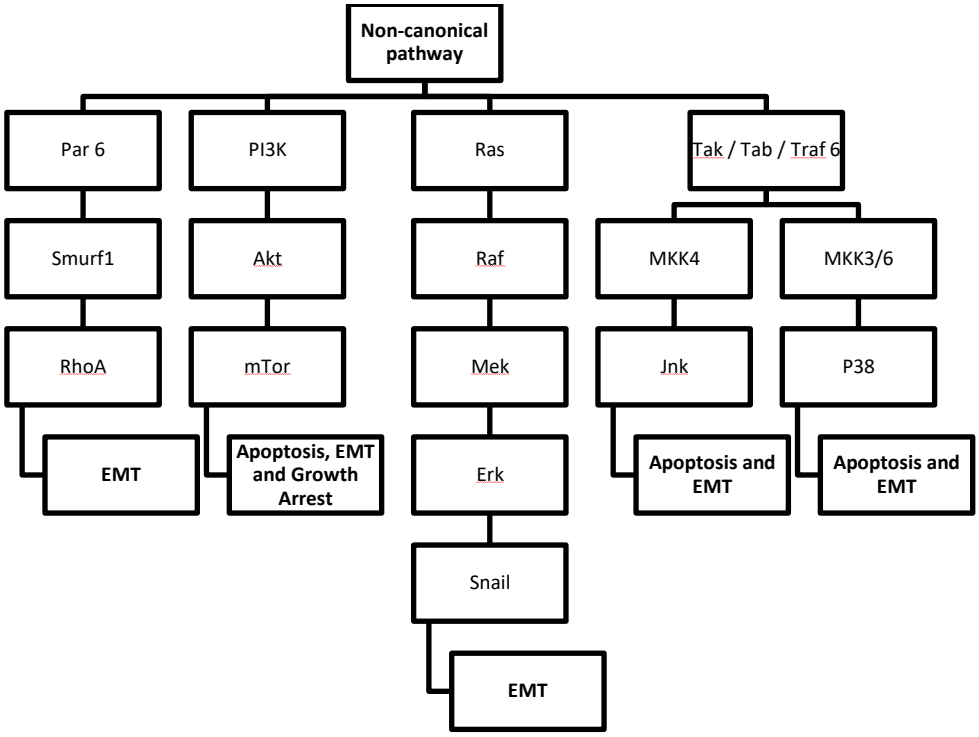

Figure 1-7 Summary of non-canonical TGF-β signalling. The interactions that this pathway has are not fully understood and this diagram is a simplified representation of the complex interplay of factors involved in many of the roles that TGF-β has including Epithelial-Mesenchymal Transition (EMT), apoptosis and cell growth arrest.

TGF-β signalling not only occurs via the Smad pathway but also by a number of non-canonical signalling pathways including the MAP Kinase pathways, Rho-like GTPase pathways and the phosphatidylinositol-3-kinase (PI3K)/AKT pathways, as represented in Figure 1-7 (94). Many studies have been performed to assess the role of each of these pathways in fibrosis. It is unclear what each pathway does in turn as they appear to strongly interact, both with other non-canonical pathways and the Smad pathway above and is dependent upon the cell type. However, it can be seen that these pathways have multiple crucial cellular effects. It has also been shown that when TGF-β is used to stimulate cells into producing COL1A2, this effect occurs through the Smad and non-Smad signalling pathway (95).

1.4.3 Platelet Derived Growth Factors

There are other signalling molecules that appear to play a crucial role in fibrosis. One such molecule is Platelet Derived Growth Factor (PDGF) and its receptors (PDGFR). The PDGFs are four possible subunits (A-D) that act upon two possible PDGFRs (α and β). The PDGFRs are transmembrane proteins that belong to the tyrosine kinase family. Binding to the receptor activates a number of intracellular signalling pathways including the PI3K / AKT pathway and the MAP Kinase pathways, described in more detail above. Its activation appears to play a fundamental role in cell proliferation, cell growth, differentiation and migration (96). The importance of PDGF in fibrosis was assessed when rats were exposed to asbestos, inducing the onset of pulmonary fibrosis. Within 5 hours there was a significant increase in the mRNA production of PDGFRα, however this was not a prolonged response and tapered back to baseline levels over the time course of up to 8 days (97). Expression of the PDGF-A gene is also increased in the bleomycin-induced mouse model of pulmonary fibrosis (98).

An inhibitor of PDGFR signalling, crenolanib, was used to examine its effect in fibrosis. Mice were challenged with angiotensin II, which causes effects similar to those seen in SSc in both the skin and heart. Treatment with crenolanib reduced fibrosis, confirmed by a reduction of picrosirius red staining in histology specimens, a surrogate marker for collagen formation (99). In another study to assess the effect of inhibiting PDGFR signalling, mice were irradiated to induce pulmonary fibrosis. Treatment with PDGFR tyrosine kinase inhibitors attenuated the fibrotic response with an improvement in mouse survival (100). The importance of these molecules in fibrosis are shown by the use of the drug nintedinib in IPF (17). This is a potent inhibitor of the tyrosine kinases and appears to slow disease progression in IPF. This confirms the critical role that this molecule has in perpetuating fibrosis.

1.4.4 The Production of the Myofibroblast and its Role in Fibrosis

Stimulation of fibroblasts with TGF-β causes proliferation and activation of the cell, leading to the secretion of ECM proteins. Some of these fibroblasts become synthetic cells, known as a myofibroblast. It is the myofibroblast that is the key cell in fibrosis, responsible for increasing the production of collagens, fibronectin and other ECM components. The hallmark of this cell type is its expression of α-SMA which gives it contractile properties. It has an active role in wound healing, where its migratory and contractile properties are required. Myofibroblasts are driven by myocardin related transcription factors (MRTF) (101). MRTFs are transcriptional co-activators. They are formed in the cytoplasm of cells and translocate to the nucleus in mechanical stress or growth factor stimulation. Here they bind with serum response factor (SRF) to cause gene transcription, in particular, transcription of α-SMA.

There are a number of studies that have been published that give evidence for the SRF / MRTF pathway playing a key role in fibrosis. Genetically modified mice that have a knockout for the MRTF-A gene were protected from bleomycin-induced lung fibrosis suggesting that this is a key molecule in this process (102). It has also been found that MRTF-A is more widely expressed in the skin of patients with diffuse SSc than in healthy control skin. When these dermal fibroblasts are isolated and cultured they produce more collagen, α-SMA and CCN2. These cells were treated with CCG-1423, originally described as a Rho inhibitor and blocks the SRF / MRTF pathway. By inhibiting this pathway *in vitro* there was a reduction in the expression of these genes (103).

Sisson et al treated cells and mice with a different SRF / MRTF pathway inhibitor (CCG-203971) which again acts to block nuclear localisation of MRTF preventing its downstream effects. When performed *in vitro* this intervention prevented differentiation to the myofibroblast, with a reduction in α-SMA and decreased expression of fibronectin (104). The authors also examined the effects of this drug *in vivo* using the bleomycin-induced lung fibrosis mouse model. They found that it significantly reduced the lung collagen content after injury, observed using picrosirius red staining.

1.4.5 Epithelial-Mesenchymal Transition (EMT)

Although some myofibroblasts appear to derive from activated fibroblasts this does not account for all of these cells. It seems that there are many cell types that can become mesenchymal and thus contribute to the fibrotic process and add to the myofibroblast pool. Indeed, TGF-β is also responsible for a process called epithelial-mesenchymal transition (EMT) where epithelial cells transdifferentiate into cells of mesenchymal type and secrete ECM contributing to the profibrotic process. EMT was initially described in embryology but is now recognised as occurring in adult cells (105). EMT is characterised by loss of the junctions between cells, loss of apical-basal polarity and associated changes in the cell cytoskeleton. Several transcription factors including Snail Family Transcriptional Repressor 1 (Snail, SNAI1), Snail Family Transcriptional Repressor 2 (Slug, SNAI2), Twist and Zinc-finger-E-box-binding (ZEB) control the regulation of the genes that lead to EMT (106). Snail and Slug reduce the expression of E-cadherins, claudins and occludins. This destabilises the tight cell-cell adherence between epithelial cells and reduces its barrier function. There is a corresponding increase in N-cadherin, fibronectin and collagen. N-cadherin is expressed by mesenchymal cells and gives weaker cell adhesion. This allows cells to migrate more easily. The cells also re-organise their actin cytoskeleton, increasing contractility and motility (107). It is accepted that EMT can be induced in various epithelial cell lines by stimuli such as TGF-β. This leads to an increase in collagen type I and III and a corresponding reduction in expression of E-cadherin (108). However, interestingly, even when EMT is stimulated *in vitro* and there is an upregulation of *COL1A1* mRNA, the amount of collagen type 1 protein produced and deposited was significantly less than that of fibroblasts (109). Although it is recognised that these processes occur *in vitro* the contribution that EMT makes in animal models of fibrosis and human fibrotic diseases is more controversial.

EMT was first described *in vivo* in 2002 in an animal model of renal fibrosis where over a third of the fibroblast population was thought to have arisen through EMT (110). Using this theory, it was suggested that similar mechanisms may occur in ILD. Studies have shown that EMT, including that occurring from type II alveolar epithelial cells, contribute up to 50% of the myofibroblast population (111) (72). However, these models used the marker SP100A4, also known as fibroblast-specific protein-1, as a fibroblast specific marker. However, this protein is also found in macrophages, neutrophils and endothelial cells so is not "fibroblast specific" and this error may have led to an overestimation of the contribution that EMT plays (106), (112).

1.4.6 Endothelial-Mesenchymal Transition (Endo-MT)

More recent studies suggest that several other cell types may contribute as precursors of the myofibroblast. Endothelial cells can transform into a mesenchymal cell type, acquiring the ability to express α-SMA and collagen, via a process called endothelial-mesenchymal transition (Endo-MT). Endothelial cells respond in a similar way to epithelial cells when treated with TGF-β *in vitro*. There is a reduction in expression of cell junction proteins that cause adherence between cells including vascular endothelial (VE)-cadherin and CD31. Similarly, endothelial cells have been shown to contribute to the myofibroblast pool in bleomycin-induced pulmonary fibrosis (113). Other evidence supportive of Endo-MT occurring in ILD comes from biopsy specimens of patients with SSc-ILD. These revealed that cells expressing the endothelial cell specific marker CD31 also expressed high levels of mesenchymal-specific genes such as collagen type I and fibronectin suggestive that endothelial cells were gaining a mesenchymal phenotype (114).

1.4.7 Evidence for Other Precursors of the Myofibroblast

Fate mapping strategies have been used to assess the contribution that lung pericytes have in fibrosis. Pericytes are mesenchymal cells that share a basement membrane with endothelial cells. Hung et al suggested that almost 70% of the cells in the lung that were α-SMA positive derived from pericytes after bleomycin treatment (115).

A final cell type implicated in fibrosis are fibrocytes. Fibrocytes are mesenchymal cell progenitors that are found in the bone marrow. They can also differentiate into fibroblasts and myofibroblasts once they reach a specific organ. Cell lineage tracing has suggested that fibrocytes may contribute up to 15% of the myofibroblast population in a model of kidney fibrosis (110) and lung biopsy samples from patients with IPF have shown that fibrocytes contribute to fibroblastic foci (116). A summary of these processes is shown in Figure 1-8 below (101).

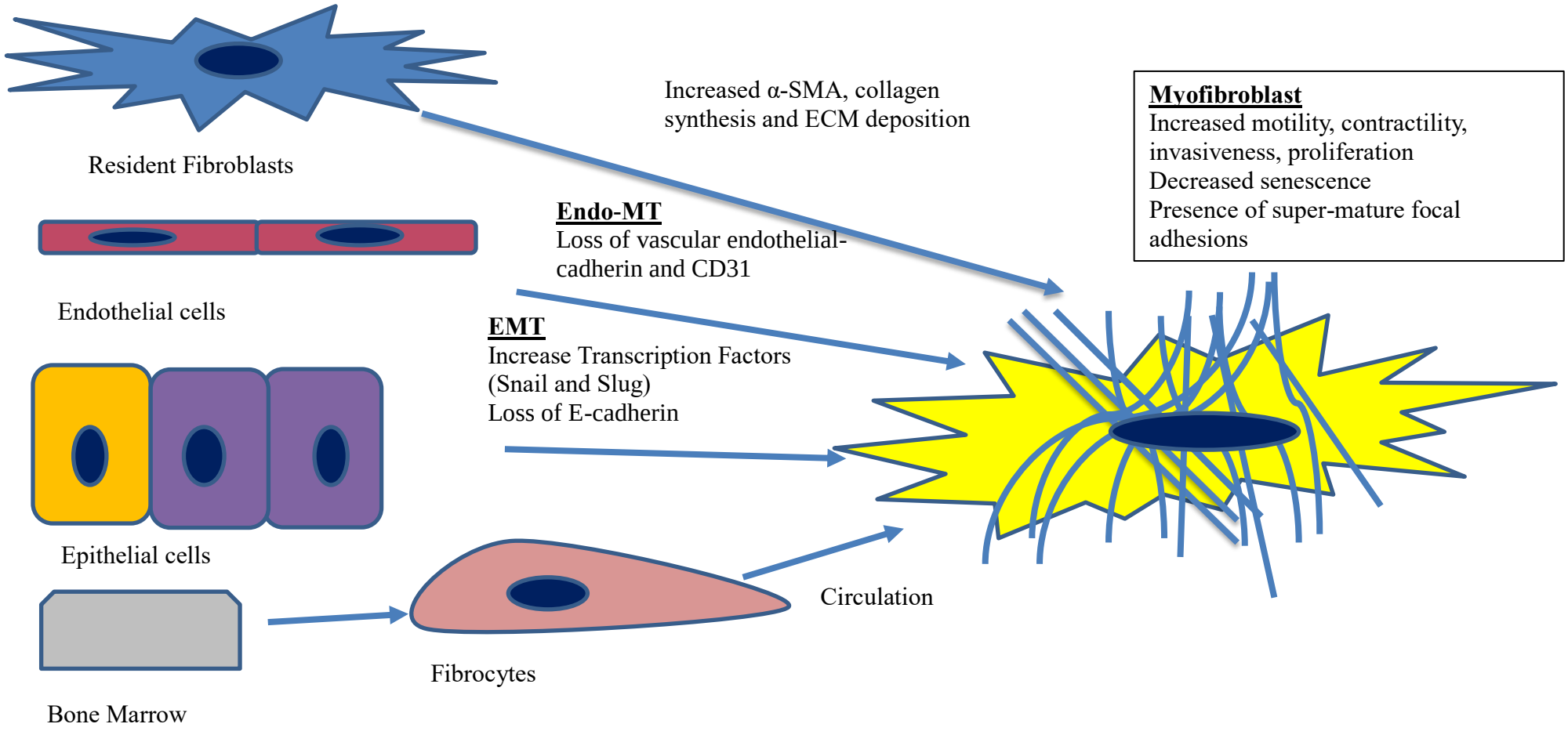

Figure 1-8 A representation of the development of the myofibroblast. The myofibroblast may derive from a number of cell types. It may be from active fibroblasts resident in the particular tissue, from endo-MT, EMT and from circulating fibrocytes produced by bone marrow. Endo-MT; endothelial -mesenchymal transition, EMT; epithelial-mesenchymal transition.

As discussed, it appears that processes such as EMT and Endo-MT are driven by the canonical and non-canonical pathways driven by TGF-β signalling. These signalling pathways also have an impact on downstream mediators of fibrosis. A particular molecule of interest in fibrosis is CCN2 which belongs to a family of proteins that appear to interact and have a variety of effects discussed in more detail below.

1.4.8 The CCN Family

The CCN family are a group of multifunctional proteins of which there are 6 members. Each protein has a similar structure and contains 5 exons that code for similar regions depicted below in Figure 1-9 (117).

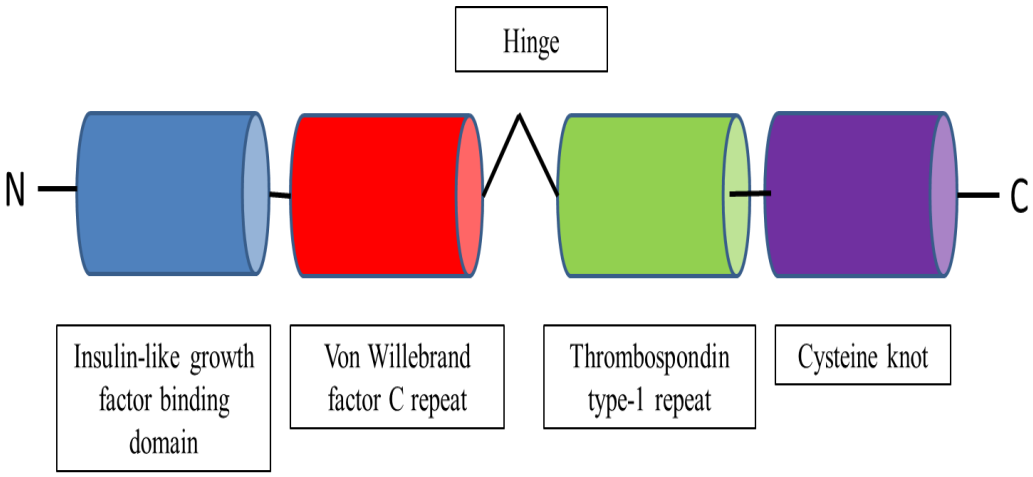

Figure 1-9 Diagram of the shared structure of the CCN family of proteins. Each has 5 exons as depicted above.

As a group they have a role in cell adhesion, migration and signalling due to their connection to the ECM (117). They have a role in angiogenesis which is important for tissue development and wound healing. They also act in regulating cell proliferation. The proteins appear to have differing roles in fibrosis with some, for example CCN2, having pro-fibrotic effects, and CCN3 appearing to have a negative regulatory role.

1.4.8.1 CCN1

The first member of the CCN family can also be referred to as cysteine-rich protein 61 (Cyr61). Functions include cell adhesion, migration, differentiation and angiogenesis (118). Mice that lack the CCN1 gene die *in utero* due to defects in cardiovascular development (Mo FE, 2006).

The role of CCN1 in fibrosis is controversial with studies showing opposing effects. Work produced by Jun and colleagues showed that CCN1 is highly expressed in healing skin wounds. In these wounds cellular senescence is important to restrict fibrosis once the wound has healed. It appears that CCN1 is required for the cellular senescence process acting through integrin-mediated receptors suggesting an antifibrotic effect (118). Further work *in vivo* verified this result showing similar evidence for cellular senescence in murine models of myocardial and liver fibrosis (119, 120). Kim et al used an established model of liver fibrosis, administering carbon tetrachloride to the animal to provoke injury eventually leading to hepatic fibrosis. These mice showed an upregulation of CCN1, which was thought to trigger cellular senescence. By administering purified CCN1 protein to mice with established hepatic fibrosis, the authors showed a regression of the fibrotic tissue within the liver and a reduction in mRNA of collagen.

However, this antifibrotic role has not been confirmed in further studies. A previously accepted murine model of renal fibrosis was used to identify the role of CCN1 in kidney injury. These mice undergo surgery to cause unilateral urethral obstruction, which causes fibrosis in the obstructed kidney. This injury led to an increase in production of the CCN1 protein at day 1 which remained elevated until day 10 after injury. Interestingly, the authors blocked the effects of CCN1 using an

antibody which reduced the initial fibrotic response, however this could not be sustained (121). CCN1 expression is also increased in the lungs of mice exposed to bleomycin and this increase occurs during the initial inflammatory stage (122). The same authors also found that the overexpression of CCN1 using adenovirus-mediated gene transfer directly to the lungs induced lung injury in mice by causing a neutrophilic alveolitis measured in broncho-alveolar lavage (BAL) fluid (122). Evidence from these studies suggests that CCN1 may be upregulated in acute lung injury and have a pro-inflammatory response, which is clearly contradictory to previous work. One reason for this discrepancy may be that CCN1 has a different role depending on the tissue that it is expressed in.

In human lung tissue from patients with IPF, CCN1 mRNA and protein levels were elevated. This was in association with increased levels of pro-fibrotic genes such as collagen, FN and α-SMA (123). The effect that CCN1 was inducing was further investigated by culturing these fibroblasts *ex vivo* and using RNA-interference to knockdown CCN1 expression. This reduced the constitutive expression of these pro-fibrotic genes again suggesting CCN1 may play a pro-fibrotic role in lung fibrosis. Similar effects have been shown in models of myocardial fibrosis (120).

1.4.8.2 CCN2

This protein was previously referred to as Connective Tissue Growth Factor (CTGF). It has a pivotal role in embryogenesis as CCN2 knock-out mice die shortly after birth due to severely malformed ribcages (124). It has roles in angiogenesis, tissue repair and fibrosis where it appears to act as a downstream mediator of TGF-β. Much work has been undertaken showing evidence that CCN2 plays a key role in propagating fibrosis. When CCN2 was given to mice in isolation it did not induce fibrosis and when TGF-β was given alone there was an initial fibrotic effect in the skin but it did not lead to a sustained response. However, when both molecules were administered in combination there was a sustained fibrotic response, suggesting an interaction between the two molecules for propagation of fibrosis (125). There also appear to be other regulators of CCN2 expression including hypoxia and mechanical stretch (126, 127).

Studies have shown that CCN2 is overexpressed in fibroblasts isolated from skin biopsy specimens of patients with SSc (128). There is also a correlation between the level of CCN2 in the circulating plasma of patients with SSc and disease severity (129).

Murine models have also been used to assess the role that CCN2 has in fibrosis. Mice were genetically modified to lack expression of CCN2 within skin fibroblasts. When they were administered subcutaneous bleomycin to induce a fibrotic response, the mice who lacked CCN2 were protected from developing skin fibrosis (130). To assess whether CCN2 has a similar pro-fibrotic role in lung fibrosis, mice were exposed to inhaled bleomycin *in vivo*. This led to an increase in levels of *CCN2* mRNA which preceded an increase in *COL1A2* (95).

These mouse model experiments led to an interest in developing a drug to inhibit CCN2 in patients with fibrotic diseases. The above study by Ponticos et al treated mice with a specific anti-CCN2 antibody (FG-3019) after treatment with bleomycin. Histological sections 7 and 14 days after treatment showed that less type I collagen and α-SMA was produced in the lungs of animals treated with the antibody. In a similar way, a monoclonal antibody to CCN2 was given to mice being administered angiotensin II, which is a known inducer of skin fibrosis (99). Mice treated with the drug showed a significant reduction in skin thickness and collagen production when compared to untreated mice 14 days after treatment. In fact, the above drug has been used in phase 2 clinical trials of patients with IPF (131). This was well tolerated and showed some promising results, with 30% of treated subjects showing an increase in Forced Vital Capacity (FVC) from baseline.

1.4.8.3 CCN3

CCN3 is also referred to as nephroblastoma overexpressed gene (NOV) and is known to play a role in embryogenesis, inflammation and tissue repair (132). CCN3 knockout mice survive *in utero* but may show cardiac and skeletal abnormalities, muscle atrophy and cataracts (133).

Riser et al used TGF-β to stimulate the upregulation of CCN2 and type I collagen *in vitro* using mesangial cells from rat glomeruli, and then showed that concomitant treatment with CCN3 inhibited this effect. They investigated this further by showing a lack of change in the downstream phosphorylation of Smad, suggesting the effect of CCN3 was not a direct, blocking effect on TGF-β (134). Overexpression of CCN3, by insertion of a CCN3 vector in fibroblasts, leads to similar reductions of CCN2 and type I collagen (135). This was suggestive that CCN3 has an antifibrotic effect.

CCN3 effects have also been investigated *in vivo* using the unilateral ureteral obstructive model of renal fibrosis where there was an increase in protein expression after injury, both in the obstructed kidney and in the circulating plasma. However, in CCN3 null mice where this increase could not occur, there was a reduction in fibrosis (132). Again, this result appears contradictory to previous work, where CCN3 appears antifibrotic. To date the effects of CCN3 in a murine model of pulmonary fibrosis have not been investigated.

1.4.8.4 CCN4

CCN4 is also referred to as WNT1-inducible signalling protein (WISP-1). Treatment of epithelial cells with CCN4 leads to EMT with an increase in α-SMA positive cells (136). In the carbon tetrachloride murine model of liver fibrosis, it was shown that blockade of CCN4 using an antibody reduced the amount of collagen in the liver, suggesting that CCN4 acts as a pro-fibrotic mediator (137).

In type II epithelial cells isolated from lungs of mice treated with bleomycin there is an increase in CCN4 expression. If mice were treated with CCN4 antibody prior to receiving bleomycin there was a reduction in fibrosis, again suggesting a pro-fibrotic role of CCN4. This increase was also present in type II epithelial cells isolated from biopsy specimens from patients with IPF (136).

1.4.8.5 CCN5

CCN5, also referred to as WNT2-inducible signalling protein (WISP-2), is unique within the CCN family as it does not have a C-terminal domain. This domain is important as in other CCN proteins it has been found to bind to integrins, other matrix molecules and important signalling molecules such as Notch 1 (117). CCN5 appears to have a critical role in embryogenesis as CCN5 null mice do not survive *in utero* and its expression is widespread early in embryonic development (138).

When CCN5 was overexpressed in primary human lung fibroblasts cultured from patients with IPF there was reduced expression of CCN2, α-SMA and type 1 collagen. This suggests that CCN5 has anti-fibrotic effects (139).

1.4.9 Fibroblast Surface Markers and their Role in Fibrosis

1.4.9.1 Thy-1

Thy-1 is a glycophosphatidylinositol anchored cell surface protein, found on the surface of fibroblasts as well as many other cells and tissues in the body including neurons and T-lymphocytes. There is a variety of evidence to suggest that thy-1 has a role in lung fibrosis. Thy-1 null mice administered bleomycin experienced more severe lung fibrosis, with a greater accumulation of collagen, than their wild type counterparts (140). Biopsy specimens from patients with IPF found that myofibroblasts within the fibroblastic foci also appear to be thy-1 negative. In contrast, in healthy lungs the majority of fibroblasts are thy-1 positive (140). This is suggestive that thy-1 expression has a protective role in fibrosis.

Having recognised the multitude of cell types and transformations which could contribute to lung fibrosis, and given that it is recognised that elevated serum levels of TGF-β are detectable in ILD patients (141), it was wondered whether ILD patient plasma could cause changes in fibroblasts or epithelial cells towards that of a myofibroblast phenotype. This appears of considerable importance, as it could give clues as to what may be happening in the lungs of ILD patients, and by which pathway fibrosis is affecting the lung. It is clear that this may be different depending upon the underlying cause, i.e. in IPF which is predominantly fibrotic or CTD-ILD which is more strongly associated with inflammation. By recognising the pathways that drive the fibrotic response it will aid the development of future therapeutic targets for a more personalised medicine approach for ILD patients. Currently there are only two drugs, pirfenidone and nintedanib, that have been shown to have any impact upon the relentless progression of IPF. However, these drugs only appear to slow progression of the disease and do not stop the ongoing fibrosis. CTD-ILD appears to respond to steroids and immunosuppressive agents suggesting a different underlying aetiology. If the mechanisms of the disease are better understood then

affecting part of the pathway driving the fibrotic response may allow termination of disease progression. This work strives to recognise any key molecules involved in fibrosis when lung cell types are treated with ILD plasma.

The key aims of the work that is presented in the next few chapters include:

1) To identify the proportion of patients diagnosed with IPF who have a recognised antibody associated with CTD-ILD in their serum. This will ascertain whether patients are being incorrectly diagnosed with IPF, thereby receiving incorrect treatment that may not be beneficial. It will also show whether the IPF population used in later chapters has a number of patients with covert CTD-ILD, affecting any comparisons that can be made.
2) To design an *in vitro* model of fibrosis that can measure changes in fibrotic markers. Two cell types have been chosen, fibroblasts and epithelial cells, as previous literature has implicated these cell types as key cells in the fibrotic response.
3) To use this model by treating cell lines with plasma from patients with fibrotic lung diseases. Two diseases were chosen, IPF (a predominantly fibrotic disease that affects the lungs) and SSc-ILD (a disease that has an inflammatory component and responds to immunosuppression).
4) To adapt the *in vitro* model by using stretch to imitate the constant movement of the lungs and to assess what impact this movement has upon the fibrotic response in the lungs.

2 Materials and Methods

2.1 Recruitment of ILD Patients to Enable Clinical Research

2.1.1 United Kingdom – Biomarkers in Interstitial Lung Disease (UK-BILD) Study

As ILD is relatively rare it was necessary to set up a UK-wide collaborative network designed to enable recruitment of a sufficient number of cases to permit research into disease mechanisms. The UK-BILD study was thus established to allow this research to be undertaken. It is now an established large-scale, national collaboration involving 38 centres across the UK, a list of which is given in Appendix 1. It was designed as a cross-sectional study recruiting patients across the spectrum of ILD subgroups. This multicentre, collaborative approach allows sufficient numbers of patients to be recruited, particularly in rarer disease subtypes, to allow statistically meaningful within and between subgroup comparisons to be made.

2.1.2 Ethical Approval

In order to recruit into UK-BILD, ethical approval was sought from the Research Ethics Committee (REC). An ethical application was made and called; "Identifying disease susceptibility genes and autoantibodies associated with the development and clinical characteristics of interstitial lung disease (ILD) in patients with and without proven connective tissue diseases (CTDs)". This received favourable ethical opinion on the 11th March 2011, Research Ethics Committee (REC) reference number 11/H1010/4 (see Appendix 3 for REC approval form), later also referred to as the "UK-BILD study". Following its ethical approval, the study received endorsement for portfolio support (UK-Clinical Research Network (UKCRN) ID: 15775) and is now supported by UKCRN nurses at the 38 individual recruitment centres.

2.1.3 Recruitment of Centres and Patients into UK-BILD

Patients with a definite diagnosis of ILD were recruited into UK-BILD in a cross-sectional manner. Patients were identified as being eligible for study enrolment by research teams at ILD or Rheumatology centres. To be eligible for the study patients must be 18 years or older at time of ILD diagnosis and have evidence of ILD on their HRCT scans. Pulmonary function testing must show evidence of restriction (reduced vital capacity, often with an increased forced expiratory volume in 1 second / forced vital capacity (FEV1/FVC) ratio) and impaired gas exchange. Those with a diagnosis of IPF must have met criteria for this diagnosis based on the 2011/13 ATS/ERS guidelines. The disease duration should be longer than 3 months. The exclusion criteria included drug-induced ILD and those unable or unwilling to give consent for study inclusion.

Key clinical data was completed on a two-page proforma, an example of which is included in appendix 2, and sent via secured NHS email to be recorded on a centralised database.

One EDTA tube and one serum gel tube (10ml blood per tube) were taken from patients and sent to the Centre for Integrated Genomic Medical Research (CIGMR) at the University of Manchester. Once samples were received, they were separated by centrifugation into plasma (stored for mechanistic research), serum (stored for serotyping by immunoprecipitation) and DNA samples (stored for future genotyping projects), labelled using the laboratory information management tracking system and stored at -80°C for future use. Each centre has required Research and Development (R&D) approval through its individual site prior to commencing recruitment. The first patient was collected on 7th January 2015. There are now 38 centres recruiting patients with ILD. Appendix 1 shows the centres that are currently recruiting patients. As of the 16th May 2017, this study has recruited over 2624 patients of many different ILD subgroups, a breakdown of which is shown in chapter 3.

Data was collected as part of the study including patient demographics (age, gender and ethnicity), smoking history, the date of ILD onset, any CTD or respiratory symptoms and signs and a history of previous or current malignancy in a cross-sectional manner. The data collection sheet is shown in Appendix 2.

Smoking data was collected on patients to determine if they were current smokers, previous smokers or never smokers. To determine if they were heavy smokers a pack year calculation was performed. This is calculated by (number of cigarettes smoked per day / 20) multiplied by the number of years smoked. Patients were subdivided into heavy smokers (greater than 40 pack year history), moderate smokers (20-40 pack year history) or light smokers (less than 20 pack year history).

Patients with a diagnosis of IPF were separated into 3 distinct categories. The first two categories of IPF are termed "definite IPF". The first category includes patients who have a characteristic appearance on HRCT with a reticular pattern, honeycombing and a lack of ground glass change (ie, a definite UIP pattern) and these patients do not require a histological specimen for confirmation of their diagnosis. The second category is for patients who lack honeycombing and have a scan appearance more consistent with fibrotic NSIP but undergo diagnostic lung biopsy which confirms a UIP pattern. The third category is termed "probable IPF", where the patient has a HRCT pattern similar to the second category (fibrotic NSIP) but is unable to undergo surgical lung biopsy, most likely due to poor lung function or underlying co-morbidity. However, if these patients are of an older age group, discussed in an MDT clinical setting and another cause is not recognised they can be diagnosed with probable IPF. These diagnostic guidelines have recently been updated (142).

Physicians recruiting patients to the study were required to identify specific CTD and respiratory symptoms and signs when examining patients. CTD symptoms included Raynaud's phenomenon, arthralgia and myalgia. Signs included sclerodactyly, calcinosis, Mechanic's hands, periungal erythema and telangiectasia. Many of these signs, if present, may be subtle and were included on the form as a prompt for physicians to specifically look for these. Respiratory signs included clubbing, crackles and evidence of pulmonary hypertension, diagnosed according to either echocardiographic or right heart catheter criteria.

2.1.4 Recruitment of Healthy Control Subjects

Healthy control subject plasma was obtained through the Myositis Research Tissue Bank (MRTB) and their samples were requested via the MRTB Steering Committee. The Bank received favourable ethical opinion on the 10th November 2015, REC reference number 15/NW/0826. There was limited data available regarding these patients however they were recruited to a tissue bank for use as healthy control subjects and their age and gender had been recorded.

2.2 Serotyping of IPF Patients using Immunoprecipitation

Immunoprecipitation is the gold standard technique for the detection of autoantibodies in patients' sera. The aim is to purify specific proteins from a cell extract, human plasma or serum samples. Usually it involves an antibody to recognise the protein of interest but in this scenario it is the antibody itself that is of interest. For this reason, human serum is incubated alongside protein A beads that are immunoglobulin-binding proteins that can bind to any autoantibodies present in the patient serum. The sample is then washed to remove any unbound proteins. This mixture is then incubated with the radiolabelled cell extract to form a complex. These are washed again to remove any unbound protein. Elution occurs to de-couple the antigen, and the remaining proteins are then ran on a sodium dodecyl sulphate (SDS)-polyacrylamide gel to separate the protein by molecular weight. Autoradiography is then undertaken and analysed to assess for the presence of particular bands associated with particular autoantibodies. This process is depicted in Figure 2-1.

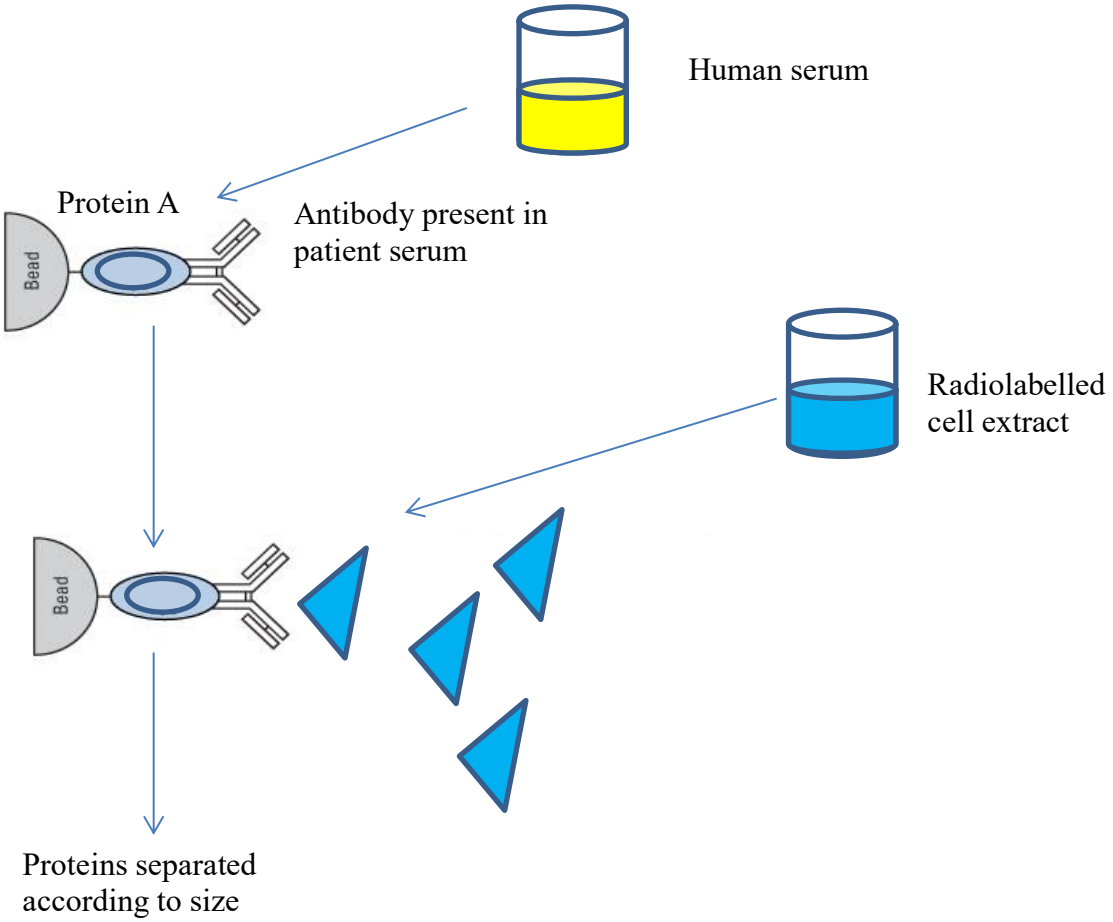

Figure 2-1 Simplified description of technique used in immunoprecipitation procedure. Human serum was incubated alongside protein A beads that bind to any autoantibodies present in the serum. This mixture was then incubated with radiolabelled cell extract. Proteins were separated according to molecular weight and autoradiography was used to detect the presence of bands which may correlate with a corresponding autoantibody.

This technique was performed in a specialised laboratory with a high specificity and sensitivity. This was not performed by myself but was undertaken by Dr Zoe Betteridge at the National Immunoprecipitation Laboratory, University of Bath. It has been described previously in work performed by the group (143).

Briefly, 10ul patient sera was mixed with 2mg protein-A-sepharose beads in IPP buffer. This allows for binding of the autoantibodies present in the sera. K562 cells were labelled with [35S]-methionine, a radioactive material, and then lysed. Beads were washed in IPP buffer before being added to the radioactive cell extract. Samples were mixed at 4°C for 2 hours. Beads were washed in IPP buffer with a final wash in Tris buffered saline (TBS) buffer. They were then re-suspended in sodium dodecyl sulphate (SDS), heated and separated by molecular weight on a 9% SDS-polyacrylamide gel electrophoresis (SDS-PAGE). They are then analysed by auto-radiography to give a band at certain molecular weights. An example gel is shown below, some lanes are used as positive controls, in which samples from patients with recognised autoantibodies are run alongside the IPF samples for quality control purposes. It should be noted that autoantibodies are usually mutually exclusive and the positive controls used in the gel below were using mixed patient sera.

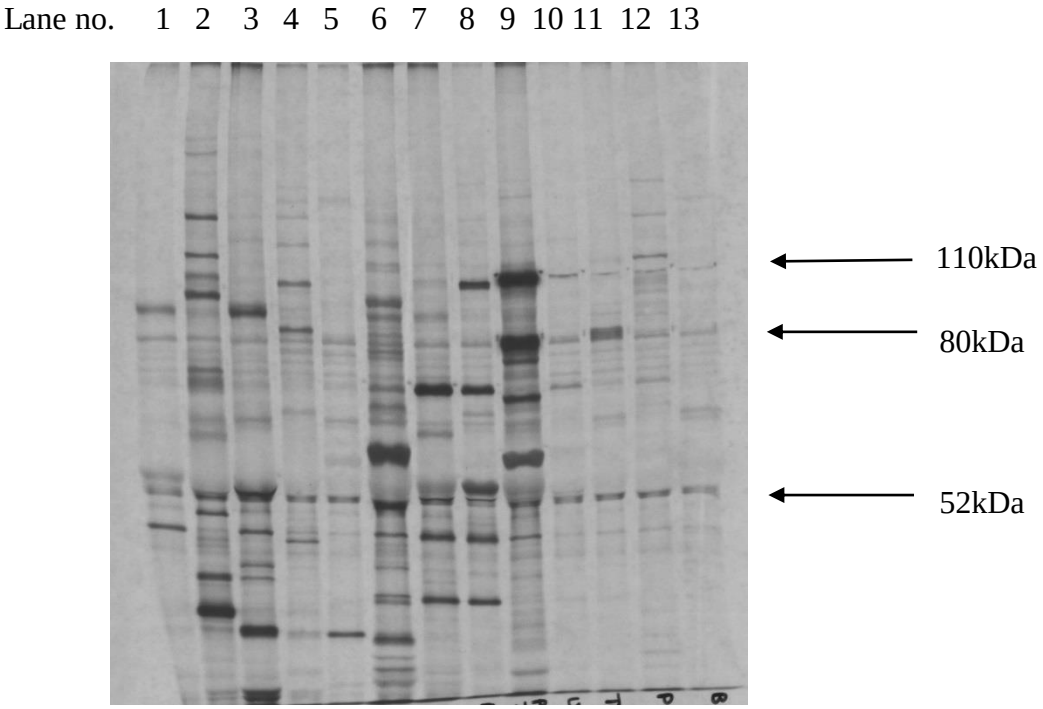

Figure 2-2 Example of immunoprecipitation gel kindly provided by Dr Zoe Betteridge. Lane 1 is provided as a negative control. Positive controls are shown in lane 3 (U1, Jo-1, NXP-2 and RNAPol II), lane 6 (Ro-60, La, PM-Scl), lane 7 (Anti-Mitochondrial Antibody (AMA)) and lane 9 (PL-7, PL-12 and Zo). Lanes 2, 4, 5, 8, 11, 12 and 13 were from various patients recruited through the UK-BILD study. All lanes show strong unknown bands at various molecular weights, with lane 2 showing RNAPol II and lane 8 showing AMA.

2.3 Cell Culture

2.3.1 General Cell Culture Materials

Cell culture was performed for both MRC5 fibroblast cells, a human foetal fibroblast cell line and A549 epithelial cells, a human cancerous lung epithelial cell line. The following materials were used in all cell culture work undertaken;

Plastics

- T75 cell culture flask, Cellstar, Sigma-Aldrich, Dorset, UK
- Centrifuge tube (15ml), Cellstar, Sigma-Aldrich, Dorset, UK

Reagents

- Dulbecco's phosphate buffered saline (PBS), Sigma-Aldrich, Dorset, UK
- Penicillin-streptomycin (100x), Sigma-Aldrich, Dorset, UK
- Trypsin-EDTA Solution (10x), Sigma-Aldrich, Dorset, UK
- Fetal Bovine Serum (FBS), qualified, EU-approved, South America origin (500ml), Thermo Fisher Scientific, Paisley, UK
- TCH Defined Serum Replacement, 50X concentrate, MP Biomedicals, Leicester, UK
- Dimethyl Sulphoxide (DMSO) Hybri-Max, Sigma-Aldrich, Dorset, UK
- Trypan Blue Solution, Sigma-Aldrich, Dorset, UK

Cytokine

- Recombinant Human TGF-β1, Lot#0713AF354, Peprotech, London, UK.

Equipment

- Heraeus Multifuge X1 Centrifuge, Thermo Fisher Scientific, Runcorn, UK

Materials for MRC5 Fibroblasts

- MRC5 cell line, Sigma-Aldrich, Dorset, UK
- Minimum Essential Medium (MEM) (1x) with Earle's salts and L-glutamine, Gibco by Life Technologies, Thermo Fisher, Runcorn, UK
- Minimum Essential Media Non-Essential Amino Acids (100x), Gibco by Life Technologies, Thermo Fisher, Runcorn, UK

Medium used for culture of MRC5 cells				
Serum supplemented medium	Minimum Essential Medium (MEM) (1x) with Earle's salts and L-glutamine	1% Minimum Essential Media Non-Essential Amino Acids (100x)	1% Penicillin-streptomycin (100x)	10% Fetal Bovine Serum (FBS)
Serum free medium	Minimum Essential Medium (MEM) (1x) with Earle's salts and L-glutamine	1% Minimum Essential Media Non-Essential Amino Acids (100x)	1% Penicillin-streptomycin (100x)	
Serum replacement medium	Minimum Essential Medium (MEM) (1x) with Earle's salts and L-glutamine	1% Minimum Essential Media Non-Essential Amino Acids (100x)	1% Penicillin-streptomycin (100x)	2% TCH Defined Serum Replacement, 50X concentrate

Table 2-1 Medium used for culture of MRC5 cells.

Materials for A549 Epithelial Cells

- A549 cell line, ATCC, CCL-185, Middlesex, UK
- F-12K Kaighn's modification of Ham's F-12 with L-glutamine, sterile filtered medium, ATCC, Middlesex, UK

Medium used for culture of A549 cells			
Serum supplemented medium	F-12K Kaighn's modification of Ham's F-12 with L-glutamine	1% Penicillin-streptomycin (100x)	10% Fetal Bovine Serum (FBS)
Serum free medium	F-12K Kaighn's modification of Ham's F-12 with L-glutamine	1% Penicillin-streptomycin (100x)	
Serum replacement medium	F-12K Kaighn's modification of Ham's F-12 with L-glutamine	1% Penicillin-streptomycin (100x)	2% TCH Defined Serum Replacement, 50X concentrate

Table 2-2 Medium used for culture of A549 cells.

2.3.2 General Cell Culture Methods

Cell lines (either MRC5 or A549) were cultured in T-75 flasks (Sigma-Aldrich, UK) along with 10ml of their respective serum supplemented medium (described above). The flasks were placed in a standard 5% CO_2 incubator at a temperature of 37°C.

Cells were split once they reached 80% confluence. The used culture medium was discarded and cells washed twice with PBS (Sigma-Aldrich, UK). Trypsin (Sigma-

Aldrich, UK) was added and the flask placed in the incubator at 37°C for 5 minutes until cells were removed from the bottom of the flask. Serum supplemented medium (5ml) was added to the flask, the mixture placed in a 15ml centrifuge tube and spun at 1000xg for 5 minutes. The excess medium was then removed and the remaining cell pellet was re-suspended in 1ml medium. For all described experiments a cell count was performed using a haemocytometer. To undertake this 10ul of the re-suspended cell pellet, 10ul trypan blue (Sigma-Aldrich, UK) and the appropriate dilution were mixed in a sterile Eppendorf. Using this mixture, 10ul was placed on the haemocytometer and a count undertaken.

2.3.2.1 Cell Culture Experiment Assessing the Effect of TGF-β

Cells (MRC5 cells, passage 11-13 or A549 cells, passage 22) were plated at a density of $1x10^5$ cells per well in a 6 well plate and cultured for 24 hours. Cells were given 2ml per well of serum supplemented medium. After 24 hours this medium was replaced with serum free medium (described in Table 2-1 and Table 2-2). MRC5 cells were serum starved for 16 hours and A549 cells were serum starved for 8 hours. The medium was then replaced with serum supplemented medium (2ml) and cells treated with TGF-β (Peprotech, UK) of varying concentrations. The MRC5 cells were treated with 0.5ng/ml, 1ng/ml and 2ng/ml TGF-β alongside untreated control wells. The A549 cells were treated with TGF-β 1.5ng/ml or 3ng/ml alongside untreated control wells. The conditioned medium was removed, placed in sterile Eppendorf tubes and stored at -80°C for use in western blot experiments. RNA was extracted, see section 2.7 for method, at 24, 48, 72 and 96 hours respectively.

2.3.2.2 Cell Culture Experiment Assessing the Effect of TGF-β but Using Serum Supplementation Instead of Serum Starvation

To reduce the impact of serum starvation, the above experiment was repeated using a similar method. However, medium was not replaced with serum free medium but by serum replacement medium containing 2% TCH (MP Biomedicals, UK), as described in Table 2-1 and Table 2-2. TCH ensures that cells are kept in a consistent growth environment but are free from growth factors and steroid hormones, ensuring that these molecules found in FBS do not impact upon cells. After 16 hours, cells were treated with TGF-β (0.5ng/ml, 1ng/ml and 2ng/ml in the MRC5 cells or 1.5ng/ml and 3ng/ml in the A549 cells) alongside untreated, control wells. RNA was extracted at 48 hours only.

2.3.2.3 Cell Culture Experiment Assessing the Effect of Patient Plasma

Cells (MRC5 cells, passage 12-20 or A549 cells, passage 16-24) were plated at a density of $1x10^5$ cells per well in a 6 well plate for 24 hours with each well receiving 2ml of serum supplemented medium. After 24 hours this medium was removed, discarded and cells were washed with warmed PBS and replaced with 1.2ml serum replacement medium. After 16 hours cells were treated with 100ul patient or healthy control plasma and RNA extracted at 24, 48 and 72 hours respectively.

2.3.2.4 MRC5 Stretch experiment with TGF-β or Patient Plasma

2.3.2.4.1 Extra Materials Required

- Bioflex 6 well culture plates, Flexcell International Corporation, Burlington, North Carolina, USA
- Flexcell Strain Unit, FX-4000, Flexcell International Corporation, Burlington, North Carolina, USA

MRC5 cells (passage 14-17) were seeded onto bioflex 6 well plates (Flexcell, Burlington, USA) at a density of $2.5x10^5$ and covered with 2ml serum supplemented medium per well. Once cells were fully confluent, the medium was removed, the cells washed with warmed PBS and the medium replaced with serum replacement medium overnight. After 16 hours, cells were left untreated, treated with stretch only, treated with TGF-β only (2ng/ml) or treated with a combination of TGF-β (2ng/ml) and stretch. Stretch was applied at 6.66% in pulsed sine wave intervals at 1 Hertz (Hz). After 24 hours, RNA was extracted using the method described in section 2.7.

In a similar experiment to assess the impact of stretch and patient plasma, cells were kept in the same conditions and then treated with 100ul IPF patient plasma or 100ul healthy control plasma respectively. One plate was stretched while the other was kept in the same incubator but without stretch applied. Again, cells were stretched at 6.66% in pulsed sine wave intervals at 1 Hz for 24 hours. RNA was extracted using the protocol described in section 2.7.

2.3.2.5 A549 Stretch Experiment with TGF-β

2.3.2.5.1 Extra Materials Required

- Silicon stretch chambers, custom made
- Laminin from Engelbreth-Holm-Swarm murine sarcoma (basement membrane), Sigma-Aldrich, Dorset, UK
- Heraeus Multifuge X1 Centrifuge, Thermo Fisher Scientific, Runcorn, UK

Laminin (4ug/ml) was placed on stretch chambers and incubated at 37°C for 2 hours to coat the chamber and allow for cell attachment and growth. A549 cells (passage 19-23) were plated at a density of $1x10^6$ and left to grow in 4ml serum supplemented medium until confluent. The cells were washed with PBS and the medium replaced with serum supplemented medium overnight. Cells were then split into 4 groups

with the experiment repeated in duplicate; (a) untreated with no stretch; (b) treated with TGF-β (1.5ng/ml) with no stretch; (c) untreated with stretch; (d) treated with TGF-β (1.5ng/ml) and stretch. Stretch was set to 6.6% at 1 Hz. RNA was extracted at 24 hours as per methods described in section 2.7.

This experiment was performed in a similar manner using patient plasma. Once cells were grown in serum supplemented medium, 150ul patient plasma or healthy control plasma was added to each chamber and cells either stretched or left in the same incubator without stretch for 24 hours. RNA was then extracted using methods previously described.

2.4 Immunocytochemistry

2.4.1 Immunocytochemistry Materials

- Phosphate Buffered Saline tablet, Sigma-Aldrich, Dorset, UK
- 0.01% Phosphate Buffered Saline and Tween (PBST) prepared as described in Appendix 4
- Neutral Buffered Formalin (NBF) 10%, Leica Biosystems, Milton Keynes, UK
- Goat serum, Vector Laboratories, Burlingame, California, USA
- Vectashield Hard Set Mounting medium with dapi, Vector Laboratories, Burlingame, California, USA
- Glass cover slip, 22x22mm, Scientific Laboratory Supplies Ltd, Manchester, UK
- Nikon eclipse Ti confocal microscope, Amsterdam, Netherlands
- Phalloidin, A12379, Alexa Fluor, Life Technologies, USA

Primary Antibodies Used for Immunocytochemistry				
Protein	Company	Product Code	Antibody Type	Dilution
Collagen 1	Abcam	ab34710	Rabbit polyclonal	1/500
α-SMA	Abcam	ab5694	Rabbit polyclonal	1/250
Thy-1	Abcam	ab133350	Rabbit monoclonal	1/250

Table 2-3 Primary Antibodies for Immunocytochemistry

Secondary Antibodies Used for Immunocytochemistry			
Antibody	Company	Product code	Dilution
532 goat anti-rabbit IgG	Alexa fluor, Life Technologies	A-11009	1/1000

Table 2-4 Secondary Antibodies for Immunocytochemistry

2.4.2 Immunocytochemistry Methods

Cells were plated at a density of $1x10^5$ in 6 well plates or $2.5x10^4$ in 12 well plates, cultured and treated with TGF-β or patient plasma as described previously. The addition of a glass cover slip was placed in the bottom of each well. This was to allow optimum views when using the microscope for staining. After 48 hours cells were washed carefully with PBS. Cells were fixed by adding 1ml NBF (Leica Biosystems, Milton Keynes, UK) per well in a fume hood and incubating for 15 minutes at room temperature. The NBF was removed and the cells washed twice with 0.01% PBST to permeabilise the membrane.

Phalloidin (Life Technologies, USA) was diluted in 1.5ml methanol and made to a dilution of 1 in 40 with PBST, added to each well and incubated under light-sensitive conditions for a further 40 minutes at room temperature. The phalloidin was removed by three 5-minute washes with PBST.

A blocking solution of 5% goat serum (diluted with PBST) was then added to each well (1ml per well) and the plate left to incubate at room temperature for 2 hours. The primary antibody (made to the dilution specified above) was made in 5% goat serum diluted with PBST and added to each well. This was left overnight at 4°C. The antibody was removed by three 5-minute washes with PBST.

The secondary antibody, made to the dilution specified above, was added to each well (750ul per well). This was incubated at room temperature for 2 hours. Again, the antibody was removed and the cells given a short wash with PBST. The glass cover slip was removed from each well and added to glass slides using hard set mountant along with Dapi staining. Cells were then imaged using a confocal microscope (Nikon eclipse Ti, Netherlands). When not in use, slides were stored at 4°C.

2.5 Cell Proliferation Assay

2.5.1 Cell Proliferation Assay Materials

- Cell culture materials as documented above
- Alamar Blue Cell Viability Reagent, Invitrogen, Paisley, UK
- Fluostar Optima Microplate reader, BMG Labtech, Ortenberg, Germany

2.5.2 Cell Proliferation Assay Methods

Initially, a standard curve was produced for both the MRC5 fibroblasts and the A549 epithelial cells respectively. To undertake this, cells were plated at increasing densities and left to settle for 2 hours. Alamar blue reagent (10%) (Invitrogen, Paisley, UK) was then added to each well and the plate kept under light sensitive conditions at 37°C for 3 hours prior to measurement of fluorescence.

To calculate proliferation, cells were plated at 6250 cells per well in a 96 well plate along with 150ul of serum replacement medium. After 24 hours, cells were washed with PBS and changed to serum supplemented medium overnight. Cells were then treated with TGF-β (concentrations as previously described) or patient plasma (6.25ul per well). Alamar blue (10%) was then added to wells after 24, 48, 72 and 96 hours respectively and left for 3 hours under light sensitive conditions until measurement of fluorescence.

2.6 PCNA Staining for Cell Proliferation

2.6.1 PCNA Staining for Cell Proliferation Materials

- Cell culture materials as per section 2.3
- PBS tablet, Sigma-Aldrich, Dorset, UK
- 0.01% PBST prepared as described in Appendix 4
- Analytical reagent grade methanol, Fisher Chemical, Fisher Scientific, Leicestershire, UK
- Goat serum, Vector Laboratories, Burlingame, California, USA
- Bovine serum albumin (BSA) lyophilized powder, Sigma-Aldrich, Dorset, UK
- Glycine for electrophoresis, Sigma-Aldrich, Dorset, UK
- Anti-PCNA antibody, ab18197, Rabbit polyclonal, dilution

- Alexa Fluor 532 goat anti-rabbit IgG, molecular probes by life technologies, Oregon, USA
- Vectashield hard set mounting medium with dapi, Vector Laboratories, Burlingame, California, USA
- Glass cover slip, 22x22mm, Scientific Laboratory Supplies Ltd, Manchester, UK
- Nikon eclipse Ti confocal microscope, Amsterdam, Netherlands

2.6.2 PCNA Staining for Cell Proliferation Methods Performed for Cells Treated with TGF-β or Patient Plasma

Cells were plated at a density of $5x10^4$ in 12 well plates and cultured in conditions previously described (see section 2.3.2). The MRC5 cells were treated with 1ng/ml or 2ng/ml TGF-β alongside untreated, control wells respectively. A549 cells were treated with 1.5ng/ml or 3ng/ml TGF-β. After 48 hours 1ml 100% methanol was added to each well and incubated at room temperature for 5 minutes until cells were fixed. Cells were washed and incubated in 1% BSA, 10% normal goat serum, 0.3M glycine in 0.1% PBST for 1 hour to permeabilise the cells and block non-specific protein-protein interactions. Cells were then diluted with the Anti-PCNA antibody, diluted 1/1000, at 4°C overnight. Cells were washed with PBS and the secondary antibody (Alexa Fluor 532 goat anti-rabbit IgG, diluted 1 in 1000) was added for 2 hours. This was then removed by two 5-minute washes. The cover slip was then removed and placed onto slides using mountant containing dapi.

The experiment was repeated as described above except each well was treated with 50ul patient or healthy control plasma respectively.

2.7 RNA Extraction, cDNA synthesis and Quantitative Polymerase Chain Reaction (qPCR)

2.7.1 RNA Extraction Materials

- Trizol reagent, Ref 155096-018, Thermo Fisher, Runcorn, UK
- Chloroform, Ref C2432, Sigma-Aldrich, Dorset, UK
- Isopropanol 99.5% pure, Acros organics, Thermo Fisher Scientific, Runcorn, UK
- Molecular grade ethanol, Sigma-Aldrich, Dorset, UK
- Diethylpyrocarbonate (DEPC)-Treated water, nuclease free, Ambion, Thermo Fisher Scientific, Runcorn, UK
- GeneJET RNA cleanup and concentration Micro kit, Ref K0842, Thermo Scientific, Runcorn, UK
- 25cm cell scraper, Sarstedt, Leicester, UK
- Eppendorf centrifuge 5417R, Eppendorf, Stevenage, UK
- Nanodrop 2000 spectrophotometer, Thermo Scientific, Runcorn, UK

2.7.2 RNA Extraction Methods

Cells were cultured and treated as previously described (see section 2.3.2). To extract RNA, cells were washed with 1ml warmed PBS. Once washed, 500ul of Trizol (Thermo-Fisher, Runcorn, UK) was added to each well and incubated at room temperature for 5 minutes. The cells were then scraped and the mixture added to a sterile 1.5ml Eppendorf tube. Chloroform (200ul) was added to each Eppendorf and the mixture shaken vigorously for 15 seconds. The tube was then left to stand for 15 minutes before being placed in the centrifuge and spun at 12,000xg for 15 minutes at a temperature of 4°C. This separated the mixture into three distinct phases. The upper colourless phase, containing the RNA, was removed by careful pipetting to ensure that it was not contaminated from the other layers, and placed into a sterile 1.5ml Eppendorf. To precipitate the RNA, 500ul isopropanol (Acros organics,

Runcorn, UK) was then added and the sample was briefly vortexed before being left to stand for 10 minutes at room temperature. The Eppendorf was placed in the centrifuge and spun at 12,000xg for 10 minutes at 4°C. Residual liquid was removed from the Eppendorf tube leaving a small cell pellet at the bottom of the tube. To wash the RNA pellet, 500ul of 75% ethanol (Signa-Aldrich, Dorset, UK) was added to the pellet and spun at 12,000xg for 5 minutes at 4°C. Again, the residual liquid was removed leaving the RNA pellet at the bottom of the tube. This was left to air dry for 5 minutes and 200ul DEPC-treated water (Thermo-Fisher, Runcorn, UK) was added. An RNA clean-up kit (Thermo-Fisher, Runcorn, UK) was then used, following the instructions provided by the company, to produce a 10ul sample of RNA. The nanodrop (Thermo-Fisher, Runcorn, UK) was used to quantify the amount of RNA as well as to measure the sample purity.

2.7.3 cDNA Synthesis Materials

- High-Capacity cDNA Reverse Transcription Kit, Ref 4368814, Life Technologies, Thermo Fisher, Runcorn, UK
- Biorad T100 Thermal Cycler, Bio-rad Laboratories, Watford, UK
- 0.2ml Flat Cap PCR Tube, Star lab, Milton Keynes, UK

2.7.4 cDNA Synthesis Methods

For each sample, 1ug cDNA was made, using the RNA extracted as described previously. Quantities of RNA necessary for this concentration were calculated from nanodrop values. The above cDNA kit was used as per manufacturer instructions. In brief, 2ul reverse transcription buffer, 0.8ul deoxyribonucleotide triphosphate (dNTP), 2ul random primers, 1ul multiscribe reverse transcriptase and 1ug RNA were added for each sample. The thermocycler was programmed under the following conditions; 10 minutes at 25°C, 2 hours at 37°C, 5 minutes at 85°C and

continuous hold at 4°C. The product, 20ul of cDNA, was diluted 1 in 20 and stored at -20°C prior to use.

2.7.5 Design of Primers

qPCR primers used were as follows. A detailed description of primer testing is given in section 4.1.

Primer	Primer Sequence	Temp	Reference and Product Size
RPLPO (Forward)	3'-CACTGAGATCAGGGACATGTTG-5'	60.3	NM_001002.3 77 bp
RPLPO (Reverse)	3'-CTTCACATGGGGCAATGG-5'	56.0	
Collagen 1a1 (Forward)	3'-GGACACAGAGGTTTCAGTGGT-5'	59.8	NM_000088 185 bp
Collagen 1a1 (Reverse)	3'-GCACCATCATTTCCACGAGC-5'	59.4	
Collagen 3a1 (Forward)	3'-GAAAGATGGCCCAAGGGGTC-5'	61.4	NM_000090 103 bp
Collagen 3a1 (Reverse)	3'-TATACCTGGAAGTCCGGGGG-5'	61.4	
Fibronectin Extra Domain A (Forward)	3'-TCCAAGCGGAGAGAGT-5'	51.7	(144) 360 bp
Fibronectin Extra Domain A (Reverse)	3'-GTGGGTGTGACCTGAG-5'	54.3	
Slug (Forward)	3'-CGCCTCCAAAAAGCCAAAC-5'	56.7	(145) 149 bp
Slug (Reverse)	3'-CGGTAGTCCACACAGTGATG-5'	59.4	

Snail (Forward)	3’-ACCCCAATCGGAAGCCTAACT-5’	59.8	(146) 75 bp
Snail (Reverse)	3’-GGTCGTAGGGCTGCTGGAA-5’	61.0	
E-cadherin (Forward)	3’-TCATGAGTGTCCCCCGGTAT-5’	59.4	(147)
E-cadherin (Reverse)	3’-GTCAGTATCAGCCGCTTCAGAT-5’	60.3	
N-cadherin (Forward)	3’-CCACAG CTCCACCATATGACT-5’	59.8	(145) 133 bp
N-cadherin (Reverse)	3’-CCCCAGTCGTTCAGGTAATC-5’	59.4	
CCN1 (Forward)	3’-GTGACGAGGATAGTATCAAGGACC-5’	62.7	NM_001554.4 198 bp
CCN1 (Reverse)	3’-ATTTCTGGCCTTGTAAAGGGTTG-5’	58.9	
CCN2 (Forward)	3’-GCTTACCGACTGGAAGACACG-5’	61.8	NM_001901.2 233 bp
CCN2 (Reverse)	3’-CGGATGCACTTTTTGCCCTT-5’	57.3	
CCN3 (Forward)	3’-CACGGCGGTAGAGGGAGATA-5’	61.4	NM_002514.3 251 bp
CCN3 (Reverse)	3’-GGGTAAGGCCTCCCAGTGAA-5’	61.4	
CCN4 (Forward)	3’-AAGAGAGCCGCCTCTGCAACTT-5’	62.1	NM_003882.3 105 bp
CCN4 (Reverse)	3’-TCATGGATGCCTCTGGCTGGTA-5’	62.1	
PDGFR-α (Forward)	3’-TGGGAGGGTGGTCTGGATGAG-5’	63.7	(148) 174 bp
PDGFR-α (Reverse)	3’-GATGAAGGTGGAACTGCGGGAAC-5’	64.2	
MRTF-A (Forward)	3’-TCCACCCCCACACTCATTAAG-5’	59.8	NM_020831.4 67 bp
MRTF-A (Reverse)	3’-TCTTGCTGCGCTGTGACTTC-5’	59.4	
Thy-1 (Forward)	3’-CCTGACCCGTGAGACAAAGAAG-5’	62.1	(149) 130 bp

Thy-1 (Reverse)	3'-GCTAGTGAAGGCGGATAAGTAGAG-5'	62.7	

Table 2-5 List of primers used for qPCR. If primers had previously been used a reference is given in column 4. Ideal annealing temperatures are given in column 3, however the annealing temperature used in all experiments was 60°C.

2.7.6 Quantitative PCR (qPCR) Materials

- qPCR strip tubes and caps 0.1ml, Ref 981103, Qiagen, Manchester, UK
- SensiMix SYBR Hi-ROX Kit (SYBR green), Ref QT605-02, Bioline, London, UK
- Rotor Gene 6000 72 well plate qPCR machine, Corbett Life Science, Qiagen, Manchester, UK

2.7.7 qPCR Methods

A master mix containing SYBR green (10ul per sample), forward primer (0.6ul per sample), reverse primer (0.6ul per sample) and water (6.8ul per sample) was made. Diluted cDNA (2ul) was added to each well alongside the master mix (18ul). qPCR was set up and performed using Rotor Gene 6000, 72 well plate quantitative PCR machine.

A single hold step at 95°C for 10 minutes was commenced. This was then followed by 40 cycles of 95°C for 10 seconds, 60°C for 15 seconds and 72°C for 20 seconds. A melt step was added to ensure single product formation.

2.7.8 Statistical Analysis for qPCR

To calculate the fold change of particular genes of interest, the average CT value of the housekeeping gene (RPLPO) was subtracted from the average CT value of the experimental gene of interest giving a delta CT value (ΔCT). The ΔCT of the control cells was then subtracted from the ΔCT value of the TGF-β treated cells giving a delta-delta CT (ΔΔCT) value. Given that calculations were logarithm base 2, the value of 2^(-ΔΔCT) was used to calculate a fold change. Values were transferred to Prism software for calculation of significance using a two-way anova with Bonferroni post-test.

When cells were treated with human plasma a fold change was not calculated so that variation between individual patients could be assessed. Again, ΔCT values were calculated by subtracting the mean CT value of the housekeeping gene (RPLPO) with the mean CT value of the gene of interest for that individual patient or control sample. An average ΔCT value was calculated for the control samples and all values plotted in relation to the mean value of this healthy control group. Again values are in logarithm base 2. Prism software was used to calculate significance using an unpaired two-tailed t-test.

2.8 Agarose Gel

2.8.1 Agarose Gel Materials

- cDNA sample that had undergone qPCR as described above
- 2% agarose gel, prepared as described in Appendix 4
- Safe View Nucleic Acid Stain, NBS Biologicals, Cambridgeshire, UK
- TAE buffer prepared as described in Appendix 4
- 100 base pair ladder, New England Biolabs, Hertfordshire, UK
- Biorad Chemidoc, Biorad laboratories limited, Hertfordshire, UK

2.8.2 Agarose Gel Methods

To test that each primer produced just a single product a 2% agarose gel was made. The above contents were mixed in a sterile bottle and heated in the microwave to ensure the agarose had fully dissolved in the TAE. Safe view nucleic acid stain (2ul) was then added to the solution to allow visualisation of the product. The gel was poured into the appropriate casing and left for 30 minutes until fully set. The comb was removed and the gel immersed into 1% TAE buffer. 20ul of sample was loaded into each well and a reference ladder (New England Biolabs, Hertfordshire, UK) was added to the end well in each case. The sample was ran through the gel at 70-90 vaults until appropriately separated and then imaged using the chemidoc system (Biorad laboratories, Hertfordshire, UK).

2.9 Western Blot

2.9.1 Western Blot Materials

2.9.1.1 Trichloroacetic Acid Protein Precipitation Materials

- Trichloroacetic acid (TCA), Sigma-Aldrich, Dorset, UK
- Urea-lysis buffer, prepared as described in Appendix 4

2.9.1.2 Gel Preparation and Gel Electrophoresis

- Protogel 30% (w/v) acrylamide: 0.8% (w/v) Bis-Acryl-amide stock solution, Geneflow, Staffordshire, UK
- 4X Protogel resolving buffer 1.5M Tris-Hcl, 0.4% SDS, pH8.8, Geneflow, Staffordshire, UK
- Protogel stacking buffer 0.5M Tris-HCl, 4% SDS, pH 6.8, Geneflow, Staffordshire, UK
- Ammonium persulphate (10%)

- Tetramethylethylenediamine (TEMED), Sigma-Aldrich, Runcorn, UK
- Ultrapure 10X Tris/Glycine/SDS running buffer, diluted to 1X, Geneflow, Staffordshire, UK
- Protein loading buffer blue (2x), National Diagnostics, Nottingham, UK
- Precision Plus Protein Dual Color standards ladder, BioRad, Hertfordshire, UK

2.9.1.3 Transfer

- Transfer Buffer prepared as described in Appendix 4
- Whatman chromatography paper, Sigma-Aldrich, Dorset, UK
- Amersham Protran premium 0.45um nitrocellulose blotting membrane, GE Healthcare Life Sciences, Buckinghamshire, UK

2.9.1.4 Blocking and Antibody Incubation

- Tris Buffered Saline (TBS) prepared as described in Appendix 4
- Tris Buffered Saline with Tween (TBST) prepared as described in Appendix 4
- Ponceau S, Sigma-Aldrich, Dorset, UK
- Marvel skimmed milk powder, Premier Foods, St Albans, UK

Primary Antibodies Used for Western Blot				
Company	**Protein**	**Product Code**	**Antibody Type**	**Dilution**
Abcam	Collagen 1	ab34710	Rabbit polyclonal	1 in 1000
Sigma-Aldrich	Fibronectin	F3648	Rabbit polyclonal	1 in 1000

Table 2-6 Primary Antibodies used in Western Blot with company, product code and dilution specified.

Secondary Antibodies Used for Western Blot			
Company	**Antibody**	**Product Code**	**Dilution**
Dako	Swine anti-rabbit	P0217	1 in 5000

Table 2-7 Secondary Antibodies used in Western Blot with company, product code and dilution specified.

2.9.1.5 Imaging

- Super Signal West Dura Extended Duration Substrate, Thermo Scientific, Rockford, USA

2.9.1.6 Equipment

- Eppendorf centrifuge 5417R, Eppendorf, Stevenage, UK
- Geneflow electrophoresis gel tank, Geneflow Limited, Staffordshire, UK
- BioRad criterion blotter for transfer, BioRad, Hertfordshire, UK
- Biorad Chemidoc, Biorad laboratories limited, Hertfordshire, UK

2.9.1.7 Sample

- Protein samples prepared by mixing 5ul protein sample, 5ul distilled water and 10ul of 2 x loading buffer.

2.9.2 Western Blot Methods

2.9.2.1 Trichloroacetic Acid Protein Precipitation

Conditioned medium (400ul) from each well was treated with 5% TCA (Sigma-Aldrich, Dorset, UK), vortexed and placed at 4°C overnight. Eppendorfs were then centrifuged for 30 minutes at 13,000 rpm at 4°C. Supernatant was removed. Samples were centrifuged for a further 10 minutes at 13,000 rpm at 4°C to remove residual TCA. Protein pellets were then re-suspended in urea-lysis buffer (20ul). Samples were stored at -80°C until required for western blot.

2.9.2.2 Western Blot Gel Preparation and Gel Electrophoresis

An 8% acrylamide resolving gel was prepared using 2.7ml 30% acrylamide, 2.5ml resolving buffer, 4.72ml distilled water, 200ul 10% ammonium persulphate (APS) and 20ul TEMED. The lower resolving gel was allowed to set for roughly 30 minutes at room temperature. A small amount of ethanol was added along the top of each gel to remove any bubbles. This was poured away prior to adding the stacking gel.

A 4% stacking gel was prepared using 1.3ml 30% acrylamide, 2.5ml stacking buffer, 6.1ml distilled water, 100ul ammonium persulphate and 25ul TEMED. Combs were added for the formation of wells and the gel was allowed to set prior to use.

Gels were immersed in 1 x running buffer. Samples (prepared as described above) were added to each well. A ladder (5ul) was added to the end well of each sample for reference. Samples were ran through the gel at 80V for 30 minutes, and this speed was increased to 100V until the proteins were separated.

2.9.2.3 Western Blot Transfer

Proteins were transferred onto nitrocellulose membranes using the wet transfer method. Items were soaked in transfer buffer before being stacked into a cassette in the order below. The criterion blotter tank was filled with transfer buffer, the cassette was inserted and a charge ran at 250mA for 2 hours to transfer the protein to the nitrocellulose membrane.

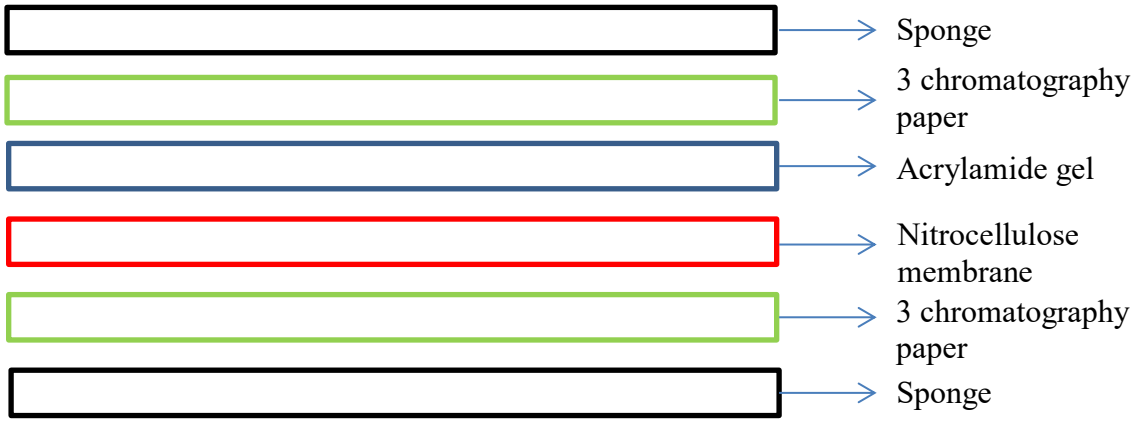

Figure 2-3 Diagram of the gel and membrane sandwich showing the order in which materials were stacked to facilitate the transfer.

2.9.2.4 Western Blot Blocking and Antibody Incubation

A Ponceau S stain (Sigma-Aldrich, Dorset, UK) was used to stain each blot and an image recorded for normalisation of the sample. The stain was removed after rinsing with TBST.

A 3% milk solution (40ml) was then used as a blocking agent for 1 hour. The membrane was washed 3 times for 10 minutes each using TBST. The primary antibody was added and incubated at 4°C on a rocker overnight. The primary antibody was removed by washing the membrane 3 times for 10 minutes each at room temperature. The secondary antibody was added for 2 hours and incubated at room temperature. This was then removed by further washing of the membrane with TBST.

2.9.2.5 Western Blot Imaging and Analysis

The gel was imaged by washing the membrane with horse radish peroxidase (HRP) solution. The Biorad Chemidoc was used to image the membrane. Analysis was performed using Image J software to measure densitometry of the protein bands. Loading was normalised against ponceau staining.

3 Immunoprecipitation to Assess for Covert CTD-ILD in Patients Diagnosed with IPF

In this chapter the proportion of patients diagnosed with IPF that actually have an underlying CTD disclosed by serology was assessed. Comprehensive serology was undertaken by immunoprecipitation, seen as the "gold-standard technique" for antibody interrogation and discovery, and is discussed in more detail in the materials and methods section. Whether patients are assigned an "idiopathic" label but actually have an underlying CTD has been analysed in previous studies. However, these were not performed in a UK population and patients had the diagnosis "Idiopathic Interstitial Pneumonia (IIP)" which includes any HRCT pattern consistent with "idiopathic" disease whereas this chapter specifically assesses patients assigned an IPF diagnosis. The importance of distinguishing between IPF and other idiopathic diagnoses is now vital due to new treatment options and drug discovery in IPF. Patients with a cellular NSIP or an organising pneumonia pattern are treated with steroids and therefore have treatment that would be given for an underlying CTD. However, with an IPF diagnosis steroid treatment has been shown to shorten life expectancy and patients should instead be treated with newer, anti-fibrotic medications such as pirfenidone and nintedanib (15). It is, therefore, vital that the issue of diagnostic error in IPF in UK hospitals is assessed and quantified.

As previously mentioned there have been other studies to assess the role of serology in diagnosing patients with ILD. A study published by Song et al retrospectively analysed patients diagnosed with IIP in a Korean hospital, who had undergone line-blot immunoassay able to detect 11 myositis autoantibodies. The authors found that 38% of patients had a recognised MSA or MAA present (70). Unfortunately, the authors did not discuss HRCT patterns of these patients, nor if their serology results led to a change in clinical management. Similarly, when serology was assessed in a Japanese population, 6.6% of patients had evidence of an antisynthetase antibody. It should be noted that, although none of the latter patients had evidence of a UIP pattern on HRCT, 2 patients who underwent a lung biopsy had a UIP pattern histologically, allowing for the possibility of a diagnosis of IPF (69). The authors used the immunoprecipitation procedure but were only detecting six antisynthetase

antibodies and were not assessing for the rarer synthetases or other CTD antibodies, making this study less comprehensive for detecting antibodies.

Another Japanese study followed 168 patients with a diagnosis of IIP. Using an enzyme-linked immunosorbent assay (ELISA) system, 10.7% of patients were positive for antisynthetase antibodies. These authors did collect data regarding the HRCT pattern of each group, and 5.6% of patients assigned an IPF diagnosis had an antisynthetase and 12.1% of patients with an HRCT pattern other than UIP had an antisynthetase antibody present (150). To our knowledge no study has analysed patients with a diagnosis of IPF made in a UK centre and undertaken immunoprecipitation to assess for the presence of a CTD-associated antibody. It is vital to ascertain the degree of diagnostic error to assess whether patients assigned an IPF diagnosis are being treated appropriately in the UK.

3.1 Case Recruitment and Accrual

As mentioned in the previous chapter, patients with ILD were recruited into the UK-BILD study. This is a multi-centre collaboration involving 38 UK sites. Figure 3-1 gives a breakdown of patients recruited into the study by ILD sub-group. It should be noted that recruitment of IPF patients was suspended as it was ascertained that enough participants had been recruited for any future genetic research within 1 year of opening. According to the histogram showing accrual, it would appear that sarcoid is almost as prevalent as IPF, but this is misleading as IPF cases had reached this number within 1 year of recruitment and then further case recruitment was suspended, allowing other subgroups to appear more prevalent in relation.

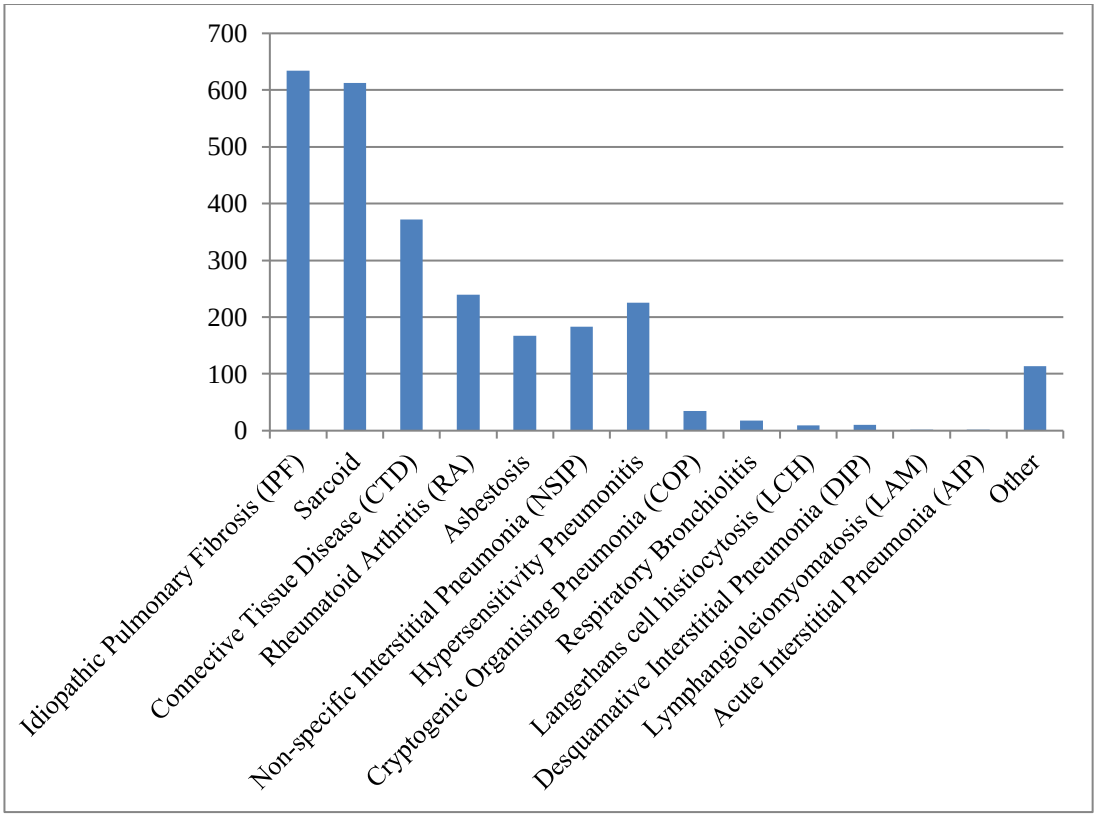

Figure 3-1 Recruitment of patients into the UK-BILD study separated into ILD subgroups. There have been 2624 patients recruited into the study, with IPF the most prevalent form of ILD.

As can be seen in Figure 3-1 even with 38 centres recruiting there are still very few cases collected into some of the rarer forms of ILD, such as Acute Interstitial Pneumonia (AIP). It is therefore essential that multi-centre collaboration continues to allow for investigation into some of these rarer subgroups.

3.2 Autoantibody Results

Autoantibody testing by immunoprecipitation was performed by Dr Zoe Betteridge a postdoctoral scientist located at the University of Bath. The procedure was undertaken on 249 patients diagnosed with IPF and recruited into UK-BILD. Immunoprecipitation was performed using the materials and methods as described in section 2.2.

The procedure produces a gel, which is analysed by autoradiography and this gives bands at certain molecular weights which may correlate with a recognised autoantibody. An example is given in the materials and methods section and a further example is given below;

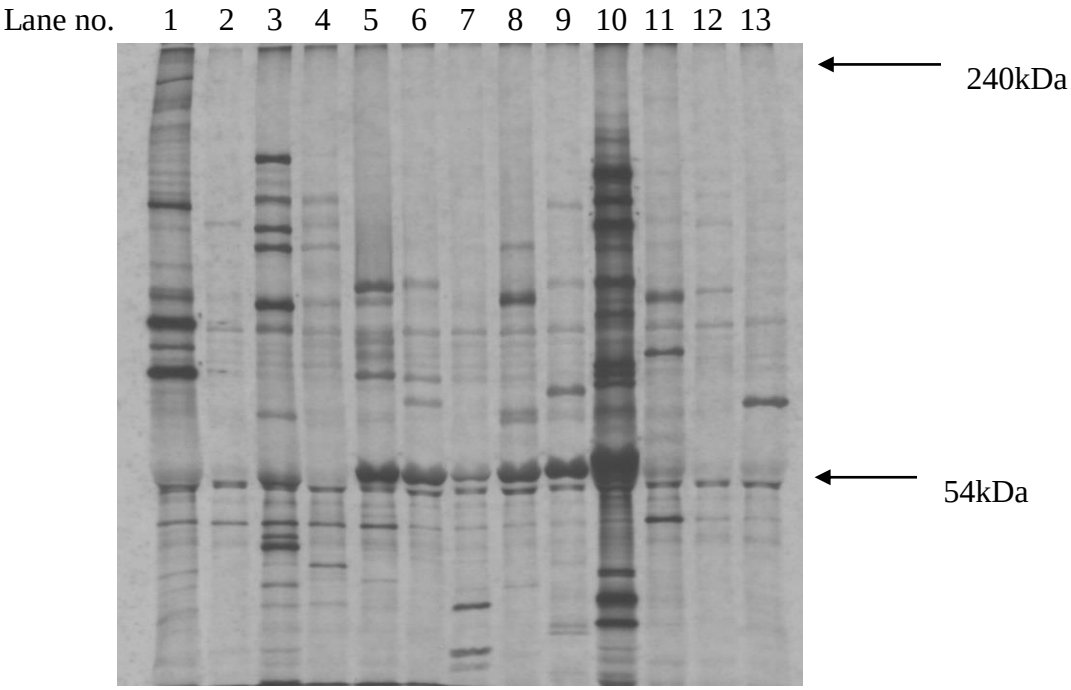

Figure 3-2 Further example of an immunoprecipitation gel kindly provided by Dr Zoe Betteridge. The above example shows positive controls in lane 1 (anti-Ku and anti-Mi-2), lane 2 (anti-MDA5), lane 3 (anti-SAE and anti-RNAPI / III), lane 4 (anti-U3 and anti-TIF1), lane 5 (anti-SRP and anti-topoisomerase), lane 10 (anti-OJ) and lane 11 (anti-EJ). The other lanes show various patients from the UK-BILD study. Lane 6 shows an unknown strong band at 54 kDa, it shows weak bands at 68, 70 and 105 kDa. Lane 7 shows strong bands present at 28, 31 and 54 kDa, it shows weak bands at 30 and 120 kDa. Lane 8 shows strong bands present at 54, 65 and 90 kDa and weaker bands at 64, 120 and 200 kDa. Lane 9 shows strong bands present at 54 kDa. Weaker bands were present at 30, 31, 66, 68, 105 and 150 kDa. Thereby lanes 6-9 all had the same strong, unknown band present at 54kDa, discussed in more detail below. Lane 12 shows a strong band at 95 kDa and weaker bands at 130, 150 and 170 kDa. Lane 13 shows a strong unknown band at 65 kDa and a weaker band present at 140 kDa.

Patients were therefore divided into those with no strong bands present on immunoprecipitation, those with strong bands present but not corresponding to a recognised CTD-associated autoantibody, those that had a recognised MSA / MAA present and patients who had a strong band present at 54 kDa. The results are shown in the table below;

Immunoprecipitation Result	**Number of patients**
No strong bands present on immunoprecipitation	146 (58.6%)
Strong bands present on immunoprecipitation but not corresponding with a recognised CTD-associated antibody	91 (36.5%)
MSA / MAA positive result	4 (1.6%)
54 kDa band present	7 (2.8%)

Table 3-1 Results of Immunoprecipitation. Table showing patients assigned a diagnosis of IPF and whether a recognised antibody was shown in their sera. One patient was excluded from analysis due to reasons described below.

Of the 249 patients tested, 4 (1.6%) had a recognised MSA or MAA present in their sera. One patient had an anti-mitochondrial antibody present which was associated with confirmed primary biliary cirrhosis, but the antibody is not associated with ILD, so this patient was taken out of the analysis. The other antibodies present included anti-OJ, anti-PM-Scl, anti-ku and anti-RNA Pol II, with one patient in each group respectively. There were also 7 (2.8%) patients who had an unknown but very strong identical band present at 54 kDa, represented separately in row 4 of Table 3-1. It is difficult to undertake subgroup comparisons given the small numbers of patients who had evidence of a recognised MSA / MAA or a new band found at 54kDa. Any p values would not be meaningful given that the group sizes are so uneven and that there were so few patients with an antibody present.

A further 91 IPF patients (36.5%) had strong unknown bands on immunoprecipitation, but which did not correspond to any known CTD autoantigen. These were analysed separately to the 146 (58.6%) patients diagnosed with IPF who did not have strong bands present when examined by immunoprecipitation. The data is not published, but from the experience of the National Immunoprecipitation Laboratory at the University of Bath only ~ 20% of healthy control patients have bands present on immunoprecipitation but these are generally weak and non-specific. They estimate that less than 10% of these healthy subjects would be expected to have strong bands present. This suggests that there is a larger prevalence of strong bands in patients with IPF, suggestive of a currently unelucidated immunological component to the disease. The group has therefore been separated to assess if there are any distinguishing characteristics in these patients.

3.3 Patient Demographics

Demographic data was collected on the UK-BILD proforma and included information regarding age, gender and ethnicity. Initially the demographic data of the patients was compared to assess if there was a significant difference between age or gender of the four groups. All UK-BILD patients in the study were Caucasian to allow for any future genetic testing to occur once it could be assured that all patients were antibody negative. It can be seen from Table 3-2 that predominantly more males are affected at 70 years old. This did not differ between those who were antibody negative with no strong bands on immunoprecipitation, those with strong bands present, those who had an underlying MSA / MAA or those with the 54kDa band. This is similar to demographic data previously published that also suggest that IPF is more prevalent in older, male patients (11). These subtle clues are important for clinicians to rule out an underlying CTD, for example a younger patient would be less likely to have IPF and many CTDs (e.g. SSc) have a higher prevalence in female patients.

Demographic information	No strong bands (n=146)	Unknown strong bands (n=91)	MSA / MAA positive result (n=4)	54 kDa Band (n=7)
Gender	Male 117 (80.1%) Female 29 (19.9%)	Male 64 (70.3%) Female 27 (29.7%)	Male 3 (75%) Female 1 (25%)	Male 5 (71.4%) Female 2 (28.6%)
Age	Median age: 74 years Age range: 50-94 years	Median age: 72 years Age range: 50-89 years	Median age: 70 years Age range: 58-76 years	Median age: 71 years Age range: 63-83 years
Ethnicity	Caucasian 146 (100%)	Caucasian 91 (100%)	Caucasian 4 (100%)	Caucasian 7 (100%)

Table 3-2 Patient demographic data showing proportion of males, age when recruited to the study and ethnicity.

3.4 Smoking Data

Data was collected within the UK-BILD study regarding smoking history. It was recorded whether patients were past, current or never smokers and the pack year history was recorded to give an idea of heavy smoking.

Smoking history	Pack Year History	No strong bands (n=146)	Unknown strong bands (n=91)	MSA / MAA positive result (n=4)	54kDa Band (n=7)
Current smoker		**1 (0.7%)**	**3 (3.3%)**	**0 (0%)**	**2 (28.6%)**
	<20 pack years	1 (0.7%)	2 (2.2%)	0 (0%)	0 (0%)
	>20 but <40 pack years	0 (0%)	0 (0%)	0 (0%)	1 (14.3%)
	>40 pack years	0 (0%)	1 (1.1%)	0 (0%)	1 (14.3%)
Ex-smoker		**110 (75.3%)**	**63 (69.2%)**	**3 (75%)**	**3 (42.9%)**
	<20 pack years	48 (32.9%)	30 (33%)	2 (50%)	3 (42.9%)
	>20 but <40 pack years	40 (27.4%)	24 (26.4%)	1 (25%)	0 (0%)
	>40 pack years	21 (14.4%)	9 (9.9%)	0 (0%)	0 (0%)
	Unknown	1 (0.7%)	0 (0%)	0 (0%)	0 (0%)
Never smoker		**36 (24.7%)**	**25 (27.5%)**	**1 (25%)**	**2 (28.6%)**

Table 3-3 Patient demographic data showing differences in smoking history between patients with IPF who had no strong bands, the presence of unknown strong bands on immunoprecipitation, those with an MSA / MAA present and those with an unknown band at 54kDa.

Interestingly, the majority of patients with IPF were previous smokers. However, there was a significant proportion of patients who have never smoked. There did not appear to be any appreciable difference in smoking history between the three groups of patients although it is difficult to draw firm conclusions based on the limited number of patients in the MSA / MAA positive or 54kDa groups.

3.5 IPF Diagnostic Subgroup

Patients were divided by IPF diagnostic subgroup, separated according to HRCT appearances and the availability of lung histology as discussed in the introduction (section 1.3.3). The proportion of patients from each category is shown in the table below.

IPF Subgroup	No strong bands (n=146)	Unknown strong bands (n=91)	MSA / MAA positive result (n=4)	54 kDa band (n=7)
Definite UIP	90 (61.6%)	67 (73.6%)	3 (75%)	4 (57.1%)
Definite Fibrotic NSIP	17 (11.6%)	7 (7.7%)	1 (25%)	0 (0%)
Probable Fibrotic NSIP	39 (26.7%)	17 (18.7%)	0 (0%)	3 (42.9%)

Table 3-4 Patients separated according to IPF diagnostic subgroup.

It is possible that more patients who are found to have an underlying CTD would be in the probable category. These patients have less obvious changes on HRCT with a fibrotic NSIP pattern distinguished by a lack of honeycombing, and cannot undergo lung biopsy due to underlying co-morbidities. However, more antibody positive patients had a definite UIP pattern on HRCT and were not from the less robust diagnostic categories. It is already known that patients can have a UIP pattern with CTD-ILD, and this can lead to diagnostic error. However, it should be considered that these are very small numbers of patients and overall the diagnosis of IPF is very definite.

3.6 Specificity of CTD Features

Clinicians were asked to record information regarding the presence of symptoms of an underlying CTD in all patients recruited to the UK-BILD study.

CTD Feature	No strong bands (n=146)	Strong bands (n=91)	MSA / MAA positive result (n=4)	54 kDa band (n=7)
Raynaud's phenomenon	4 (2.7%)	0 (0%)	0 (0%)	0 (0%)
Arthritis	3 (2.1%)	1 (1.1%)	0 (0%)	0 (0%)
Sclerodactyly	0 (0%)	0 (0%)	0 (0%)	0 (0%)
Calcinosis	0 (0%)	0 (0%)	0 (0%)	0 (0%)
Raised CK	1 (0.7%)	0 (0%)	0 (0%)	0 (0%)
Mechanics hands	0 (0%)	0 (0%)	0 (0%)	0 (0%)
Myalgias	0 (0%)	0 (0%)	0 (0%)	0 (0%)
Periungal erythema	11 (7.5%)	9 (9.9%)	0 (0%)	1 (14.3%)
Telangiectasia	1 (0.7%)	0 (0%)	0 (0%)	0 (0%)

Table 3-5 Prevalence of CTD features in patients assigned a diagnosis of IPF before immunoprecipitation had been undertaken. Groups are divided into those without strong bands on immunoprecipitation, those with strong bands present although of no known antibody, those with recognised MSA / MAA present and those with an unknown band present at 54kDa.

As would be expected, patients assigned a diagnosis of IPF had very few CTD features present. Interestingly, those patients with an MSA or MAA present also did not have any CTD features, including any subtle abnormalities such as mechanic's hands or symptoms common in the general population such as myalgia. Features such as periungal erythema (7.5%), Raynaud's phenomenon (2.7%) and arthritis (2.1%) were present in the group that were completely negative on immunoprecipitation, presumably meaning they were not specific for an underlying CTD. It should be noted that one limitation of assessing for these features is that

recruitment was conducted at individual centres and clinicians may have various expertise in assessing for subtle signs.

3.7 Specificity of Respiratory Features

In a similar manner, clinicians were asked to record the presence of respiratory features in patients recruited to the study. These respiratory features are shown in Table 3-6 below.

Respiratory Feature	**No strong bands (n=146)**	**Strong bands (n=91)**	**MSA / MAA positive result (n=4)**	**54 kDa band (n=7)**
Clubbing	47 (32.2%)	30 (33%)	3 (75%)	2 (28.6%)
Pulmonary Arterial Hypertension (PAH)	5 (3.4%)	1 (1.1%)	0	0
- Echo Criteria	5 (3.4%)	0	0	0
- Right heart catheter criteria	0	1 (1.1%)	0	0

Table 3-6 Prevalence of respiratory features in patients with a diagnosis of IPF. Groups divided into those who lack strong bands on immunoprecipitation, those with strong bands present although no known antibody, those with recognised MSA / MAA present and those with an unknown band present at 54kDa.

Clubbing is present in a significant number of patients with IPF but this was also present in patients with an MSA or MAA present, suggesting the presence of clubbing did not accurately exclude an underlying CTD. A small number of patients who were antibody negative had PAH. In IPF, PAH is usually associated with very severe, end-stage disease (151). PAH was not present in patients with an underlying MSA / MAA or with the 54kDa band present, however, such small numbers of patients were examined in these groups that it is under powered to assess the significance.

3.8 Association with Malignancy

Participating centres were required to document whether patients had a current or previous history of malignancy. The results are shown in the table below and have been divided into skin, haematological and solid organ tumours.

Type of Malignancy	No strong bands (n=146)	Strong bands (n=91)	MSA / MAA positive result (n=4)	54 kDa band (n=7)
Skin	4 (2.7%) Basal Cell Carcinoma (2) Squamous Cell Carcinoma (2)	2 (2.2%) Basal Cell Carcinoma (1) Squamous Cell Carcinoma (1)	0	0
Haematological	2 (1.4%) Chronic Lymphocytic Leukaemia (1) Leukaemia (unspecified) / Non-Hodgkin's Lymphoma (1)	1 (1.1%) Non-Hodgkin's Lymphoma (1)	0	0
Solid Organ	10 (6.8%) Prostate (2) Breast + Renal (1) Breast (1) Bladder (2) Colon (3) Laryngeal (1)	2 (2.2%) Colon (1) Tongue (1)	0	0

Table 3-7 Prevalence of skin, haematological and solid organ malignancies in patients with a diagnosis of IPF. Groups divided into those who lack strong bands on immunoprecipitation, those with strong bands present although no known antibody, those with recognised MSA / MAA present and those with an unknown band present at 54kDa.

The prevalence of malignancy in this cohort was 8.4%, however the average age of the patients was 73 years old and many of those were previous smokers. A range of malignancies was noted with no noticeable pattern emerging.

Time since malignancy diagnosed (years)	**No strong bands (n=146) Malignancy Diagnosis (n=16 – 2 patients with multiple malignancies)**	**Strong bands (n=91) Malignancy Diagnosis (n=5)**	**MSA / MAA positive result (n=4) Malignancy Diagnosis (n=0)**	**Unknown bands at 54 kDa (n=7) Malignancy Diagnosis (n=0)**
Less than 1 year	0	0	0	0
1-5 years	4	2	0	0
6-10 years	4	2	0	0
More than 10 years	9	1	0	0
Unknown	1	0	0	0

Table 3-8 Number of years since a malignancy diagnosis depending on IPF subgroup. For patients with multiple diagnoses of malignancy each has been counted separately, hence the numbers do not tally to the total number of patients as one patient had both breast and renal cancer and another had an unspecified diagnosis of leukaemia followed by a separate diagnosis of Non-Hodgkin's Lymphoma.

As noted in Table 3-8 above many of the malignancy diagnoses are historic and this would be expected in an older population. The group did not appear to be linked to any recent diagnoses of malignancy, with no patients being diagnosed in the preceding year. It should be noted that this was a cross-sectional study and therefore it did not follow patients to assess if they develop a subsequent malignancy.

3.9 MSA / MAA Positive Group

As such a small number of MSA and MAA were found it is easier to discuss the implications of each antibody in turn.

Anti-OJ is an MSA and one of the 8 recognised antisynthetase antibodies, directed against anti-isoleucyl-tRNA synthetase. Anti-OJ positive patients may present with a negative Antinuclear Antibody (ANA) as the synthetase antigen is cytoplasmic rather than nuclear. It is one of the rarer antisynthetase antibodies, found in less than 5% of patients with IIM and an MSA present. However, it can be found in patients who present with ILD alone and so the frequency may be higher than predicted (39, 40). As it is such a rare antibody most of the available data is based on retrospective observations of small patient cohorts. One study found that 63% of patients with the antibody presented with ILD alone, with just 13% and 25% of patients having a classical DM rash or PM signs respectively (40). During the follow up period, 100% of patients developed ILD. Another study of 7 patients with the antibody similarly showed that 100% of the patients had ILD whereas just 4 patients developed muscle weakness, suggesting it is more strongly associated with ILD than with myositis (39). The estimated 5-year survival of patients with anti-OJ antibodies is estimated at 60% in a study where pulmonary fibrosis accounted for 50% of all deaths in patients with ASS (152).

Anti-PMScl was present in the serum of 1 patient. This antibody occurs in myositis-scleroderma overlap disease and is a recognised MAA. Hep-2 screening on patients with this antibody usually shows a homogeneous nucleolar staining pattern (153). In a meta-analysis that included 116 patients with anti-PMScl antibodies, 76% of patients had evidence of sclerodactyly and 74% had Raynaud's phenomenon showing its clear association as an overlap antibody. It also has a strong association with ILD, with 38% of patients having documented evidence of ILD (45).

The presence of another MAA was discovered in 1 patient, which was the anti-ku antibody. This is found in a variety of CTD diagnoses including SSc, SLE, RA and UCTD (154). Hep-2 screening on patients with anti-ku shows dense, fine speckled staining of the nucleus, with nucleoli staining possible (153). The presence of the antibody is specific for an autoimmune disease. One study retrospectively examined

30 patients with the antibody. It was strongly associated with arthralgia which was reported in almost 80% of patients and Raynaud's phenomenon in just over half of the patients. Nearly 40% of patients had myositis and the same proportion had evidence of ILD on HRCT scan. Of these, 3 patients had a UIP pattern present suggesting that the diagnosis could be mistaken for IPF (155).

The final antibody detected by immunoprecipitation was anti-RNAP II. There are 3 antibodies directed against the RNA polymerases, labelled RNAP I, II and III respectively. The anti-RNAP antibodies are found in around 20% of patients with SSc (61, 156). Anti-RNAP I and III frequently occur together, are found in patients with SSc and those with the antibody have a higher frequency of SSc renal crisis. Anti-RNAP II antibodies may be found in SSc as well as occurring in SLE and UCTD. They are often found alongside other autoantibodies including Anti-RNAP I and III and anti-topoisomerase (157). As anti-RNAP autoantibodies are not frequently found in isolation, it is difficult to assess their association with ILD. However, when associated with anti-topoisomerase antibody 55-75% of patients developed ILD and 50% of patients developed ILD when it was associated with Anti-RNAP I and III (156).

3.10 Discussion

This chapter highlights the fact that chest physicians are very good at distinguishing IPF from other ILD subsets. It should be noted that immunoprecipitation may rule out a number of CTDs, but does not exclude other mimicking conditions such as asbestosis. However, the working hypothesis for this component of the PhD was that chest physicians were potentially missing subtle features of an underlying CTD. This, however, does not appear to be the case.

There are only a very small number of patients who had CTD-associated antibodies detected in their sera, and thus suggestive of an underlying CTD. It is vital that IPF and CTD-ILD groups are accurately distinguished as there are treatment differences between IPF patients and CTD patients. Patients with an underlying CTD respond well to immunosuppression while such treatment increases mortality in those with IPF. This study therefore provides reassurance that the majority of patients assigned

an IPF diagnosis by use of guidelines and HRCT are indeed commencing the correct treatment.

Of the IPF patients uncovered as having an underlying CTD, all 4 were diagnosed in secondary care rather than in tertiary ILD centres. Although the numbers were very small, and this should be kept in mind, it does support previous work that IPF diagnoses should be made in a specialist setting with a specialised MDT (158).

Although the number of patients with an underlying autoantibody associated with ILD in this cohort is low, it is of interest to discuss whether patients with different scan appearances may actually have a higher prevalence of undisclosed CTDs. For example, in a diagnosis such as COP or cellular NSIP would a higher proportion of patients have an underlying CTD, as disclosed by serotyping using immunoprecipitation? The HRCT appearances of COP and cellular NSIP are much more common in myositis and SSc and it is therefore possible that there are more covert CTD cases in this group of patients.

This work has also shown the importance of Hep-2 ANA testing. Many of the autoantibodies recognised in this cohort show particular patterns by Hep-2 screening and therefore this specialised test may be helpful to clinicians who do not have access to immunoprecipitation which can be costly and labour intensive.

The work undertaken here has shown that IPF is a distinct disease and gives a group of patients, that have actively had the presence of an underlying CTD excluded, to do further studies. It has given confidence that respiratory physicians are good at clinically distinguishing between IPF and other causes of ILD.

4 Developing an *in vitro* Model of Fibrosis to Investigate Underlying Pathogenesis

In this chapter the development of an *in vitro* model of fibrosis, to investigate the underlying pathological mechanisms relating to the fibrotic process is presented. This model was used to assess for biomarkers of disease. Two cell types, implicated in the development of pulmonary fibrosis, were cultured and treated with TGF-β, a pro-inflammatory cytokine that is known to induce fibrosis. This preparatory work was undertaken to recreate the basic *in vitro* response of different cell types driven by TGF-β, and to develop methods by which to measure changes in cellular pathways and inflammatory cytokines in an accurate and reproducible way. Perfecting this model will allow investigation into the mechanisms driving fibrosis in two cell types, the MRC5 fibroblasts and the A549 epithelial cells.

Fibroblasts and epithelial cells were chosen for this work as they are two cell types implicated in processes of fibrosis, which are discussed in more detail in the initial introduction. The MRC5 cell line are normal human lung fibroblasts developed from the lung tissue of a human foetus in 1966, the cells are therefore of a normal phenotype (159). MRC5 fibroblasts are therefore an established cell line, which has been used in a variety of studies. These cells are present in the normal pulmonary interstitium and it was previously thought that an external trigger activates the fibroblast leading to its transformation into a myofibroblast, cells that are more contractile than fibroblasts with an increase in the presence of α-SMA. Myofibroblasts produce and secrete excess ECM proteins including collagen and FN-EDA. However, the hypothesis that myofibroblasts are activated fibroblasts which are solely responsible for excessive ECM production is no longer accepted and it has been suggested that myofibroblasts are derived from a variety of cell types. Hence work has also been undertaken on epithelial cells.

The A549 alveolar epithelial cell line was derived from an adenocarcinoma of the lung in 1972 (160). They are type II alveolar epithelial cells, and they are also an established cell line that has been used in multiple studies. It has been noted that, despite being from a cancerous cell lineage, these cells retain the phenotype and metabolic properties of type II alveolar epithelial cells (108). Unfortunately, there

are obvious drawbacks to using a cancerous cell line as cells will not be truly "normal" in phenotype. There is evidence to suggest that EMT occurs in fibrosis, described in detail in the initial introduction, and this causes transition of epithelial cells into a myofibroblast. This process likely contributes to a small percentage of the myofibroblast pool.

The aim of this chapter is to assess what effects a pro-inflammatory cytokine will have when used at different concentrations to treat these two different cell types. The chapter will investigate whether these effects are measurable using a variety of techniques, including qPCR, immunocytochemistry and western blot, to assess changes in fibrosis associated genes and proteins. It will also assess the reproducibility of the TGF-β driven changes.

4.1 Validation of qPCR Primer Sets

To create accurate primers for qPCR a literature search was undertaken to assess if primers had been used previously for investigating the gene of interest. If such work had been undertaken, the sequence was transferred to the National Centre for Biotechnology Information (NCBI) primer-BLAST page to assess primer specificity (161). If the primer pair was designed the same website was used to ensure specific targets. The ideal primer should give an amplified region between 60-150 base pairs (bp) and should be separated by an exon-exon boundary to reduce the risk of amplification from genomic DNA contamination. The produced primer pair was then tested by using a four-fold serial dilution to produce a standard curve to assess for the assay efficiency. Efficiency was calculated from the slope of the standard curve, with a value of -3.32 indicating 100% efficiency. A melt curve was checked to ensure that a single product was formed (Figure 4-1). As a final check, the PCR product was run on a gel to ensure that only a single product had been produced (Figure 4-2).

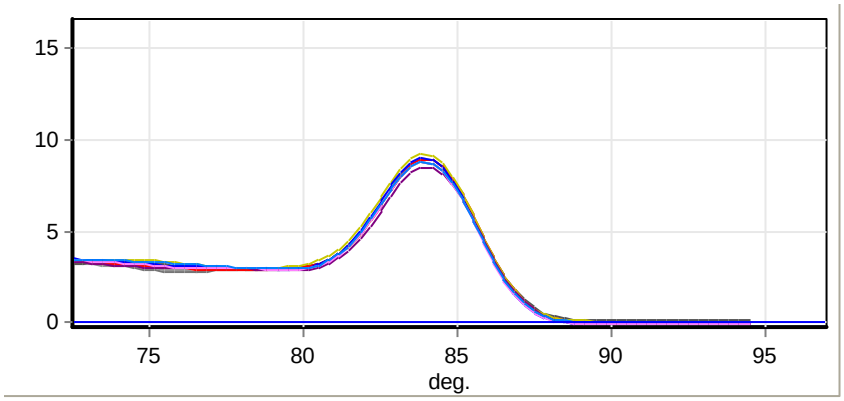

Figure 4-1 Melt curve to show only a single product had been formed. At the end of the qPCR cycles, SYBR green fluoresces as it is incorporated into the double-stranded DNA product. The reaction mixture is then heated in increments, until this strand denatures into single-stranded DNA, releasing the SYBR green and reducing the measured fluorescence. If only a single product has been formed, a single peak should be produced, occurring at the same temperature for all samples. The melt curve for *RPLPO* is given as a representative example above, and shows a single peak occurring at 83°C.

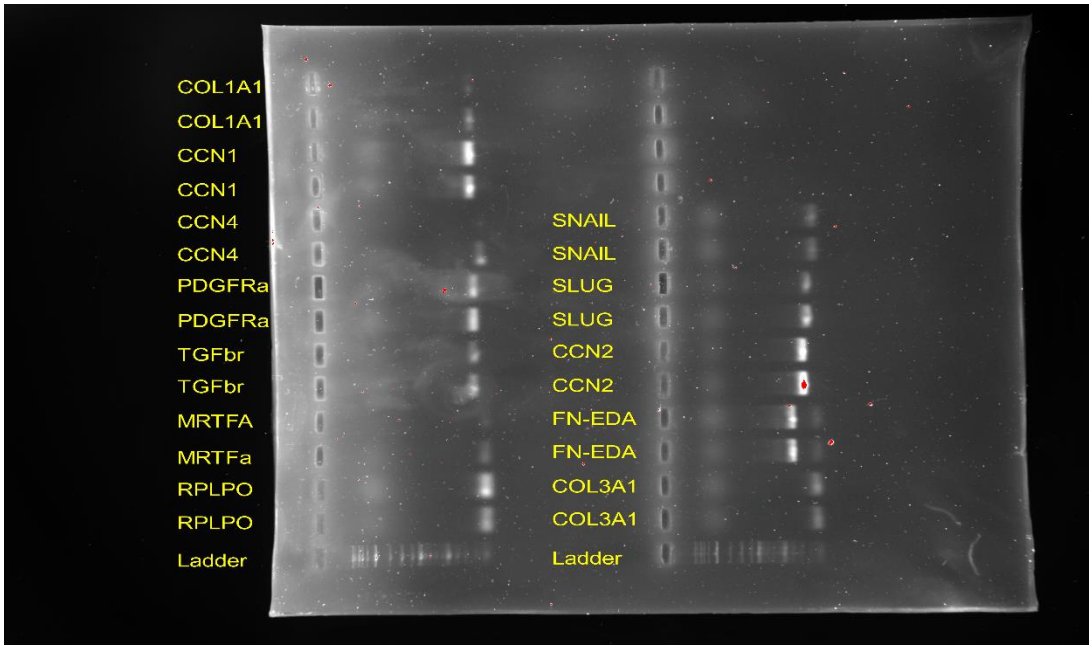

Figure 4-2 Agarose gel showing single product formation for qPCR products. Products for the housekeeping gene *RPLPO*, *MRTFa*, *TGF-β receptor* (not used), *PDGFR-α*, *CCN4*, *CCN1*, *COL1A1*, *COL3A1*, *Fibronectin-EDA*, *CCN2*, *slug* and *snail* are represented in the above figure.

4.2 The Effect of TGF-β Treatment on Fibroblast (MRC5) Cells

Preliminary work was undertaken to assess if treating MRC5 fibroblasts with increasing concentrations of the pro-inflammatory cytokine TGF-β would cause a change in the morphology of the cells. This was initially assessed visually, with a representative example of changes observed after 48 hours given in Figure 4-3.

4.2.1 The Effect of TGF-β Treatment on the Morphology of MRC5 Fibroblasts

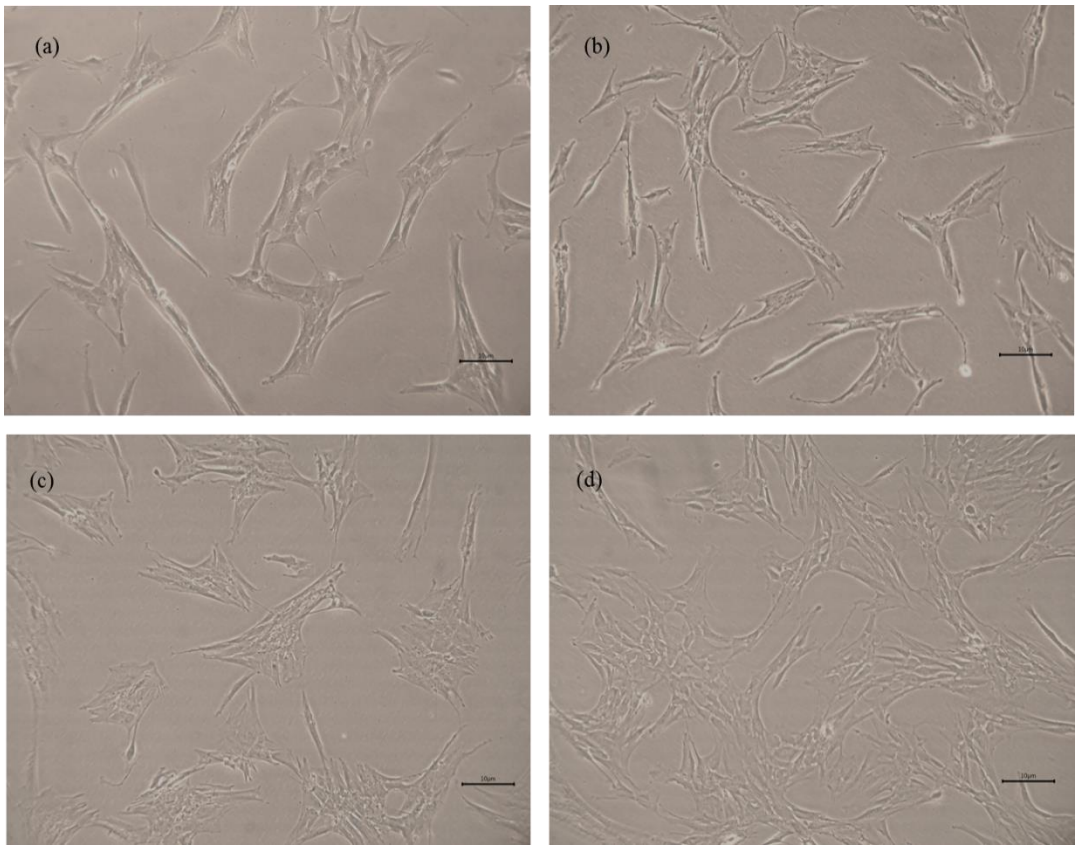

Figure 4-3 Change in morphology of MRC5 cells treated with TGF-β. (a) Control cells maintained in baseline conditions without TGF-β, (b) MRC5 cells treated with 0.5ng/ml TGF-β for 48 hours, (c) MRC5 cells treated with 1ng/ml TGF-β for 48 hours; (d) MRC5 cells treated with 2ng/ml TGF-β for 48 hours. Fibroblasts treated with increased concentrations of TGF-β appeared enlarged with a possible increase in proliferation. Magnification x10 objective lens, scale bar 10µm.

Figure 4-3 shows that treatment with TGF-β led to enlarged cells with the possibility of increased proliferation (discussed in further detail later in the chapter). Previous literature has suggested that these cells are a "myofibroblast", activated fibroblasts that produce αSMA.

4.2.2 Immunolocalisation of Fibroblast Markers in MRC5 cells Treated with TGF-β

Immunocytochemistry was undertaken to assess if myofibroblast transformation had occurred, and whether the treated cells were producing more of this contractile protein.

(a) 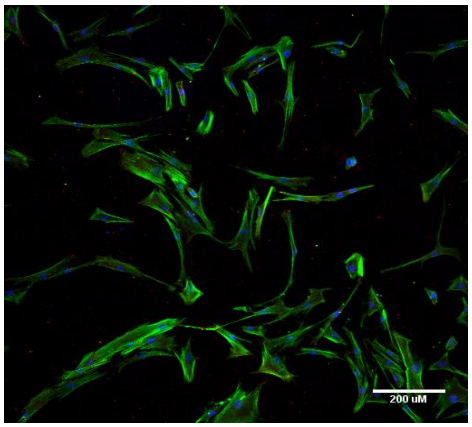

(b) 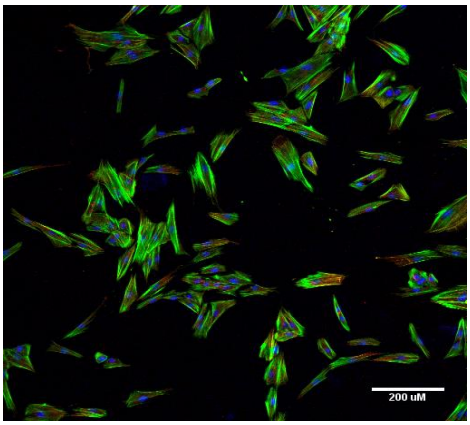

Figure 4-4 MRC5 cells stained for phalloidin (green) and α-SMA (red). (a) Staining for αSMA in untreated control cells after 48 hours showed no red colour, (b) cells under same conditions but treated with TGF-β 2ng/ml for 48 hours. MRC5 cells treated with TGF-β showed increased red staining to confirm production of more α-SMA in the treated cells. Magnification x10 objective lens, scale bar 200μm.

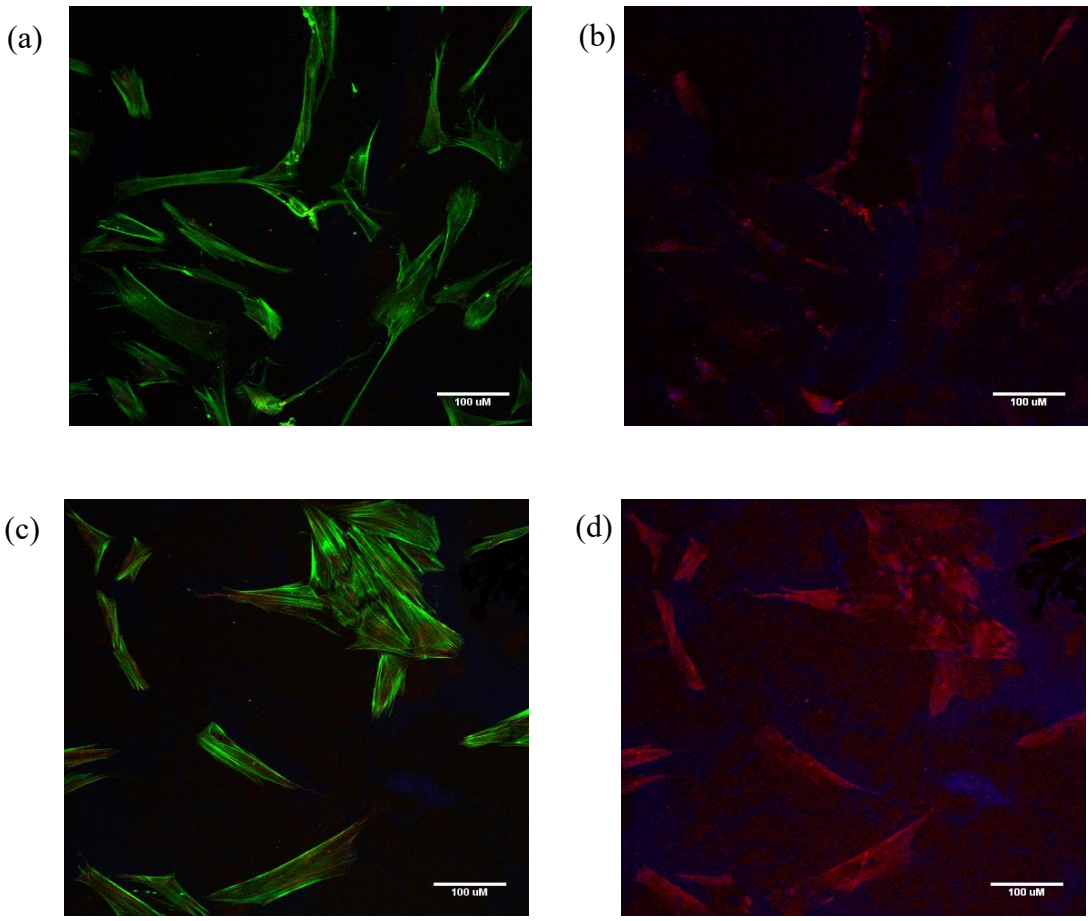

Figure 4-5 MRC5 cells stained for phalloidin (green) and α-SMA (red) after 48 hours shown at higher magnification. (a) control cells stained for phalloidin and α-SMA, (b) same image with phalloidin staining removed, (c) cells treated with TGF-β 2ng/ml for 48 hours and stained for phalloidin and α-SMA, (d) same image with phalloidin staining removed. The image shows that more α-SMA is produced by cells treated with TGF-β, again suggesting that cells were becoming more "myofibroblast-like". Magnification x20 objective lens, scale bar 100μm.

Figure 4-4 and Figure 4-5 show the results of immunocytochemistry performed on MRC5 cells to assess for changes in α-SMA production. The images show very little production of α-SMA in the untreated, control cells. After treatment with TGF-β, there was an increase in expression of α-SMA within the cell. This association has been shown in previous literature (162). This result suggests that the cells are responding to TGF-β by increasing production of α-SMA to become more "myofibroblast-like".

Cells were also stained for COL1A1, the results of which are shown in Figure 4-6 and Figure 4-7.

(a) (b)

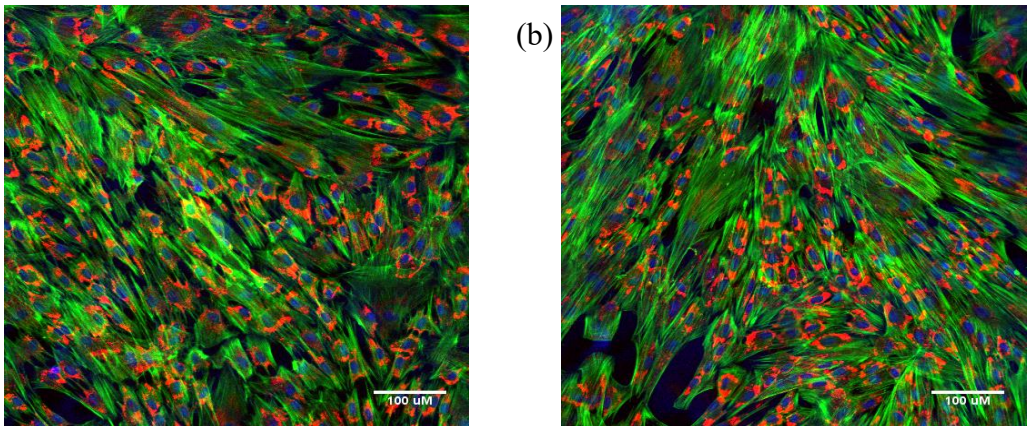

Figure 4-6 MRC5 cells stained for phalloidin (green) and COL1A1 (red). (a) Untreated control cells in baseline conditions, (b) cells under same conditions but treated with TGF-β 2ng/ml for 48 hours. It is difficult to establish any differences in the production of COL1A1 from these images given the abundance of COL1A1 in baseline conditions. Magnification x20 objective lens, scale bar 100µm.

(a) 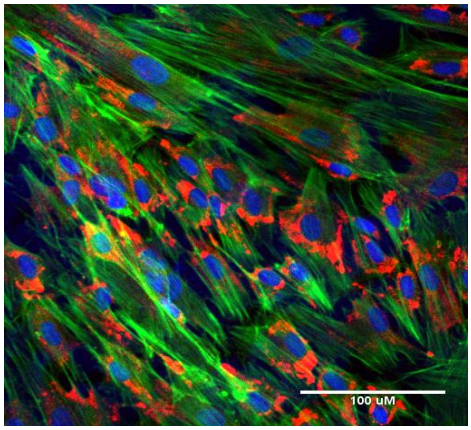

(b) 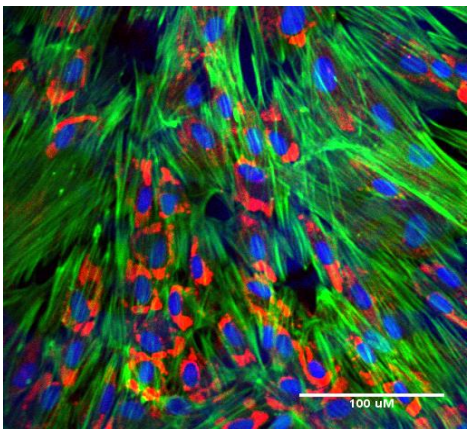

Figure 4-7 MRC5 cells stained for phalloidin (green) and COL1A1 (red). (a) Untreated control cells in baseline conditions, (b) cells under same conditions but treated with TGF-β 2ng/ml for 48 hours. It remains difficult to assess for any increase in COL1A1 production. Magnification x40 objective lens, scale bar 100µm.

The images above show that the MRC5 fibroblasts already produced a lot of COL1A1 before treatment with TGF-β. It was unclear from the immunocytochemistry images whether more COL1A1 was produced after treatment as such a large amount is produced before treatment with TGF-β. The COL1A1 is found in the cytoplasm of the cell, surrounding the nucleus.

4.2.3 The Effect of TGF-β Treatment on the Proliferation of MRC5 Fibroblasts

It was unclear whether the MRC5 fibroblasts were proliferating in response to treatment with TGF-β, or whether the cells were becoming larger to give the impression of an increase in cell number. For this reason, a number of experiments were performed to assess if this treatment induces an increase in cell number at 24, 48, 72 and 96 hour time points respectively.

Initially a fluorescence assay was used, the trade name being alamar blue. This contains a weakly fluorescent indicator dye called Resazurin, which permeates through the cell where it is affected by cell metabolism and on being reduced to Resorufin becomes strongly fluorescent. The fluorescence emitted is then measured with results being directly proportional to the number of metabolically active cells.

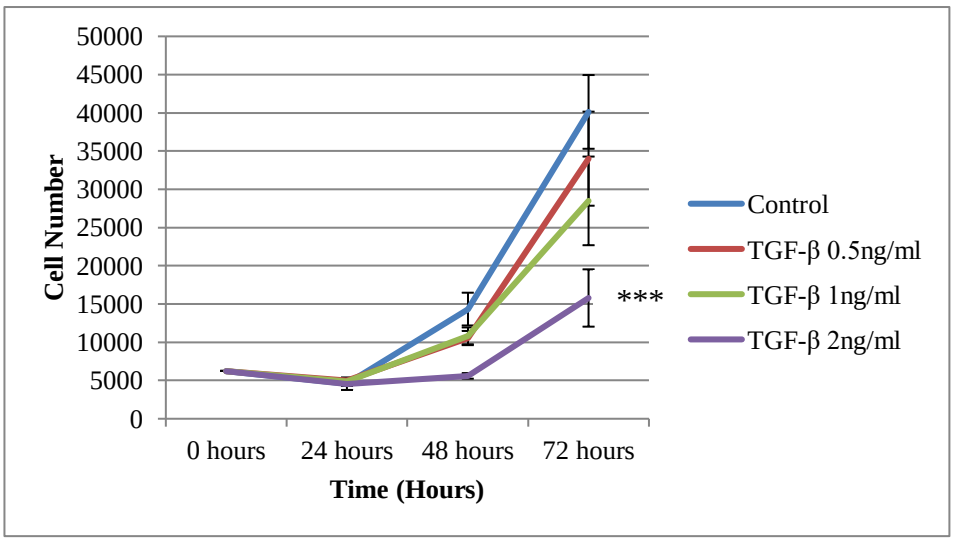

Figure 4-8 MRC5 cells treated with increasing concentrations of TGF-β and then fluorescence measured with alamar blue. These results show that treatment with TGF-β reduces proliferation of MRC5 fibroblasts in a dose-dependent response. Results are expressed as mean values (n= 4) with error bars +/- SD. Two-way anova with Bonferroni post-test was performed, ***$p<0.001$.

The only significant difference in this experiment was shown between control cells and cells treated with TGF-β 2ng/ml where there was a significant reduction in cell proliferation at the 72 hour time point. Surprisingly, although not significant, there appeared to be a general reduction in proliferation of cells treated with TGF-β, with a dose-response trend. However, these results seem to oppose the findings in the cell morphology experiment. It may be that fibroblasts stimulated with TGF-β enlarge which gives the appearance of apparently increased proliferation. It may also cause changes in the cell, which prevents them from remaining healthy and metabolically active, thus leading to the differences seen in the alamar blue assay at 72 hours.

As a further experiment, MRC5 cells were stained for Proliferating Cell Nuclear Antigen (PCNA) antibody. This molecule has an essential role in DNA replication and is thus expressed in proliferating cells.

(a) (b)

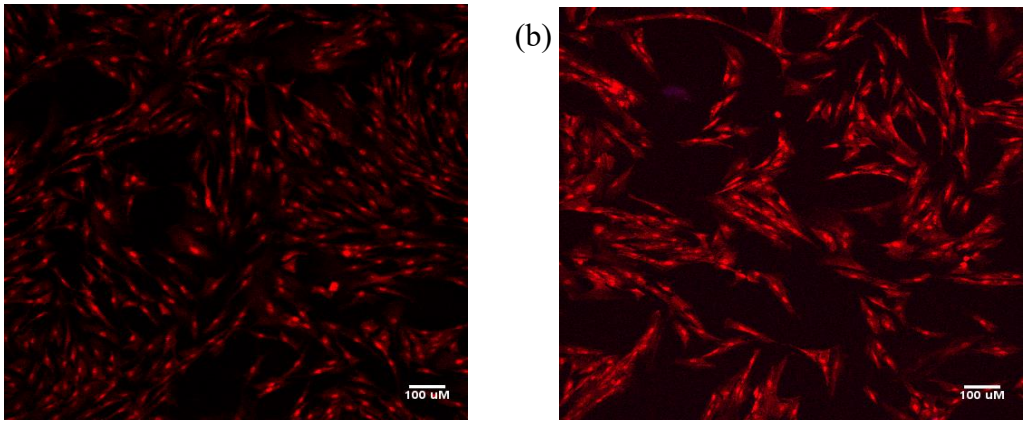

Figure 4-9 MRC5 proliferation assessed by PCNA staining. (a) Untreated, control cells under baseline conditions, (b) Cells treated with TGF-β 2ng/ml for 48 hours. There appears to be a reduction in proliferation of MRC5 fibroblasts in cells treated with TGF-β shown by a reduction in cell number above. Magnification x10 objective lens, scale bar 100μm.

Figure 4-9 shows that cells appeared to be proliferating well at 48 hours, whether untreated or treated with TGF-β 2ng/ml. There did appear to be a reduction in the number of proliferating cells present after 48 hours when they were treated with TGF-β. Although this difference was not significant until 96 hours in the alamar blue assay, this result did suggest a definite reduction in cellular proliferation.

4.2.4 The Effect of TGF-β on Gene Expression in MRC5 Fibroblasts

It was then investigated whether treatment with TGF-β could induce changes in fibroblasts that could be measured at an mRNA level, with changes in transcription of genes for proteins that form the ECM. The mRNA levels were assessed by qPCR at 24 hour intervals over a 96 hour treatment period. The levels of *COL1A1*, *COL3A1* and *FN-EDA* expression in treated cells were compared with untreated control cells, the results are shown in the figures Figure 4-10 – Figure 4-12 below.

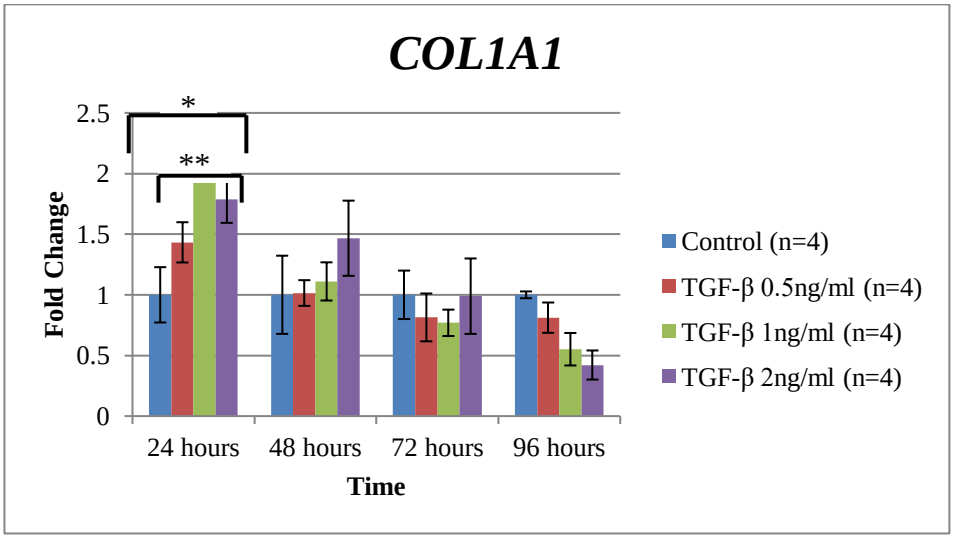

Figure 4-10 Fold change in *COL1A1* in MRC5 cells after treatment with TGF-β over 96 hours. The results show there was a significant increase in gene expression of *COL1A1* after 24 hours, however the results were not sustained at the later time points. Results are mean values (n=4) with error bars +/- SEM. Two-way anova with Bonferroni post-test performed, *$p<0.05$, **$p<0.01$.

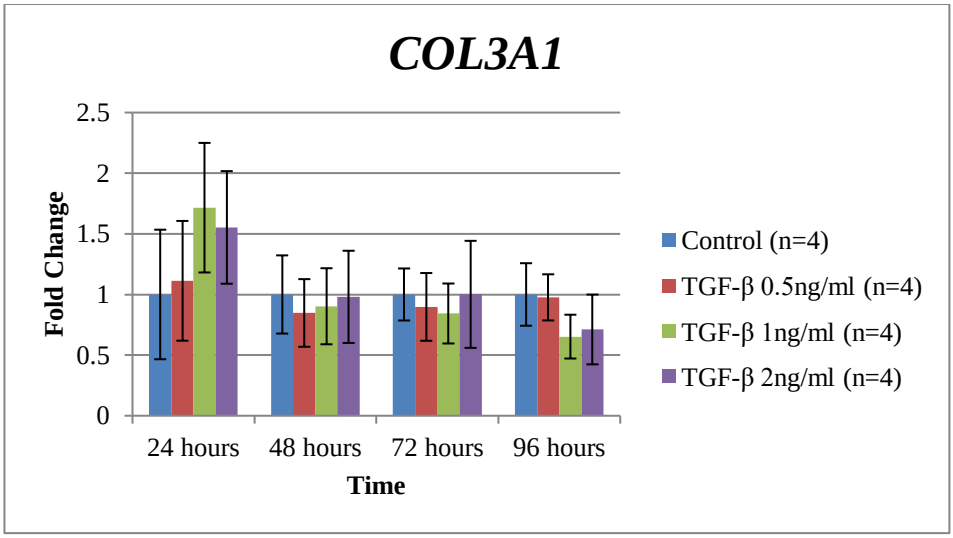

Figure 4-11 Fold change in *COL3A1* in MRC5 cells after treatment with TGF-β over 96 hours. There were no significant changes in *COL3A1* gene expression at any TGF-β concentration or at any length of treatment. Results are mean values (n=4) with error bars +/- SEM. Two-way anova with Bonferroni post-test performed.

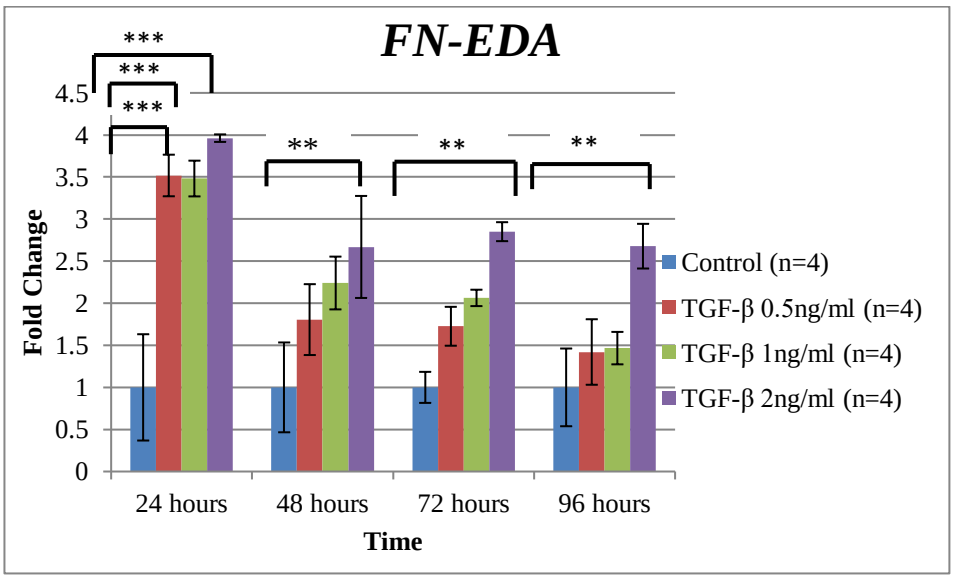

Figure 4-12 Fold change in *FN-EDA* in MRC5 cells after treatment with TGF-β over 96 hours. There was a significant increase in expression of *FN-EDA*, which was sustained at all time points with the highest concentration of TGF-β used (2 ng/ml). Results are mean values (n=4) with error bars +/- SEM. Two-way anova with Bonferroni post-test performed, *p<0.05, **p<0.01, ***p<0.001.

Figure 4-10 showed a 2-fold increase in the transcription of *COL1A1* by MRC5 fibroblasts treated with TGF-β occurring after 24 hours. This response tapered after 72 and 96 hours. There was no significant difference in transcription of *COL3A1* throughout the time course however, at 24 hours there did appear to be a non-significant increase in transcription of *COL3A1*. Again, this response tapered after 48 hours, represented in Figure 4-11. For both genes, there was an initial increase in transcription which was not sustained throughout the 96 hour time course.

Figure 4-12 showed a significant increase in *FN-EDA* present at 24 hours at all doses of TGF-β used, and at 48, 72 and 96 hours, at the highest dose of TGF-β. Unlike collagen, this appeared to be a truly dose-dependent effect.

Although the data presented above has shown that the MRC5 fibroblasts upregulate transcription of ECM genes, it is possible that this may not translate into ECM protein production. For example, RNA binding proteins can affect RNA levels and then reduce the amount of translated protein produced. To assess if this occurred, a western blot experiment was undertaken on the conditioned medium to assess if the treated cells were producing more COL1A1 and FN.

4.2.5 The Effect of TGF-β on Protein Production by MRC5 Fibroblasts

Western blots were produced from conditioned medium taken after 96 hours of TGF-β treatment. Protein was precipitated and western blot performed as per methods described in section 2.9. The predicted molecular weight of COL1A1 is 139kDa.

(a)

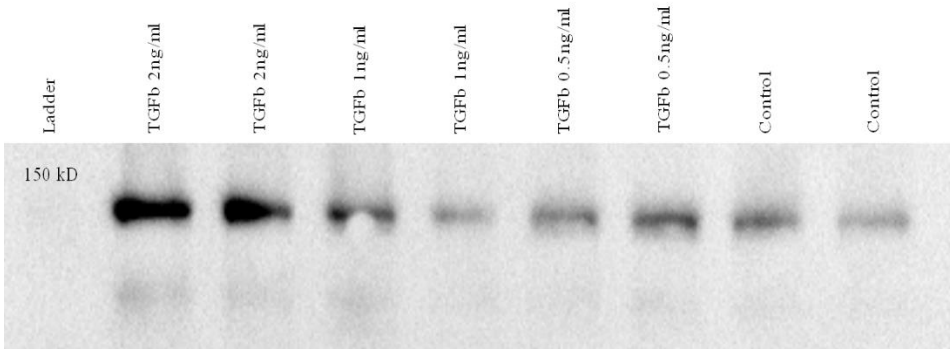

(b)

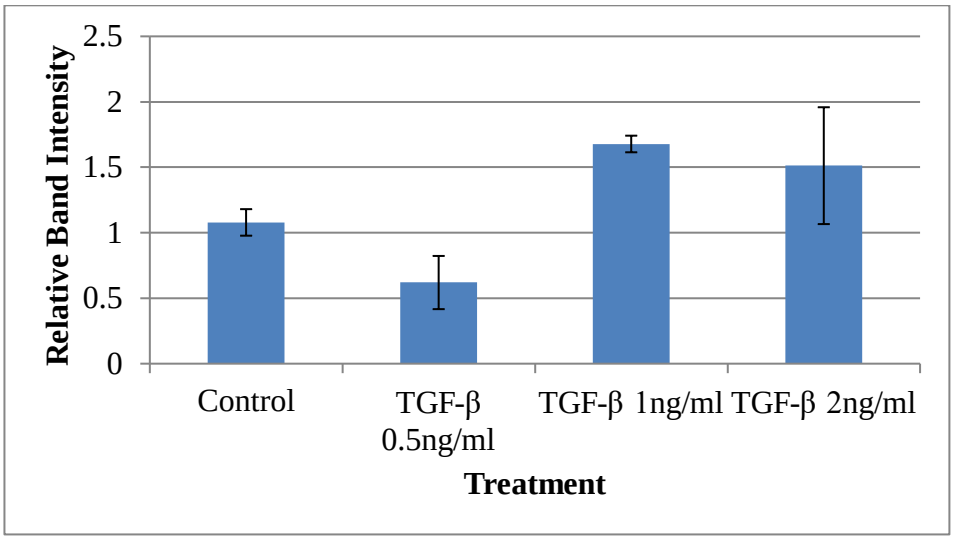

Figure 4-13 Western blot for COL1A1 from conditioned medium of MRC5 cells treated with increasing concentrations of TGF-β over 96 hours. (a) Annotated western blot gel image, (b) analysis of western blot with results normalised for protein loading against ponceau S staining. Although visually there appeared to be an increase in COL1A1 protein, when results were normalised there was no significant differences found. Results are mean values (n=2) of the relative band intensity with error bars +/- SEM. One-way anova with Bonferroni's multiple comparison test performed.

Although visually there appeared to be an increase in COL1A1 secretion by MRC5 fibroblasts, once normalised, there was no significant difference apparent despite the results showing an upregulation in *COL1A1* at 24 hours at an mRNA level.

A western blot was also produced to measure the change in FN secreted by MRC5 cells after 96 hours. The predicted molecular weight of FN is 220kDa.

(a)

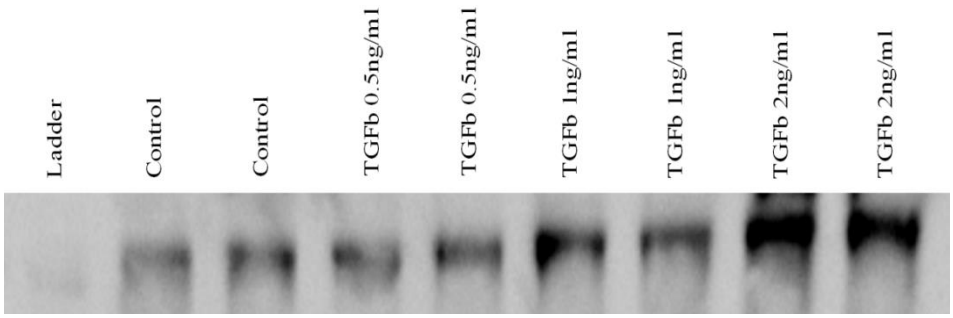

(b)

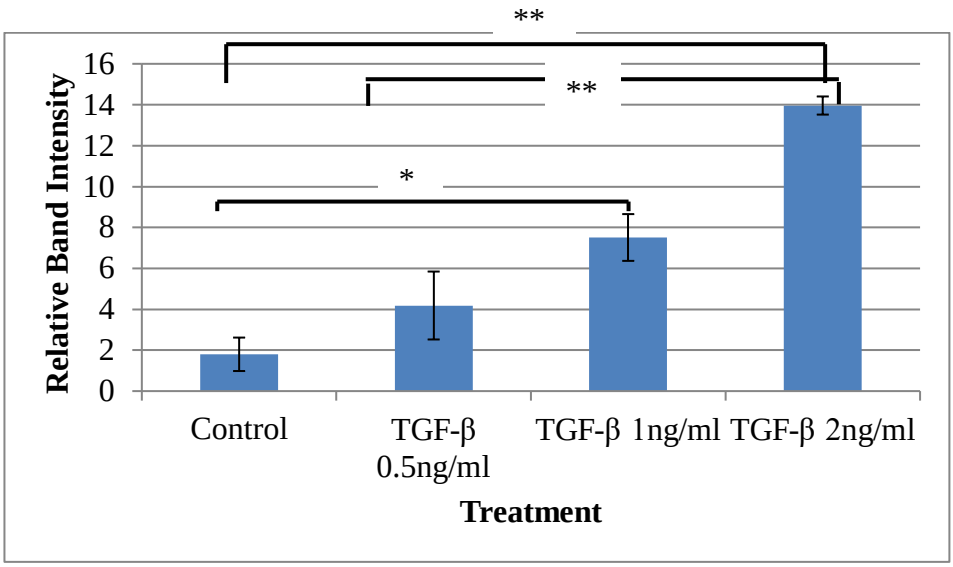

Figure 4-14 Western blot for FN secreted by MRC5 cells treated with increasing concentrations of TGF-β for 96 hours. (a) Annotated western blot gel image, (b) analysis of western blot with results normalised for protein loading against ponceau S staining. There was a significant increase in production of FN with increasing concentrations of TGF-β, with a dose-dependent response. Results are mean values (n=2) with error bars +/- SEM. One-way anova performed with Bonferroni multiple comparison test, *$p<0.05$, **$p<0.01$.

The western blot of FN appeared to show an upregulation in secretion of the protein after treatment with increasing concentrations of TGF-β. This would match the upregulation of the *FN-EDA* splice variant transcription observed and shown earlier in the chapter. It should be noted that the protein assessed using western blot was the regular form of FN and not the FN-EDA form in which expression was measured.

4.3 The Effect of TGF-β Treatment on Epithelial Cells (A549)

As previously discussed, alveolar epithelial cells are likely implicated in pulmonary fibrosis, potentially undergoing EMT and then becoming mesenchymal cells, and becoming capable of producing more ECM. For this reason, they were chosen as an interesting cell type to assess the impact of TGF-β. In a similar way to the MRC5 fibroblasts, they were treated with increasing concentrations of TGF-β to assess for changes in pro-fibrosis markers.

4.3.1 The Effect of TGF-β Treatment on the Morphology of A549 Epithelial Cells

Initially A549 cells were treated with increasing concentrations of TGF-β and images were recorded at 24, 48, 72 and 96 hours respectively. The Figure below demonstrates the changes observed in cell morphology after 48 hours TGF-β treatment.

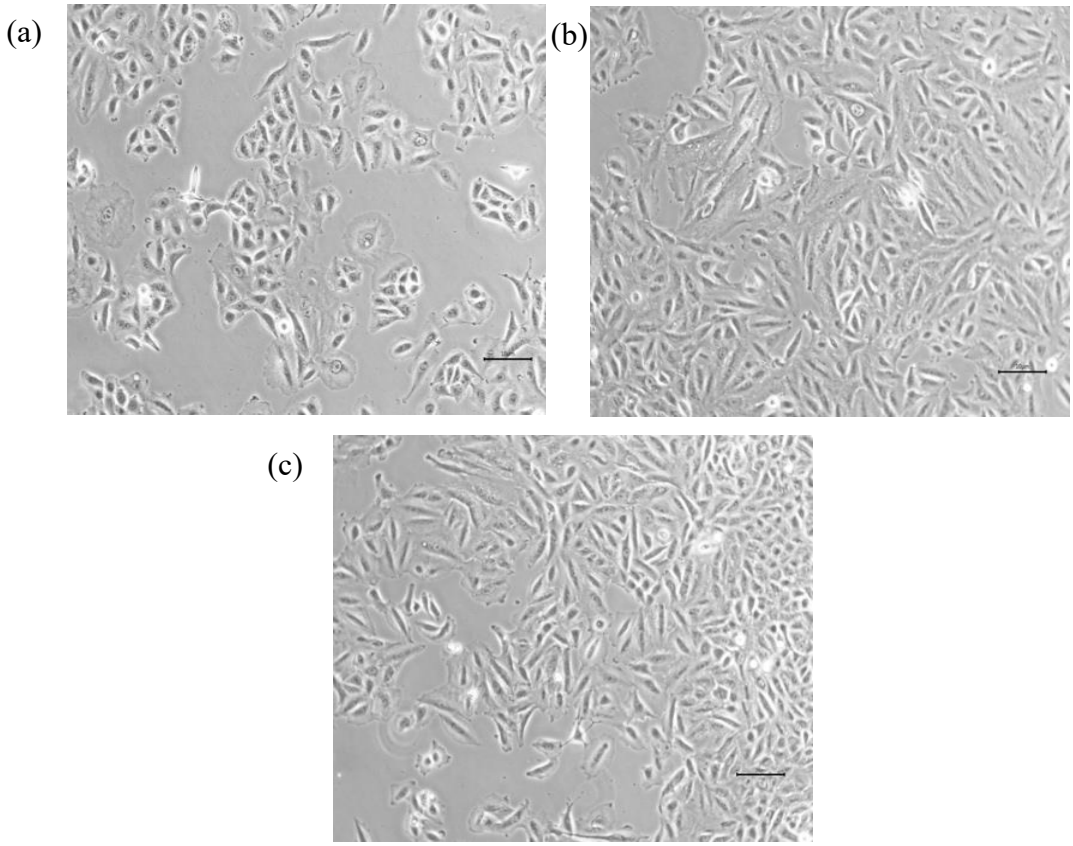

Figure 4-15 Change in morphology of A549 cells treated with TGF-β for 48 hours. (a) Control cells treated in baseline conditions without the addition of TGF-β, (b) A549 cells treated with 1.5ng/ml TGF-β, (c) A549 cells treated with 3ng/ml TGF-β for 48 hours. These figures demonstrate the subtle changes in morphology brought about by TGF-β treatment, with slightly more elongation of the usually tightly packed cuboidal cells. Magnification x10 objective lens, scale bar 10μm.

A549 cells treated with TGF-β showed a subtle change in appearance. Figure 4-15 shows that the epithelial cells have lost their cuboidal shape with tightly adherent junctions and have become elongated, spindle-shaped cells. Further immunohistochemistry staining and qPCR was performed to assess if these cells were undergoing EMT.

4.3.2 Immunolocalisation of EMT Proteins in A549 cells treated with TGF-β

To assess these morphological changes further the epithelial cells were stained for both COL1A1 and αSMA. These proteins may be produced by epithelial cells that have undergone EMT and are more mesenchymal in phenotype.

(a) 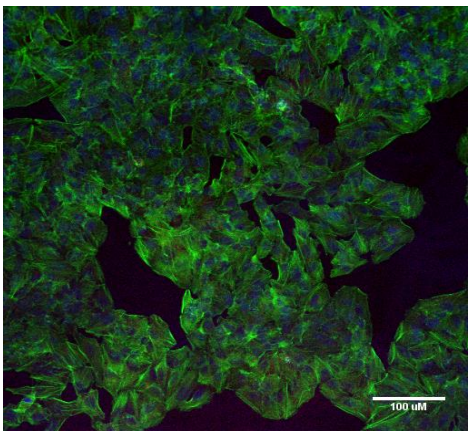

(b) 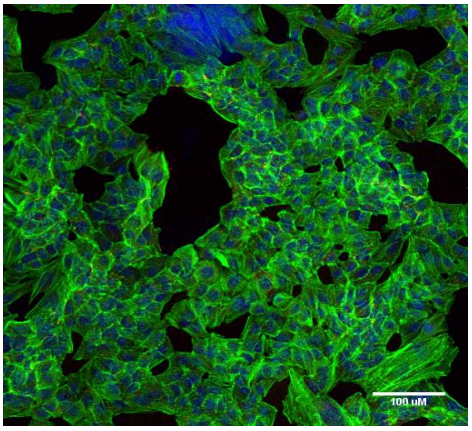

Figure 4-16 A549 cells stained for phalloidin (green) and COL1A1 (red). (a) control cells cultured in baseline conditions, (b) cells treated with TGF-β 3ng/ml for 48 hours. The phalloidin staining, appreciated better at low magnification, allows the tight, cobblestone appearance of the A549 epithelial cells to be assessed. It is difficult to detect the COL1A1 staining in this image so the figure below shows the samples at higher magnification. Magnification x20 objective lens, scale bar 100µm.

(a) 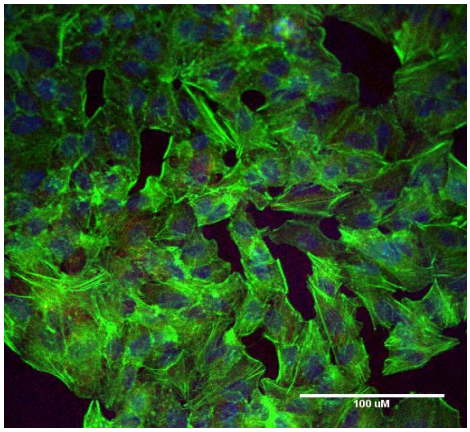

(b) 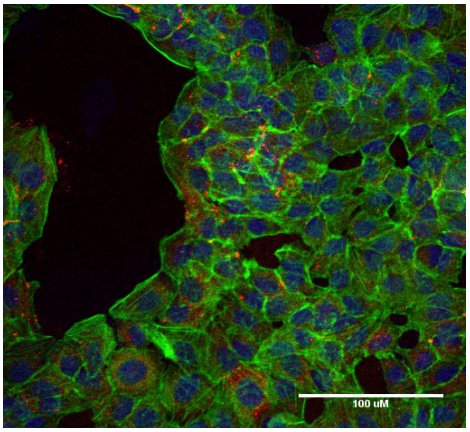

Figure 4-17 A549 cells stained for phalloidin (green) and COL1A1 (red). (a) control cells cultured in baseline conditions without TGF-β treatment, (b) cells treated with TGF-β 3ng/ml for 48 hours. At this higher magnification it was noted that more COL1A1 is produced by treated cells, evidenced by increased red staining of the cells. Magnification x40 objective lens, scale bar 100µm.

A549 cells treated with TGF-β showed an increase in production of COL1A1, as represented by an increase in red staining in Figure 4-16 and Figure 4-17. This was further quantified using qPCR and western blot, shown later in the chapter.

The A549 cells were then stained for α-SMA to assess if there was an increase in production of this protein, suggesting that EMT was occurring in response to TGF-β treatment.

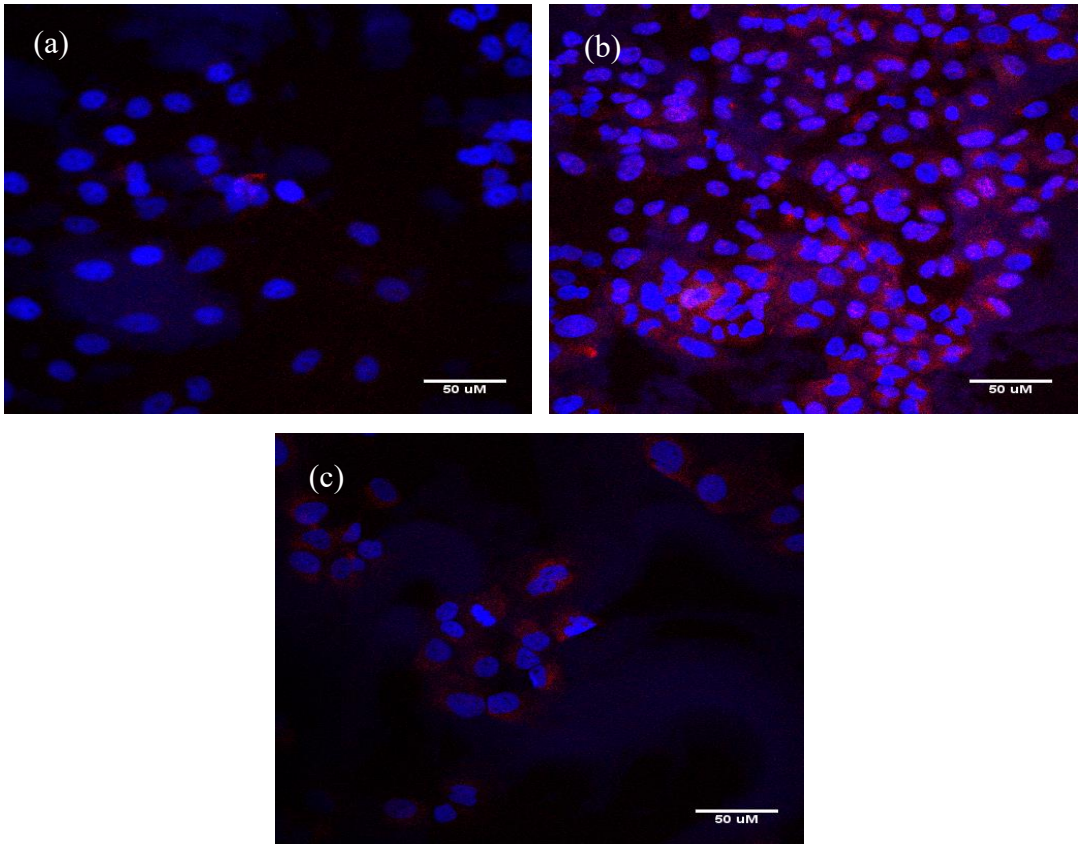

Figure 4-18 A549 epithelial cells stained for αSMA (red) alongside nuclear DAPI staining (blue) for 48 hours. (a) control cells cultured in baseline conditions, (b) cells treated with TGF-β 1.5ng/ml, (c) cells treated with TGF-β 3ng/ml. The images show that more α-SMA was produced in response to TGF-β treatment suggesting that EMT may be occurring. Magnification x40 objective lens, scale bar 50µm.

Figure 4-18 shows that A549 cells produced α-SMA in response to TGF-β. As can be seen from these images control cells produce very little of this protein, which stained red, suggesting that the cells were undergoing EMT in response to TGF-β treatment.

4.3.3 The Effect of TGF-β Treatment on the Proliferation of A549 Epithelial Cells

It was investigated whether TGF-β induced a proliferative response in A549 epithelial cells. An alamar blue assay was performed to measure the number of metabolically active cells at different time points and thus give an estimate of the proliferation of the A549 cells over a 72 hour time course.

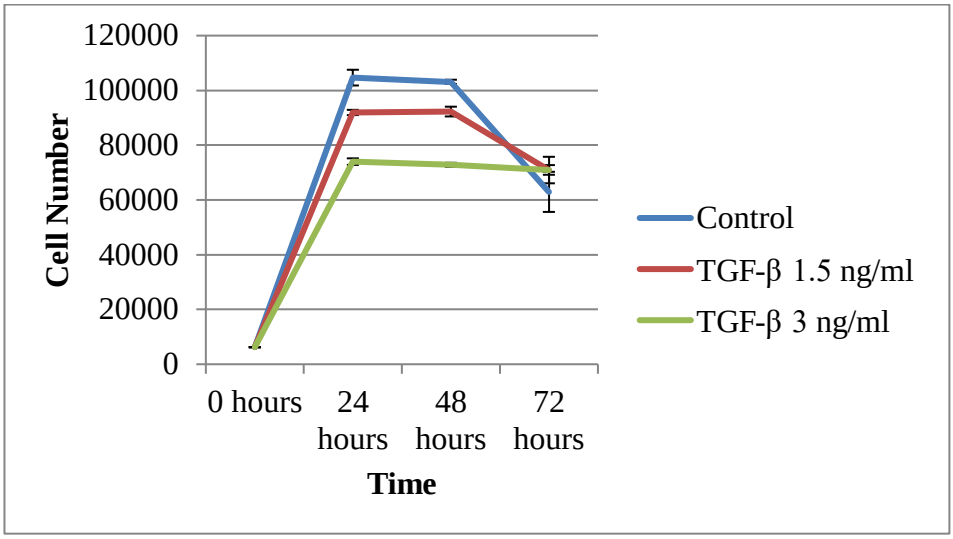

Figure 4-19 Alamar blue assay assessing the proliferation of A549 cells treated with increasing concentrations of TGF-β over 72 hours. There were no significant differences noted, however A549 cells treated with TGF-β seemed to proliferate less than control cells. Results are mean values (n=4) with error bars +/- SEM. Two-way anova with Bonferroni post-test was performed.

Figure 4-19 shows the growth of A549 epithelial cells over 72 hours after treatment with 1.5ng/ml and 3ng/ml TGF-β respectively. Although the cells grew well over the time course, there did not appear to be any significant difference between the growth of control cells and those that were treated. In fact, there was trend for proliferation to be less in cells that were treated with TGF-β, although this was non-significant.

4.3.4 The Effect of TGF-β Treatment on Gene Expression in A549 Epithelial Cells

It was then investigated if treatment with TGF-β could cause a change in transcription levels of genes associated with production of the ECM or EMT over the time course.

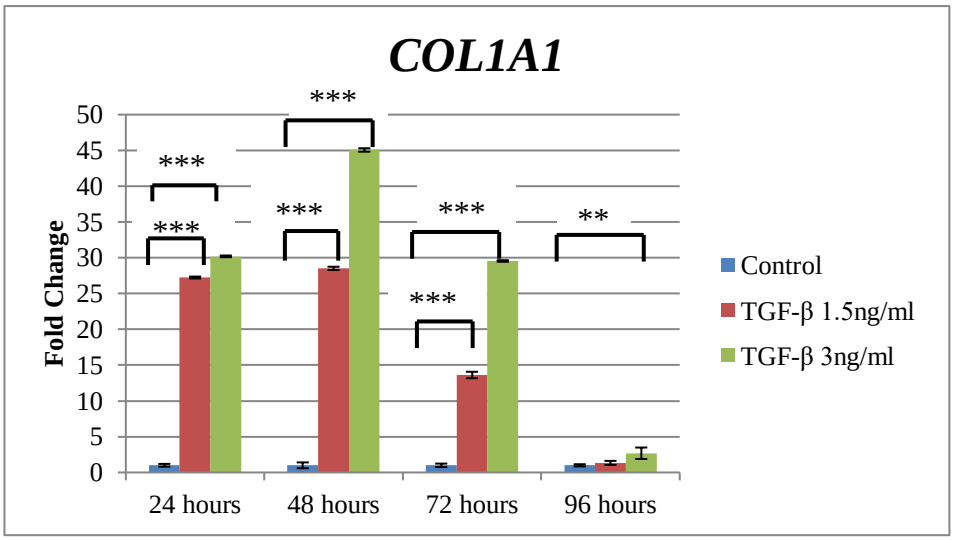

Figure 4-20 Fold change in mRNA levels of *COL1A1* in A549 cells treated with 1.5ng/ml TGF-β and 3ng/ml TGF-β over 96 hours in comparison to untreated, control cells. There was a significant increase in expression of *COL1A1* at all concentrations of TGF-β used. This was still present after 72 hours treatment. Results are mean values (n=4) with error bars +/- SEM. Two-way anova with Bonferroni post-test was performed, *p<0.05, **p<0.01, ***p<0.001.

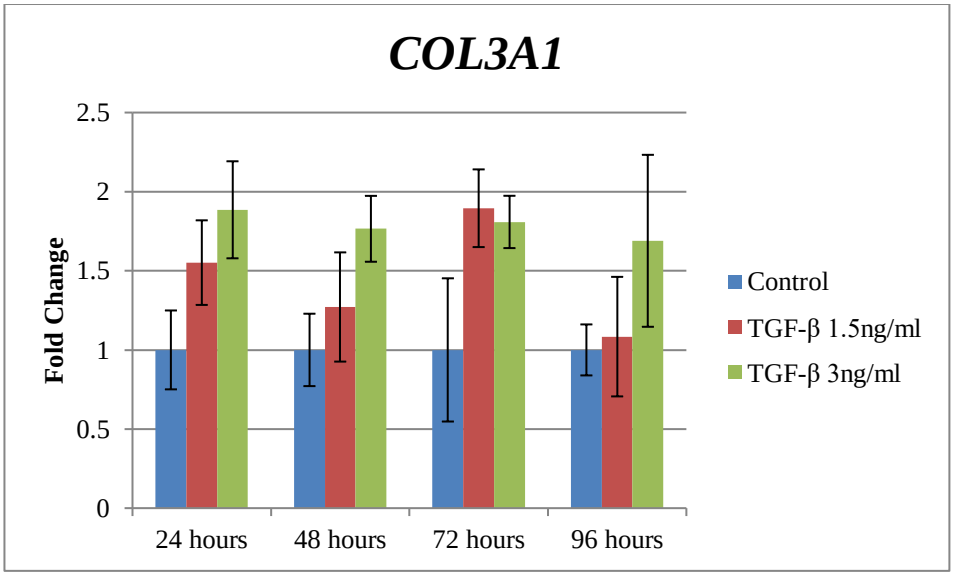

Figure 4-21 Fold change in mRNA levels of *COL3A1* in A549 cells treated with 1.5ng/ml TGF-β and 3ng/ml TGF-β over 96 hours in comparison to untreated, control cells. There were no significant changes in expression of *COL3A1* after treatment with TGF-β. Results are mean values (n=4, n=3 at 96 hours) with error bars +/- SEM. Two-way anova with Bonferroni post-test performed.

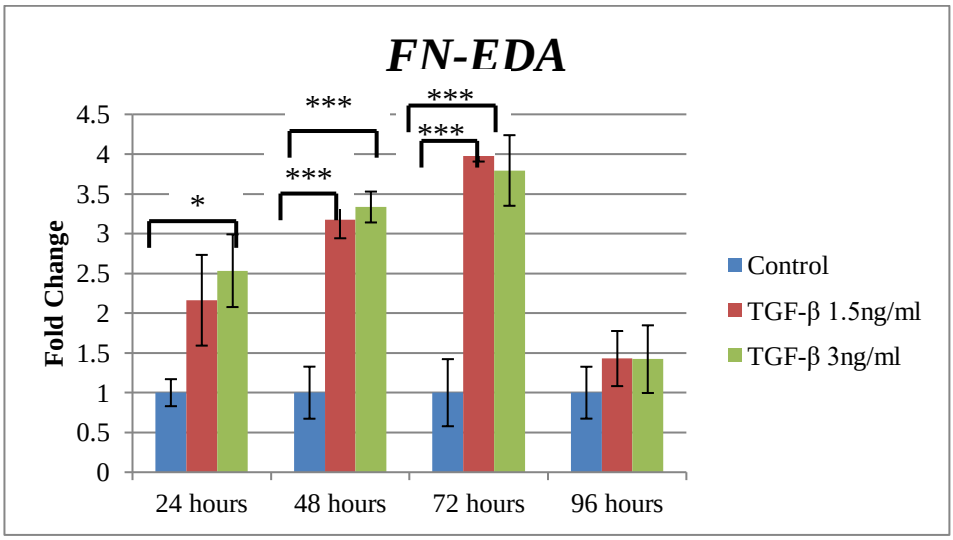

Figure 4-22 Fold change in mRNA levels of *FN-EDA* in A549 cells treated with increasing concentrations of TGF-β over 96 hours in comparison to untreated, control cells. There was a significant increase in expression of *FN-EDA*, sustained to 72 hours treatment. Results are mean values (n=4) with error bars +/- SEM. Two-way anova with Bonferroni post-test performed, *p<0.05, **p<0.01, ***p<0.001.

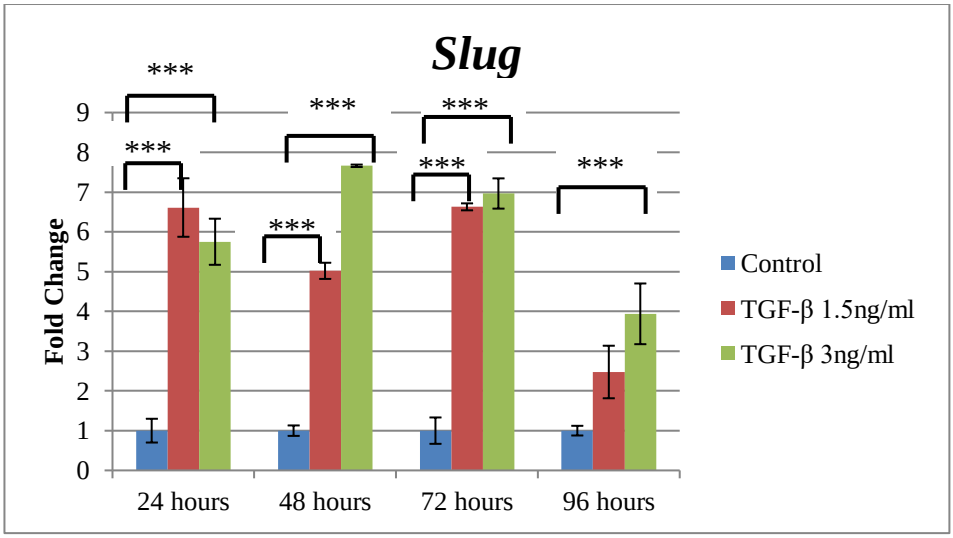

Figure 4-23 Fold change in mRNA levels of *Slug* in A549 cells treated with 1.5ng/ml TGF-β and 3ng/ml TGF-β over 96 hours in comparison to untreated, control cells. These results showed a significant increase in *Slug* after TGF-β treatment. Results are mean values (n=4) with error bars +/- SEM. Two-way anova with Bonferroni post-test performed, ***p<0.001.

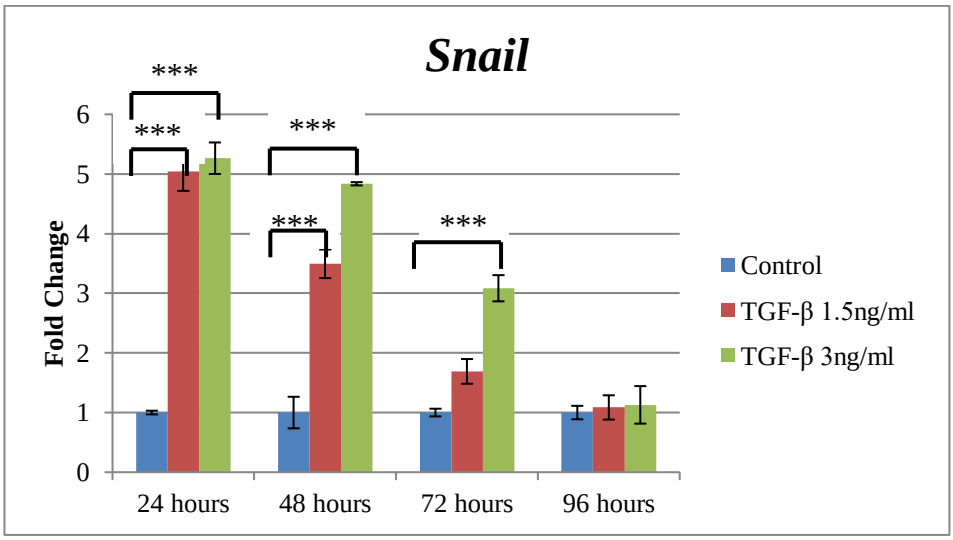

Figure 4-24 Fold change in mRNA levels of *Snail* in A549 cells treated with 1.5ng/ml TGF-β and 3ng/ml TGF-β over 96 hours in comparison to untreated, control cells. This demonstrated a significant increase in expression of *Snail* with up to 72 hours TGF-β treatment. Results are mean values (n=4) with error bars +/- SEM. Two-way anova with Bonferroni post-test performed, ***p<0.001.

Figure 4-20 shows a significant increase in transcription of *COL1A1* mRNA in response to treatment with TGF-β. This was a very significant change (45 times higher in cells treated with the highest dose of TGF-β at 48 hours) and the response was sustained up to 96 hours after initial treatment. It was also a dose-dependent effect with the higher treatment dose of TGF-β having the largest effect. This may be because these cells produce very little *COL1A1* under normal, control conditions, so once stimulated to produce collagen this effect appears profound. However, there was no significant effect on mRNA levels of *COL3A1* after treatment with either concentration of TGF-β (as represented in Figure 4-21). There was also a dose-dependent upregulation of *FN-EDA*, again sustained to at least 72 hours treatment (see Figure 4-22).

These changes were associated with a dose-dependent increase in the mRNA level of the transcription factors S*lug* and *Snail* (represented in Figure 4-23 and Figure 4-24 respectively). The changes in ECM genes peaked around 48-72 hours, whereas the changes in transcription factors peaked earlier (around 24-48 hours).

4.3.5 The Effect of TGF-β on Protein Production by A549 Epithelial Cells

Given that TGF-β treatment had such a profound effect in the transcription of *COL1A1*, a western blot was also performed to assess for upregulation of the transcribed protein (see Figure 4-25).

(a)

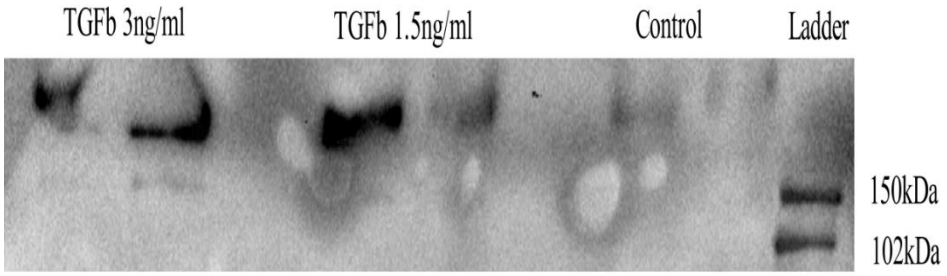

(b)

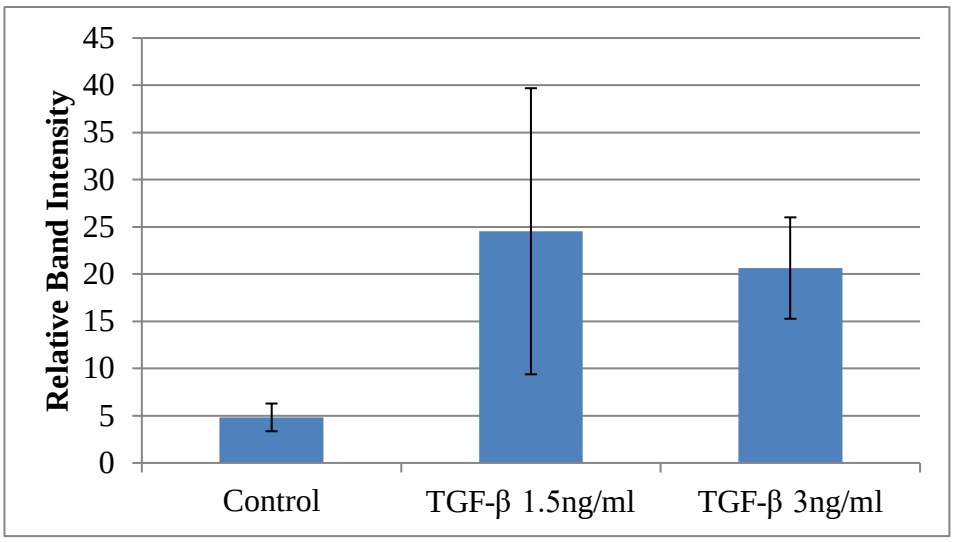

Figure 4-25 Western blot for COL1A1 secreted by A549 cells treated with increasing concentrations of TGF-β for 96 hours. (a) Western blot image, (b) analysis of western blot showing relative band intensity. There was no significant change in the production of COL1A1 in epithelial cells treated with TGF-β. Results are mean values (n=2) with error bars +/- SEM. One-way anova performed with Bonferroni multiple comparison test.

Figure 4-25 shows a tendency to an increase in the production of COL1A1 produced by A549 cells in response to treatment with TGF-β. Unfortunately, there was a lot of variation within the experiment and this was not found to be significant, although the result suggests that more COL1A1 may be produced by A549 cells stimulated with TGF-β.

4.4 The Use of TCH (A Serum Replacement Product) in Experiments Requiring Serum Starvation

4.4.1 MRC5 cells Cultured in TCH Supplemented Medium

Serum starvation is used in multiple types of *in vitro* studies, but there is no standard practice to guide how such studies should be undertaken (163). For example, cells may be starved for anything from 15 minutes to several hours. As serum contains variable amounts of growth factors and cytokines, removing it makes experiments more reproducible and ensures that cells are only being stimulated by the experimental cytokine being added (in this case, TGF-β). However, there has been evidence to suggest serum starvation impacts upon the growth of cells causing environmental stress and perhaps even being an apoptotic trigger (164). For this reason, TCH was used as an alternative to FBS. This is a serum replacement product that lacks steroid hormones, growth factors and cytokines. The MRC5 and A549 cell types are listed by the company as being cultured successfully using this supplement (165).

To improve reproducibility and to ensure that any changes in the cells were not imposed due to serum starvation, the cells were cultured using this serum replacement (as described in materials and methods chapter, section 642.3.2.2).

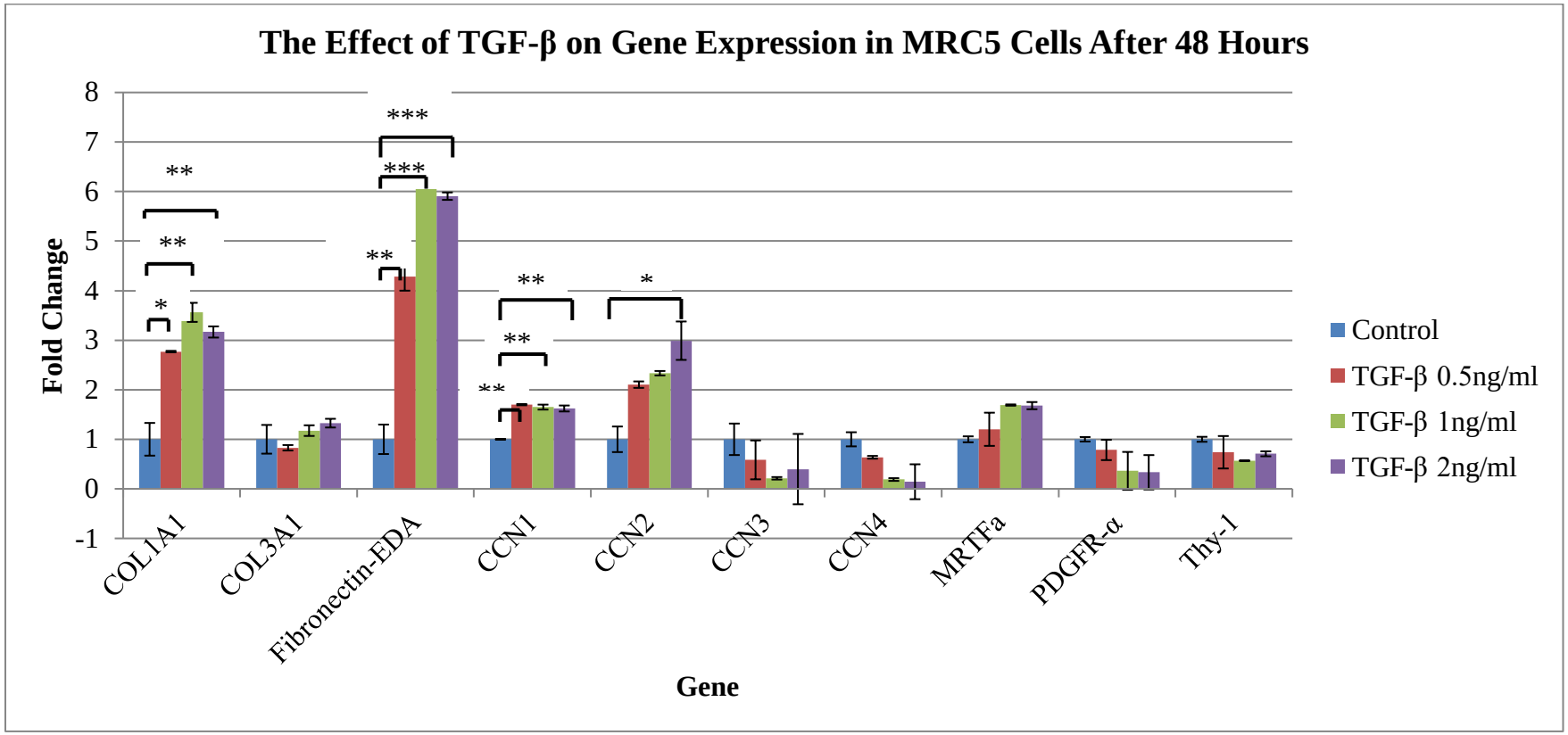

Figure 4-26 Changes in fibrosis associated genes in MRC5 cells treated with increasing concentrations of TGF-β for 48 hours. There were significant increases in *COL1A1*, *FN-EDA*, *CCN1* and *CCN2* when MRC5 cells were treated with TGF-β for 48 hours. Results are mean values (n=3) with error bars +/- SEM. A one-way anova was used for each gene with Bonferroni correction for multiple comparisons.

This experiment, the results of which are shown in Figure 4-26, showed that treating cells with TGF-β had similar effects whether cells are serum starved or TCH is used. There is an increase in expression of genes associated with the production of ECM, including *COL1A1* and *FN-EDA*. However, when cells were serum starved any significant increase in *COL1A1* only occurred at 24 hours and had tapered after 48 hours. However, this was sustained until 48 hours when cells were given TCH suggesting that serum starvation was detrimental to the MRC5 cells. There was not a significant increase in *COL3A1*, which was similar to previous data when cells were serum starved prior to TGF-β treatment.

Interestingly, *CCN1*, the role of which is controversial in fibrosis research, was also upregulated. *CCN2* was upregulated after TGF-β treatment, which concurs with published literature, and this effect appeared dose-dependent. *CCN3*, a molecule that may have an antifibrotic effect, was attenuated 48 hours after cells were stimulated with TGF-β, although this effect was not shown to be significant. Surprisingly, *CCN4* was also attenuated after TGF-β treatment, which is in contradiction to previous literature that states CCN4 is a pro-fibrotic mediator (137). However, this response was not significant. The above data was also at a single time point and so the results may be different if the mRNA was assessed after 12 hours or 24 hours of TGF-β treatment.

MRTFa, a transcriptional co-activator is translocated to the nucleus when stimulated by growth factors such as TGF-β. Here it can initiate transcription of genes involved in fibrosis, including *COL1A1* and *α-SMA*. This experiment showed a trend to an increase in *MRTFa* in response to TGF-β, although this was not significant at 48 hours. It was therefore decided to stain the MRC5 cells for MRTFa, i.e. to assess if there was a change in location of the MRTFa protein (i.e. had the protein translocated from the cytoplasm of the cell to the nucleus in response to TGF-β), as suggested to occur by the current literature. The results are shown in Figure 4-27 below.

Thy-1 is a glycophosphatidylinositol anchored cell surface protein found on the surface of fibroblasts. There is evidence to suggest that mesenchymal cells involved in fibrosis lose expression of this protein. For this reason, change in gene expression for this protein was measured after treatment with TGF-β. There appeared to be a

downward trend in *Thy-1* expression but this did not meet significance. However, given the recent controversial literature surrounding the role of this protein in IPF the MRC5 fibroblasts were stained for Thy-1 protein to assess if there was a change in expression with TGF-β treatment. There were no significant changes in *PDGFR-α* when cells were treated with TGF-β, although there was a trend for a reduction in gene expression of this receptor.

4.4.2 The Effect of TGF-β Treatment on the Immunolocalisation of MRTFa in MRC5 cells

(a) (b)

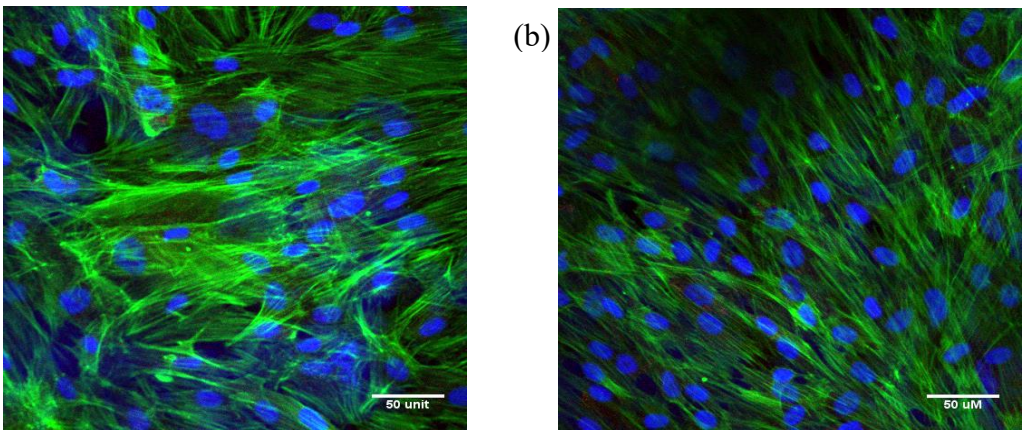

Figure 4-27 MRC5 cells showing staining with nuclear DAPI (blue), phalloidin (green) and MRTFa (red). (a) untreated control cells, (b) cells under same conditions but treated with TGF-β 2ng/ml for 48 hours. No significant changes were noted in the expression or localisation of MRTFa in the treated MRC5 fibroblasts. Magnification x40 objective lens, scale bar 50µm.

Figure 4-27 shows the expression of MRTFa in MRC5 fibroblasts. It shows that only a small amount of MRTFa was expressed in control cells and this did not appear to be significantly upregulated after 48 hours of TGF-β treatment, concurring with the mRNA data shown in Figure 4-26.

4.4.3 The Effect of TGF-β Treatment on the Immunolocalisation of Thy-1 in MRC5 Cells

As previously discussed Thy-1 is a cell surface protein that belongs to the immunoglobulin-like gene family (166). It is lost from the surface of fibroblasts located in fibroblastic foci of patients with IPF (140).

As can be seen from the qPCR data shown in Figure 4-26, the treatment of fibroblasts with TGF-β appeared to down-regulate expression of Thy-1, although this change was not statistically significant. Staining was then undertaken to assess if there was any change in Thy-1 expression of the fibroblasts, visible by immunocytochemistry.

(a) 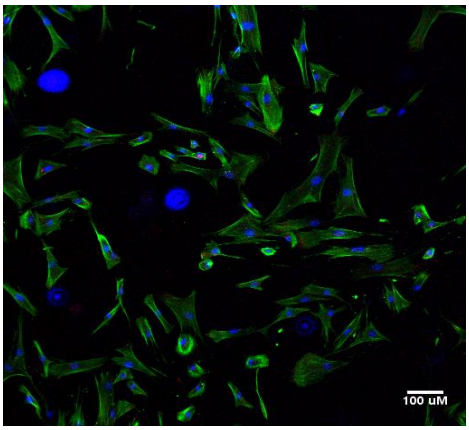

(b) 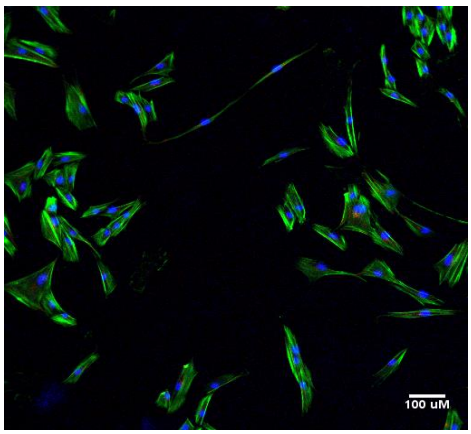

Figure 4-28 MRC5 cells stained for phalloidin (green) and Thy-1 (red). (a) control, untreated cells, (b) cells treated with TGF-β 2ng/ml for 48 hours. There appeared to be little change in expression of Thy-1 in fibroblasts treated with TGF-β. Magnification x10 objective lens, scale bar 100µm.

(a) 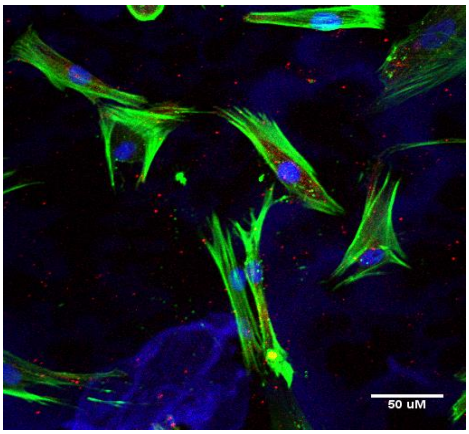

(b) 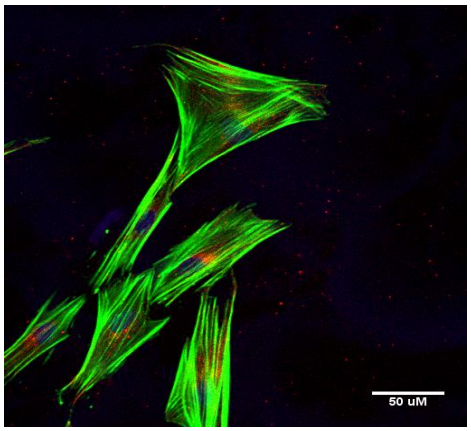

Figure 4-29 MRC5 cells stained for phalloidin (green) and Thy-1 (red). (a) control, untreated cells, (b) cells treated with TGF-β 2ng/ml for 48 hours. A higher magnification showed there was no difference in the localisation of the Thy-1 protein after treatment with TGF-β. Magnification x40 objective lens, scale bar 50µm.

Figure 4-28 shows little or no change in the expression of Thy-1 when visualised by immunocytochemistry staining, concurring with the qPCR data already shown in Figure 4-26. Interestingly, however, very little staining was seen on the cell membrane, as would be expected from a cell surface protein and there did not appear to be a change in the location of the protein after treatment with TGF-β.

4.4.4 A549 cells Cultured in TCH Serum Supplemented Medium

The experiment, using serum replacement medium instead of serum starvation when treating cells with TGF-β, was repeated using the A549 epithelial cells. These cells appeared more sensitive to serum starvation and, unlike the MRC5 fibroblasts, could only be starved for 8 hours as they did not survive when starved overnight. It was therefore important that they were given serum supplementation to ensure that they stayed healthy prior to treatment.

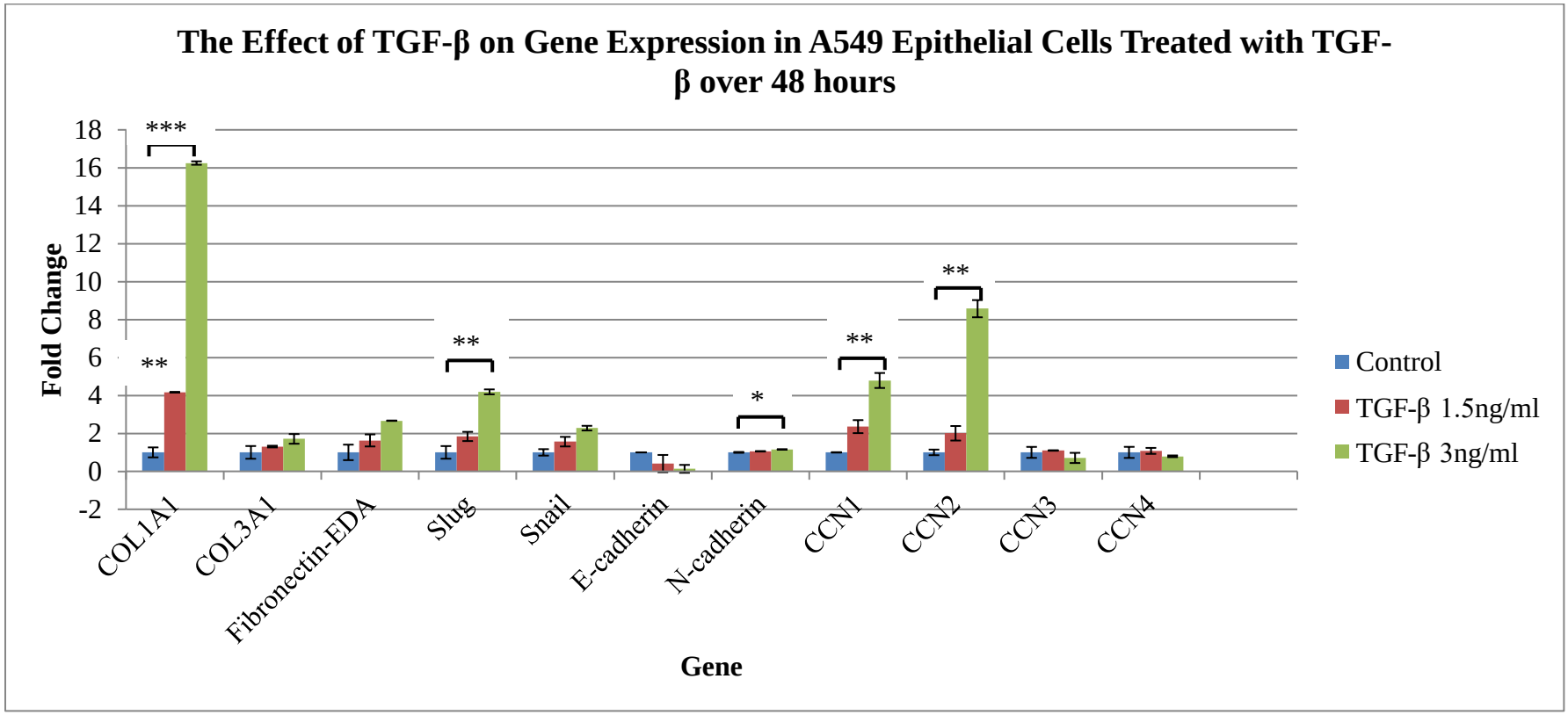

Figure 4-30 Changes in fibrosis genes in A549 cells treated with increasing concentrations of TGF-β over 48 hours. Cells were not serum starved prior to treatment but were cultured in serum replacement medium. There were significant increases in *COL1A1*, *Slug*, *N-cadherin*, *CCN1* and *CCN2* when A549 cells were treated with TGF-β. Results are expressed as mean values (n=2) with error bars +/- SEM. (* $p<0.05$, ** $p<0.01$, *** $p< 0.001$)

Figure 4-30 showed an increase in transcription of *COL1A1* when A549 cells were treated with TGF-β and serum replacement medium for 48 hours, corresponding with previous data when cells were serum starved. *FN-EDA* and *COL3A1* were not significantly increased, although *FN-EDA* did show a trend to upregulation but this was not significant. This may be due to a slight variation in the control wells. There was also a trend for a reduction in *E-cadherin*, which did not reach significance and also an associated upregulation of *N-cadherin*, both features associated with EMT (108, 167). As expected, the transcription factors S*lug* and *Snail* were upregulated in a dose-dependent manner. The CCN family showed a similar pattern of response as shown in the MRC5 fibroblasts, with an upregulation of *CCN1* and *CCN2* seen at the higher dose of TGF-β and a corresponding, although non-significant, reduction in *CCN3* and *CCN4* respectively.

5 Utilising the *in vitro* Model to Assess Changes Induced by Plasma From Patients with Fibrotic Diseases

In chapter 4 it was demonstrated that a cellular model had been produced, in which fibrotic change can be measured in cell lines from two cell types previously implicated in fibrosis. This was shown when a cytokine known to induce pro-fibrotic changes in cells, in this case TGF-β, was added to the cell medium in various experimental set-ups. Changes were shown in cell morphology (using immunocytochemistry), proliferation (using alamar blue assays), mRNA (using qPCR) and protein production (using western blot and immunocytochemistry).

In this chapter the same model was used to assess whether treating cell lines with plasma from patients with ILD could cause similar changes to those seen when cells were treated with a pro-inflammatory cytokine (as described in chapter 4). Cells treated with plasma from healthy subjects were used as a control. The hypothesis was that plasma from ILD patients would induce changes in the cells to suggest that systemic factors are present in the plasma, and that such treatment would initiate and propagate a pro-fibrotic response. Despite extensive literature searching it appears to be unknown whether treating cell lines directly with plasma from ILD patients can induce any such changes in related cell lines. However, it is wondered if there are cytokines present in patient plasma that may propagate the fibrotic pathways.

There has been some recent literature to suggest that plasma and serum have differing properties. Serum is the liquid part of whole blood obtained after it has been coagulated and then separated by centrifugation. However, this process may lead to the release of a number of pro-inflammatory cytokines, making the results less reliable. Plasma is obtained from tubes that have been treated with heparin prior to the blood being taken, preventing it from coagulating. There is some evidence to suggest that using plasma instead of serum may improve the reproducibility of experiments (168).

5.1 The Effects of Plasma from Patients with IPF on Different Cell Lines

5.1.1 Patient demographics of IPF patients compared to healthy control subjects

The first group of patients assessed were those with IPF. As discussed in more detail in the introduction, this group of patients develop fibrosis in the lungs but not in other organs. The underlying cause is unknown and patients develop fibrosis spontaneously and at a rapid pace (median mortality is just 3 years).

The plasma used was from patients recruited through the UK-BILD study. The demographic profile of these patients was compared to that of the healthy control subjects used. Whereas the UK-BILD proforma was completed for all ILD patients, limited data was available regarding healthy control subjects. However, the table below compares the demographic data that was available between the two groups. Of note, patients in the healthy control group were younger than those in the IPF group. Finding healthy control subjects can be difficult given the number of elderly people with co-morbidities. All patients used had a diagnosis of definite IPF according to ATS / ERS diagnostic guidelines and had a UIP pattern on HRCT scanning.

	IPF Patients (n=14)	**Healthy Controls (n=7)**	**Significant difference between groups**
Gender	Male 10 (71.4%) Female 4 (28.6%)	Male 4 (57.1%) Female 3 (42.9%)	ns
Age (years)	Median 68 (55-83)	Median 48 (42-58)	***p<0.0001
Ethnicity	Caucasian 14 (100%)	Unknown	N/A

Table 5-1 Demographic details for IPF patients and healthy controls. A Fisher's exact test was used to compare gender and an unpaired two-tailed t-test was used to calculate significance between age in the two groups. Healthy control subjects were significantly younger than patients with IPF. ns = no significant difference.

	IPF Patients
Time from ILD diagnosis (days)	Median 533.5 (Range 42 – 1826) 17.5 months (Range 1.4 – 60 months)
Smoking History (Pack year smoking history)	Never 3 (21%) Ex <20 3 (21%) >20 but <40 5 (36%) >40 3 (21%) Current 0 (0%)
Respiratory features	Clubbing 4 (29%) Crackles 11 (79%) Pulmonary hypertension 0 (0%) Malignancy history 0 (0%)

Table 5-2 ILD data regarding plasma from patients with IPF used to treat cells. Data collected includes time from ILD diagnosis, smoking history, diagnostic category and presence of respiratory features.

Interestingly patients had been diagnosed with IPF for a median of 1.5 years. The median time from diagnosis to death is estimated at around 3 years (14). It is therefore clear that the studied patients were well established in the course of their illness. No patients in the cohort were currently smoking but the majority (79%) were ex-smokers. All patients had been diagnosed by HRCT with a definite UIP pattern on the HRCT scan and therefore did not require diagnostic lung biopsy. On examination, end-inspiratory crackles were present in 79% and clubbing in 29% of cases respectively. No IPF patients had pulmonary hypertension, which may have its own unique cytokine profile.

5.1.2 The Effect of IPF Plasma Treatment on the Morphology of MRC5 Fibroblasts

Cells were treated directly with patient and healthy control plasma, as described in materials and methods section 2.3.2.3. Images were taken at 24, 48 and 72 hours to assess if there were any morphological changes induced by the patient plasma. The images given in the figures below are representative examples of the changes observed.

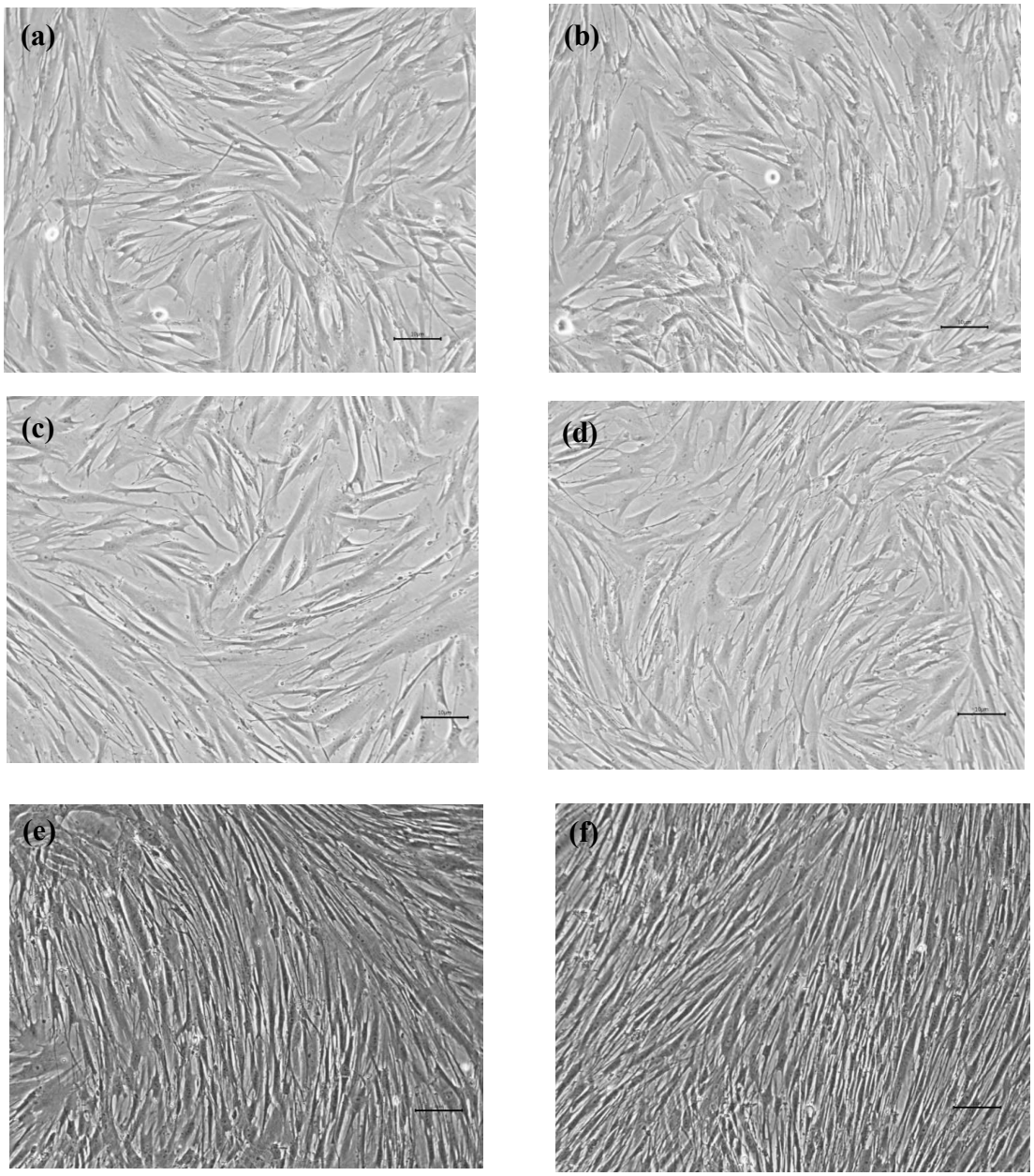

Figure 5-1 MRC5 cells treated over time course with 100ul plasma. (a) Cells treated with healthy control plasma for 24 hours, (b) Cells treated with IPF plasma for 24 hours, (c) Cells treated with healthy control plasma for 48 hours, (d) Cells treated with IPF plasma for 48 hours, (e) Cells treated with healthy control plasma for 72 hours, (f) Cells treated with IPF plasma for 72 hours. There were no differences observed in cell morphology between cells treated with healthy control plasma and IPF patient plasma. Magnification x10 objective lens, scale bar 10µm.

The above figures show that MRC5 fibroblasts proliferated well with the addition of human plasma. There did not appear to be any differences in cell morphology between MRC5 cells treated with plasma from healthy control subjects or those treated with plasma from IPF patients. However, after 72 hours, the plasma treated cells appeared more spindle shaped and less healthy when compared to cells grown with TCH or treated with TGF-β, shown in the previous chapter. The reason for this is unclear and immunocytochemistry, shown later in this chapter, was thus performed to assess these changes in more detail. There was the possibility of an increase in proliferation of the MRC5 cells treated with IPF plasma, although it was difficult to assess whether this was a true effect or based on variable factors when plating cells, or from taking pictures in different parts of the 6 well plate. Changes in proliferation may be subtle and it is difficult to assess visually across a few images in a 6 well plate. For this reason, cell proliferation was assessed using an alamar blue assay (see later).

5.1.3 The Effect of IPF Plasma Treatment on the Proliferation of MRC5 Fibroblasts

As previously described in materials and methods section 2.5, an alamar blue assay was used to assess cell viability and cell proliferation. Cells were treated with plasma from healthy controls or from IPF patients, and fluorescence measured at different time points to assess if there was an increase in the number of viable, proliferating cells. The results are shown in the figure below;

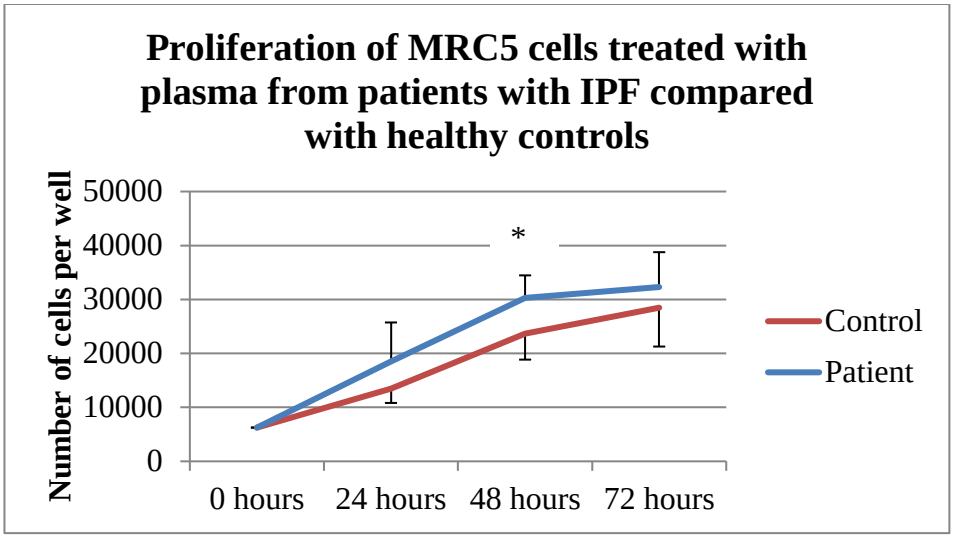

Figure 5-2 Proliferation of MRC5 cells, measured using an alamar blue assay, the red line represents wells treated with healthy control plasma (n=7) and the blue line represents wells treated with plasma from patients with IPF (n=14). There was increased proliferation of MRC5 cells treated with plasma from patients with IPF which was statistically significant after 48 hours. Results are expressed as mean values +/- SD. A two-way anova with Bonferroni post-test was performed for analysis, * $p<0.05$.

Figure 5-2 shows there was a general increase in proliferation of MRC5 fibroblasts treated with IPF patient plasma in comparison to healthy control plasma. However, this effect was only significant at 48 hours ($p<0.05$), although the trend was for an increase at all time points.

5.1.4 The Effect of 24 hours IPF Plasma Treatment on Gene Expression in MRC5 Fibroblasts

After images were obtained, RNA was extracted as described in materials and methods section 2.7. This RNA was then converted to cDNA, and then qPCR performed as previously described. The first genes to be investigated were those that build the ECM. These include *COL1A1*, *COL3A1* and *FN-EDA*. All genes were examined when cells were treated with TGF-β in the previous chapter and both *COL1A1* and *FN-EDA* were significantly upregulated by TGF-β treatment. *COL3A1* was not upregulated in this model, although it is implicated in fibrosis (77).

Individual points, representing a single patient result, were plotted as there was a large variation between subjects and this would not be fully recognised using a standard bar chart. This variation may be accounted for by variations in patient's ages, differences in their disease severity as well as differences in disease duration. For this reason, individual points were plotted to assess if there were not only trends between patients and controls but between individual patients as well. For example, if a patient was producing an increased amount of *COL1A1*, does that patient also produce more *FN-EDA*? These scatter plots allow for this variation to be investigated. As this study is only exploratory, the statistics were not corrected for multiple comparisons, therefore any p value must be interpreted with caution.

The values were plotted in relation to the mean value of the healthy control group. The values are presented in logarithmic base 2 form, this is a delta CT calculation to show the baseline of the gene in question, as there are variations in mRNA levels. In each of the plots, zero is a mean control and every one unit is a doubling of the mRNA levels. The data has been presented as dot plot to show the variation of the patient cohort.

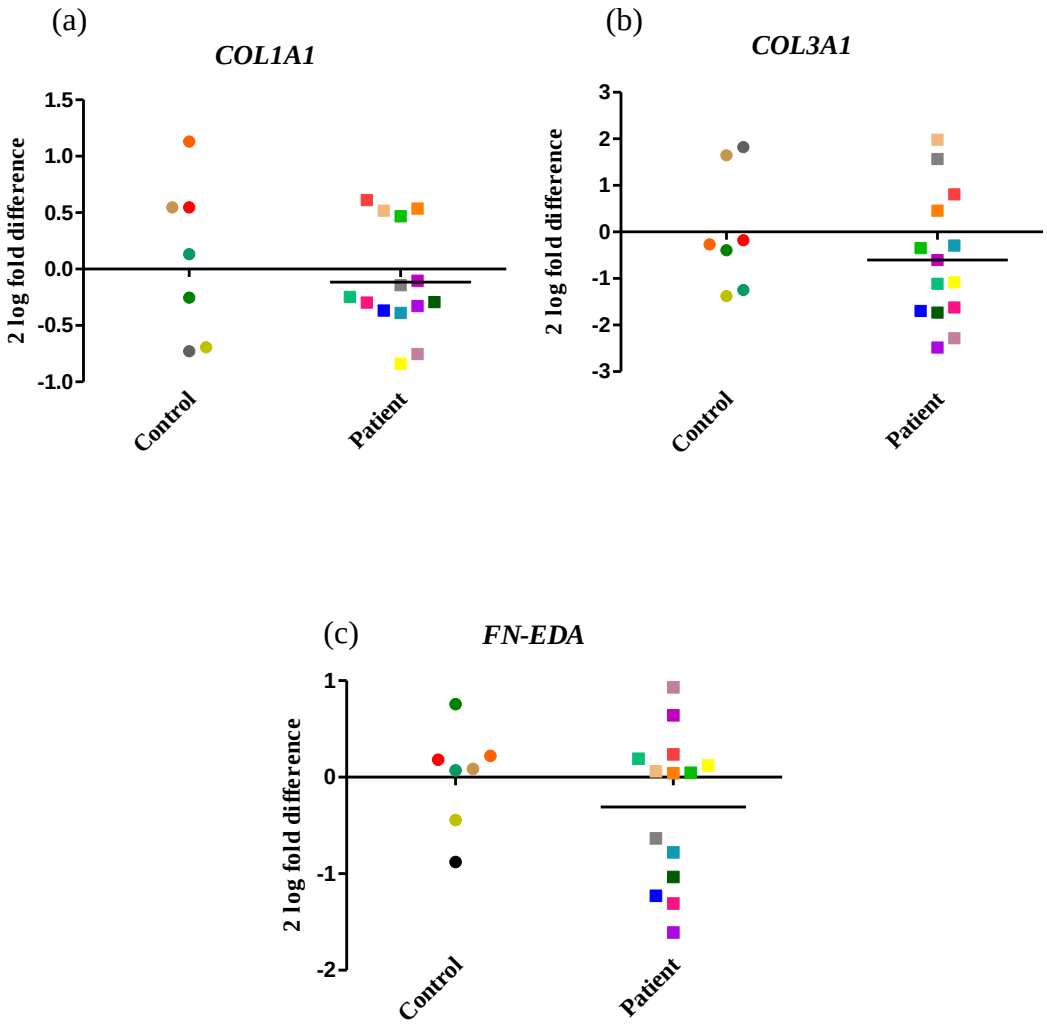

Figure 5-3 Two log of the fold difference values plotted individually for ECM genes showing healthy control values against those with IPF after treatment of cells for 24 hours. (a) *COL1A1*, (b) *COL3A1*, (c) *FN-EDA*. There were no significant differences for any of the ECM genes between cells treated with healthy control plasma and those treated with IPF plasma. Bar shows mean value for IPF patients. Unpaired two-tailed t-test performed for analysis.

There were no differences in the amount of *COL1A1*, *COL3A1* and *FN-EDA* produced by the MRC5 cells treated with IPF plasma for 24 hours compared to those cells treated with healthy control plasma. There was variation present between both control and patient groups but both produced similar changes in transcription levels of genes that form proteins in the ECM. The CCN genes were then evaluated in a

similar way, to assess if treatment with IPF plasma caused changes in these genes. The results are shown in the figure below;

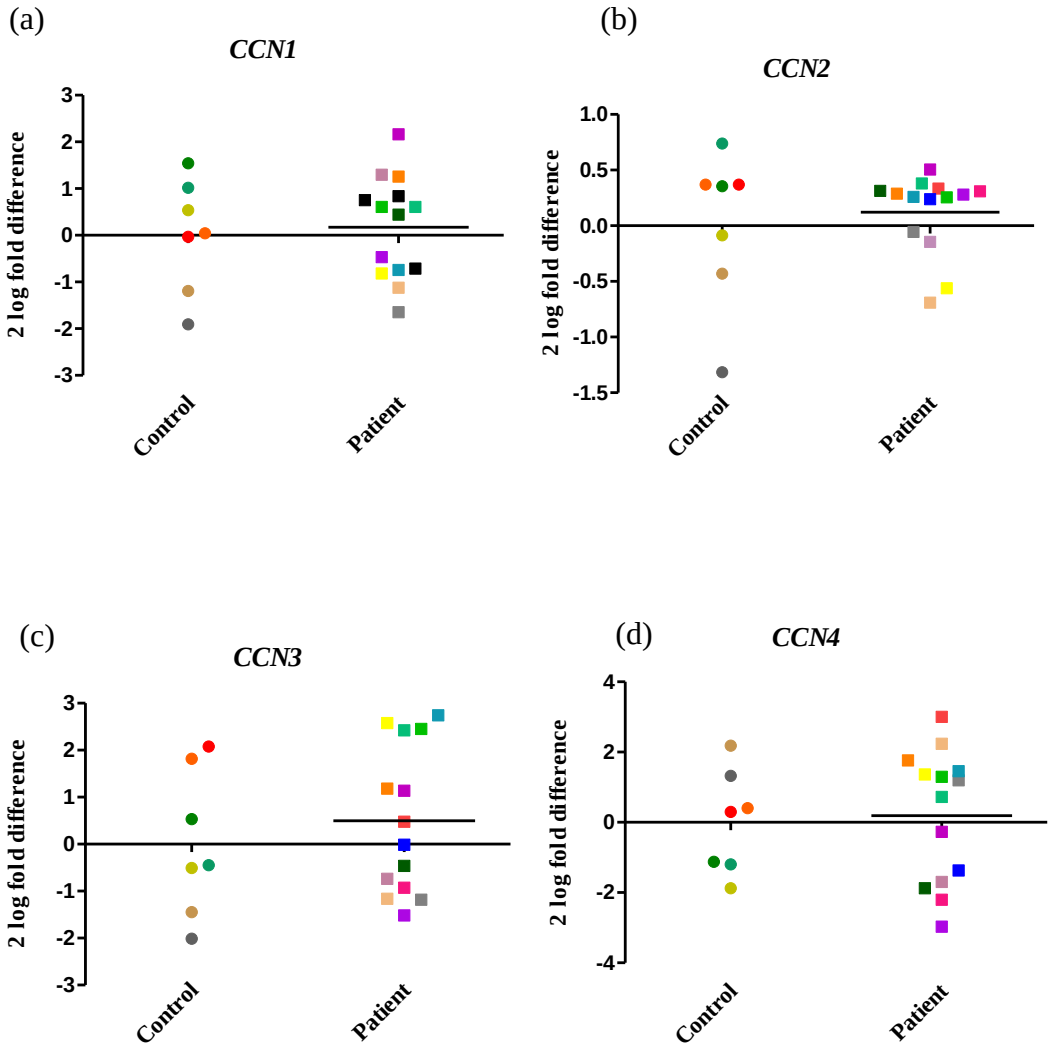

Figure 5-4 Two log of the fold difference values showing individual results for genes of the CCN family comparing healthy control plasma with IPF patient plasma after treatment of cells for 24 hours. (a) *CCN1*, (b) *CCN2*, (c) *CCN3*, (d) *CCN4*. There were no significant differences between the two groups. Bar shows mean value for IPF patients. Unpaired two-tailed t-test performed for analysis.

Figure 5-4 shows that there were no differences in transcription of *CCN1-4* between cells treated with plasma from healthy controls and those treated with plasma from IPF patients after 24 hours. As discussed in the introduction, it is recognised that

these genes interact and may exert opposing effects. As points were plotted individually there were no obvious patterns seen in individual patients. For example, patients producing more *CCN2* did not appear to be producing less *CCN3*. As no changes were seen within the genes encoding for the ECM proteins or within the CCN family, changes within other genes associated with fibrosis were also analysed.

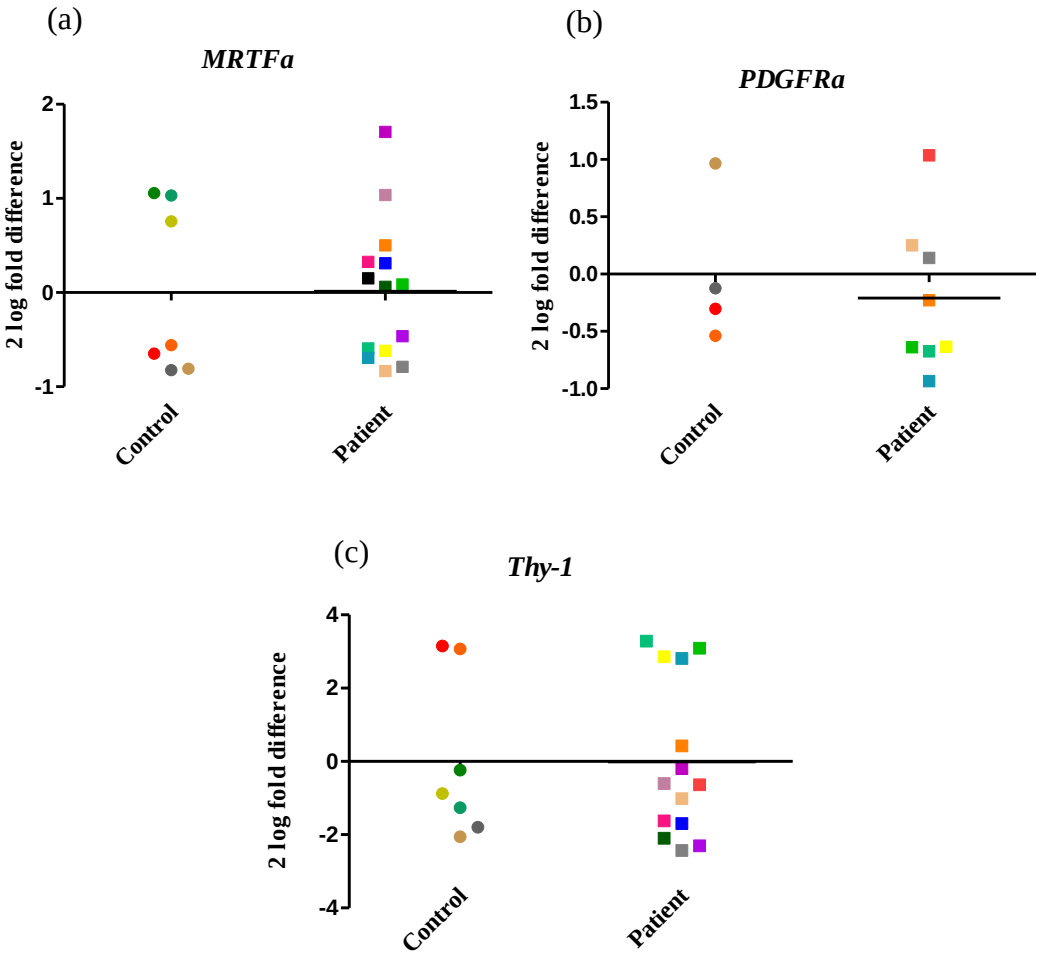

Figure 5-5 Two log of the fold difference values plotted individually for other genes relevant in fibrosis showing healthy control values against those with IPF after treatment of cells for 24 hours. (a) *MRTFa*, (b) *PDGFR-α*, (c) *Thy-1*. There were no differences between the other genes involved in fibrosis tested in the MRC5 cells. Bar shows mean value for IPF patients. Unpaired two-tailed t-test performed for analysis.

Figure 5-5 shows there was no change in *MRTFa*, a molecule that drives fibroblasts to become myofibroblasts. There was also no change in *PDGFR-α*, a receptor on the cell surface that may be expected to change as an early response to fibrosis. There were also no differences in transcription levels of *Thy-1*, a molecule that has been found to be downregulated in the fibroblastic foci of patients with IPF.

Given that changes may take longer than 24 hours to develop, this experiment was repeated at 48 and 72 hours. The data is not shown but changes were similar to those at 24 hours and no significant differences were present in any of the genes associated with fibrosis. It can therefore be concluded that treatment of MRC5 fibroblasts with plasma from patients with IPF induced no significant changes in transcription of any genes associated with pro-fibrosis, as assessed in this experimental model. It does, however, appear to induce an increase in proliferation of fibroblasts which is sustained to 72 hours. This increase in proliferation does not seem to be driven by any of the pro-fibrotic genes assessed above.

5.1.5 The Effect of IPF Plasma Treatment on the Morphology of A549 Epithelial Cells

A549 epithelial cells were treated with IPF patient plasma in a similar manner to the MRC5 fibroblasts above. Images were taken prior to RNA extraction at 24, 48 and 72 hours respectively.

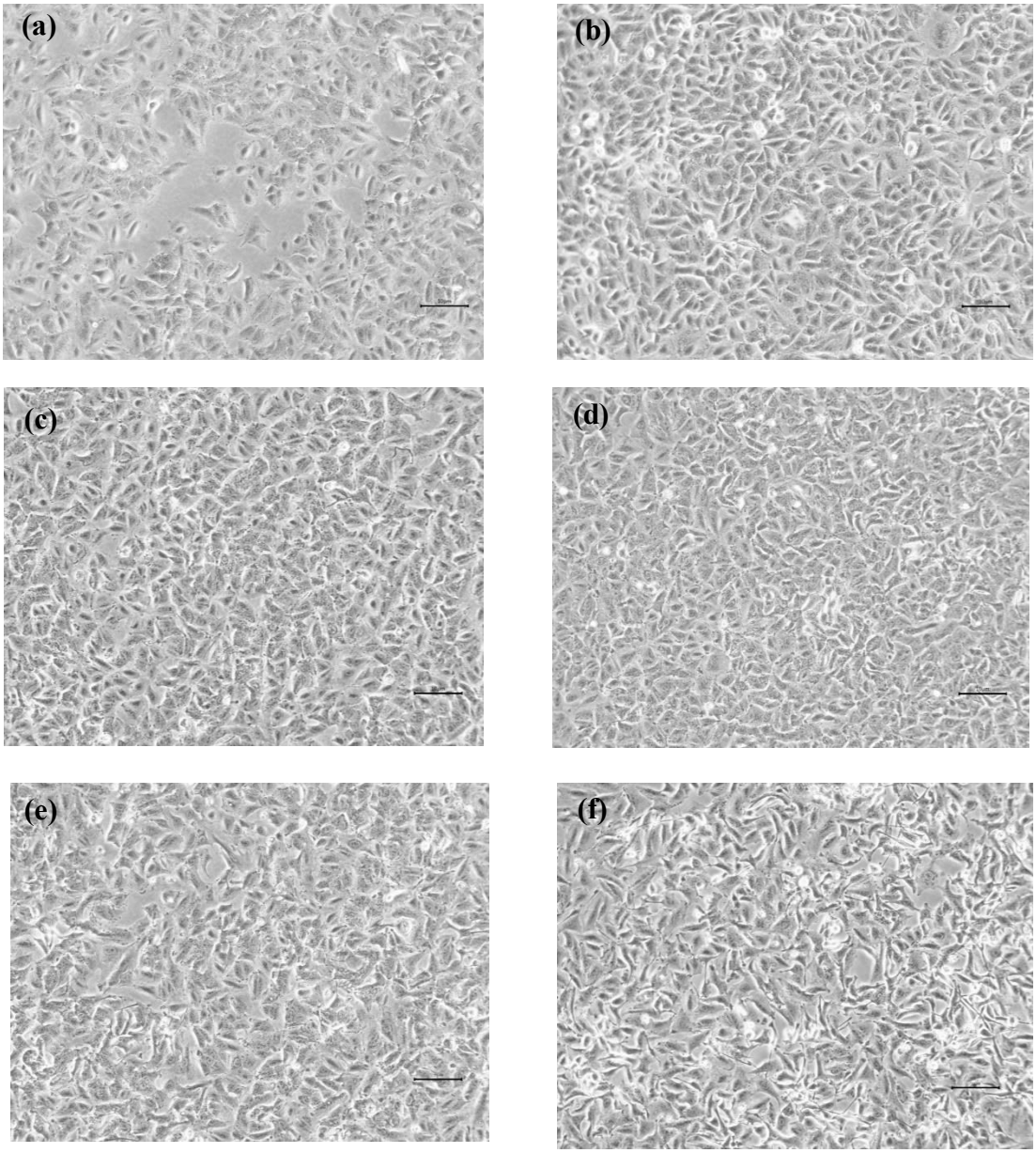

Figure 5-6 A549 epithelial cells treated over time course with plasma. (a) Cells treated with healthy control plasma for 24 hours, (b) Cells treated with IPF plasma for 24 hours, (c) Cells treated with healthy control plasma for 48 hours, (d) Cells treated with IPF plasma for 48 hours, (e) Cells treated with healthy control plasma for 72 hours, (f) Cells treated with IPF plasma for 72 hours. There were no obvious differences in the morphology of the epithelial cells between the two groups. Magnification x10 objective lens, scale bar 10µm.

Figure 5-6 shows that the A549 cells proliferated well with both healthy control plasma and IPF plasma. In most cases the cells were almost confluent after 48 hours. There were no obvious phenotypic changes between A549 cells in the 2 groups at any of the time points. To assess the possibility of an increase in cellular proliferation, cell growth was tested using an alamar blue assay.

5.1.6 The Effect of IPF Plasma Treatment on the Proliferation of A549 Epithelial Cells

An alamar blue assay was used to assess for cell proliferation. It has been shown in the previous chapter that the A549 cells do not respond to TGF-β by increasing proliferation. It was felt interesting to assess the effect that IPF patient plasma has on the growth rate of cells compared to healthy control plasma.

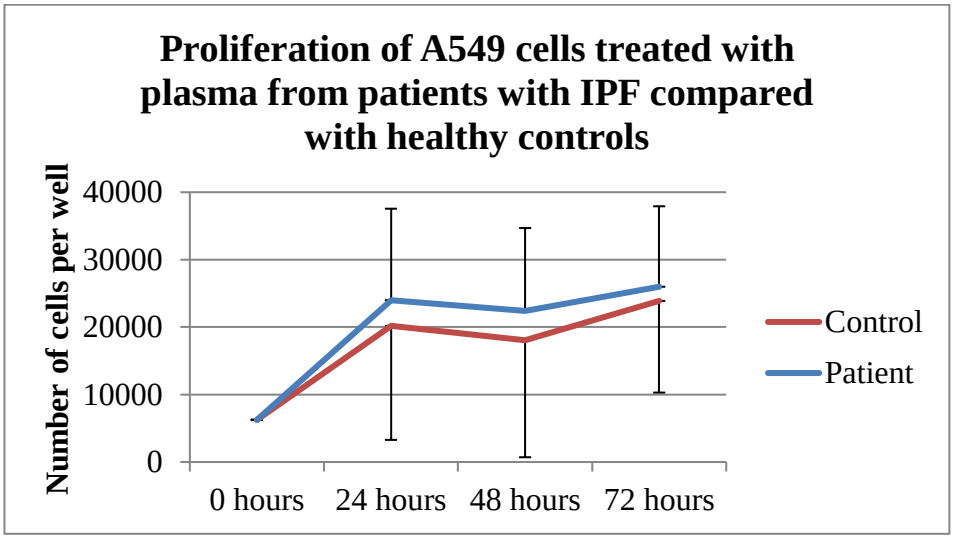

Figure 5-7 Proliferation of A549 cells, measured using an alamar blue assay. The red line represents wells treated with healthy control plasma (n=7) and the blue line represents wells treated with plasma from patients with IPF (n=14). There were no significant differences in proliferation between A549 cells treated with healthy control plasma and those treated with IPF plasma. Results are expressed as mean values +/- SD. Two-way anova with Bonferroni post-test was performed for analysis.

Figure 5-7 showed cellular proliferation of the A549 cells and there was no significant difference between cells treated with plasma from IPF patients versus that of healthy control subjects. However, there was a trend to an increase in proliferation of the A549 cells treated with patient plasma. This effect was present at 24 hours and sustained to 72 hours. There was a large amount of variation between subjects, so a much larger sample size would be needed to assess if this is a real difference.

5.1.7 The Effect of IPF Plasma Treatment on Gene Expression in A549 Epithelial Cells

A549 cells were treated with plasma from either IPF patients or from healthy control subjects. Images were taken and RNA extracted at 24 hours. qPCR was performed for genes involved in fibrosis. The first genes of interest were genes that encode for proteins that form the ECM including *COL1A1*, *COL3A1* and *FN-EDA*.

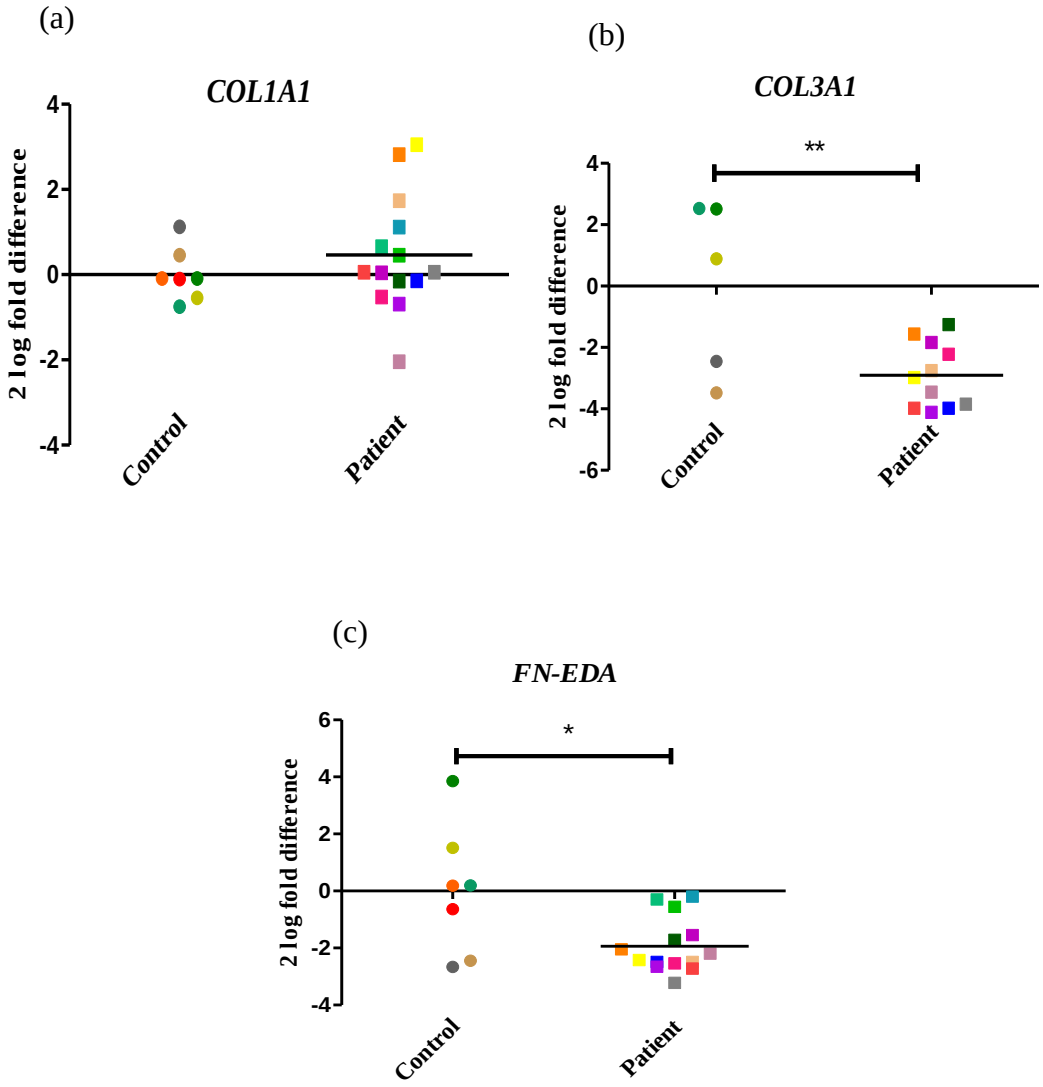

Figure 5-8 Two log of the fold difference values plotted individually for ECM genes showing A549 cells treated with healthy control plasma against those treated with plasma from IPF patients for 24 hours. (a) *COL1A1*, (b) *COL3A1*, (c) *FN-EDA*. Treatment with IPF plasma led to a significant reduction in expression of *COL3A1* and *FN-EDA*. Bar represents mean value for IPF patients. Unpaired two-tailed t-test performed for analysis, * $p<0.05$, ** $p<0.01$.

Figure 5-8 shows the individual values for genes that make up the ECM, comparing A549 cells treated with healthy control plasma versus cells treated with IPF plasma. After 24 hours there was no difference in *COL1A1* produced by either group. However, there was a reduction in *COL3A1* ($p<0.01$) with a corresponding decrease

in *FN-EDA* ($p<0.05$) in cells treated with plasma from IPF patients. This change was noted at 24 hours but when these genes were investigated at 48 and 72 hours (not shown) there were no significant differences seen, so any changes occurring in the genes appear to happen at an early stage, when cells are first treated with IPF plasma.

The transcription factors *Snail* and *Slug*, as well as the cell surface markers *E-cadherin* and *N-cadherin*, were thus studied to assess if EMT could explain the changes occurring in the cells.

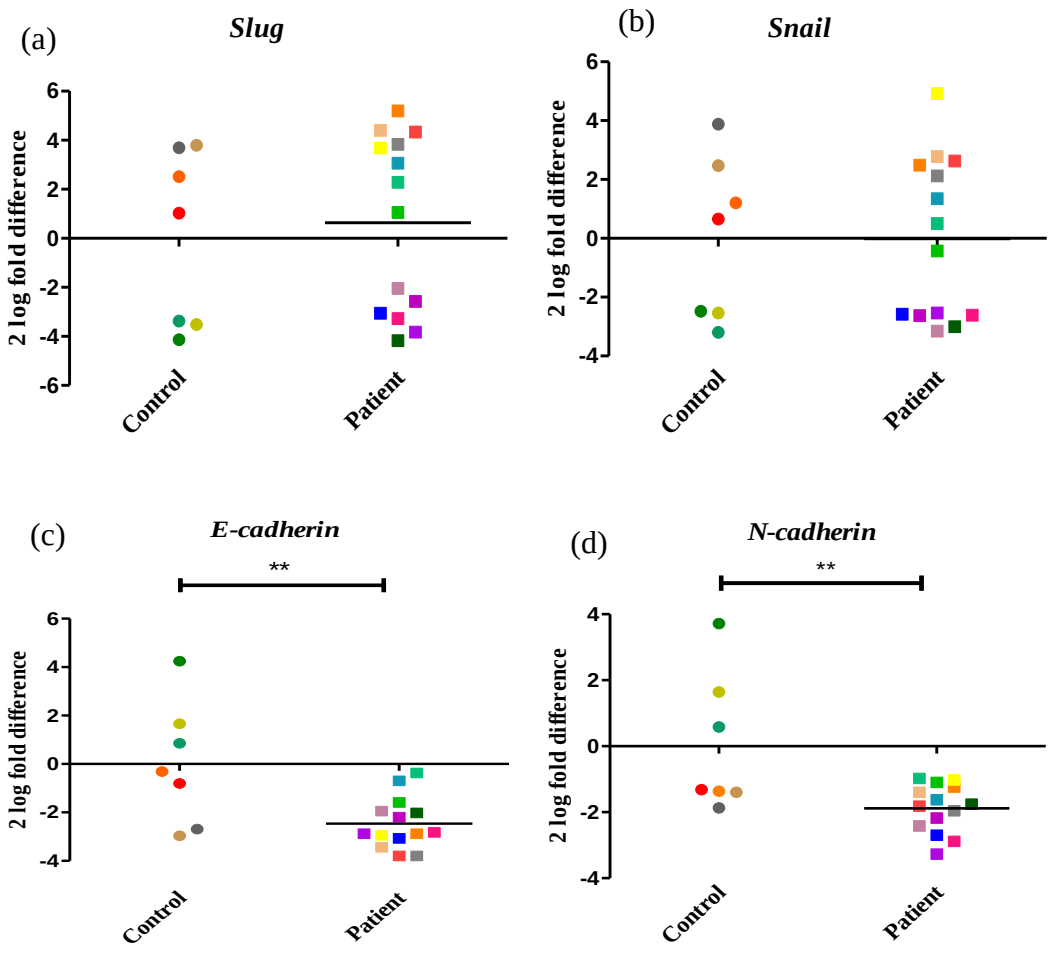

Figure 5-9 Two log of the fold difference values plotted individually for the transcription factors *Snail* and *Slug* and cell surface markers *E-cadherin* and *N-cadherin* showing healthy control values against those with IPF after treatment of A549 cells for 24 hours. (a) *Snail*, (b) *Slug*, (c) *E-cadherin*, (d) *N-cadherin*. There was a significant downregulation of *E-cadherin* and *N-cadherin* when cells were treated with IPF patient plasma. Bar represents mean value for IPF patients. Unpaired two-tailed t-test performed for analysis, ** $p<0.01$.

There were no changes in the transcription factors *Slug* and *Snail* between healthy controls and IPF patients. However, there was a significant downregulation ($p<0.01$) in *E-cadherin*, which is an early change occurring in cells undergoing EMT (108). However, there was also a decrease in *N-cadherin* ($p<0.01$) which does not usually occur in EMT, but may explain some of the changes seen in the transcription of *COL3A1* and *FN-EDA* which were downregulated, again changes that do not typically occur in EMT.

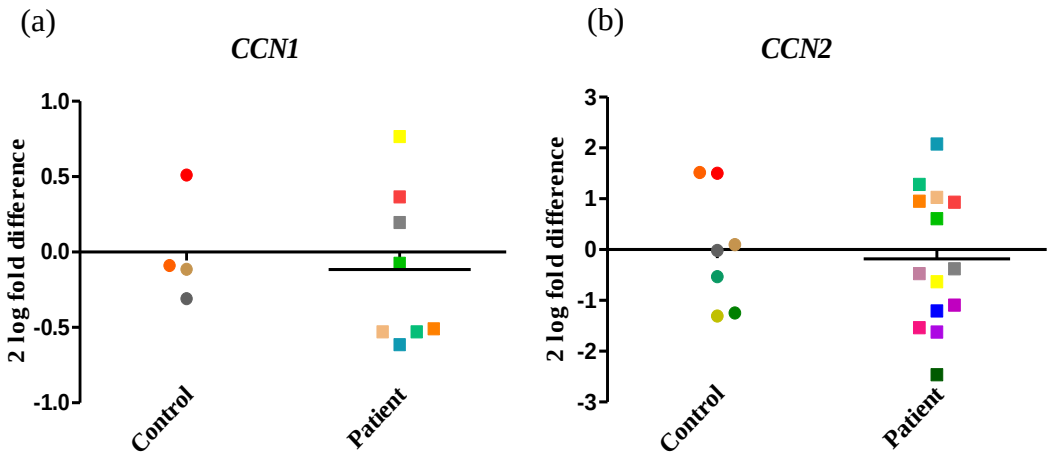

Figure 5-10 Two log of the fold difference values plotted individually for CCN genes showing healthy control values against those with IPF after treatment of A549 cells for 24 hours. (a) *CCN1*, (b) *CCN2*. There were no significant differences in *CCN1* or *CCN2* when cells were treated with IPF plasma. Bar represents mean value for IPF patients. Unpaired two-tailed t-test performed for analysis.

When the CCN family of genes were evaluated, there was no change in the CCN genes (*CCN1* or *CCN2*) after 24 hours of plasma treatment. This suggests that these genes were not responsible for any differences seen in the ECM proteins.

Overall, there were a number of significant differences in A549 cells treated with IPF plasma after 24 hours of treatment. This included a significant reduction in transcription of *COL3A1* ($p<0.01$) and *FN-EDA* ($p<0.05$). There were no corresponding changes in *COL1A1* at this time point. When the CCN family was explored, to assess if it was responsible for these changes, no significant differences were found. There was no change after 24 hours in the transcription factors *Snail* or *Slug*. There was also a significant reduction in *N-cadherin* ($p<0.01$), a marker on the surface of the cell that is increased when cells undergo EMT.

The cells were then examined after 48 and 72 hours to assess the trend at these later time points. The data is not shown but there were no significant differences between A549 cells treated with healthy control plasma and those treated with IPF plasma at these time points. The trend, however, was similar to the significant results with reductions in the ECM proteins when treated with IPF plasma.

5.2 The Effects of Treatment with Plasma from Patients with SSc-ILD on Different Cell Lines

As there were directionally surprising and small degree only changes noted between IPF patients and healthy control subjects in mRNA of several genes involved in fibrosis, this experiment was repeated using plasma from patients with diffuse SSc. The reasons for this choice of patient group included;

(a) IPF is a disease characterised by a pro-fibrotic response in the lungs only, i.e. no other organs are targeted for fibrotic changes. It could thus be hypothesised that the factors triggering and propagating pro-fibrosis are localised solely to the lungs, with only very small quantities circulating in the affected patient's plasma. On the other hand, diffuse SSc is recognised to also cause fibrosis of the skin and other internal organs, including the kidneys, lungs and GI tract. It is therefore possible that higher levels of pro-fibrotic cytokines would be circulating in the plasma of SSc patients, to have an effect on so many distant organs other than the lungs.

(b) Results from section 1 show that the IPF population used is likely homogeneous, and that a diagnosis of IPF is likely correct and reliable. Similarly, diffuse SSc is likely to be a robust diagnosis as the clinical features are usually clearly apparent, so that SSc is unlikely to be misdiagnosed.

(c) SSc-ILD is usually associated with an NSIP pattern on HRCT (169) but a small proportion of patients have a UIP pattern making this a useful comparison group. It may explain the differences in mechanisms that may give similar HRCT appearances to those of IPF.

5.2.1 Patient demographics of SSc patients with ILD

The table below shows the demographic data available for patients with SSc-ILD and the healthy controls. Again, the UK-BILD proforma had been completed for all patients with SSc-ILD meaning that there was more data available for these patients. Only limited data was available for the healthy control patients.

	Healthy Controls used for qPCR experiments (n=2)	**SSc-ILD Patients used for qPCR experiments (n=4)**	**Significant difference between groups**
Gender	Male 1 (50%) Female 1 (50%)	Male 1 (25%) Female 3 (75%)	ns
Age (years)	34.5 (Range 31-38)	62 (Range 46-76)	ns
Ethnicity	Unknown	Caucasian 14 (100%)	N/A

Table 5-3 Demographic details of SSc patients and healthy controls used to assess changes in mRNA transcription. This compares demographic data available for gender, age and ethnicity. A Fisher's exact test was used to compare gender and an unpaired two-tailed t-test was used to calculate significance between age in the two groups. ns = no significant difference.

	Healthy Controls used for Proliferation experiments (n=3)	**SSc-ILD Patients used for Proliferation experiments (n=10)**	**Significant difference?**
Gender	Male 1 (33%) Female 2 (66%)	Male 1 (10%) Female 9 (90%)	ns
Age (years)	33 (Range 31-38)	55.5 (Range 46-76)	**p<0.01
Ethnicity	Unknown	Caucasian 10 (100%)	N/A

Table 5-4 Demographic data for SSc patients and healthy controls used in the cell proliferation experiment. This compares demographic data available for gender, age and ethnicity. A Fisher's exact test was used to compare gender and an unpaired two-tailed t-test was used to calculate significance between age in the two groups. Healthy controls were significantly younger than the SSc-ILD patients. ns = no significant difference

	SSc-ILD Patients in qPCR experiments (n=4)	**SSc-ILD Patients in Proliferation experiments (n=10)**
Time from ILD diagnosis (days)	Median 766 (Range 430-1978)	Median 860.5 (Range 66-2849)
Smoking history (Pack year smoking history)	Never 3 (75%) Ex <20 0 (0%) >20 but <40 1 (25%) >40 0 (0%) Current 0 (0%)	Never 6 (60%) Ex <20 2 (20%) >20 but <40 1 (10%) >40 1 (10%) Current 0 (0%)
SSc Diagnostic Category	Diffuse SSc 4 (100%) Limited SSc 0 (0%)	Diffuse SSc 10 (100%) Limited SSc 0 (0%)
CTD features	Raynaud's 3 (75%) Arthralgias 2 (50%) Sclerodactyly 3 (75%) Calcinosis 0 (0%)	Raynaud's 8 (80%) Arthralgias 5 (50%) Sclerodactyly 6 (60%) Calcinosis 0 (0%)

	Raised CK 0 (0%) Mechanics hands 0 (0%) Myalgias 0 (0%) Periungal erythema 1 (25%) Telangiectasia 1 (25%)	Raised CK 0 (0%) Mechanics hands 0 (0%) Myalgias 1 (10%) Periungal erythema 3 (30%) Telangiectasia 1 (10%)
Respiratory features	Clubbing 0 (0%) Crackles 3 (75%) Pulmonary hypertension 0 (0%) Malignancy 0 (0%)	Clubbing 0 (0%) Crackles 7 (70%) Pulmonary hypertension 0 (0%) Malignancy 1 (10%)

Table 5-5 Collected ILD data regarding the SSc patients. Data collected includes time from ILD diagnosis, smoking history, diagnostic category and presence of CTD or respiratory features.

5.2.2 The Effect of Plasma from Patients with SSc-ILD on the Morphology of MRC5 Fibroblasts

Using methods described for treating cell lines with plasma, described in section 2.3.2.3, MRC5 cells were treated with plasma from healthy control subjects or that from patients with diffuse SSc-ILD. Images were taken at 24, 48 or 72 hours and are shown in the figure below.

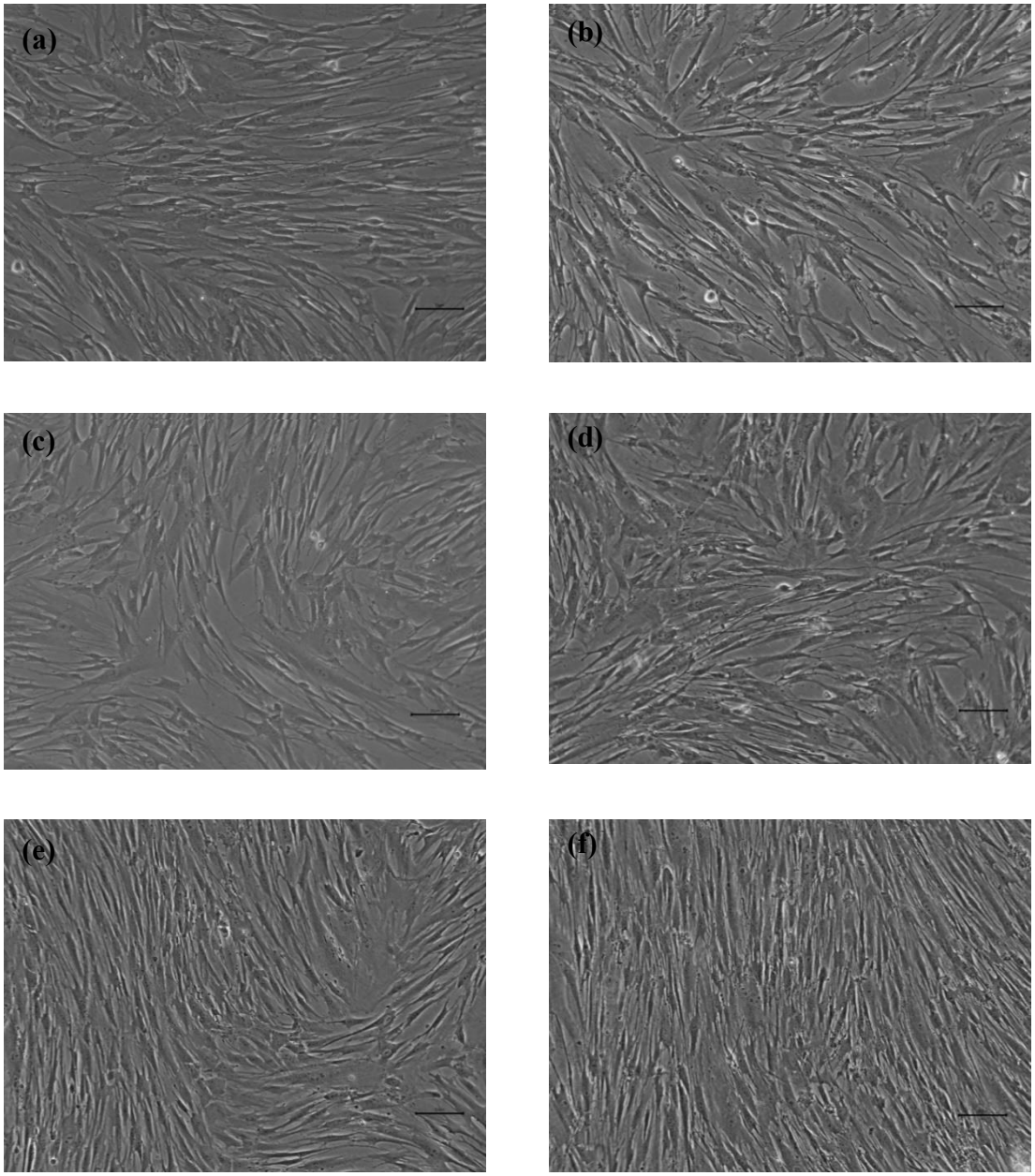

Figure 5-11 MRC5 cells treated over time course with healthy control or diffuse SSc plasma. (a) Cells treated with healthy control plasma for 24 hours, (b) Cells treated with SSc patient plasma for 24 hours, (c) Cells treated with healthy control plasma for 48 hours, (d) Cells treated with SSc patient plasma for 48 hours, (e) Cells treated with healthy control plasma for 72 hours (f) Cells treated with SSc patient plasma for 72 hours. There were no obvious differences in cell morphology between cells treated with healthy control plasma and those treated with SSc-ILD plasma at any time point. Magnification x10 objective lens, scale bar 10µm.

There were no obvious changes in MRC5 cell morphology between cells treated with healthy control plasma and those treated with plasma from patients with SSc-ILD. The cells appeared over-confluent after 72 hours which is similar to the effects after treatment with IPF plasma. It is unclear whether there is a difference in proliferation of the cells, and so a further experiment was undertaken to assess for proliferation.

5.2.3 The Effect of Plasma from Patients with SSc-ILD on the Proliferation of MRC5 Fibroblasts

An alamar blue assay was undertaken to assess for cell health and proliferation of MRC5 fibroblasts when treated with plasma from patients with diffuse SSc. The results are shown in the figure below;

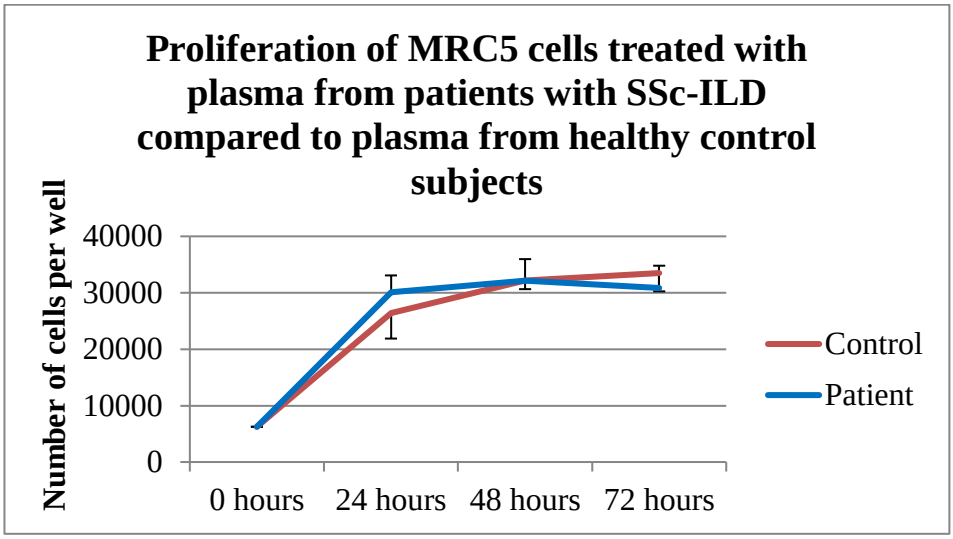

Figure 5-12 Proliferation of MRC5 fibroblasts measured with alamar blue, when treated with plasma from healthy, control subjects (represented by red line, n=3) in comparison to cells treated with SSc patient plasma (represented by blue line, n=10). There were no significant differences in proliferation of MRC5 cells when cells were treated with healthy control plasma or SSc-ILD patient plasma. Results are expressed as mean values +/- SD. Two-way anova with Bonferroni post-test was performed for analysis.

There was little or no difference in proliferation between cells treated with healthy control plasma and those treated with diffuse SSc patient plasma. Cells probably reached maximum confluency in the 96 well plate by 48 hours, so it was difficult to interpret cell proliferation past this point but at 72 hours the cells did remain healthy and viable, despite the phenotypic changes shown in more detail in the figures below.

5.2.4 Immunolocalisation of Thy-1 produced in MRC5 Fibroblasts Treated with Healthy Control Plasma Compared with Plasma from Patients with IPF and with SSc-ILD over 48 hours

To assess the morphology of the MRC5 cells treated with plasma in greater detail and the localisation of proteins involved in fibrosis, immunocytochemistry was performed. MRC5 cells were plated in 6 well plates and treated with patient plasma for 48 hours. After 48 hours cells were fixed, permeabilised and stained for phalloidin, Thy-1 and nuclear DAPI. This staining is shown in the figure below;

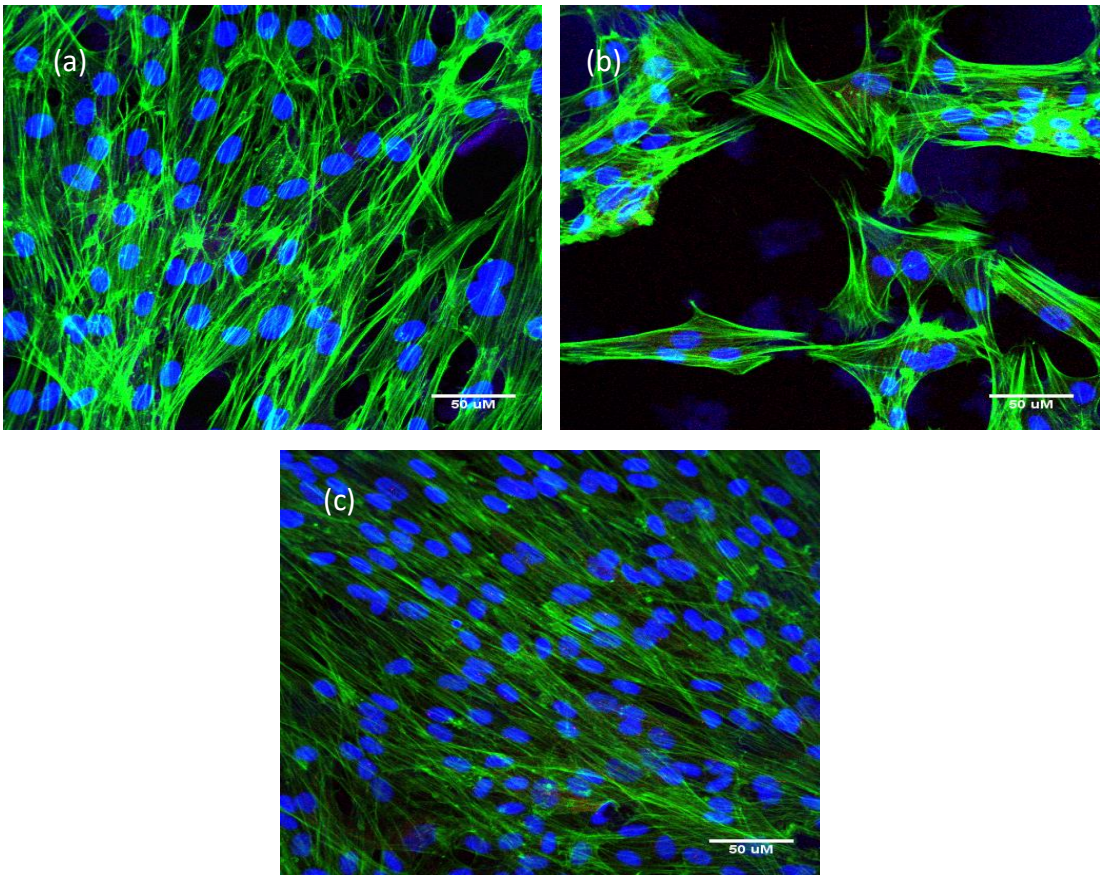

Figure 5-13 MRC5 cells treated with plasma and stained for Thy-1. Green represents phalloidin staining, red is Thy-1 staining and nuclei are stained blue. (a) Healthy control plasma, (b) Plasma from patient with IPF, (c) Plasma from patient with diffuse SSc. The images above are given as representative examples. There was very little Thy-1 staining but the images show the changes in the MRC5 fibroblasts that have become more spindle-shaped. Magnification x40 objective lens, scale bar 50µm.

The images show that very little Thy-1 (represented by red staining) was produced by cells either treated with healthy control plasma, plasma from IPF patients or those with SSc-ILD. However, the phalloidin staining in this image shows the change in the morphology of MRC5 cells after treatment with plasma for 48 hours, from healthy controls or from patients with ILD, very clearly. This shows that the cytoplasm appeared more spindle shaped. There were definite changes in the cytoplasm of the cell, however, this occurred in the cells treated with healthy control plasma or those treated with plasma from patients with ILD, suggesting that it is the

plasma treatment that changed the cell morphology not a secreted circulating factor from patients with a particular systemic disease.

5.2.5 Immunolocalisation of COL1A1 Produced by MRC5 Fibroblasts Treated with Healthy Control Plasma Compared with Plasma from Patients with IPF and with SSc-ILD

In a similar manner MRC5 cells were stained for COL1A1. The results of this staining are shown in the figures below;

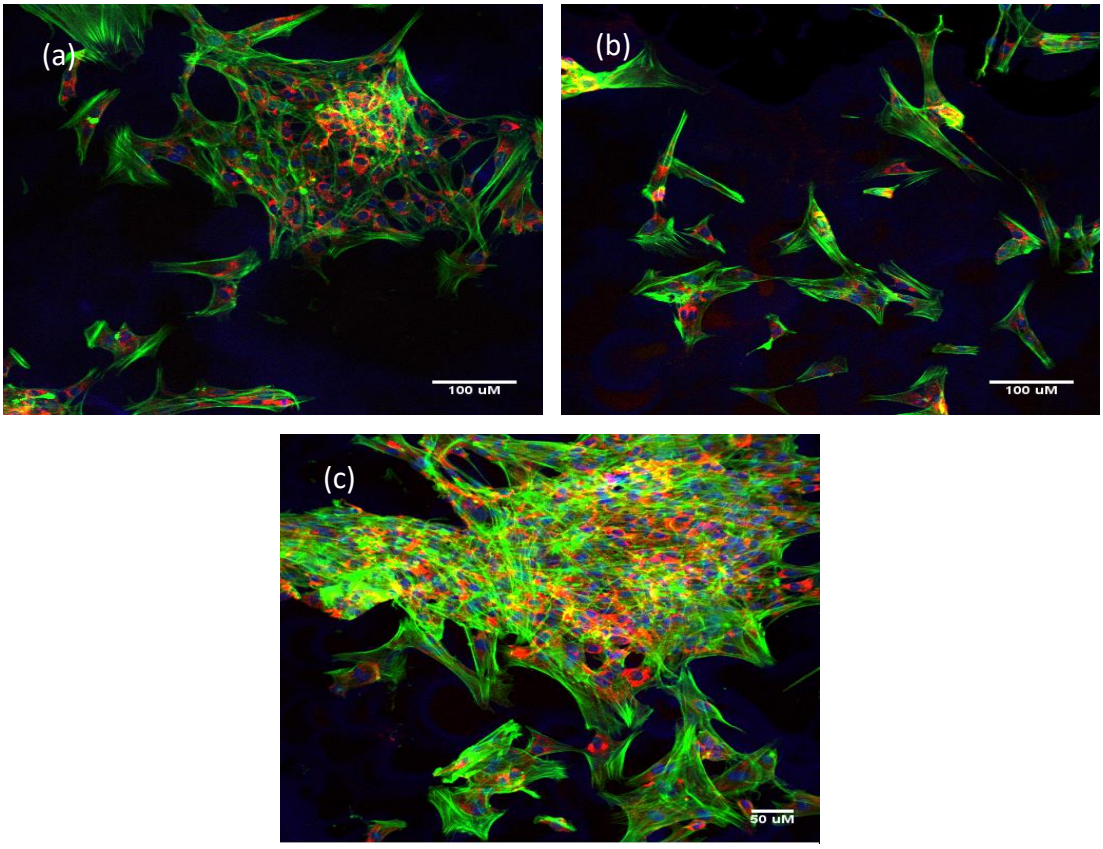

Figure 5-14 MRC5 cells treated with plasma and stained for COL1A1. Green represents phalloidin staining, blue is nuclear staining and red is COL1A1. (a) Healthy control plasma, (b) Plasma from patient with IPF, (c) Plasma from patient with SSc-ILD. Cells had become more disorganised with plasma treatment but were still producing COL1A1. Magnification x20 objective lens, scale bar 100µm.

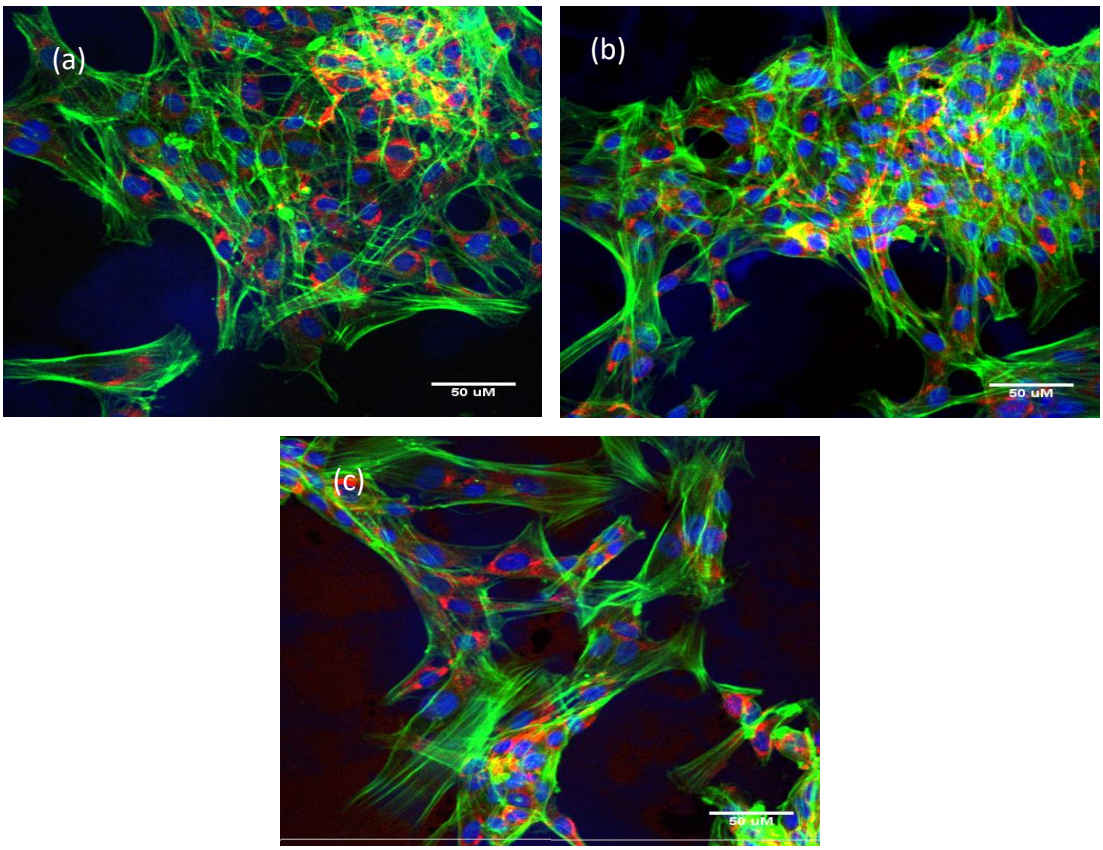

Figure 5-15 MRC5 cells treated with plasma and stained for COL1A1. (a) Healthy control plasma, (b) Plasma from patient with IPF, (c) Plasma from patient with diffuse SSc. This figure shows that there was no obvious difference in the quantity of COL1A1 produced by the cells when treated with different patient plasma. Magnification x40 objective lens, scale bar 50µm.

Figure 5-14 and Figure 5-15 demonstrate that cells became disorganised after treatment with human plasma. Although the cytoplasm becomes more spindle shaped, the MRC5 cells treated with healthy plasma or plasma from ILD patients of either subgroup continued to produce COL1A1. There did not appear to be an appreciable difference in the amount of COL1A1 that was produced, which is similar to the changes seen in mRNA transcription.

5.2.6 Immunolocalisation of α-SMA Produced by MRC5 Fibroblasts Treated with Healthy Control Plasma Compared with Plasma from Patients with IPF and with SSc-ILD

MRC5 cells were stained for α-SMA to assess if treatment with plasma from ILD patients caused an increase in production of this protein. Results are shown in the figure below;

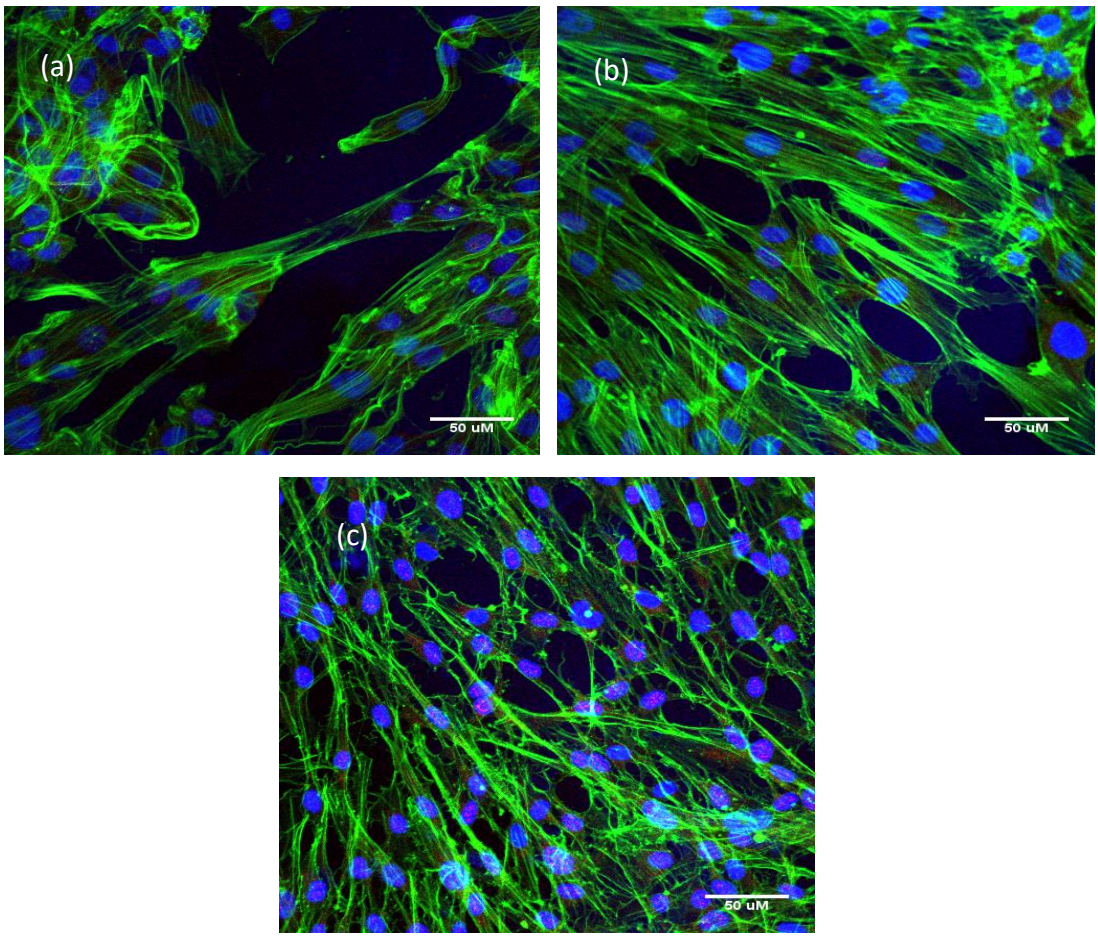

Figure 5-16 MRC5 cells treated with plasma and stained for α-SMA. Green represents phalloidin staining, blue is nuclear staining and red is α-SMA. (a) Healthy control plasma, (b) Plasma from patient with IPF, (c) Plasma from patient with SSc-ILD. There was no difference in the amount of α-SMA produced by MRC5 cells whether treated with healthy control plasma, IPF plasma or SSc-ILD plasma. Magnification x40 objective lens, scale bar 50µm.

Again, Figure 5-16 shows that the MRC5 cells remained disorganised after treatment with plasma. There did not appear to be any difference in the amount of αSMA produced in either patient group after 48 hours of treatment.

5.2.7 The Effect of SSc-ILD Plasma Treatment on Gene Expression in MRC5 Fibroblasts

MRC5 cells were plated in 6 well plates and treated with plasma from healthy control subjects or plasma from patients with SSc-ILD. After images were taken, RNA was extracted at 24 and 48 hours. The figures below show changes in gene expression after 24 hours.

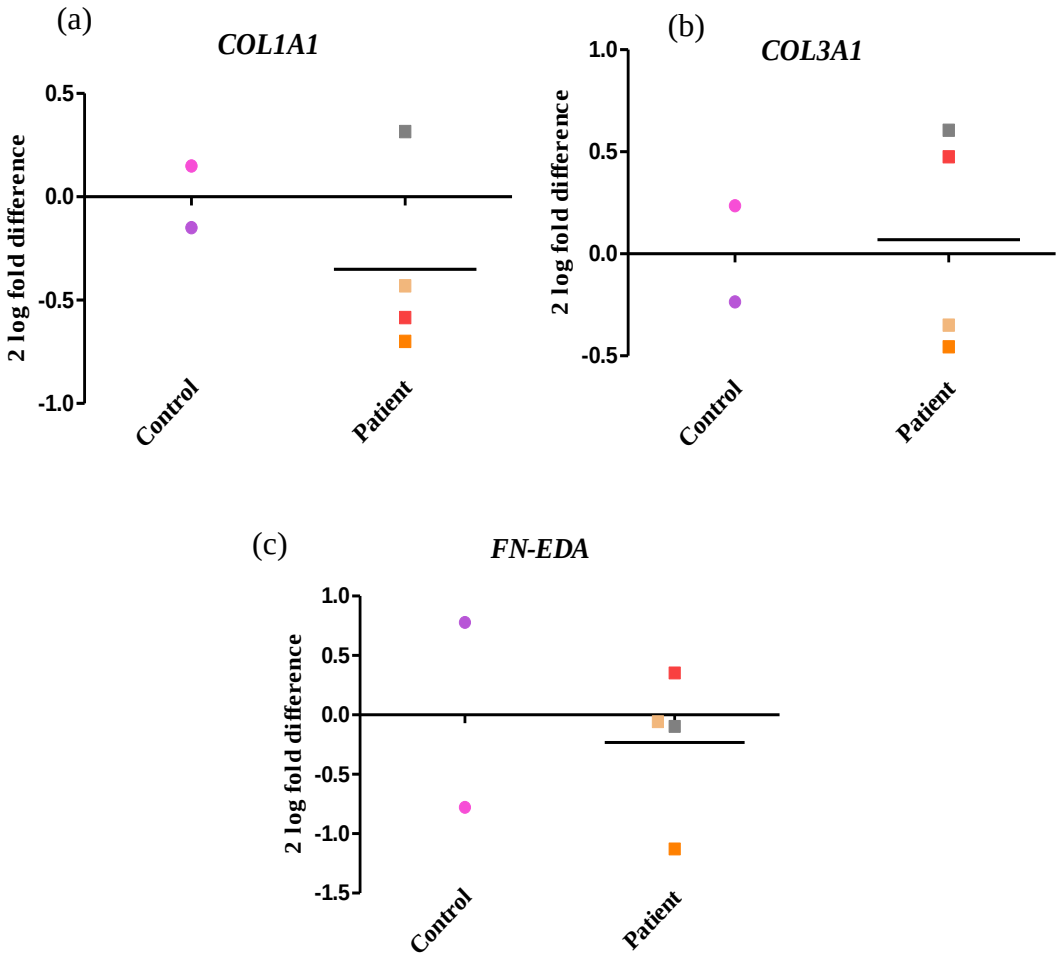

Figure 5-17 Two log of the fold difference values plotted individually for ECM genes showing MRC5 cells treated with healthy control plasma against those treated with plasma from patients with SSc-ILD for 24 hours. (a) *COL1A1*, (b) *COL3A1*, (c) *FN-EDA*. There were no significant differences in any of the ECM genes when MRC5 cells were treated with plasma from patients with SSc-ILD. Bar represents mean value for SSc-ILD patients. Unpaired two-tailed t-test performed for analysis.

There were large variations between the results arising from patient and control plasmas. It was thus difficult to draw conclusions from this data particularly when such a small number of subjects were studied. However, there were no significant differences in production of any of the genes for ECM proteins after 24 hours of treatment using diffuse SSc-ILD patient plasma in comparison to treatment with healthy control plasma.

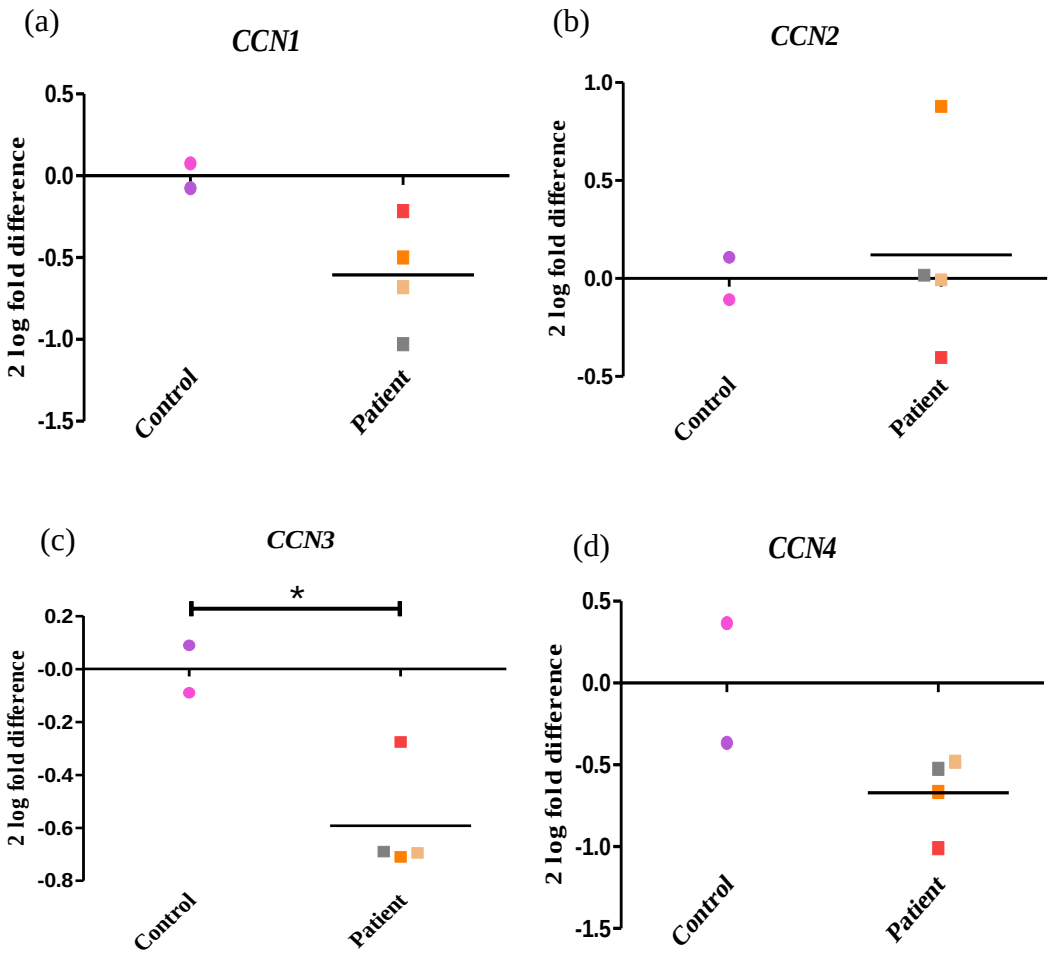

Figure 5-18 Two log of the fold difference values plotted individually for the CCN genes showing MRC5 cells treated with healthy control plasma against those treated with plasma from patients with SSc-ILD for 24 hours. (a) *CCN1*, (b) *CCN2*, (c) *CCN3*, (d) *CCN4*. There was a significant downregulation in expression of *CCN3* in cells treated with SSc-ILD plasma. Bar represents mean value for patients with SSc-ILD. Unpaired two-tailed t-test performed for analysis, * $p<0.05$.

The CCN family of genes was then assessed to see if there were any noticeable differences in these proteins after 24 hours treatment. There appeared to be a slight downregulation in *CCN1* although this did not meet significance. This was associated with a significant reduction ($p<0.05$) in *CCN3* in cells treated with SSc-ILD plasma. There appeared to be a corresponding decrease in *CCN4* in cells treated with plasma from patients with SSc-ILD although this was non-significant.

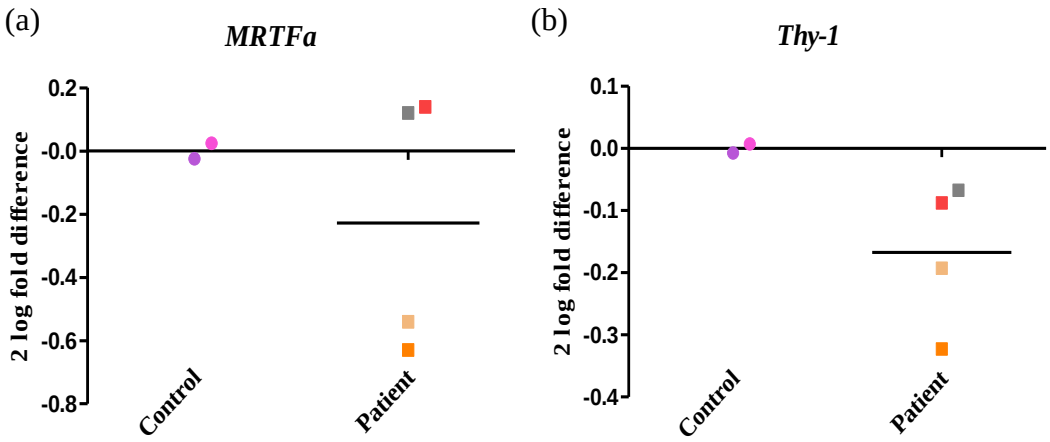

Figure 5-19 Two log of the fold difference values plotted individually for other genes involved in fibrosis showing MRC5 cells treated with healthy control plasma against those treated with plasma from patients with SSc-ILD for 24 hours. (a) *MRTFa*, (b) *Thy-1*. There was no significant difference in either gene in MRC5 cells treated with SSc-ILD plasma. Bar represents mean value for patients with diffuse SSc. Unpaired two-tailed t-test performed for analysis.

Figure 5-19 shows no significant difference between the production of *MRTFa* or *Thy-1* in those treated with healthy control plasma or SSc-ILD patient plasma.

Overall, treatment of MRC5 cells with plasma from patients with diffuse SSc caused a significant down regulation of CCN3 but very little change in the other genes associated with fibrosis. It is difficult to draw strong conclusions from this data as only very small numbers of healthy control subjects and patients with diffuse SSc were compared. When the same patients were analysed after 48 or 72 hours there were no significant differences found between healthy controls and patients with SSc-ILD in any of the fibrosis genes examined, suggesting that no differences are occurring at the later time points.

This corresponds to the changes seen in MRC5 cells treated with IPF patient plasma, where very little difference in mRNA production occurred. The A549 epithelial cells were then assessed to see if any changes were induced in this cell type.

5.2.8 The Effect of Plasma from Patient with SSc-ILD on the Morphology of A549 Epithelial Cells

In a similar way, A549 cells were plated and treated with plasma from patients with SSc-ILD or healthy control plasma for 24, 48 and 72 hours. The figure below shows representative images taken at each time point.

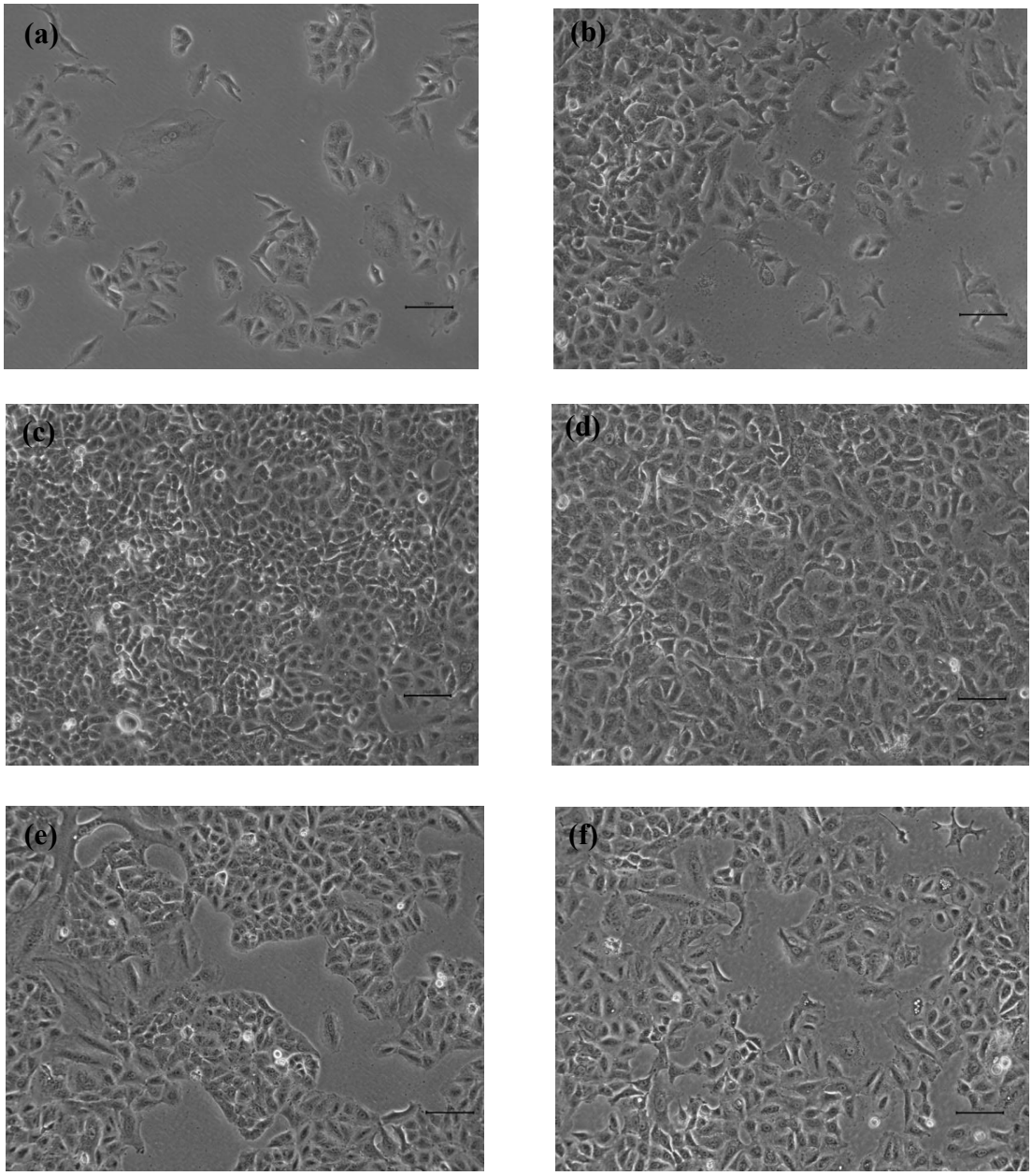

Figure 5-20 A549 cells treated over time course with healthy control or SSc-ILD plasma. (a) Cells treated with healthy control plasma for 24 hours, (b) Cells treated with SSc patient plasma for 24 hours, (c) Cells treated with healthy control plasma for 48 hours, (d) Cells treated with SSc patient plasma for 48 hours, (e) Cells treated with healthy control plasma for 72 hours (f) Cells treated with SSc patient plasma for 72 hours. There were no differences in epithelial cell morphology between cells treated with healthy control plasma and those treated with plasma from patients with SSc-ILD. Magnification x10 objective lens, scale bar 10µm.

There did not appear to be any obvious changes in morphology of A549 cells treated with SSc-ILD patient plasma. Cells appeared most confluent at 48 hours in both patient and control wells. At 72 hours cells appeared less confluent but it was unclear whether this was due to cell death or variation within the well. A proliferation assay was undertaken to assess this further.

5.2.9 The Effect of Plasma from Patients with SSc-ILD on the Proliferation of A549 Epithelial Cells

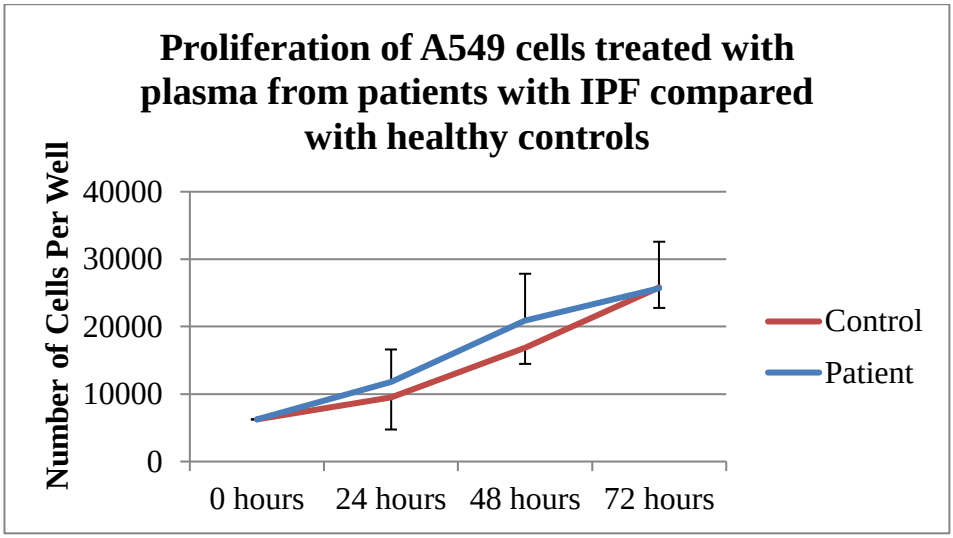

Figure 5-21 Proliferation of A549 epithelial cells measured with alamar blue, when treated with plasma from healthy, control subjects (represented by red line, n=3) in comparison to cells treated with plasma from patients with SSc-ILD (represented by blue line, n=10). A549 cells appeared to proliferate at a similar rate whether cells were treated with healthy control plasma or SSc-ILD plasma. Results are expressed as mean values +/- SD. Two-way anova with Bonferroni post-test was performed for analysis.

There were no significant differences in proliferation when A549 cells were treated with plasma from patients with SSc-ILD compared to healthy control plasma. Cells appeared to grow consistently throughout the 72 hours, with no appreciable difference between the two groups.

5.2.10 Immunolocalisation of α-SMA produced by A549 Epithelial Cells Treated with Healthy Control Plasma Compared with Plasma from Patients with SSc-ILD

A549 cells were stained for αSMA to assess whether there was an upregulation of this protein with plasma treatment, suggesting EMT was occurring.

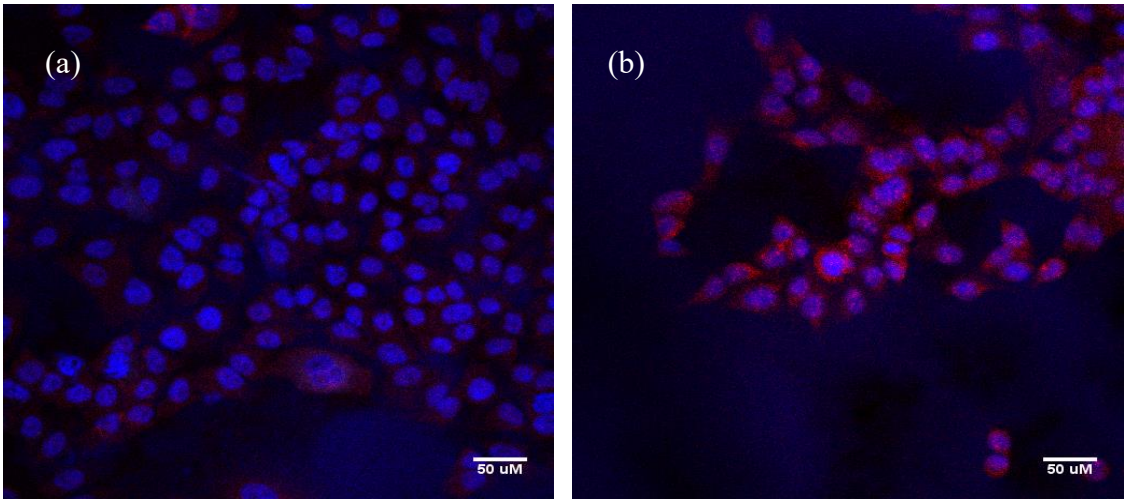

Figure 5-22 A549 cells treated with plasma and stained for αSMA. Blue is nuclear staining and red is αSMA. (a) Healthy control plasma, (b) Plasma from patient with SSc-ILD. There appeared to be more α-SMA produced in the A549 cells treated with SSc-ILD plasma, as represented by increased red staining in image (b). Magnification x40 objective lens, scale bar 100µm.

Figure 5-22 shows that A549 cells produced αSMA when treated with patient plasma, and there appeared to be more αSMA produced by A549 cells treated with plasma from patients with SSc-ILD compared to those treated with healthy control plasma. This was then compared to qPCR data available for the genes involved in production of the ECM, described below.

5.2.11 The Effect of SSc-ILD Plasma Treatment on Gene Expression in A549 Epithelial Cells

RNA was extracted after treatment of the A549 cells for 24 and 48 hours. The results at 24 hours are shown in the figure below. However, they should be interpreted with caution as there are noticeable large differences present between patients and very small numbers were used for this exploratory experiment.

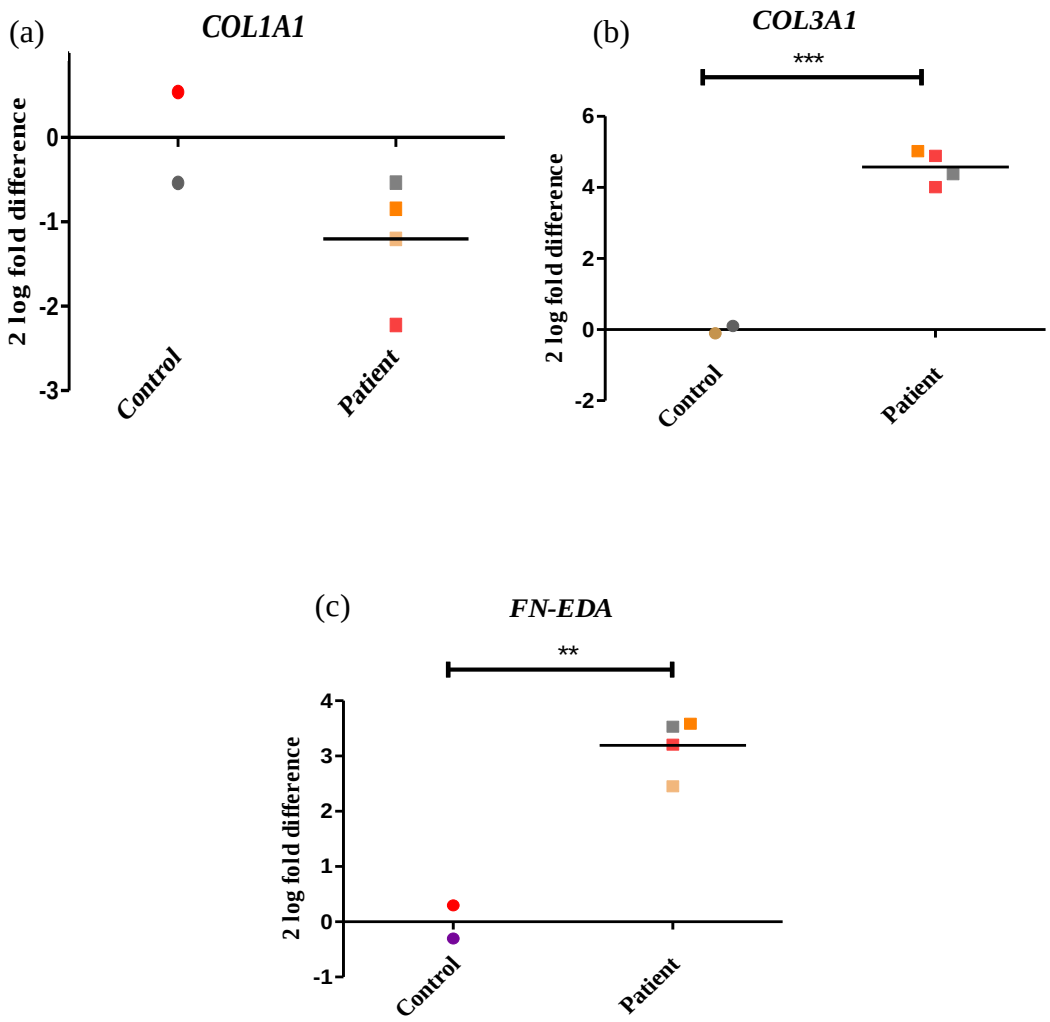

Figure 5-23 Two log of the fold difference values plotted individually for ECM genes showing A549 cells treated with healthy control plasma against those treated with plasma from patients with SSc-ILD for 24 hours. (a) *COL1A1*, (b) *COL3A1*, (c) *FN-EDA*. There was a significant increase in gene expression for *COL3A1* and *FN-EDA* in A549 cells treated with SSc-ILD plasma. Bar represents mean value for SSc-ILD patients. Unpaired two-tailed t-test performed for analysis, **p<0.01, ***p<0.001.

Figure 5-23 shows an upregulation of *COL3A1* (p<0.001) and *FN-EDA* (p<0.01) in A549 cells treated with plasma from patients with SSc-ILD plasma. qPCR was then performed on the CCN family to assess if these changes could be explained due to changes in this family of genes.

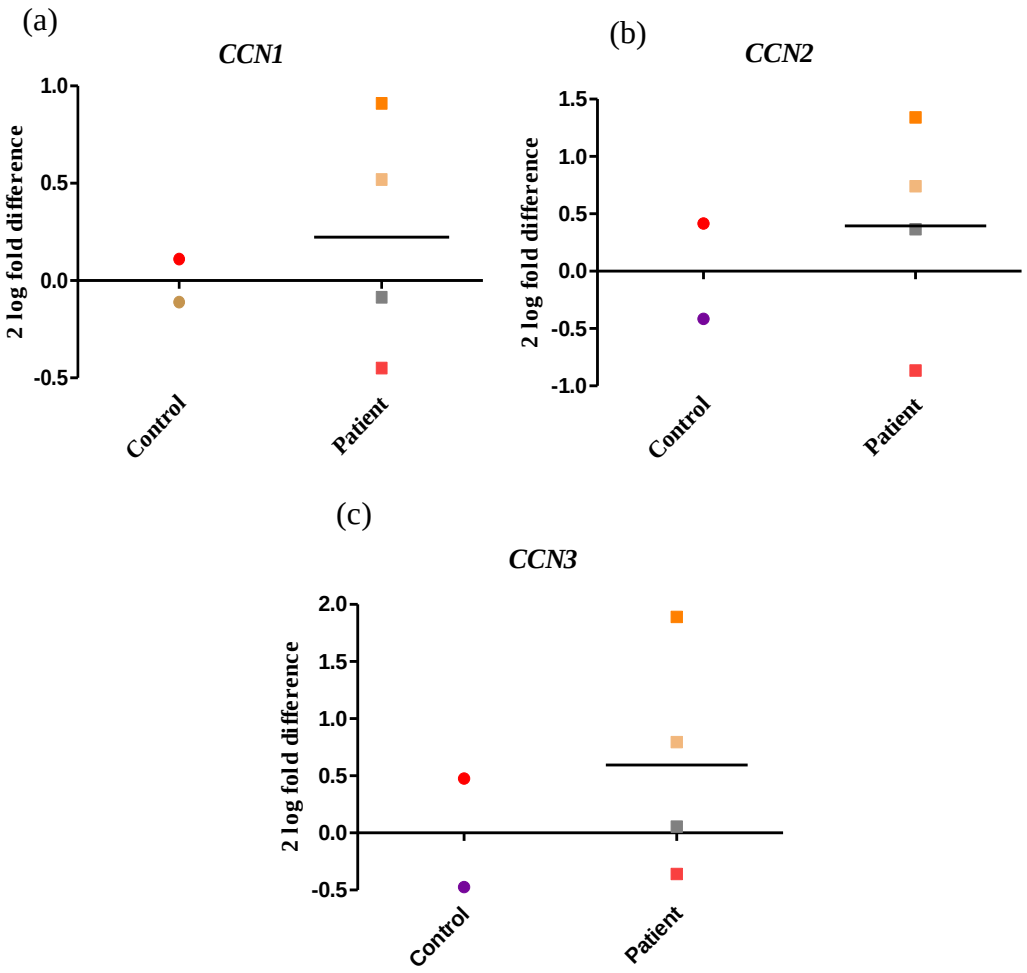

Figure 5-24 Two log of the fold difference values plotted individually for CCN genes showing healthy control values against those with SSc-ILD after treatment of A549 cells for 24 hours. (a) *CCN1*, (b) *CCN2*, (c) *CCN3*. There were no significant differences in gene expression of any of the CCN genes tested in this experiment when cells were treated with SSc-ILD patient plasma. Bar represents mean value for patients with SSc-ILD. Unpaired two-tailed t-test performed for analysis.

Figure 5-24 shows that there were no significant differences seen in any of the CCN family of genes after 24 hours. It was then assessed if these changes could be explained by changes in the transcription factors *Slug* and *Snail*, or the markers of EMT, *E-cadherin* and *N-cadherin*, that occur earlier in the fibrosis pathway.

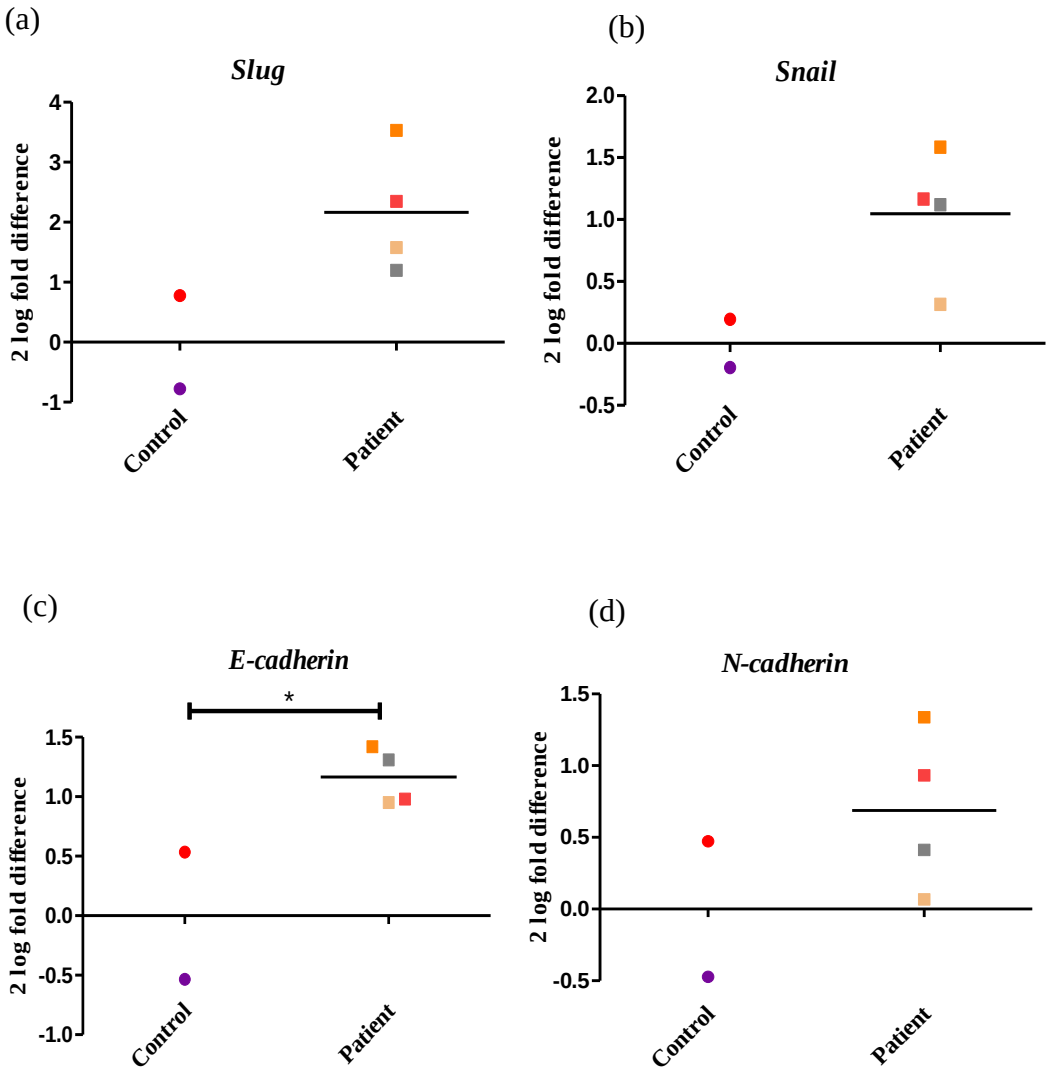

Figure 5-25 Two log of the fold difference values plotted individually for the transcription factors *Snail* and *Slug* and cell surface markers *E-cadherin* and *N-cadherin* showing healthy control values against those with plasma from patient with SSc-ILD after treatment of A549 cells for 24 hours. (a) *Snail*, (b) *Slug*, (c) *E-cadherin*, (d) *N-cadherin*. There was a significant increase in expression of *E-cadherin* in cells treated with SSc-ILD patient plasma when compared with healthy control plasma. Bar represents mean value for SSc-ILD patients. Unpaired two-tailed t-test performed for analysis, * $p<0.05$.

There appeared to be an upregulation in both *Slug* and *Snail*, although this difference did not meet significance, and would need to be confirmed using a larger patient group. There was a significant increase in *E-cadherin* production, which is surprising and would not explain the changes seen in production of ECM proteins. There was also a trend to upregulation of *N-cadherin* although this trend did not meet significance. However, it is recognised that this protein is increased in EMT and would be associated with the changes seen in ECM proteins, shown in Figure 5-23. RNA was extracted and qPCR performed for cells at 48 hours. Although there was a trend for a continued increase in production of *COL3A1*, this did not meet significance. There was no significant difference between groups for any of these genes when they were assessed at 48 hours.

In conclusion, treatment of A549 epithelial cells with plasma from patients with SSc-ILD, caused a significant upregulation in the production of *COL3A1* ($p<0.001$) and *FN-EDA* ($p<0.01$) mRNA. Interestingly, there was no significant difference in production of *COL1A1*.

6 Adapting the *in vitro* Model to Assess the Impact of Stretch on Fibrotic Pathways

The lungs are not an immobile organ but are constantly moving to allow respiration. For this to occur cells in the lung are undergoing constant stress in the form of stretch. Many lung cell studies have tried to replicate this movement both *in vitro* and *in vivo* and have found that these shear forces alone do impact upon cellular responses to wound healing and pro-fibrotic stimulation (170). It was therefore appropriate to investigate what happens to stretched pulmonary cells in the presence of TGF-β, and how key pro-fibrotic genes behave under such a stretch regime. Both fibroblasts and epithelial cells have thus been investigated *in vitro,* the results of which are shown in this chapter.

It is already recognised that lung-derived cells respond differently to stretch depending on the density of the cells that are experimentally plated (171). The particular substrate that the cells are grown on, for example a collagen coating or a FN coating, will have an impact upon how the cells react, as well as the substrate used, e.g. tissue culture plastic (172). There are also different responses depending on the degree of stretch applied and whether the resulting force is unidirectional or bidirectional in nature (173). These variables will thus have an impact upon the response of the cells to both stretch and TGF-β treatment. The conditions used for the current experiments were therefore carefully chosen to try to mirror the environment pulmonary parenchymal cells are subjected to *in vivo*.

Initially MRC5 cells were stretched using the methods described in section 2.3.2.4. A higher density of cells was plated than described in previous chapters, and the cells were cultured until almost confluent prior to treatment as cell density may impact their response and this ensured this variable was standardised. The plated cells were either treated with TGF-β (2ng/ml), stretch, a combination of both TGF-β (2ng/ml) and stretch or cultured in the same conditions but left untreated. Stretch was applied using the Flexcell Strain Unit at 6.66% length in pulsed sine wave intervals at a frequency of 1 Hz.

6.1.1 The Effect of Stretch +/- TGF-β (2ng/ml) on the Morphology of MRC5 Cells

The experiments assessed whether stretch forces applied to the MRC5 fibroblast cells in culture caused a change in their morphology. Figure 6-1 (below) shows that when stretch was applied to the cells, they became slightly more organised spatially and began to follow a single direction. It should be noted that the stretch applied to the fibroblasts was biaxial, with cells grown as a monolayer.

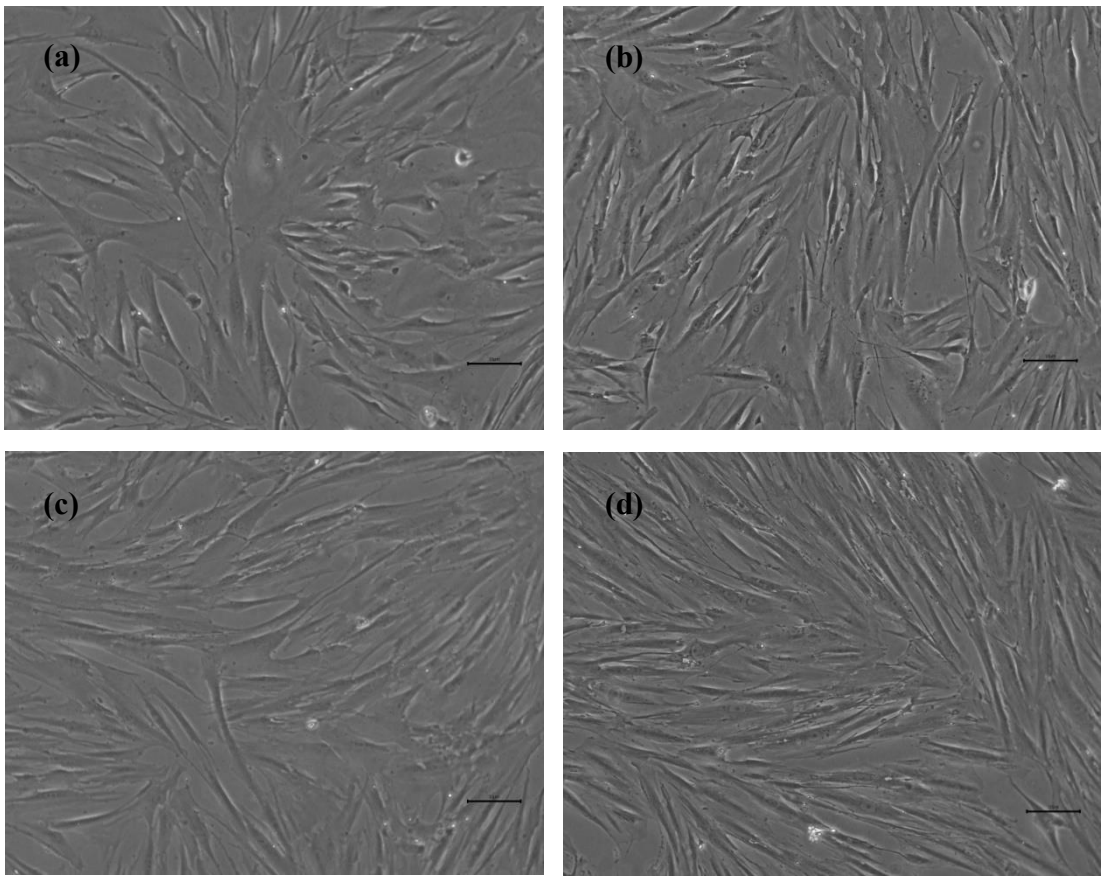

Figure 6-1 Change in morphology of MRC5 cells treated with TGF-β +/- stretch for 24 hours. (a) Control cells treated in the same conditions without the addition of TGF-β or stretch, (b) MRC5 cells treated with stretch only, (c) MRC5 cells treated with TGF-β (2ng/ml), (d) MRC5 cells treated with TGF-β (2ng/ml) and stretch. Cells became more organised and began to follow a similar direction. Magnification x10 objective lens, scale bar 10μm.

6.1.2 The Effect of TGF-β (2ng/ml) +/- Stretch Treatment on Gene Expression in MRC5 Fibroblasts

Once images had been taken, mRNA was extracted from cells using methods previously described in section 2.7. The first genes to be assessed were those that code for ECM proteins, including those for *COL1A1* and *FN-EDA*.

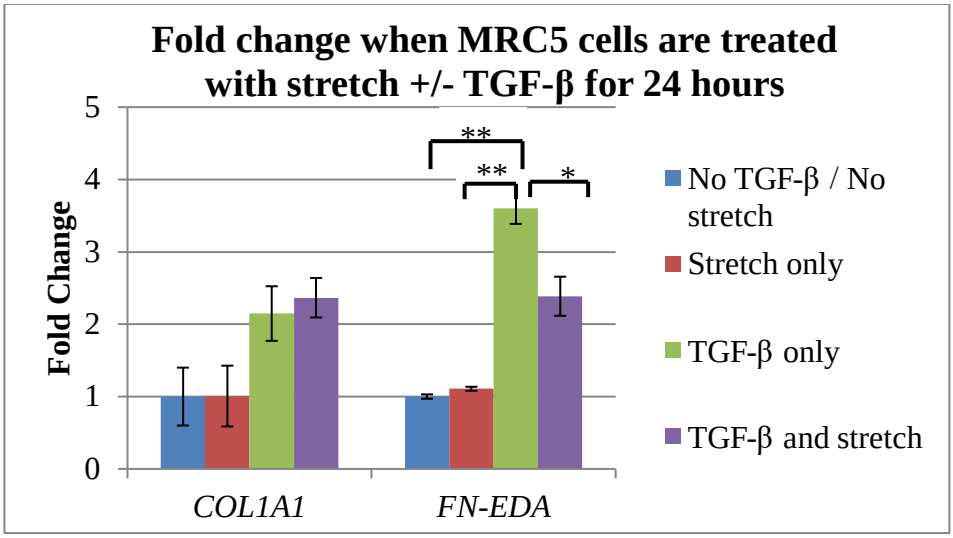

Figure 6-2 Fold change in *COL1A1* and *FN-EDA* in MRC5 cells after treatment with stretch +/- TGF-β (2ng/ml) over 24 hours. There was a significant increase in *FN-EDA* when cells were treated with TGF-β, which was attenuated when combined with stretch. Results shown are mean values (n=4) with error bars +/- SEM. One-way anova with Bonferroni post-test performed, *p<0.05, **p<0.01.

Figure 6-2 shows that there were no changes in *COL1A1* when the MRC5 cells were treated with stretch alone. As shown in chapter 4, there was however an upregulation in gene expression of *COL1A1* after treatment with TGF-β (2ng/ml) to just over twice the baseline levels, which was also shown in this experiment. When stretch was used alongside TGF-β, the transcription of *COL1A1* stayed at around twice the baseline levels, similar to the changes seen with TGF-β treatment alone.

Similarly, there was no change in *FN-EDA* expression when the cells were treated with stretch alone. There was a 3.5-fold increase in transcription of *FN-EDA* when

MRC5 cells were treated with TGF-β ($p<0.01$), with these results mirroring those seen in chapter 4. Interestingly, when stretch was also deployed alongside TGF-β treatment, there was a reduction in the amount of *FN-EDA* produced ($p<0.05$). This was surprising as it was expected that these stressed cells may produce more *FN-EDA*. Other genes involved in fibrosis were therefore examined to try to explain these changes.

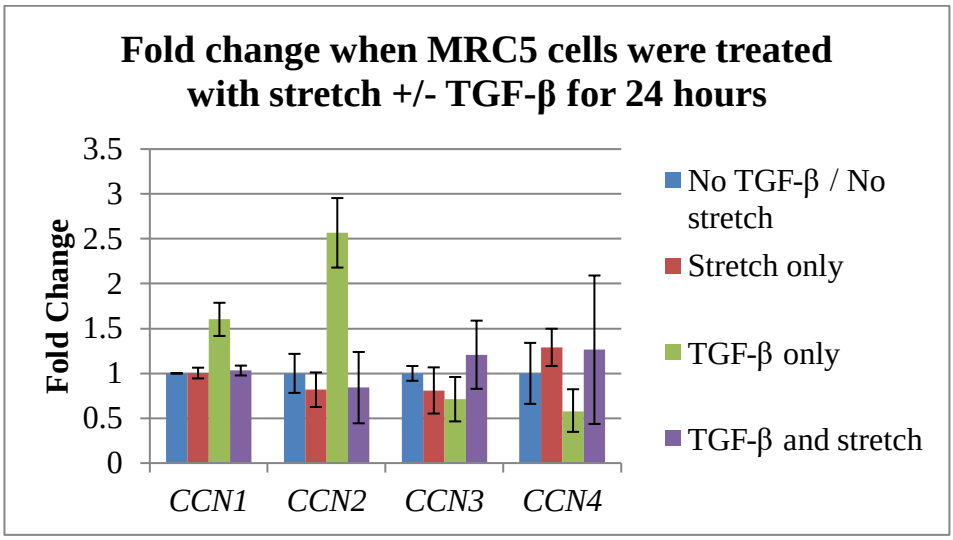

Figure 6-3 Fold changes in *CCN1*, *CCN2*, *CCN3* and *CCN4* in MRC5 cells after treatment with stretch +/- TGF-β over 24 hours. There were no significant differences in any of the CCN genes regardless of treatment with TGF-β, stretch or a combination of the two. Results are mean values (n=4) with error bars +/- SEM. One-way anova with Bonferroni post-test performed.

Figure 6-3 shows there were no significant differences between any members of the CCN family when the MRC5 cells were treated with stretch, TGF-β or a combination of the two. There was an upregulation of both *CCN1* and *CCN2* when the cells were treated with TGF-β alone, which occurred simultaneously alongside a decrease in the amount of *CCN3* and *CCN4*, but none of these results were statistically significant. These results were similar to those seen in chapter 5, although these genes were only checked at the 48 hour time point whereas the above results are after 24 hours. When stretch was applied together with TGF-β treatment,

there was a downregulation of both *CCN1* and *CCN2* to baseline levels. This may explain why there was a corresponding reduction of mRNA transcription of *FN-EDA* when the cells are treated with both stretch and TGF-β. In the case of *CCN3* and *CCN4*, there appeared to be an increase in transcription of these genes when cells were treated with TGF-β and stretch, although this did not meet significance due to large error bars.

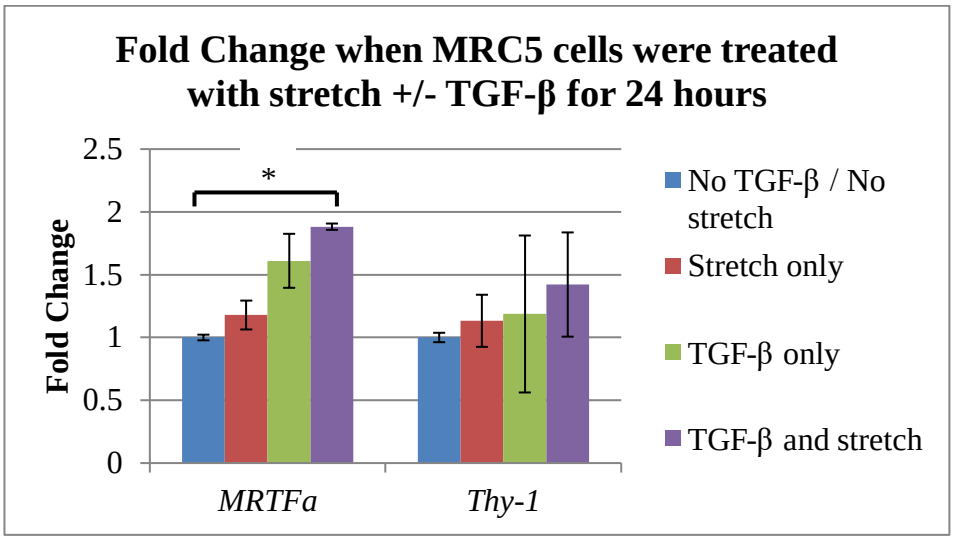

Figure 6-4 Fold change in *MRTFa* and *Thy-1* in MRC5 cells after treatment with stretch +/-TGF-β (2ng/ml) over 24 hours. There was a significant upregulation of *MRTFa* when MRC5 cells were treated with TGF-β and stretch. Results are mean values (n=4) with error bars +/- SEM. One-way anova with Bonferroni post-test performed, *$p<0.05$.

There were minor changes in *MRTFa* or *Thy-1* gene expression when MRC5 cells were treated with stretch for 24 hours. When the cells were treated with TGF-β there was a minor upregulation of *MRTFa* although this was not significant. This was however significantly upregulated when the cells were treated with both TGF-β and stretch together ($p<0.05$). There was no substantial change in transcription of *Thy-1* in cells treated with TGF-β, stretch or both together.

6.1.3 The Effect of Treatment with Human Plasma +/- Stretch on Gene Expression in MRC5 Fibroblasts

This stretch experiment design was then modified to assess the effect of human plasma on the transcription of these proteins. MRC5 cells were thus plated onto bioflex plates as described, and treated with human plasma (100ul per well), with one plate receiving either healthy control or IPF patient plasma without stretch and the other plate receiving the same plasma but having stretch applied. RNA was extracted after 24 hours of stretch. The results should be interpreted with caution as they were generated using small numbers of patients. This movement added an extra dimension to the model established in the previous chapters.

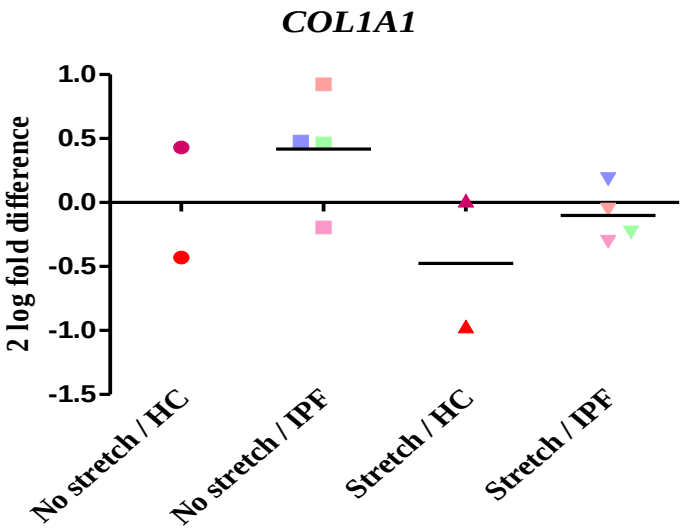

Figure 6-5 Two log of the fold difference values plotted individually for transcription of *COL1A1* showing cells treated with healthy control plasma and not subjected to stretch, cells treated with plasma from IPF patients not subjected to stretch, healthy control plasma values alongside stretch treatment and IPF plasma alongside stretch treatment applied for 24 hours. There was no significant difference in gene expression of *COL1A1* whether cells were cultured in static conditions or treated alongside stretch. Bars show mean values. One-way anova performed for statistical analysis. HC, healthy control; IPF, Idiopathic Pulmonary Fibrosis.

There were no significant differences noted in transcription of *COL1A1* between cells treated with IPF patient plasma or healthy control plasma. This result applied whether cells were static or subjected to stretch. There did appear to be a slight decrease in the amount of *COL1A1* produced by the cells in either group when they were subjected to stretch although this difference was not significant.

(a)

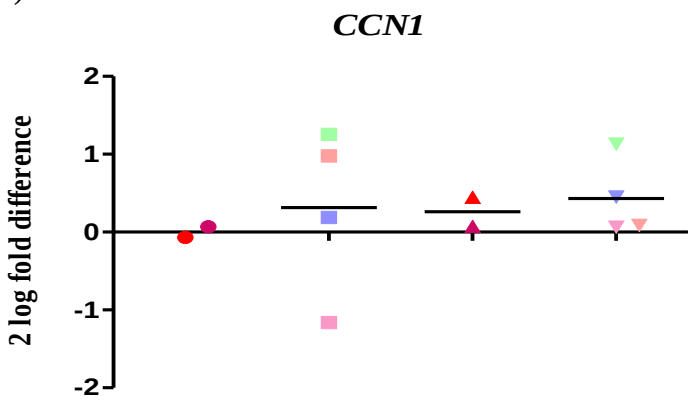
CCN1
2 log fold difference
2
1
0
-1
-2

(b)

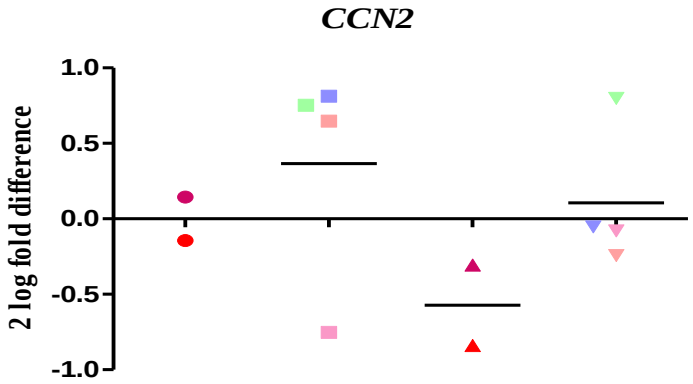
CCN2
2 log fold difference
1.0
0.5
0.0
-0.5
-1.0

(c)

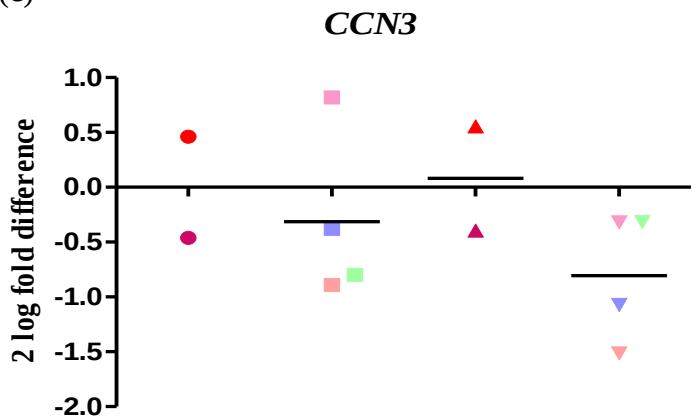
CCN3
2 log fold difference
1.0
0.5
0.0
-0.5
-1.0
-1.5
-2.0

(d)

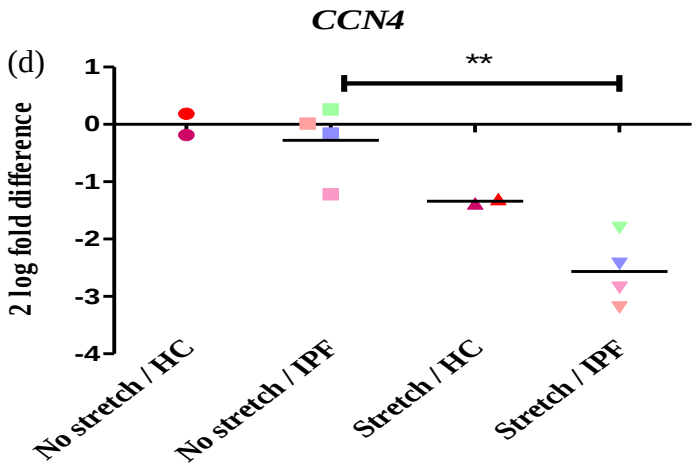
CCN4
**
2 log fold difference
1
0
-1
-2
-3
-4
No stretch / HC
No stretch / IPF
Stretch / HC
Stretch / IPF

Figure 6-6 (overleaf) Two log of the fold difference values plotted individually for transcription of the CCN genes showing cells treated with healthy control plasma and not subjected to stretch, cells treated with plasma from IPF patients not subjected to stretch, healthy control plasma values alongside stretch treatment and IPF plasma alongside stretch treatment after 24 hours. (a) *CCN1*, (b) *CCN2*, (c) *CCN3*, (d) *CCN4*. There was a significant reduction in expression of *CCN4* when MRC5 cells were treated with IPF plasma alongside stretch, as shown in (d). Bars show mean values. One-way anova performed for analysis, ** $p<0.01$. HC, healthy control; IPF, Idiopathic Pulmonary Fibrosis.

There were no differences in transcription of *CCN1*, *CCN2* or *CCN3* between cells treated with IPF patient plasma or those treated with healthy control subject plasma. These results were similar to those shown in chapter 5. There were also no significant differences noted when the cells were stretched.

CCN4 is also shown in the figure above. There was no significant difference between unstretched cells treated with IPF plasma and healthy control plasma, in accordance with the data shown in chapter 5. However, when cells were stretched there was a decrease in transcription of *CCN4* that reached significance ($p<0.01$) in cells treated with plasma from IPF patients. There also appeared to be a decrease in CCN4 transcription when the cells were stretched in the presence of healthy control plasma, although this did not meet significance.

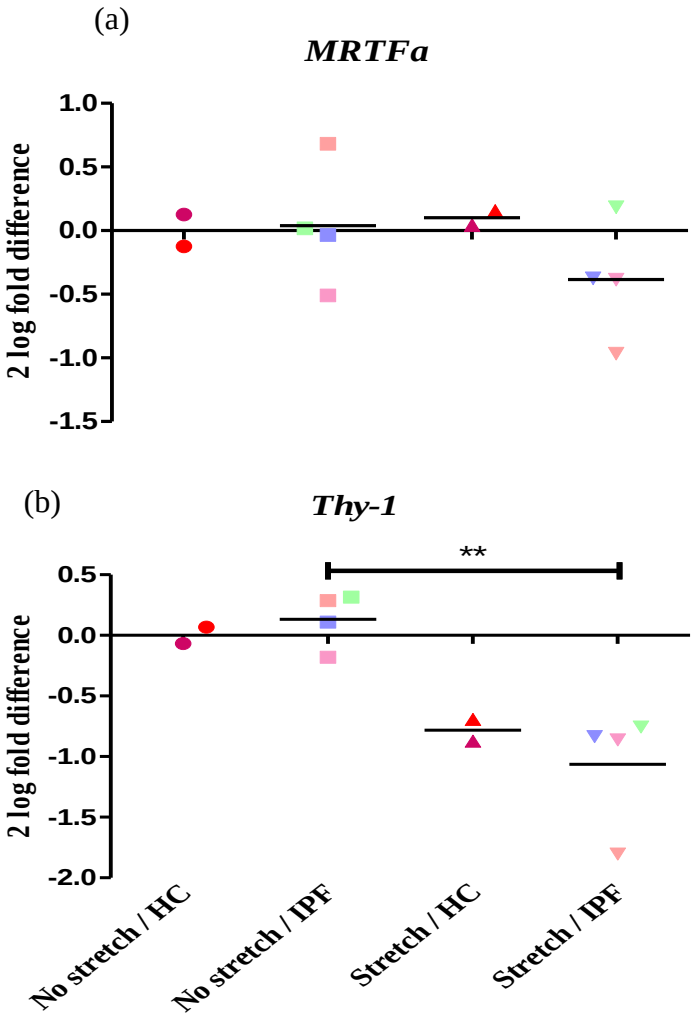

Figure 6-7 Two log of the fold difference values plotted individually for transcription of the other genes involved in fibrosis, showing results from MRC5 cells treated with healthy control plasma and not subjected to stretch, cells treated with plasma from IPF patients not subjected to stretch, healthy control plasma values with stretch and IPF plasma alongside applied stretch after 24 hours. (a) *MRTFa*, (b) *Thy-1*. There was a significant reduction in expression of *Thy-1* when MRC5 cells were treated with IPF plasma alongside stretch. Bars show mean values. One-way anova performed for analysis, ** $p<0.01$. HC, healthy control; IPF, Idiopathic Pulmonary Fibrosis.

MRC5 cells were also investigated for changes in gene expression of *MRTFa* and *Thy-1* in the presence of IPF patient plasma. There was no difference in transcription of *MRTFa* in cells treated with healthy control plasma or plasma from patients with IPF. When cells were stretched it caused no difference in transcription compared to cells that were not stretched and whether cells were treated with IPF plasma or healthy control plasma.

When *Thy-1* was similarly tested, there were no differences when cells were treated with either IPF plasma or healthy control plasma and cultured under static conditions, again mirroring the results shown in chapter 5. However, when the cells were stretched there was a downregulation of *Thy-1* which reached significance when the cells were treated with IPF plasma. This may not have met significance in cells treated with healthy control plasma due to the small number of patients assessed in this group.

6.1.4 The Effect of Treatment with TGF-β (1.5ng/ml) +/- Stretch on the Morphology of A549 Epithelial Cells

A549 cells were stretched using the methods described in section 2.3.2.5. The stretch chambers used for this experiment were from a custom-built machine which stretches cells in a unidirectional manner, thus differing from the MRC5 experiment described above where the cells were stretched in a bidirectional manner.

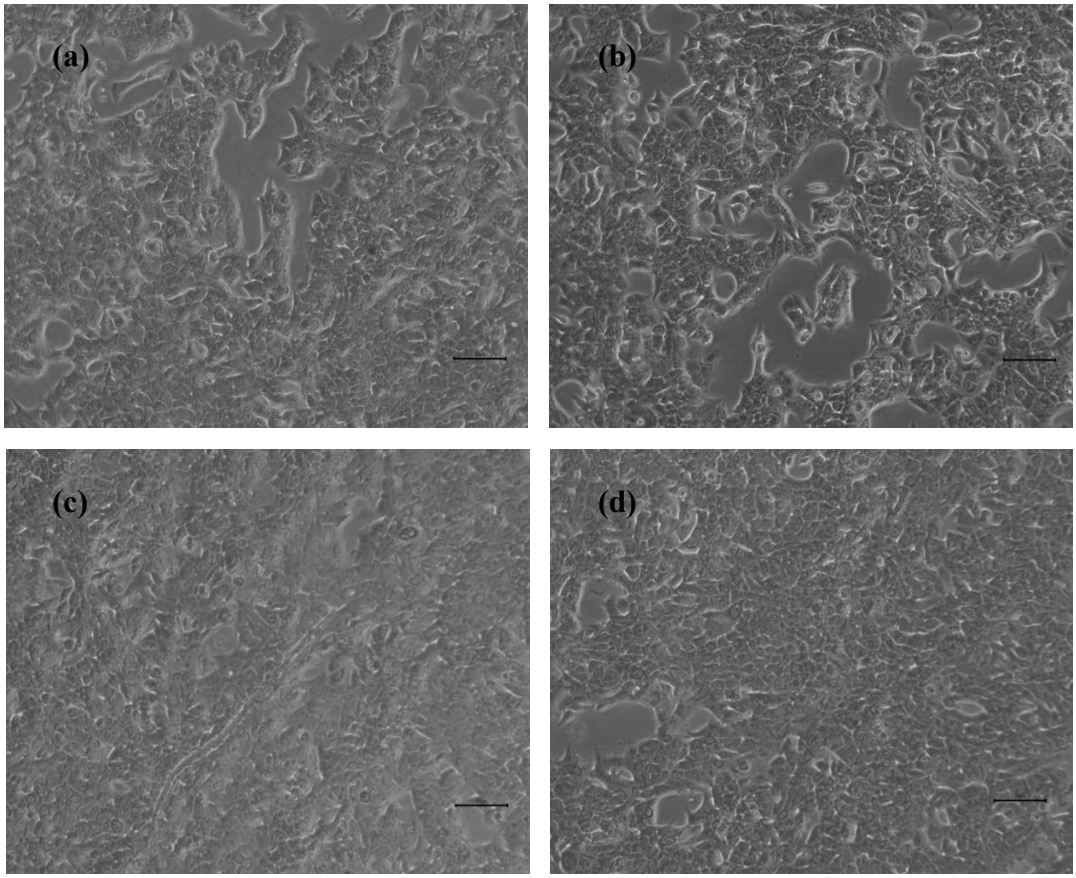

Figure 6-8 Change in morphology of A549 cells treated with TGF-β (1.5ng/ml) +/- stretch for 24 hours. (a) Control cells treated in the same conditions without the addition of TGF-β or stretch, (b) A549 cells treated with stretch only, (c) A549 cells treated with TGF-β (1.5ng/ml), (d) A549 cells treated with TGF-β (1.5ng/ml) and stretch. There were no changes in the morphology of the A549 cells when treated with stretch. In these images it is difficult to appreciate whether there is any change when cells were treated with TGF-β, the reasons for this are discussed in more detail below. Magnification x10 objective lens, scale bar 10μm.

There did not appear to be any obvious change in the morphology of the A549 cells when they were subjected to stretch. It was also difficult to assess whether there was any difference in the morphology of the epithelial cells when they were treated with TGF-β. One limitation of using the custom-built stretch machine was that chambers needed to be coated prior to each experiment. This meant that a laminin coating was put onto the chambers before they were incubated prior to use. This

may mean that the coating of the chamber may not have been uniform leading to cells in some areas of the chamber not being confluent. The material of the chamber was also much softer meaning that the cells may behave differently due to the change of material that they are plated on.

6.1.5 The Effect of TGF-β (1.5ng/ml) +/- Stretch Treatment on Gene Expression in A549 Epithelial Cells

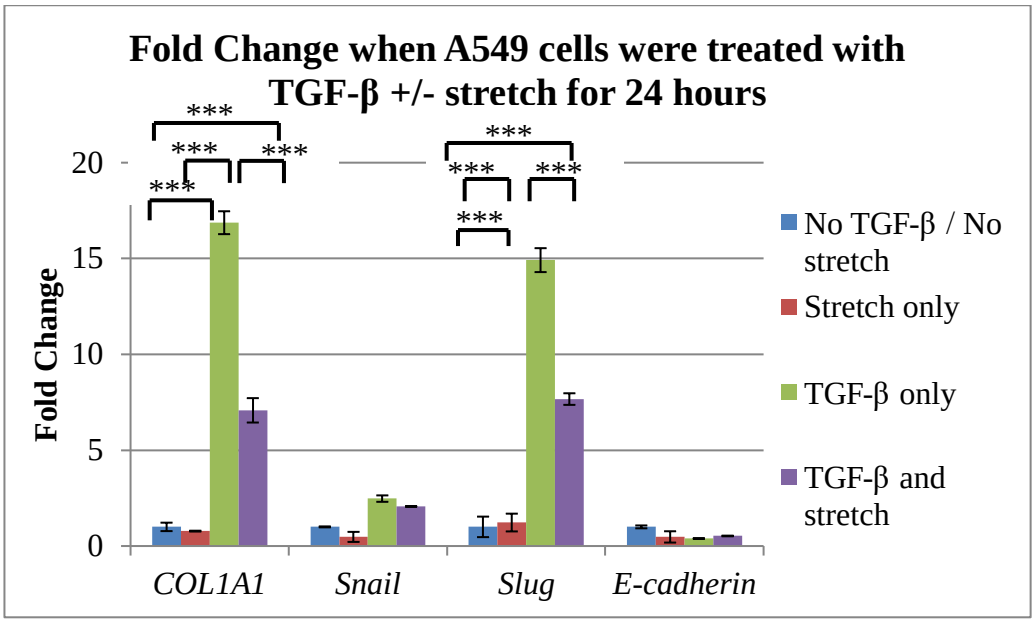

Figure 6-9 Fold change in *COL1A1*, *Snail*, *Slug* and *E-cadherin* in A549 cells following treatment with TGF-β +/- stretch over 24 hours. Stretch alone did not lead to any significant differences in any of the above genes. When treated with TGF-β there was a significant increase in *COL1A1* and *Slug*, which was attenuated when cells were treated alongside stretch. Results are mean values (n=4) with error bars +/- SEM. One-way anova with Bonferroni post-tests were performed, ***p<0.001.

This figure shows there was very little or no change in the transcription of *COL1A1* produced by A549 cells subjected to stretch alone. However, when these cells were

treated with TGF-β there was over a 16-fold increase in *COL1A1* mRNA, as previously shown in chapter 4. However, this response was attenuated when the cells were treated with TGF-β and subjected to unidirectional stretch for 24 hours. Other genes were then explored to assess if this impact could be explained.

The transcription factors *Slug* and *Snail* were therefore assessed. The result showed similar patterns of change to those seen in *COL1A1* with a more obvious increase observed in *Slug*. There was very little change in either *Snail* or *Slug* when the A549 cells were subjected to stretch alone. There was however a large increase in in transcription of *Slug* and *Snail* after treatment with TGF-β, mirroring effects previously seen in chapter 4. This response was attenuated when the cells were treated with both TGF-β and stretch for 24 hours, perhaps explaining the trend seen for *COL1A1*. There was very little difference seen in *E-cadherin*, whether cells were treated with stretch, TGF-β or a combination of both. This trend followed that seen in chapter 4.

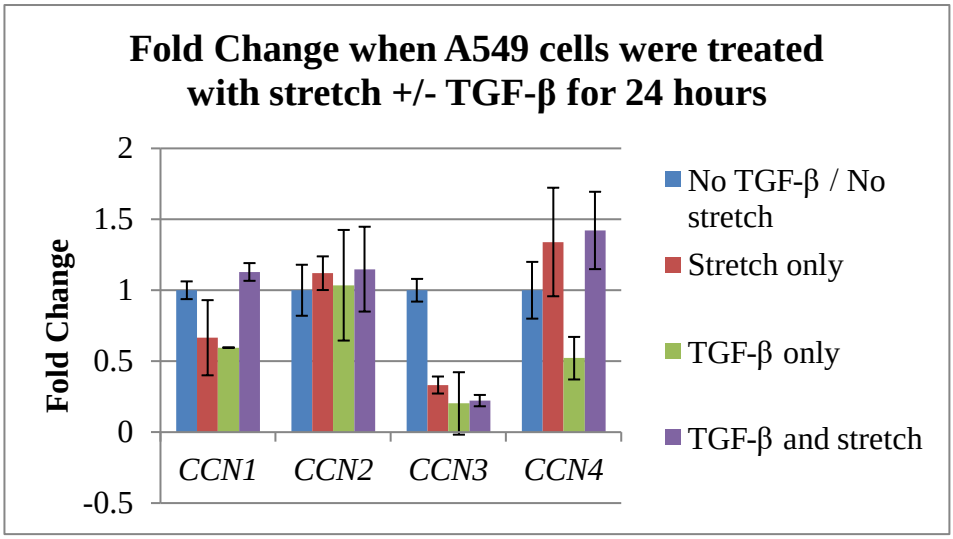

Figure 6-10 Fold change in *CCN1*, *CCN2*, *CCN3* and *CCN4* in A549 cells after treatment with TGF-β (1.5ng/ml) +/- stretch over 24 hours. There were no significant differences in expression of the CCN genes whether exposed to stretch, TGF-β or a combination of both. Results are mean values (n=4) with error bars +/- SEM. One-way anova with Bonferroni post-test performed.

Treating the A549 cells with either TGF-β, stretch or a combination of the two did not induce any significant changes in the expression of the CCN genes within the A549 epithelial cells. This differed from chapter 4 where treatment with TGF-β alone led to a significant increase in *CCN1* and *CCN2*. However, in chapter 4 these changes were measured at 48 hours and the changes above are measured at 24 hours. Also, the significant differences in chapter 2 were only seen when cells were treated with 3ng/ml TGF-β ($p<0.01$), but the cells above were treated with a smaller concentration (1.5ng/ml) which may also explain the differences observed.

6.1.6 The Effect of Human Plasma +/- Stretch Treatment on Gene Expression in A549 Epithelial Cells

This model was then adapted to assess the effects of plasma from patients with IPF in combination with stretch.

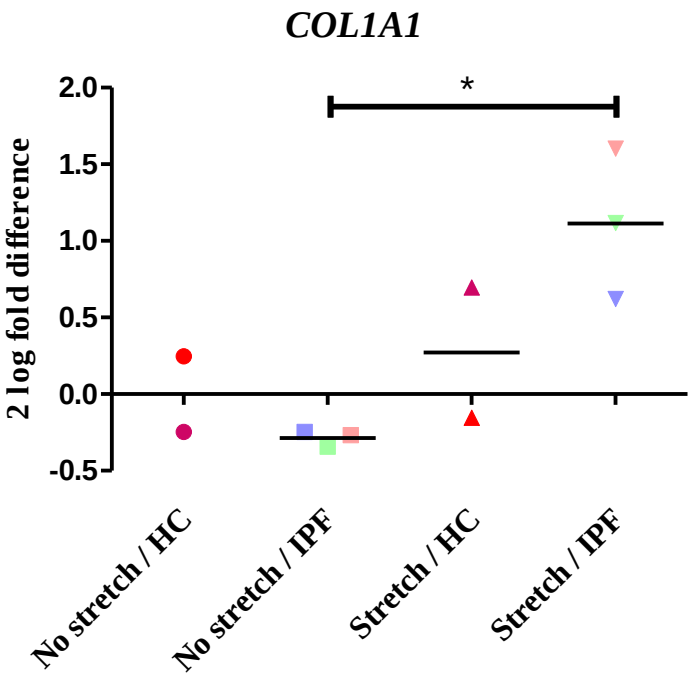

Figure 6-11 Two log of the fold difference values plotted individually for transcription of *COL1A1* showing cells treated with healthy control plasma and not subjected to stretch, cells treated with IPF patient plasma and not subjected to stretch, healthy control plasma values alongside stretch treatment and IPF plasma alongside stretch treatment after 24 hours. When cells were treated with IPF plasma alongside stretch there was a significant increase in expression of *COL1A1*. Bars show mean values. One-way anova performed for analysis, * $p<0.05$. HC, healthy control; IPF, Idiopathic Pulmonary Fibrosis.

In A549 cells there were no significant differences between cells that were treated with healthy control plasma or IPF patient plasma and cultured under static conditions. However, there appeared to be upregulation in *COL1A1* transcription once these cells were subjected to stretch, which did reach significance in the cells treated with IPF patient plasma ($p<0.05$).

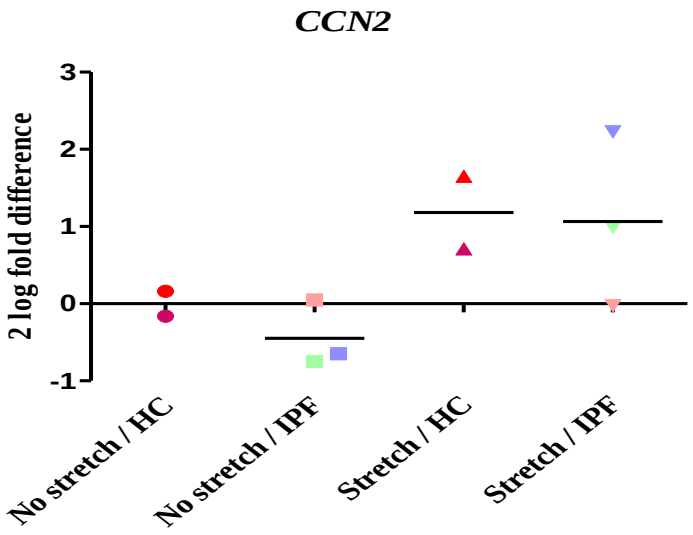

Figure 6-12 Two log of the fold difference values plotted individually for transcription of *CCN2* showing cells treated with healthy control plasma and not subjected to stretch, cells treated with IPF patient plasma and not subjected to stretch, healthy control plasma values alongside stretch treatment and IPF plasma alongside stretch treatment after 24 hours. There was no significant difference in CCN2 when A549 epithelial cells were treated with IPF plasma and stretch. Bars show mean values. One-way anova performed for analysis. HC, healthy control; IPF, Idiopathic Pulmonary Fibrosis.

CCN2 was then investigated to assess if this upregulation could be explained through regulation of this gene which seems to hold such a crucial role in fibrosis. Again, when cells were not subjected to stretch there appeared to be no difference in *CCN2* transcription whether cells were treated with IPF patient plasma or healthy control plasma. However, once stretch was applied there appeared to be a corresponding upregulation of *CCN2*, mirroring the effects seen in the transcription of *COL1A1*. However, as there was variation between subjects this effect did not meet significance.

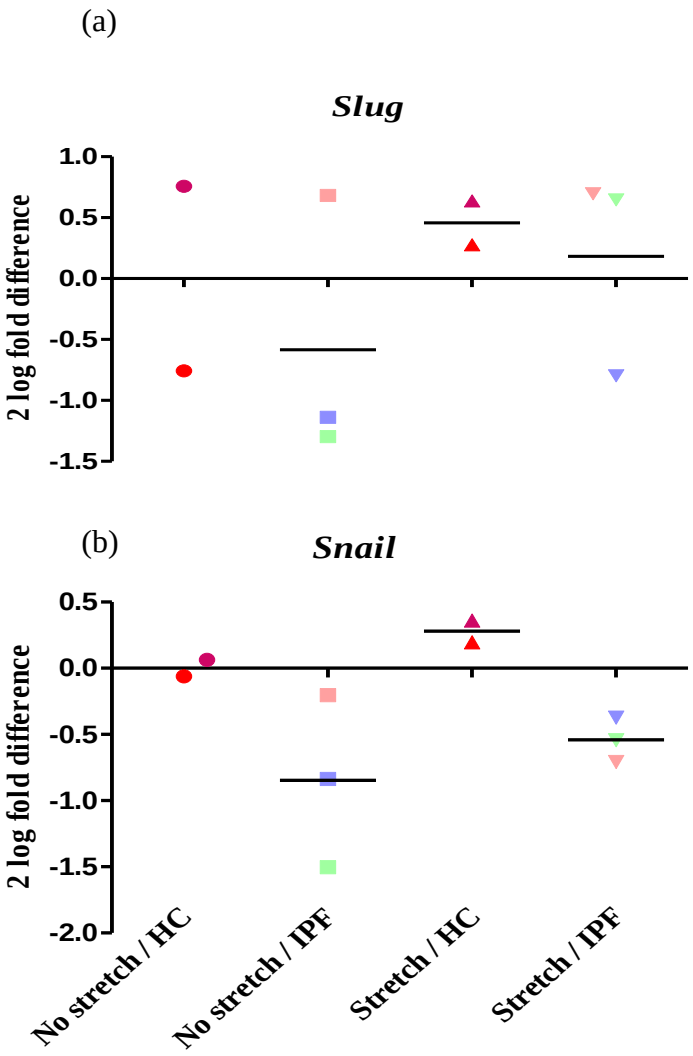

Figure 6-13 Two log of the fold difference values plotted individually for transcription of *Slug* and *Snail* showing cells treated with healthy control plasma not subjected to stretch, cells treated with plasma from patients with IPF and not subjected to stretch, healthy control plasma alongside stretch treatment and IPF plasma values alongside stretch treatment after 24 hours. There were no significant differences in either transcription factor when cells were treated with IPF plasma when in static conditions or when subjected to stretch. Bars show mean values. One-way anova performed for analysis. HC, healthy control; IPF, Idiopathic Pulmonary Fibrosis.

There were no significant differences noted in the transcription factors *Slug* or *Snail* when cells were treated with healthy control plasma or IPF patient plasma, as previously shown in chapter 5. When these cells were exposed to stretch, there were no significant differences noted in either of these genes.

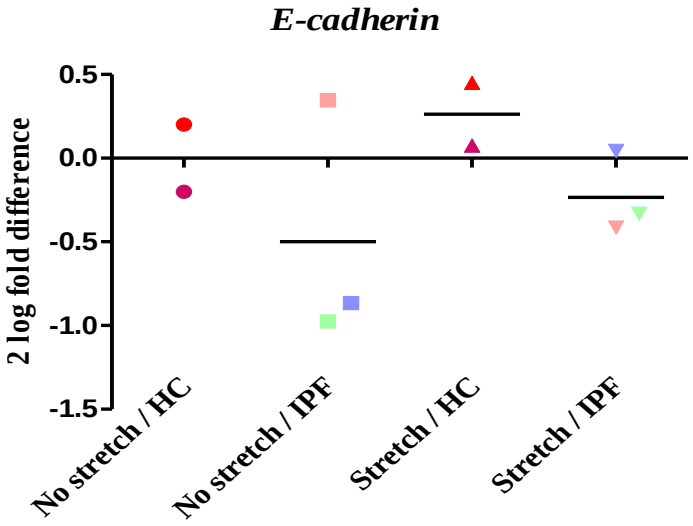

Figure 6-14 Two log of the fold difference values plotted individually for *E-cadherin* showing cells treated with healthy control plasma not subjected to stretch, cells treated with plasma from IPF patients and not subjected to stretch, healthy control plasma alongside stretch treatment and IPF plasma values alongside stretch treatment after 24 hours. There were no significant differences in E-cadherin when cells were treated with IPF plasma and subjected to stretch. Bars show mean values. One-way anova performed for analysis. HC, healthy control; IPF, Idiopathic Pulmonary Fibrosis.

Finally, *E-cadherin* expression was assessed to see if its regulation was changed when cells were stretched. There were no significant differences apparent between transcription of mRNA for this protein when comparing treatment with healthy control plasma and IPF patient plasma or when comparing the effect of stretch.

7 Discussion

The results presented in this thesis examine the important molecular processes involved in inducing and propagating lung fibrosis in IPF and those occurring in CTD-ILD. A number of techniques were used throughout the thesis to achieve some key objectives;

1) To assess whether the IPF population of the UK-BILD study is truly homogeneous or whether there are a number of patients misdiagnosed as IPF who have an autoantibody present in their sera associated with an underlying CTD.
2) To develop an *in vitro* cellular model with which to assess changes in genes associated with fibrosis which is both reliable and reproducible.
3) To utilise this cellular model by treating cells with plasma from patients with fibrotic diseases and assess if there are differences in the response of the cells when compared to healthy controls and when compared to each other.
4) To imitate the continued movement of the lungs, and the shear forces that cells within the lung are exposed to, by stretching the cells in culture. This model was used to assess whether this has any effect on the cellular response, firstly using TGF-β and then when cells were treated with IPF plasma.

The major findings of this work included:

1) Respiratory physicians are good at diagnosing IPF and an underlying CTD is not missed very frequently (less than 2% of patients). It can be inferred that the UK-BILD cohort of patients with IPF are a homogeneous population with which to do further work.
2) A cellular model was produced that was able to identify and measure extracellular matrix and other fibrosis associated gene induction by TGF-β.
3) The model was utilised using plasma from patients with fibrotic diseases. This appears a novel way to investigate fibrotic pathways.

The results of each chapter, with their strengths and limitations, will now be discussed in more detail below.

7.1 Immunoprecipitation Results

The results presented in chapter 3 used immunoprecipitation to identify autoantibodies in the sera of patients with IPF. It was hypothesised that patients were being misdiagnosed and actually had an underlying CTD, which would hinder any comparisons between IPF and CTD-ILD undertaken in later chapters. More importantly, it also has considerable clinical implications for patients as the treatments for the two conditions is different. CTD-ILD usually responds to steroids and immunosuppression, however this is harmful in IPF and actually increases mortality (15), perhaps due to side effects such as increased rates of infection. Conversely, if patients are misdiagnosed with IPF they may miss out on therapeutic options in the form of steroids. It was therefore of vital importance that the diagnostic error in IPF in a UK population was measured. Although this has been investigated previously in Japanese and Korean populations it was unknown in the UK population with IPF (69, 70). Serum samples from 249 patients with IPF were screened for autoantibodies using the gold-standard test of immunoprecipitation. The results of the UK-BILD population revealed that just 4 patients (1.6%) had an underlying MSA / MAA in their sera. These included anti-OJ, anti-Ku, anti-PM-Scl and anti-RNA Pol II. Each antibody and their associated features are discussed in more detail in chapter 3.

When analysed these patients did not have any overt features suggestive of an underlying CTD according to the UK-BILD proforma. For this reason, it may be argued that although a patient has the presence of an autoantibody it cannot be concluded that they have the associated disease. For example, it is known that patients may be anti-CCP antibody positive for several years prior to the development of Rheumatoid Arthritis (174). However, it is also recognised that a patient can have ILD as a lone feature of an underlying CTD and that other features such as mechanic's hands may be subtle or may develop later during the course of the disease (175). One limitation of this study is that these subtle features are

assessed by clinicians at each centre and depends upon the expertise of the individual physician.

Overall, the results give confidence that respiratory physicians are accurate when making a diagnosis of IPF and the reassurance that patients are likely receiving the correct treatment. The 4 patients who had a CTD-associated autoantibody present in their sera were diagnosed in non-specialist ILD centres. It does suggest that an IPF diagnosis is more certain when made in a specialist ILD setting, however this is a very small number of patients and overall the diagnosis of IPF is secure. Interestingly, there appeared to be more patients with IPF with strong bands found on immunoprecipitation (36.5% rather than less than 10% in a healthy population, data according to expert opinion at the University of Bath). There did not appear to be any obvious demographic differences between patients with strong bands and those with no bands present. The significance of these bands is unclear, it may be that these patients run a different disease course but as this is a cross-sectional study this cannot be investigated and any future longitudinal studies may be able to assess the relevance of this finding.

There was also a novel band noted, present at 54 kDa, with examples given in Figure 3-2 and consistent with an associated autoantibody, found in 7 patients diagnosed with IPF. Unfortunately, experiments to classify this antibody have been unsuccessful so far. It did not appear to be consistent with any overt CTD features in this population. Again, longitudinal studies, with collection of Pulmonary Function Test (PFT) data, may be helpful to assess if these patients respond differently to treatment or have a different disease course than the antibody negative population.

7.2 The Development of an *in vitro* Model in MRC5 Fibroblasts

As chapter 3 has shown that the IPF population from the UK-BILD study is homogeneous, the samples collected were then used in further chapters to assess differences in the fibrotic pathways between IPF and CTD-ILD. Firstly, an *in vitro* assay was established to ensure that a reliable and reproducible model was produced. Cells were cultured and treated with TGF-β, a pro-inflammatory cytokine that promotes fibrosis. It was chosen as it is a key molecule in the pathway of fibrosis and may cause effects similar to those when cells are treated with human plasma from patients with fibrotic diseases. Two cell types, fibroblasts and epithelial cells, were chosen as they are key cells associated with fibrosis in the lungs. They both have the ability to become a "myofibroblast", a cell with contractile properties with current literature suggesting it is the key cell responsible for fibrotic processes. Another cell type with the ability to transition into a cell with mesenchymal properties are the endothelial cells, they do this via a process called endothelial-mesenchymal transition, discussed in more detail in the introduction. It is recognised that they are a key cell to study, particularly in SSc where endothelial dysfunction is part of the disease pathogenesis, but unfortunately due to time constraints endothelial cells were not used in this experiment. Future work may be important to assess changes in this cell type also. Initially, for this thesis and to assess the viability of this experimental method, the MRC5 fibroblasts and A549 epithelial cells were treated with increasing concentrations of TGF-β to assess the changes that occur.

When treated with increasing concentrations of TGF-β there appeared to be a corresponding increase in proliferation of MRC5 cells when they were visually assessed at different time points. However, an alamar blue assay performed to measure proliferation of the cells found that as cells were treated with increasing concentrations of TGF-β, there was actually a decrease in the proliferation of the fibroblasts. This became significant at the highest concentration of TGF-β (2 ng/ml) when cells were treated for 96 hours. The response appeared dose-dependent. This was an unexpected result given the photomicrographs of the cell plates, however it

may be that when cells were treated with TGF-β they underwent morphological changes, becoming larger and giving the impression of being more numerous. At higher TGF-β treatment concentrations they were also producing more fibrotic proteins, but this may occur at the expense of cell proliferation. Early literature published on TGF-β suggests that it has very little effect on the proliferation of fibroblasts, and actually has inhibitory effects on epithelial cells and endothelial cells (discussed later in this chapter) (176-178).

Given the morphological changes described above, immunocytochemistry was performed to assess for changes in the ECM proteins to show if treatment with TGF-β was leading to increased expression of these molecules. This showed an increase in the amount of α-SMA protein present within the fibroblasts treated with TGF-β. This protein is a hallmark of the myofibroblast, suggesting that cells were changing in response to the TGF-β treatment. Fibroblasts were also stained for COL1A1 however as this protein was so abundant prior to treatment with TGF-β it was difficult to assess whether more of this protein was being produced after treatment. Quantitative PCR and western blot techniques were therefore used to assess for changes in gene expression and protein secretion from these treated cells.

There was a significant increase in gene expression of *COL1A1* in MRC5 cells treated with TGF-β (1ng/ml and 2ng/ml) after 24 hours. This effect was to twice the control level and was not sustained at the later time points. This was associated with a significant increase in *FN-EDA* at all concentrations of TGF-β used after 24 hours. This effect was sustained at 48, 72 and 96 hours at the highest concentration of TGF-β (2ng/ml). Although *COL3A1* has been described as an important molecule in fibrosis and the production of ECM, there was no significant increase in this gene at any time point tested throughout the experiment. However, the first time point used was 24 hours and significant changes in *COL3A1* expression may be seen at earlier time points than this. These results are in line with many previous experiments that showed TGF-β involvement in matrix deposition by fibroblast cells (176, 179).

There may be several reasons for this reduction in response of *COL1A1* and *FN-EDA* over 96 hours. Binding of TGF-β to its receptor leads to a downstream response in the phosphorylation of Smad within 5 minutes (108). Therefore, the transcription of genes affected by TGF-β signalling will occur quickly and may be

seen at 24 hours rather than 96 hours when feedback mechanisms may downregulate this transcription.

It was then assessed whether this increase in gene transcription led to an increase in the production of protein secreted by fibroblasts by undertaking a western blot. Visually, by assessing the blot image, it appeared there was more COL1A1 produced by MRC5 fibroblasts after 96 hours with increasing concentrations of TGF-β. However, once this was normalised using a ponceau stain to compare protein loading between lanes, the increase was not significant. This technique was repeated for FN which produced a dose-dependent increase in FN protein and showed significant effects at 1ng/ml and 2ng/ml ($p<0.01$) which would complement the qPCR data previously discussed. These changes agree with previous literature that has shown that fibroblasts exposed to TGF-β increase mRNA production and protein synthesis of both collagen and FN, providing further evidence that this was a reliable model (179, 180).

This experiment was modified by using TCH instead of serum starving the fibroblasts. TCH is a serum replacement product, containing nutrients for cells without hormones and growth factors which may have an impact upon their growth. The ideal length of time to starve cells prior to an experiment is unknown and it may have an impact upon the health of the cell (163). The changes in gene expression of these cells was assessed at a single 48-hour time point. Although this produced no changes in *COL3A1*, there was a dose dependent increase in expression of *COL1A1* and *FN-EDA* as shown previously, however, when cells were serum starved these changes were only present at 24 hours but when cells were treated with TCH they remained significant at 48 hours. There was over a 3-fold increase in *COL1A1* and over 6-fold increase in *FN-EDA*. It may be that serum starvation had a detrimental effect on the cells and therefore cells that were not stressed prior to the experiment were able to respond to TGF-β stimulation for longer. It would also remove any variation that serum starvation may add to the experiment, thus it was used for future experiments.

During this adaptation of the original experiment several extra genes that have an effect in fibrosis were evaluated. Initially CCN genes were assessed. The CCN family of proteins share a similar structure of five domains. They have extensive

biological effects on cell adhesion, proliferation, migration, signalling and appear to play a key role in fibrosis and wound healing (117). They are secreted into the ECM where they interact with a variety of proteins to have such variable effects. They have been investigated in multiple studies and their role is not fully understood. For this reason, it was assessed what impact they had when an inflammatory cytokine (TGF-β) was added to each cell type (both MRC5 fibroblasts and A549 epithelial cells) and this could be compared with changes induced by human plasma. There was a significant increase in expression of *CCN1*, to almost twice the baseline levels occurring at all concentrations of TGF-β treatment. CCN1 has been shown in wound healing models to have a role in cellular senescence and attenuating the fibrotic response (118). Conversely, it is upregulated in models of lung fibrosis where it has a pro-inflammatory effect (122). At 48 hours, when MRC5 fibroblasts are treated with TGF-β, it appears to be upregulated, this may be either driving the pro-fibrotic response or as a negative feedback mechanism to attenuate the fibrotic response.

There was also a significant increase in *CCN2*. This has been shown to upregulate in previous work when fibroblasts were treated with TGF-β (181) where it acts as a downstream mediator and allows for a sustained fibrotic response (182). It is upregulated in murine models of fibrosis, such as the inhaled bleomycin model (95). When drugs are given that directly inhibit this molecule, for example FG-3019 (an anti-CCN2 antibody), there is less of a fibrotic response in the lungs (95).

In this experiment, there appeared to be a corresponding reduction in CCN3, although this did not meet significance. A recent study published by Liu et al suggests that TGF-β treatment reduces the expression of CCN3 in human mesangial cells. By pre-treating the cells with CCN3 prior to TGF-β exposure there was a reduction of ECM proteins produced by the cells in response to TGF-β (183). However, this protein is similar to CCN1 and its role in fibrosis does not seem completely established with contradictory literature published, with other studies suggesting a pro-fibrotic role (132).

The expression of CCN4 was also reduced in fibroblasts treated with TGF-β, although this change was not significant. This is an interesting change, as when CCN4 was blocked in a mouse model of liver fibrosis, there was a reduction in

collagen production suggesting that it acts as a pro-fibrotic marker (137). Reasons for this response may be that this protein acts differently depending on the cell type that it is expressed in. It may also be that by 48-hours it is downregulated due to negative feedback mechanisms in place that are attenuating the fibrotic response.

Further work to establish the role that these key molecules play might include assessing the pattern of expression across the 96-hour time point, to assess for negative feedback mechanisms that may occur. It may be that blocking the molecule of interest with a specific CCN antibody and then assessing the response that occurs in ECM protein markers such as COL1A1 could also give interesting results that may show some of the complex interplay between these molecules.

Other molecules assessed but that did not show significant changes included *MRTFa*, *PDGFR-α* and *Thy-1*. These molecules were chosen as there is evidence that they play a key role in fibrosis. MRTFa is a transcriptional co-activator that is formed in the cytoplasm and translocates to the nucleus where it binds to the serum response factor and causes the transcription of genes such as α-SMA. Crider et al have shown that MRTFa is a key regulator of myofibroblast formation in response to TGF-β stimulation. However, it should be noted that in this study there was only a small increase in message levels of *MRTFa* when fibroblasts (REF-52 cells) were treated with 0.25ng/ml TGF-β for 96 hours (less than twice baseline levels). The protein was shown to be a key part of the fibrosis pathway as knockdown of the molecule reduced the expression of key markers of the myofibroblast including α-SMA (184). The data shown in this experiment, using MRC5 fibroblasts, did appear to correspond showing just under a 2-fold increase in *MRTFa* expression in cells treated with TGF-β, however this small change was not found to be statistically significant.

There was no significant difference in *PDGFR-α* when fibroblasts were treated with TGF-β. Previous work showed that treatment of fibroblasts with TGF-β *in vitro* leads to a reduction in *PDGFR-α,* which corresponds with the results in this experiment, although this experiment was not statistically significant (185). PDGF is an important signalling molecule found in the ECM that appears to have effects in fibrosis. When mice were exposed to asbestos, inducing pulmonary fibrosis, there was an increase in gene expression of *PDGFR-α.* The molecule also appears to act

synergistically with TGF-β as when corneal fibroblasts were treated with TGF-β and PDGF-A there was a significant increase in myofibroblast transition, which was a much bigger effect than when they were treated with each molecule alone (186).

The gene expression of *Thy-1* was also assessed in this experiment. Thy-1 is a cell surface protein, found on the surface of a number of cell types including fibroblasts. In healthy lung specimens the majority of fibroblasts express Thy-1 on their surface. However, the lung biopsy specimens from patients with IPF lack Thy-1 expression. Gene expression of this marker was therefore measured to see if expression was downregulated when cells were treated with a pro-inflammatory cytokine and later with IPF and SSc patient plasma. The results showed that there was no significant change in this protein when fibroblasts were treated with TGF-β.

7.3 The Development of an *in vitro* Model in A549 Epithelial Cells

A similar experiment was performed in the A549 epithelial cells. This was an important cell type to investigate as type II alveolar epithelial cells have been implicated as playing a key role in the onset of IPF. There is a theory that IPF is caused by repeated subclinical injury of the lung with damage occurring to the alveolar epithelial cells and affecting the integrity of the basement membrane (187). This damaging process leads to a chain of events that permits the formation of the myofibroblast, a contractile cell which produces excess ECM (188). There is also evidence for EMT occurring, with type II alveolar epithelial cells transitioning into mesenchymal cells, adding to the myofibroblast pool (110). Epithelial cells are therefore an interesting target to investigate further. Cells were treated with TGF-β (1.5ng/ml and 3ng/ml) for 24, 48, 72 or 96 hours. Images were taken and RNA extracted at these time points. There appeared to be changes observed in the morphology of the cells with squamous epithelial cells changing from the typical tight-spaced, cobblestoned appearance to slightly more elongated cells. Proliferation of the cells was measured using an alamar blue assay and showed no significant difference in proliferation between control cells and A549 cells treated with TGF-β.

Interestingly, the A549 cells were very fast growing and reached peak confluence by 24 hours. At 72 hours the number of healthy, viable cells had reduced. Similar findings were also shown by Shipley et al, where mouse embryonic epithelial cells (AKR-2B cells) were treated with TGF-β. This caused a prolonged pre-replicative phase of the cells and did not induce proliferation. There was however a definite early change in morphology with an early increase in protein synthesis. The authors also hypothesised that cells were not replicating while there were such drastic changes in morphology occurring (189).

Immunofluorescence staining was undertaken to assess if cells were undergoing EMT in response to TGF-β. It showed that cells were producing more COL1A1 and α-SMA after 48 hours treatment and suggests that cells were undergoing EMT, producing fibrosis associated proteins in response to TGF-β treatment. These results are in accordance with previous literature that showed that when epithelial cells were treated with TGF-β *in vitro* they became more mesenchymal in phenotype, and eventually produced more collagen and fibronectin (assessed further by qPCR and western blot in the next few sections) (108). However, even when directly stimulated by TGF-β, epithelial cells did not produce as much COL1A1 as the MRC5 fibroblasts did even at baseline levels, without TGF-β stimulation, questioning the amount that EMT contributes to fibrosis (109).

Initial genes assessed were those coding for proteins that form the ECM and would expect to be increased if cells were undergoing EMT, and becoming more mesenchymal in phenotype. Changes in gene expression were measured using qPCR, with up to a 45-fold increase in gene expression of *COL1A1* after treatment with the highest concentration of TGF-β (3ng/ml). This was repeated on several occasions when A549 epithelial cells were treated with TGF-β in later chapters, confirming it was a true response. The reason for such a significant increase with TGF-β may be that these cells usually produce such small amounts of *COL1A1*, that when stimulated with TGF-β the fold change appears very large. This effect peaked after 48 hours but was sustained up to 96 hours in the experiment. There was a significant increase in *FN-EDA*, which peaked at 72 hours. Again, although *COL3A1* is implicated in fibrosis there was no significant change noted in expression of this gene.

These changes in ECM genes were associated with over 6-fold changes in the transcription factors *Slug* and *Snail*. Although there was overlap, these changes occurred prior to the peak changes in the ECM genes, suggesting that cells are first stimulated to increase production of transcription factors, which in turn drives the cells to produce more ECM proteins, thereby becoming more mesenchymal in phenotype. Previous literature has also shown that *Slug* and *Snail* are increased in response to TGF-β *in vitro*. By using small interfering RNA sequences to reduce the mRNA level of *Slug* and *Snail* the same authors showed there was a corresponding reduction in EMT associated proteins, providing evidence they are key to driving the TGF-β response (190).

Figure 4-16, 4-17 and 4-18 show that when treated with TGF-β the A549 cells were producing more COL1A1 and α-SMA using immunocytochemistry techniques. Western blot of the conditioned cell medium was used to compare how much COL1A1 was secreted by the epithelial cells but unfortunately there was a wide variation in the experiment making measurement difficult and no significant differences were observed. A recent publication has suggested that although there is a definite increase in gene expression of ECM markers in epithelial cells that have undergone EMT, this does not correlate with an increase in COL1A1 protein, suggesting its contribution to the production of ECM is limited (109).

Epithelial cells did not survive with prolonged serum starvation. When it was attempted to starve them overnight (16 hours) apoptosis and cell death occurred. For the above experiments, cells were starved for 8 hours. However, similarly to the experiment in MRC5 cells described above, the serum replacement product TCH was used instead of serum starvation to stimulate cells.

Again, the ECM genes were assessed first to see if the changes were similar to those observed when cells were serum starved. There was a significant increase in the gene expression of *COL1A1* to over 16-fold its baseline expression. This was not associated with a significant difference in *COL3A1,* in agreement with the data shown in the previous experiment. Although there was an increase in expression of *FN-EDA*, this did not meet significance, however this may be due to the small number of replicates and some variation in the control samples.

These changes appear to be driven by the transcription factors *Slug* and *Snail*, with a significant increase in *Slug* at this 48-hour time point. There appeared to be a decrease in *E-cadherin*, which is a protein required for the tight junctions seen between epithelial cells, giving the epithelium its typical cobblestone appearance. This protein was assessed as downregulation is recognised as an early response in EMT, allowing cells to lose their tight junctions and become more invasive (108). This was associated with a significant increase in *N-cadherin* ($p<0.05$), another recognised feature of EMT (167). N-cadherin is a cell adhesion molecule, expressed by mesenchymal cells, and its expression is increased in EMT. It is expressed in biopsy specimens of patients with IPF suggesting that alveolar EMT may be occurring, and making it a good molecule to assess if plasma treatment changes expression of this protein (191).

Again, the CCN family was assessed due to the crucial role it appears to play in ECM regulation. Interestingly in this experiment the CCN family showed a similar response to the changes occurring in the MRC5 fibroblasts. There was a significant increase in *CCN1* (5-fold with TGF-β 3ng/ml) and *CCN2* (8-fold with TGF-β 3ng/ml). *CCN1* is increased in lung specimens of patients with IPF and correlated with increased expression of the ECM proteins, collagen and FN (123). Previous work has shown an increase in *CCN2* in response to TGF-β stimulation, where it has been shown as a downstream, pro-fibrotic mediator of this pathway. There were no significant differences in *CCN3* or *CCN4*, although the trend appeared that there was a reduction in expression of these genes. The role of these CCN genes in fibrosis is less understood and previous literature is controversial.

The results in this chapter therefore show the establishment of a model with which to assess changes involved in fibrosis. Treatment of MRC5 fibroblasts with TGF-β reduced the proliferation of the cells which became larger in size. There is an increase in gene expression of *COL1A1* and *FN-EDA*. There was an increase in production of FN protein secreted by these cells. Treatment of A549 cells with TGF-β caused an increase in gene expression of *COL1A1, FN-EDA, Slug, Snail, CCN1, CCN2* and *N-cadherin*. There was an associated significant decrease in the expression of *E-cadherin*. Immunocytochemistry showed an increase in expression of COL1A1 and α-SMA. The changes discussed above occurred consistently and were those expected when a pro-inflammatory cytokine is placed on the cells,

suggesting that this was a reliable model with which to do further work. As shown, a number of factors influenced the changes that occurred, including the concentration of TGF-β used as well as the time points that the RNA was extracted. It was therefore hypothesised that if the same cell lines were treated with plasma from patients with a fibrotic disease this would cause changes similar to those seen in this chapter when cells were treated with TGF-β and it may reveal important proteins involved in the fibrotic pathways of lung fibrosis.

7.4 Using the *in vitro* Model to Assess Changes Induced in MRC5 Fibroblasts by Plasma from Patients with Fibrotic Diseases

The results in chapter 5 show the outcome when this model was used to compare changes in fibrotic markers when cells were treated with plasma from two different groups of patients. The first group were patients with IPF, these patients develop fibrosis affecting the lungs only but do not develop fibrosis of systemic organs. We also know from the results in chapter 3 that this is a homogeneous population. Although the cause is unknown, the disease does not appear to be preceded by inflammation but patients develop progressive fibrosis of the lungs, with a median mortality of just 3 years (14). Diffuse SSc-ILD was used as a contrasting disease. HRCT scans in this disease often show inflammation and patients generally respond to steroids and immunosuppression. Features of the disease are often overt and unlikely to be misdiagnosed. The disease leads to fibrosis in multiple organs, and patients from this cohort are known to suffer fibrosis affecting at least the skin and lungs. It is therefore a contrasting disease and allows comparison of the fibrotic pathways and key molecules involved in the fibrotic response.

Initially MRC5 fibroblasts were treated with 100ul per well of plasma from patients with IPF. As there were so few changes at 96 hours in the previous experiment with TGF-β it was decided to reduce the number of time points and so this last time point was removed. Treatment with human plasma appeared to have obvious

morphological effects on the cells, with fibroblasts appearing more spindle-shaped. This occurred whether cells were treated with plasma from healthy controls or from patients with fibrosis, suggesting it was a direct effect of the plasma not the underlying disease process. The cells appeared less healthy and to assess if they were still proliferating well an alamar blue assay was performed. This showed that MRC5 cells treated with plasma from patients with IPF were more proliferative throughout the 72 hours than those treated with plasma from healthy controls. Although this was only significant at the 48-hour time point, the trend extended throughout the entire 72-hour time course (Figure 5-2). This trend was not shown when MRC5 cells were treated with plasma from patients with SSc, where there were no significant differences in cell proliferation regardless of treatment group.

Given the obvious morphological effects induced by plasma treatment immunocytochemistry was performed to assess the cytoskeletal changes. Phalloidin staining revealed that the cells had become more spindle-shaped in response to human plasma treatment irrespective of whether the plasma was from a healthy control subject, IPF or SSc-ILD patient. When MRC5 cells were stained for COL1A1 there was continued production of the protein but there was no significant increase whether patients were treated with healthy control plasma, IPF plasma or SSc-ILD plasma. It is unclear whether these effects were anticipated as these methods appear novel and there is very little literature regarding the expected changes to cell lines when treated with human plasma.

RNA was extracted at 24, 48 and 72 hours respectively. It should be noted that no significant differences in any of the genes assessed for fibrosis were noted at 48 or 72 hours and so the data presented and discussed are changes occurring at 24 hours. There were no significant changes noted between healthy control and IPF patient plasma for any ECM protein genes, CCN genes or other proteins involved in fibrosis. When the same cell lines were treated with plasma from patients with SSc-ILD there were no significant differences noted in gene expression for any of the ECM associated proteins. The CCN genes were then explored, showing a significant downregulation in expression of *CCN3* ($p<0.05$). As previously described CCN3 is part of the CCN family and has a role in inflammation and tissue repair (132). Its impact upon the fibrotic response has been contradictory, with some literature suggesting that it has an anti-fibrotic role and other studies showing

evidence that it is pro-fibrotic (132, 135). As shown in chapter 4, *CCN3* appeared to be reduced when MRC5 cells were treated with TGF-β for 48 hours although this change was not statistically significant and this appeared to be in the same direction when cells were treated with SSc-ILD plasma. There was no difference in *CCN2*, although CCN2 has increased expression from skin fibroblasts isolated from lesions in patients with SSc (128). There were no differences in expression of *MRTFa* or *Thy-1* between cells treated with healthy plasma and those treated with SSc-ILD.

7.5 Using the *in vitro* Model to Assess Changes Induced in A549 Epithelial Cells by Plasma from Patients with Fibrotic Diseases

In a similar manner the A549 cells were treated with human plasma. Images were recorded at different time points and the cells appeared to grow well, reaching maximum confluence at around 48 hours. There did not appear to be any obvious morphological changes in the cells but this was assessed further using immunocytochemistry. When the A549 epithelial cells were stained for α-SMA, a protein expressed by myofibroblasts, there appeared to be a minor increase in production of this protein from patients with IPF or SSc-ILD compared to cells that were treated with healthy control plasma. This would be expected if cells were undergoing EMT, becoming more mesenchymal in phenotype and expressing more α-SMA.

Epithelial cells were also assessed for whether treatment with plasma from patients with ILD affected proliferation. There did not appear to be any significant differences in proliferation of A549 cells that were treated with healthy control plasma and IPF plasma or when healthy controls were compared with SSc-ILD. However, when A549 cells were treated with TGF-β of varying concentrations, shown in chapter 4, there was no change in the proliferation of cells. It was hypothesised that the cells were not replicating while undergoing such drastic changes in morphology.

Changes in gene expression were also assessed in the A549 epithelial cells treated with plasma for 24, 48 and 72 hours. Again, there were no significant differences between any of the genes explored at 48 or 72 hours when cells were treated with IPF plasma or SSc-ILD plasma and so this data was not shown. When A549 cells were treated with plasma from patients with IPF, there was very little change in *COL1A1*. There was a significant reduction in *COL3A1* ($p<0.01$) and *FN-EDA* ($p<0.05$). These changes are difficult to explain as they are unexpected. It would be hypothesised that in patients with IPF there would be a driving factor present in the plasma that would upregulate transcription of genes that code for proteins that build the ECM, given the disease leads to excess secretion of ECM. Interestingly, when A549 epithelial cells were treated with TGF-β there was a significant increase in *COL1A1* and *FN-EDA*, and although there was a trend for upregulation of *COL3A1* this was not significant. The changes seen with IPF patient plasma occur in the opposite direction, perhaps suggesting that changes are not TGF-β driven.

Other genes involved in fibrosis and EMT were then explored to see if these changes could be explained. There were no significant differences noted in the transcription factors *Slug* and *Snail*. As these transcription factors tend to cause the upregulation or downregulation of ECM proteins, any changes in these genes is likely to occur prior to any changes noted in ECM genes (i.e., at an earlier time point than 24 hours). It may be interesting therefore to assess these genes after 12 hours of IPF plasma treatment to see if they are driving these changes. *N-cadherin* was assessed and this showed a significant downregulation in expression ($p<0.01$). This is in the opposite direction to that which is expected in cells undergoing EMT, where it is upregulated, but may explain the changes noted in the ECM protein genes in this experiment. Interestingly there was a significant decrease in the expression of *E-cadherin* ($p<0.01$). As discussed previously this is an early change associated with EMT, as it is a marker of epithelial cells and reduces when cells are undergoing EMT, allowing epithelial cells to lose their tight junctions. However, this downregulation would not explain the changes occurring in gene expression of the ECM proteins in the same experiment. If cells were transitioning into a mesenchymal phenotype, reducing their expression of E-cadherin as shown, it would be expected there would be a corresponding increase in the ECM genes, which there was not. This unexpected effect on gene expression could not be explained by

changes in the CCN genes, in which there were no significant differences between cells treated with healthy control plasma and those treated with IPF plasma.

When the same cell line was treated with plasma from patients with SSc-ILD there was a significant increase in *COL3A1* ($p<0.001$). There was a corresponding increase in expression of *FN-EDA* ($p<0.01$). This change would be expected if cells were undergoing EMT, becoming more mesenchymal in phenotype and producing more ECM proteins. The CCN proteins, including *CCN1*, *CCN2* and *CCN3* were explored to assess whether these changes could be explained but there were no significant differences in expression in any of these genes which would explain the changes seen with the ECM proteins.

However, SSc-ILD plasma treatment was associated with an upregulation in the transcription factors *Slug* and *Snail*, although this did not meet significance. These markers were increased when cells were treated with TGF-β in the previous chapter, where it appeared to be an early change driving cells to increase mRNA production of ECM proteins. Earlier time points were not assessed in this experiment. However, these changes may reach significance if assessed after 12 hours, as they may be early changes driving the cells to produce more *COL3A1* and *FN-EDA*, and therefore when examined at 24 hours levels are starting to decline. There was a significant upregulation of *E-cadherin* after 24 hours, a marker that is lost from epithelial cells when transitioning into mesenchymal cells, and so a downregulation would be expected in association with the changes in ECM proteins. One explanation for this is whether this early change in the cell is a repair mechanism in response to EMT occurring.

Interestingly, *COL3A1* and *FN-EDA* were significantly downregulated when treated with IPF patient plasma, which is in the opposite direction to when cells were treated with plasma from patients with SSc-ILD. They were then associated with a significant decrease in *E-cadherin*, again in the opposite direction to when A549 epithelial cells were treated with SSc-ILD plasma. It is known that changes in cadherin are seen in cells that are undergoing EMT and may suggest that plasma is causing a change in the morphology of the epithelial cells. It is interesting that these changes are in the same genes in patients with different underlying fibrotic diseases

and perhaps indicates that they act via different fibrotic pathways. The fact that it is the same genes that show significance may suggest that this is a true interaction.

The changes expected in the cells when treated with plasma from patients with fibrotic diseases were based on the changes induced by TGF-β, a pro-inflammatory cytokine. Interestingly, in SSc there is good evidence that there are increased circulating levels of TGF-β in patient plasma and that higher levels correlate with increasing disease severity (192). Alhamad et al measured levels of circulating TGF-β in patients with IPF and there was no increase in plasma levels. There was however, an increase in active TGF-β locally in the lungs of patients and this may explain why it does not show clinical systemic effects like SSc as well as not causing the same changes observed in fibrosis associated genes in this experiment (193). As there is no increase in TGF-β levels in the plasma of patients with IPF it may explain why there is no increase in production of ECM genes when this plasma was used to treat cells. In contrast, SSc-ILD plasma, which has more active TGF-β than healthy plasma, does induce these changes. This may also explain some of the very different clinical presentations of these two distinct fibrotic diseases.

7.6 Using the *in vitro* Model to Assess Changes Induced by Plasma Treatment from Patients with Fibrotic Diseases Alongside Stretch

The final chapter of this thesis explored the stretch model, which was used to assess the effect of stretch alongside the plasma treatment. As understood, the lung is not a static organ but is constantly moving, creating shear forces within the cells. It was unknown how these cells would respond to stretch alone and respond to stretch alongside treatment with TGF-β or human plasma from patients with IPF.

In summary, 6.66% biaxial stretch treatment alone in MRC5 cells caused no significant differences in any of the genes associated with fibrosis and assessed in previous chapters. This included *COL1A1* and *FN-EDA,* genes that code for ECM proteins that are excessively produced and secreted into the extracellular space in

fibrosis. There was no change in the CCN family, *MRTFa* or *Thy-1* from baseline levels, other molecules involved in the fibrotic response. Treatment with TGF-β caused an increase in *FN-EDA* as previously shown in chapter 4. It also caused an increase in *COL1A1*, alongside an increase in *CCN1* and *CCN2* although these results did not reach significance in this experiment, although the same concentration of TGF-β was used (2ng/ml). The reason for this lack of response, as previously seen in *COL1A1*, *CCN1* and *CCN2* when MRC5 cells were treated with TGF-β, may be due to some key differences with this experiment. The first difference is that in chapter 4 qPCR was performed after the MRC5 cells were treated for 48 hours, whereas the stretched cells were assessed after just 24 hours. Also, there may be a difference in response when the cells were plated on a softer, collagen-lined base rather than tissue culture plastic.

When the fibroblasts were treated with both TGF-β (2ng/ml) and stretch the *FN-EDA* response was attenuated. This occurred alongside a reduction in *CCN1* and *CCN2* back to baseline levels, although these changes were not significant they may explain the reduction seen in *FN-EDA*. It should be noted that a reduction in *FN-EDA* with stretch treatment is surprising, as it would be expected that cells undergoing stretch would upregulate the production of ECM proteins, to counteract the shear forces produced by the movement. However, these effects have been shown in previous published literature. In a study conducted by Blaauboer et al primary human lung fibroblasts were subjected to 10ng/ml TGF-β. They were then either left to grow for 48 hours or subjected to mechanical stretch and qPCR undertaken. In this experiment, the use of stretch reduced the mRNA production of α-SMA and type-I, type-III and type-V collagen (194).

On the other hand, *MRTFa* was further increased when TGF-β and stretch were combined reaching a significant change when compared to baseline levels. The exact effect of MRTFa in fibrosis is unknown but it appears to target serum response factors, which then impact upon cell growth, proliferation and cytoskeleton organisation. It may be that in this situation, expression of *MRTFa* is required for other pathways.

The same cells were treated with human plasma and stretch using the same stretch protocol as previously tested. In agreement with the results in chapter 5 there were

no significant differences between cells treated with healthy control plasma and cells treated with plasma from IPF patients in static conditions. When cells were stretched there were no changes noted in the expression of *COL1A1*. There was a significant downregulation of *CCN4* ($p<0.01$) in cells that were treated with stretch and IPF patient plasma compared to cells treated with IPF plasma in static conditions. CCN4 has been considered part of the pro-fibrotic response, with a reduction in fibrosis if mice are treated with a CCN4 antibody prior to being exposed to inhaled bleomycin which induces lung fibrosis (136). There was also a significant decrease in *Thy-1* ($p<0.01$) in cells that were stretched in the presence of IPF patient plasma compared to cells treated with IPF plasma without stretch. It may be possible that treatment with patient plasma alongside stretch is leading to a reduction in Thy-1, a change that occurs in IPF patient tissue.

In the A549 epithelial cells 6.66% unidirectional stretch alone caused no significant differences in any of the genes tested including *COL1A1, Snail, Slug, E-cadherin* and the CCN family. As expected, treatment of the cells with TGF-β (1.5ng/ml) caused a significant increase in *COL1A1* and the transcription factor *Slug*. There was also an increase in the transcription factor *Snail* but this did not meet significance. There were no significant changes in the CCN family when the cells were treated with TGF-β alone. This differed to the results presented in chapter 4 where there was an increase in *CCN1* and *CCN2* with TGF-β treatment. It is unclear why there was this discrepancy. The results presented in chapter 4 were after 48 hours whereas the results from this work were after 24 hours and it is recognised that changes in gene expression can vary at different time points. It should also be noted that the results in chapter 4 only reached significance at the higher concentrations of TGF-β used (3ng/ml) and although there was upregulation at the smaller concentration (1.5ng/ml), this was not a significant change. More importantly it should be noted that there were differences in the material of the chamber that the cells were plated on (the cells that were used in the stretch experiment were plated in silicone chambers coated with laminin rather than cell culture plastic) potentially leading to a change in the way the cells responded to TGF-β.

When A549 epithelial cells were treated with TGF-β and stretch there was a significant attenuation of *COL1A1*. This is surprising, as it would be expected that

cells that are undergoing more shear forces would upregulate their expression of collagen. This change occurs alongside a significant reduction in the transcription factor *Slug* in the same cells treated with TGF-β and stretch.

When the A549 epithelial cells in this experiment were treated with human plasma and stretch there was a downregulation of *COL1A1* ($p<0.05$) in the group treated with stretch and IPF patient plasma compared to cells that were not stretched. There appeared to be a corresponding reduction in the transcription factors *Slug* and *Snail*, as well as *CCN2*, potentially leading to these effects but these changes did not meet significance. As discussed previously Slug and Snail appear to drive the fibrotic response, leading to changes in expression of the ECM proteins. These changes appear to mirror those effects seen when cells were treated with TGF-β and stretch.

It is interesting that the addition of stretch to TGF-β treatment attenuates any fibrotic response. It is unclear why stretch would have this effect in both fibroblasts and epithelial cells. The possibility is that this is a mechanism that has been adapted during natural breathing to prevent the lung becoming fibrotic when it is continually undergoing shear forces.

It should be noted that there have been other studies published that show conflicting evidence for an attenuated response. Heise et al isolated type II alveolar epithelial cells from mice and applied mechanical stretch (195). They noted that mechanical stretch reduced the amount of E-cadherin, and increased the amount of vimentin and α-SMA, changes associated with EMT (195). However, these changes occurred after 15% stretch was applied to the cells for 4 days. This may explain the differences seen, as 6% stretch mirrors the force that the epithelial cells undergo on a daily basis during natural breathing, a process in which a fibrotic response should not occur. An *in vivo* study injured the lungs of mice using acid aspiration to assess the effect of mechanical ventilation after injury. The mice that underwent ventilation, associated with increased stretch and shear forces, showed increased expression of TGF-β and α-SMA. There was also an increase in hydroxyproline content of the lung (a surrogate marker for excess collagen deposition) as well as histological specimens showing more evidence of fibrosis (196). It should be noted that this study is difficult to compare as it is an *in vivo* study rather than in a single cell line. These changes also occurred after 15 days, a much longer time point than

assessed in the above model. The amount of stretch force applied was also significantly greater as the authors were trying to replicate the excessive stress that occurs during mechanical ventilation. Again, these differences may explain the conflicting results. A further study took normal human lung tissue and tissue from patients with IPF and applied stretch to both specimens. There was a significant increase in the stiffness present in the IPF tissue. There was also an increase in active TGF-β and the amount of phosphorylated Smad 2 and 3 secreted by the fibrotic tissue when stretched in comparison to control tissue (197). However, the patients used in this study had established IPF and it could be argued that once the tissue has fibrosed the changes continue in a positive feedback cycle.

7.7 Conclusion and Proposed Further Work

In conclusion, the results from thesis have shown that respiratory physicians rarely misdiagnose IPF using currently available serology alongside HRCT scan appearances. This gives confidence that the majority of patients are receiving the best available treatment for their conditions. Further work would assess patients with other patterns found in ILD such as NSIP and organising pneumonia to assess if there is a higher prevalence of antibodies in these patients. It is recognised that these HRCT patterns are more commonly associated with a CTD-ILD, and so there may be more patients diagnosed with "idiopathic" disease in these subgroups that actually have an underlying CTD.

A cellular model has been produced which is capable of measuring changes in fibroblasts and epithelial cells when treated with increasing concentrations of TGF-β in a reliable and reproducible way. Evidence to suggest this was reliable includes the consistency with which the changes occurred throughout the experiments.

This model was then used to assess for changes in those cell lines occurring when they were treated with plasma from patients with ILD. The main difficulty with this experiment is a large variability between individuals and so it is difficult to undertake the experiment using sufficient numbers of patients to ensure that

significant findings are a true difference. Given the variation present it would be important to repeat this experiment and re-assess the genes that showed significant changes and ensure that these changes were reproducible. Given there were no changes at 48 and 72 hours but any significant differences found were at 24 hours it may be more important to assess earlier time points such as 12 hours, when changes in transcription factors may be more apparent.

The final chapter added the dimension of stretch to the cellular model. Cells in the lungs are continually moving to allow respiration and the aim of adapting this model was to replicate this movement to assess the effects. There appeared to be an attenuation in any response to TGF-β when stretch was added. It is hypothesised that this may be an adaptation of pulmonary cells to prevent fibrosis occurring during normal breathing. It would be interesting to assess the effects of stretch in the same cell lines at different time points, using different concentrations of TGF-β and using different stretch forces.

Although this is very preliminary work, there are trends in key genes that should be explored further to understand the pathways involved in IPF and SSc-ILD, to understand why individual patients may respond to certain therapeutic options allowing for a more personalised therapeutic choice.

8 References

1. Moore KL DA. Clinically Orientated Anatomy. Fourth ed: Lippincott, Williams and Wilkins; 1999.
2. Tortura GJ GS. Principles of Anatomy and Physiology. Tenth edition ed: John Wiley and Sons, Inc; 2002.
3. Ryerson CJ, Collard HR. Update on the diagnosis and classification of ILD. Current opinion in pulmonary medicine. 2013;19(5):453-9.
4. Han Q, Luo Q, Xie JX, Wu LL, Liao LY, Zhang XX, et al. Diagnostic yield and postoperative mortality associated with surgical lung biopsy for evaluation of interstitial lung diseases: A systematic review and meta-analysis. Journal of Thoracic and cardiovascular surgery. 2015;149(5):1394-401.
5. Lynch DA, Travis WD, Muller NL, Galvin JR, Hansell DM, Grenier PA, et al. Idiopathic interstitial pneumonias: CT features. Radiology. 2005;236(1):10-21.
6. Kim EJ, Elicker BM, Maldonado F, Webb WR, Ryu JH, Van Uden JH, et al. Usual interstitial pneumonia in rheumatoid arthritis-associated interstitial lung disease. The European respiratory journal. 2010;35(6):1322-8.
7. American Thoracic S, European Respiratory S. American Thoracic Society/European Respiratory Society International Multidisciplinary Consensus Classification of the Idiopathic Interstitial Pneumonias. This joint statement of the American Thoracic Society (ATS), and the European Respiratory Society (ERS) was adopted by the ATS board of directors, June 2001 and by the ERS Executive Committee, June 2001. American journal of respiratory and critical care medicine. 2002;165(2):277-304.
8. Bouros D, Wells AU, Nicholson AG, Colby TV, Polychronopoulos V, Pantelidis P, et al. Histopathologic subsets of fibrosing alveolitis in patients with systemic sclerosis and their relationship to outcome. American journal of respiratory and critical care medicine. 2002;165(12):1581-6.
9. Debray MP, Borie R, Revel MP, Naccache JM, Khalil A, Toper C, et al. Interstitial lung disease in anti-synthetase syndrome: initial and follow-up CT findings. European journal of radiology. 2015;84(3):516-23.
10. Wells AU. High-resolution computed tomography and scleroderma lung disease. Rheumatology. 2008;47 Suppl 5:v59-61.
11. Raghu G, Collard HR, Egan JJ, Martinez FJ, Behr J, Brown KK, et al. An official ATS/ERS/JRS/ALAT statement: idiopathic pulmonary fibrosis: evidence-based guidelines for diagnosis and management. American journal of respiratory and critical care medicine. 2011;183(6):788-824.
12. Aziz ZA, Wells AU, Hansell DM, Bain GA, Copley SJ, Desai SR, et al. HRCT diagnosis of diffuse parenchymal lung disease: inter-observer variation. Thorax. 2004;59(6):506-11.
13. Collard HR, King TE, Jr., Bartelson BB, Vourlekis JS, Schwarz MI, Brown KK. Changes in clinical and physiologic variables predict survival in idiopathic pulmonary fibrosis. American journal of respiratory and critical care medicine. 2003;168(5):538-42.
14. Kim DS, Collard HR, King TE, Jr. Classification and natural history of the idiopathic interstitial pneumonias. Proceedings of the American Thoracic Society. 2006;3(4):285-92.

15. Idiopathic Pulmonary Fibrosis Clinical Research Network, Raghu G, Anstrom KJ, King TE, Jr., Lasky JA, Martinez FJ. Prednisone, azathioprine, and N-acetylcysteine for pulmonary fibrosis. The New England journal of medicine. 2012;366(21):1968-77.
16. King TE, Jr., Bradford WZ, Castro-Bernardini S, Fagan EA, Glaspole I, Glassberg MK, et al. A phase 3 trial of pirfenidone in patients with idiopathic pulmonary fibrosis. The New England journal of medicine. 2014;370(22):2083-92.
17. Richeldi L, du Bois RM, Raghu G, Azuma A, Brown KK, Costabel U, et al. Efficacy and safety of nintedanib in idiopathic pulmonary fibrosis. The New England journal of medicine. 2014;370(22):2071-82.
18. Noble PW, Albera C, Bradford WZ, Costabel U, Glassberg MK, Kardatzke D, et al. Pirfenidone in patients with idiopathic pulmonary fibrosis (CAPACITY): two randomised trials. Lancet. 2011;377(9779):1760-9.
19. Flaherty KR, King TE, Jr., Raghu G, Lynch JP, 3rd, Colby TV, Travis WD, et al. Idiopathic interstitial pneumonia: what is the effect of a multidisciplinary approach to diagnosis? American journal of respiratory and critical care medicine. 2004;170(8):904-10.
20. Steen VD, Medsger TA. Changes in causes of death in systemic sclerosis, 1972-2002. Annals of the rheumatic diseases. 2007;66(7):940-4.
21. Dalakas MC. Polymyositis, dermatomyositis and inclusion-body myositis. The New England journal of medicine. 1991;325(21):1487-98.
22. Marie I, Josse S, Hatron PY, Dominique S, Hachulla E, Janvresse A, et al. Interstitial lung disease in anti-Jo-1 patients with antisynthetase syndrome. Arthritis care & research. 2013;65(5):800-8.
23. Solomon J, Swigris JJ, Brown KK. Myositis-related interstitial lung disease and antisynthetase syndrome. Jornol Brasileiro de Pneumologia. 2011;37(1):100-9.
24. Fathi M, Vikgren J, Boijsen M, Tylen U, Jorfeldt L, Tornling G, et al. Interstitial lung disease in polymyositis and dermatomyositis: longitudinal evaluation by pulmonary function and radiology. Arthritis and rheumatism. 2008;59(5):677-85.
25. Wollheim FA. Classification of systemic sclerosis. Visions and reality. Rheumatology. 2005;44(10):1212-6.
26. Gabrielli A, Avvedimento EV, Krieg T. Scleroderma. The New England journal of medicine. 2009;360(19):1989-2003.
27. Steele R, Hudson M, Lo E, Baron M, Canadian Scleroderma Research G. Clinical decision rule to predict the presence of interstitial lung disease in systemic sclerosis. Arthritis care & research. 2012;64(4):519-24.
28. Winstone TA, Assayag D, Wilcox PG, Dunne JV, Hague CJ, Leipsic J, et al. Predictors of mortality and progression in scleroderma-associated interstitial lung disease: a systematic review. Chest. 2014;146(2):422-36.
29. Komocsi A, Vorobcsuk A, Faludi R, Pinter T, Lenkey Z, Kolto G, et al. The impact of cardiopulmonary manifestations on the mortality of SSc: a systematic review and meta-analysis of observational studies. Rheumatology. 2012;51(6):1027-36.
30. Solomon JJ, Olson AL, Fischer A, Bull T, Brown KK, Raghu G. Scleroderma lung disease. European respiratory review : an official journal of the European Respiratory Society. 2013;22(127):6-19.
31. Dawson JK, Fewins HE, Desmond J, Lynch MP, Graham DR. Fibrosing alveolitis in patients with rheumatoid arthritis as assessed by high resolution

computed tomography, chest radiography, and pulmonary function tests. Thorax. 2001;56(8):622-7.
32. Koduri G, Norton S, Young A, Cox N, Davies P, Devlin J, et al. Interstitial lung disease has a poor prognosis in rheumatoid arthritis: results from an inception cohort. Rheumatology. 2010;49(8):1483-9.
33. Kelly CA, Saravanan V, Nisar M, Arthanari S, Woodhead FA, Price-Forbes AN, et al. Rheumatoid arthritis-related interstitial lung disease: associations, prognostic factors and physiological and radiological characteristics-a large multicentre UK study. Rheumatology. 2014;53(9):1676-82.
34. Marie I, Josse S, Decaux O, Diot E, Landron C, Roblot P, et al. Clinical manifestations and outcome of anti-PL7 positive patients with antisynthetase syndrome. European journal of internal medicine. 2013;24(5):474-9.
35. Kalluri M, Sahn SA, Oddis CV, Gharib SL, Christopher-Stine L, Danoff SK, et al. Clinical profile of anti-PL-12 autoantibody. Cohort study and review of the literature. Chest. 2009;135(6):1550-6.
36. Stone KB, Oddis CV, Fertig N, Katsumata Y, Lucas M, Vogt M, et al. Anti-Jo-1 antibody levels correlate with disease activity in idiopathic inflammatory myopathy. Arthritis and rheumatism. 2007;56(9):3125-31.
37. Hall JC, Casciola-Rosen L, Samedy LA, Werner J, Owoyemi K, Danoff SK, et al. Anti-melanoma differentiation-associated protein 5-associated dermatomyositis: expanding the clinical spectrum. Arthritis care & research. 2013;65(8):1307-15.
38. Hirakata M, Suwa A, Takada T, Sato S, Nagai S, Genth E, et al. Clinical and immunogenetic features of patients with autoantibodies to asparaginyl-transfer RNA synthetase. Arthritis and rheumatism. 2007;56(4):1295-303.
39. Sato S, Kuwana M, Hirakata M. Clinical characteristics of Japanese patients with anti-OJ (anti-isoleucyl-tRNA synthetase) autoantibodies. Rheumatology. 2007;46(5):842-5.
40. Hamaguchi Y, Fujimoto M, Matsushita T, Kaji K, Komura K, Hasegawa M, et al. Common and distinct clinical features in adult patients with anti-aminoacyl-tRNA synthetase antibodies: heterogeneity within the syndrome. PloS one. 2013;8(4):e60442.
41. Betteridge Z, Gunawardena H, North J, Slinn J, McHugh N. Anti-synthetase syndrome: a new autoantibody to phenylalanyl transfer RNA synthetase (anti-Zo) associated with polymyositis and interstitial pneumonia. Rheumatology. 2007;46(6):1005-8.
42. Koga T, Fujikawa K, Horai Y, Okada A, Kawashiri SY, Iwamoto N, et al. The diagnostic utility of anti-melanoma differentiation-associated gene 5 antibody testing for predicting the prognosis of Japanese patients with DM. Rheumatology. 2012;51(7):1278-84.
43. Moghadam-Kia S, Oddis CV, Sato S, Kuwana M, Aggarwal R. Anti-MDA5 is associated with rapidly progressive lung disease and poor survival in U.S. patients with amyopathic and myopathic dermatomyositis. Arthritis care & research. 2015.
44. Betteridge ZE, Gunawardena H, McHugh NJ. Novel autoantibodies and clinical phenotypes in adult and juvenile myositis. Arthritis research & therapy. 2011;13(2):209.
45. Lega JC, Fabien N, Reynaud Q, Durieu I, Durupt S, Dutertre M, et al. The clinical phenotype associated with myositis-specific and associated autoantibodies: a meta-analysis revisiting the so-called antisynthetase syndrome. Autoimmunity reviews. 2014;13(9):883-91.

46. Denton CP. Advances in pathogenesis and treatment of systemic sclerosis. Clinical medicine journal. 2016;16(1):55-60.
47. Selva-O'Callaghan A, Labrador-Horrillo M, Solans-Laque R, Simeon-Aznar CP, Martinez-Gomez X, Vilardell-Tarres M. Myositis-specific and myositis-associated antibodies in a series of eighty-eight Mediterranean patients with idiopathic inflammatory myopathy. Arthritis and rheumatism. 2006;55(5):791-8.
48. Gunnarsson R, Aalokken TM, Molberg O, Lund MB, Mynarek GK, Lexberg AS, et al. Prevalence and severity of interstitial lung disease in mixed connective tissue disease: a nationwide, cross-sectional study. Annals of the rheumatic diseases. 2012;71(12):1966-72.
49. Mierau R, Moinzadeh P, Riemekasten G, Melchers I, Meurer M, Reichenberger F, et al. Frequency of disease-associated and other nuclear autoantibodies in patients of the German Network for Systemic Scleroderma: correlation with characteristic clinical features. Arthritis research & therapy. 2011;13(5):R172.
50. Steen VD. Autoantibodies in systemic sclerosis. Seminars in arthritis and rheumatism. 2005;35(1):35-42.
51. Walker UA, Tyndall A, Czirjak L, Denton C, Farge-Bancel D, Kowal-Bielecka O, et al. Clinical risk assessment of organ manifestations in systemic sclerosis: a report from the EULAR Scleroderma Trials And Research group database. Annals of the rheumatic diseases. 2007;66(6):754-63.
52. Hamaguchi Y. Autoantibody profiles in systemic sclerosis: predictive value for clinical evaluation and prognosis. The Journal of dermatology. 2010;37(1):42-53.
53. Mitri GM, Lucas M, Fertig N, Steen VD, Medsger TA, Jr. A comparison between anti-Th/To- and anticentromere antibody-positive systemic sclerosis patients with limited cutaneous involvement. Arthritis and rheumatism. 2003;48(1):203-9.
54. Arnett FC, Reveille JD, Goldstein R, Pollard KM, Leaird K, Smith EA, et al. Autoantibodies to fibrillarin in systemic sclerosis (scleroderma). An immunogenetic, serologic, and clinical analysis. Arthritis and rheumatism. 1996;39(7):1151-60.
55. Aggarwal R, Lucas M, Fertig N, Oddis CV, Medsger TA, Jr. Anti-U3 RNP autoantibodies in systemic sclerosis. Arthritis and rheumatism. 2009;60(4):1112-8.
56. Fertig N, Domsic RT, Rodriguez-Reyna T, Kuwana M, Lucas M, Medsger TA, Jr., et al. Anti-U11/U12 RNP antibodies in systemic sclerosis: a new serologic marker associated with pulmonary fibrosis. Arthritis and rheumatism. 2009;61(7):958-65.
57. Kaji K, Fertig N, Medsger TA, Jr., Satoh T, Hoshino K, Hamaguchi Y, et al. Autoantibodies to RuvBL1 and RuvBL2: a novel systemic sclerosis-related antibody associated with diffuse cutaneous and skeletal muscle involvement. Arthritis care & research. 2014;66(4):575-84.
58. Betteridge Z WF, Bunn C, Denton CD, Abraham DJ, Desai S, du Bois R, Wells AU, McHugh N. Anti-EIF2B: A novel interstitial lung disease associated autoantibody in patients with systemic sclerosis [Abstract]. Arthritis Rheumatism. 2012;64(Suppl 10):854.
59. Mehra S, Walker J, Patterson K, Fritzler MJ. Autoantibodies in systemic sclerosis. Autoimmunity reviews. 2013;12(3):340-54.
60. Denton CP, Krieg T, Guillevin L, Schwierin B, Rosenberg D, Silkey M, et al. Demographic, clinical and antibody characteristics of patients with digital ulcers

in systemic sclerosis: data from the DUO Registry. Annals of the rheumatic diseases. 2012;71(5):718-21.
61. Hesselstrand R, Scheja A, Shen GQ, Wiik A, Akesson A. The association of antinuclear antibodies with organ involvement and survival in systemic sclerosis. Rheumatology. 2003;42(4):534-40.
62. Kuwana M, Kaburaki J, Mimori T, Kawakami Y, Tojo T. Longitudinal analysis of autoantibody response to topoisomerase I in systemic sclerosis. Arthritis and rheumatism. 2000;43(5):1074-84.
63. Gabrielli A, Svegliati S, Moroncini G, Avvedimento EV. Pathogenic autoantibodies in systemic sclerosis. Current opinion in immunology. 2007;19(6):640-5.
64. Castelino FV, Goldberg H, Dellaripa PF. The impact of rheumatological evaluation in the management of patients with interstitial lung disease. Rheumatology. 2011;50(3):489-93.
65. Bussone G, Mouthon L. Interstitial lung disease in systemic sclerosis. Autoimmunity reviews. 2011;10(5):248-55.
66. Song JW, Do KH, Kim MY, Jang SJ, Colby TV, Kim DS. Pathologic and radiologic differences between idiopathic and collagen vascular disease-related usual interstitial pneumonia. Chest. 2009;136(1):23-30.
67. Cotton CV, Spencer LG, New RP, Cooper RG. The utility of comprehensive autoantibody testing to differentiate connective tissue disease associated and idiopathic interstitial lung disease subgroup cases. Rheumatology. 2017;56(8):1264-71.
68. Fischer A, Antoniou KM, Brown KK, Cadranel J, Corte TJ, du Bois RM, et al. An official European Respiratory Society/American Thoracic Society research statement: interstitial pneumonia with autoimmune features. The European respiratory journal. 2015; 46(4): 976-87.
69. Watanabe K, Handa T, Tanizawa K, Hosono Y, Taguchi Y, Noma S, et al. Detection of antisynthetase syndrome in patients with idiopathic interstitial pneumonias. Respiratory medicine. 2011;105(8):1238-47.
70. Song JS, Hwang J, Cha HS, Jeong BH, Suh GY, Chung MP, et al. Significance of myositis autoantibody in patients with idiopathic interstitial lung disease. Yonsei medical journal. 2015;56(3):676-83.
71. Williamson JD, Sadofsky LR, Hart SP. The pathogenesis of bleomycin-induced lung injury in animals and its applicability to human idiopathic pulmonary fibrosis. Experimental lung research. 2015;41(2):57-73.
72. Degryse AL, Tanjore H, Xu XC, Polosukhin VV, Jones BR, McMahon FB, et al. Repetitive intratracheal bleomycin models several features of idiopathic pulmonary fibrosis. American journal of physiology lung cellular and molecular physiology. 2010;299(4):L442-52.
73. Beach TA, Johnston CJ, Groves AM, Williams JP, Finkelstein JN. Radiation induced pulmonary fibrosis as a model of progressive fibrosis: Contributions of DNA damage, inflammatory response and cellular senescence genes. Experimental lung research. 2017;43(3):134-49.
74. Liu JY, Sime PJ, Wu T, Warshamana GS, Pociask D, Tsai SY, et al. Transforming growth factor-beta(1) overexpression in tumor necrosis factor-alpha receptor knockout mice induces fibroproliferative lung disease. American journal of respiratory cell and molecular biology. 2001;25(1):3-7.
75. Wells AU, Denton CP. Interstitial lung disease in connective tissue disease-mechanisms and management. Nature reviews rheumatology. 2014;10(12):728-39.

76. Lu P, Weaver VM, Werb Z. The extracellular matrix: a dynamic niche in cancer progression. Journal of cell biology. 2012;196(4):395-406.
77. Frantz C, Stewart KM, Weaver VM. The extracellular matrix at a glance. Journal of cell science. 2010;123(Pt 24):4195-200.
78. Fan D, Takawale A, Lee J, Kassiri Z. Cardiac fibroblasts, fibrosis and extracellular matrix remodeling in heart disease. Fibrogenesis Tissue Repair. 2012;5(1):15.
79. van der Slot-Verhoeven AJ, van Dura EA, Attema J, Blauw B, Degroot J, Huizinga TW, et al. The type of collagen cross-link determines the reversibility of experimental skin fibrosis. Biochimica et biophysica acta. 2005;1740(1):60-7.
80. Pankov R, Yamada KM. Fibronectin at a glance. Journal of cell science. 2002;115(Pt 20):3861-3.
81. Kuhn C, McDonald JA. The roles of the myofibroblast in idiopathic pulmonary fibrosis. Ultrastructural and immunohistochemical features of sites of active extracellular matrix synthesis. American journal of pathology. 1991;138(5):1257-65.
82. Muro AF, Moretti FA, Moore BB, Yan M, Atrasz RG, Wilke CA, et al. An essential role for fibronectin extra type III domain A in pulmonary fibrosis. American journal of respiratory and critical care medicine. 2008;177(6):638-45.
83. Bosman FT, Stamenkovic I. Functional structure and composition of the extracellular matrix. Journal of pathology. 2003;200(4):423-8.
84. Venkatesan N, Ebihara T, Roughley PJ, Ludwig MS. Alterations in large and small proteoglycans in bleomycin-induced pulmonary fibrosis in rats. American journal of respiratory and critical care medicine. 2000;161(6):2066-73.
85. Westergren-Thorsson G, Hedstrom U, Nybom A, Tykesson E, Ahrman E, Hornfelt M, et al. Increased deposition of glycosaminoglycans and altered structure of heparan sulfate in idiopathic pulmonary fibrosis. International journal of biochemistry and cell biology. 2017;83:27-38.
86. Craig VJ, Zhang L, Hagood JS, Owen CA. Matrix metalloproteinases as therapeutic targets for idiopathic pulmonary fibrosis. American journal of respiratory cell and molecular biology. 2015;53(5):585-600.
87. Yamashita CM, Dolgonos L, Zemans RL, Young SK, Robertson J, Briones N, et al. Matrix metalloproteinase 3 is a mediator of pulmonary fibrosis. American journal of pathology. 2011;179(4):1733-45.
88. Zuo F, Kaminski N, Eugui E, Allard J, Yakhini Z, Ben-Dor A, et al. Gene expression analysis reveals matrilysin as a key regulator of pulmonary fibrosis in mice and humans. Proceedings of the National Academy of Sciences of the United States of America. 2002;99(9):6292-7.
89. Derynck R, Zhang YE. Smad-dependent and Smad-independent pathways in TGF-beta family signalling. Nature. 2003;425(6958):577-84.
90. Kulkarni AB, Huh CG, Becker D, Geiser A, Lyght M, Flanders KC, et al. Transforming growth factor beta 1 null mutation in mice causes excessive inflammatory response and early death. Proceedings of the National Academy of Sciences of the United States of America. 1993;90(2):770-4.
91. Schnaper HW, Hayashida T, Hubchak SC, Poncelet AC. TGF-beta signal transduction and mesangial cell fibrogenesis. American journal of physiology. Renal physiology. 2003;284(2):F243-52.
92. Annes JP, Munger JS, Rifkin DB. Making sense of latent TGFbeta activation. Journal of cell science. 2003;116(Pt 2):217-24.

93. Moustakas A, Souchelnytskyi S, Heldin CH. Smad regulation in TGF-beta signal transduction. Journal of cell science. 2001;114(Pt 24):4359-69.
94. Zhang YE. Non-Smad pathways in TGF-beta signaling. Cell research. 2009;19(1):128-39.
95. Ponticos M, Holmes AM, Shi-wen X, Leoni P, Khan K, Rajkumar VS, et al. Pivotal role of connective tissue growth factor in lung fibrosis: MAPK-dependent transcriptional activation of type I collagen. Arthritis and rheumatism. 2009;60(7):2142-55.
96. Kanaan R, Strange C. Use of multitarget tyrosine kinase inhibitors to attenuate platelet-derived growth factor signalling in lung disease. European respiratory review : an official journal of the European respiratory society. 2017;26(146).
97. Lasky JA, Tonthat B, Liu JY, Friedman M, Brody AR. Upregulation of the PDGF-alpha receptor precedes asbestos-induced lung fibrosis in rats. American journal of respiratory and critical care medicine. 1998;157(5 Pt 1):1652-7.
98. Maeda A, Hiyama K, Yamakido H, Ishioka S, Yamakido M. Increased expression of platelet-derived growth factor A and insulin-like growth factor-I in BAL cells during the development of bleomycin-induced pulmonary fibrosis in mice. Chest. 1996;109(3):780-6.
99. Makino K, Makino T, Stawski L, Lipson KE, Leask A, Trojanowska M. Anti-connective tissue growth factor (CTGF/CCN2) monoclonal antibody attenuates skin fibrosis in mice models of systemic sclerosis. Arthritis research & therapy. 2017;19(1):134.
100. Abdollahi A, Li M, Ping G, Plathow C, Domhan S, Kiessling F, et al. Inhibition of platelet-derived growth factor signaling attenuates pulmonary fibrosis. Journal of experimental medicine. 2005;201(6):925-35.
101. Hinz B, Phan SH, Thannickal VJ, Galli A, Bochaton-Piallat ML, Gabbiani G. The myofibroblast: one function, multiple origins. American journal of pathology. 2007;170(6):1807-16.
102. Zhou Y, Huang X, Hecker L, Kurundkar D, Kurundkar A, Liu H, et al. Inhibition of mechanosensitive signaling in myofibroblasts ameliorates experimental pulmonary fibrosis. Journal of clinical investigation. 2013;123(3):1096-108.
103. Shiwen X, Stratton R, Nikitorowicz-Buniak J, Ahmed-Abdi B, Ponticos M, Denton C, et al. A Role of Myocardin Related Transcription Factor-A (MRTF-A) in Scleroderma Related Fibrosis. PloS one. 2015;10(5):e0126015.
104. Sisson TH, Ajayi IO, Subbotina N, Dodi AE, Rodansky ES, Chibucos LN, et al. Inhibition of myocardin-related transcription factor/serum response factor signaling decreases lung fibrosis and promotes mesenchymal cell apoptosis. American journal of pathology. 2015;185(4):969-86.
105. Hay ED. An overview of epithelio-mesenchymal transformation. Acta anatomica (Basel). 1995;154(1):8-20.
106. Fragiadaki M, Mason RM. Epithelial-mesenchymal transition in renal fibrosis - evidence for and against. International journal of experimental pathology. 2011;92(3):143-50.
107. Lamouille S, Xu J, Derynck R. Molecular mechanisms of epithelial-mesenchymal transition. Nature reviews molecular cell biology. 2014;15(3):178-96.
108. Kasai H, Allen JT, Mason RM, Kamimura T, Zhang Z. TGF-beta1 induces human alveolar epithelial to mesenchymal cell transition (EMT). Respiratory research. 2005;6:56.

109. Hosper NA, van den Berg PP, de Rond S, Popa ER, Wilmer MJ, Masereeuw R, et al. Epithelial-to-mesenchymal transition in fibrosis: collagen type I expression is highly upregulated after EMT, but does not contribute to collagen deposition. Experimental cell research. 2013;319(19):3000-9.
110. Iwano M, Plieth D, Danoff TM, Xue C, Okada H, Neilson EG. Evidence that fibroblasts derive from epithelium during tissue fibrosis. Journal of clinical investigation. 2002;110(3):341-50.
111. Tanjore H, Xu XC, Polosukhin VV, Degryse AL, Li B, Han W, et al. Contribution of epithelial-derived fibroblasts to bleomycin-induced lung fibrosis. American journal of respiratory and critical care medicine. 2009;180(7):657-65.
112. Boye K, Maelandsmo GM. S100A4 and metastasis: a small actor playing many roles. American journal of pathology. 2010;176(2):528-35.
113. Hashimoto N, Phan SH, Imaizumi K, Matsuo M, Nakashima H, Kawabe T, et al. Endothelial-mesenchymal transition in bleomycin-induced pulmonary fibrosis. American journal of respiratory cell and molecular biology. 2010;43(2):161-72.
114. Mendoza FA, Piera-Velazquez S, Farber JL, Feghali-Bostwick C, Jimenez SA. Endothelial Cells Expressing Endothelial and Mesenchymal Cell Gene Products in Lung Tissue From Patients With Systemic Sclerosis-Associated Interstitial Lung Disease. Arthritis & rheumatology. 2016;68(1):210-7.
115. Hung C, Linn G, Chow YH, Kobayashi A, Mittelsteadt K, Altemeier WA, et al. Role of lung pericytes and resident fibroblasts in the pathogenesis of pulmonary fibrosis. American journal of respiratory and critical care medicine. 2013;188(7):820-30.
116. Andersson-Sjoland A, de Alba CG, Nihlberg K, Becerril C, Ramirez R, Pardo A, et al. Fibrocytes are a potential source of lung fibroblasts in idiopathic pulmonary fibrosis. International journal of biochemistry and cell biology. 2008;40(10):2129-40.
117. Holbourn KP, Acharya KR, Perbal B. The CCN family of proteins: structure-function relationships. Trends in biochemical sciences. 2008;33(10):461-73.
118. Jun JI, Lau LF. The matricellular protein CCN1 induces fibroblast senescence and restricts fibrosis in cutaneous wound healing. Nature cell biology. 2010;12(7):676-85.
119. Kim KH, Chen CC, Monzon RI, Lau LF. Matricellular protein CCN1 promotes regression of liver fibrosis through induction of cellular senescence in hepatic myofibroblasts. Molecular and cellular biology. 2013;33(10):2078-90.
120. Meyer K, Hodwin B, Ramanujam D, Engelhardt S, Sarikas A. Essential Role for Premature Senescence of Myofibroblasts in Myocardial Fibrosis. Journal of the American college of cardiology. 2016;67(17):2018-28.
121. Lai CF, Chen YM, Chiang WC, Lin SL, Kuo ML, Tsai TJ. Cysteine-rich protein 61 plays a proinflammatory role in obstructive kidney fibrosis. PloS one. 2013;8(2):e56481.
122. Grazioli S, Gil S, An D, Kajikawa O, Farnand AW, Hanson JF, et al. CYR61 (CCN1) overexpression induces lung injury in mice. American journal of physiology lung cellular and molecular physiology. 2015;308(8):L759-65.
123. Kurundkar AR, Kurundkar D, Rangarajan S, Locy ML, Zhou Y, Liu RM, et al. The matricellular protein CCN1 enhances TGF-beta1/SMAD3-dependent profibrotic signaling in fibroblasts and contributes to fibrogenic responses to lung injury. FASEB journal. 2016;30(6):2135-50.

124. Ivkovic S, Yoon BS, Popoff SN, Safadi FF, Libuda DE, Stephenson RC, et al. Connective tissue growth factor coordinates chondrogenesis and angiogenesis during skeletal development. Development. 2003;130(12):2779-91.
125. Mori T, Kawara S, Shinozaki M, Hayashi N, Kakinuma T, Igarashi A, et al. Role and interaction of connective tissue growth factor with transforming growth factor-beta in persistent fibrosis: A mouse fibrosis model. Journal of cell physiology. 1999;181(1):153-9.
126. Blaauw E, Lorenzen-Schmidt I, Babiker FA, Munts C, Prinzen FW, Snoeckx LH, et al. Stretch-induced upregulation of connective tissue growth factor in rabbit cardiomyocytes. Journal of cardiovascular translational research. 2013;6(5):861-9.
127. Kroening S, Neubauer E, Wullich B, Aten J, Goppelt-Struebe M. Characterization of connective tissue growth factor expression in primary cultures of human tubular epithelial cells: modulation by hypoxia. American journal of physiology renal physiology. 2010;298(3):F796-806.
128. Shi-wen X, Pennington D, Holmes A, Leask A, Bradham D, Beauchamp JR, et al. Autocrine overexpression of CTGF maintains fibrosis: RDA analysis of fibrosis genes in systemic sclerosis. Experimental cell research. 2000;259(1):213-24.
129. Dziadzio M, Usinger W, Leask A, Abraham D, Black CM, Denton C, et al. N-terminal connective tissue growth factor is a marker of the fibrotic phenotype in scleroderma. Quarterly journal of medicine. 2005;98(7):485-92.
130. Liu S, Shi-wen X, Abraham DJ, Leask A. CCN2 is required for bleomycin-induced skin fibrosis in mice. Arthritis and rheumatism. 2011;63(1):239-46.
131. Raghu G, Scholand MB, de Andrade J, Lancaster L, Mageto Y, Goldin J, et al. FG-3019 anti-connective tissue growth factor monoclonal antibody: results of an open-label clinical trial in idiopathic pulmonary fibrosis. The European respiratory journal. 2016;47(5):1481-91.
132. Marchal PO, Kavvadas P, Abed A, Kazazian C, Authier F, Koseki H, et al. Reduced NOV/CCN3 Expression Limits Inflammation and Interstitial Renal Fibrosis after Obstructive Nephropathy in Mice. PloS one. 2015;10(9):e0137876.
133. Heath E, Tahri D, Andermarcher E, Schofield P, Fleming S, Boulter CA. Abnormal skeletal and cardiac development, cardiomyopathy, muscle atrophy and cataracts in mice with a targeted disruption of the Nov (Ccn3) gene. BMC developmental biology. 2008;8:18.
134. Riser BL, Najmabadi F, Perbal B, Peterson DR, Rambow JA, Riser ML, et al. CCN3 (NOV) is a negative regulator of CCN2 (CTGF) and a novel endogenous inhibitor of the fibrotic pathway in an in vitro model of renal disease. American journal of pathology. 2009;174(5):1725-34.
135. Abd El Kader T, Kubota S, Janune D, Nishida T, Hattori T, Aoyama E, et al. Anti-fibrotic effect of CCN3 accompanied by altered gene expression profile of the CCN family. Journal of cell communication and signaling. 2013;7(1):11-8.
136. Konigshoff M, Kramer M, Balsara N, Wilhelm J, Amarie OV, Jahn A, et al. WNT1-inducible signaling protein-1 mediates pulmonary fibrosis in mice and is upregulated in humans with idiopathic pulmonary fibrosis. Journal of clinical investigation. 2009;119(4):772-87.
137. Li X, Chen Y, Ye W, Tao X, Zhu J, Wu S, et al. Blockade of CCN4 attenuates CCl4-induced liver fibrosis. Archives of medical science. 2015;11(3):647-53.
138. Myers RB, Rwayitare K, Richey L, Lem J, Castellot JJ, Jr. CCN5 Expression in mammals. III. Early embryonic mouse development. Journal of cell communication and signaling. 2012;6(4):217-23.

139. Zhang L, Li Y, Liang C, Yang W. CCN5 overexpression inhibits profibrotic phenotypes via the PI3K/Akt signaling pathway in lung fibroblasts isolated from patients with idiopathic pulmonary fibrosis and in an in vivo model of lung fibrosis. International journal of molecular medicine. 2014;33(2):478-86.
140. Hagood JS, Prabhakaran P, Kumbla P, Salazar L, MacEwen MW, Barker TH, et al. Loss of fibroblast Thy-1 expression correlates with lung fibrogenesis. American journal of pathology. 2005;167(2):365-79.
141. Coker RK, Laurent GJ, Jeffery PK, du Bois RM, Black CM, McAnulty RJ. Localisation of transforming growth factor beta1 and beta3 mRNA transcripts in normal and fibrotic human lung. Thorax. 2001;56(7):549-56.
142. Lynch DA, Sverzellati N, Travis WD, Brown KK, Colby TV, Galvin JR, et al. Diagnostic criteria for idiopathic pulmonary fibrosis: a Fleischner Society White Paper. The Lancet respiratory medicine. 2018;6(2):138-53.
143. Betteridge ZE, Woodhead F, Lu H, Shaddick G, Bunn CC, Denton CP, et al. Brief Report: Anti-Eukaryotic Initiation Factor 2B Autoantibodies Are Associated With Interstitial Lung Disease in Patients With Systemic Sclerosis. Arthritis & rheumatology. 2016;68(11):2778-83.
144. Khankan R, Oliver N, He S, Ryan SJ, Hinton DR. Regulation of fibronectin-EDA through CTGF domain-specific interactions with TGFbeta2 and its receptor TGFbetaRII. Investigative ophthalmology and visual science. 2011;52(8):5068-78.
145. Li N, Xu H, Fan K, Liu X, Qi J, Zhao C, et al. Altered beta1,6-GlcNAc branched N-glycans impair TGF-beta-mediated epithelial-to-mesenchymal transition through Smad signalling pathway in human lung cancer. Journal of cellular and molecular medicine. 2014;18(10):1975-91.
146. Scarpa M, Grillo AR, Brun P, Macchi V, Stefani A, Signori S, et al. Snail1 transcription factor is a critical mediator of hepatic stellate cell activation following hepatic injury. American journal of physiology gastrointestinal and liver physiology. 2011;300(2):G316-26.
147. Eurlings IM, Reynaert NL, van den Beucken T, Gosker HR, de Theije CC, Verhamme FM, et al. Cigarette smoke extract induces a phenotypic shift in epithelial cells; involvement of HIF1alpha in mesenchymal transition. PloS one. 2014;9(10):e107757.
148. Liu T, Zhang J, Zhang J, Mu X, Su H, Hu X, et al. RNA interference against platelet-derived growth factor receptor alpha mRNA inhibits fibroblast transdifferentiation in skin lesions of patients with systemic sclerosis. PloS one. 2013;8(4):e60414.
149. Sanders YY, Pardo A, Selman M, Nuovo GJ, Tollefsbol TO, Siegal GP, et al. Thy-1 promoter hypermethylation: a novel epigenetic pathogenic mechanism in pulmonary fibrosis. American journal of respiratory cell and molecular biology. 2008;39(5):610-8.
150. Nakashima R, Imura Y, Hosono Y, Seto M, Murakami A, Watanabe K, et al. The multicenter study of a new assay for simultaneous detection of multiple anti-aminoacyl-tRNA synthetases in myositis and interstitial pneumonia. PloS one. 2014;9(1):e85062.
151. Behr J, Nathan SD, Harari S, Wuyts W, Kirchgaessler KU, Bengus M, et al. Sildenafil added to pirfenidone in patients with advanced idiopathic pulmonary fibrosis and risk of pulmonary hypertension: A Phase IIb, randomised, double-blind, placebo-controlled study - Rationale and study design. Respiratory medicine. 2018;138:13-20.

152. Aggarwal R, Cassidy E, Fertig N, Koontz DC, Lucas M, Ascherman DP, et al. Patients with non-Jo-1 anti-tRNA-synthetase autoantibodies have worse survival than Jo-1 positive patients. Annals of the rheumatic diseases. 2014;73(1):227-32.
153. Chan EK, Damoiseaux J, Carballo OG, Conrad K, de Melo Cruvinel W, Francescantonio PL, et al. Report of the First International Consensus on Standardized Nomenclature of Antinuclear Antibody HEp-2 Cell Patterns 2014-2015. Frontiers in immunology. 2015;6:412.
154. Cooley HM, Melny BJ, Gleeson R, Greco T, Kay TW. Clinical and serological associations of anti-Ku antibody. The journal of rheumatology. 1999;26(3):563-7.
155. Cavazzana I, Ceribelli A, Quinzanini M, Scarsi M, Airo P, Cattaneo R, et al. Prevalence and clinical associations of anti-Ku antibodies in systemic autoimmune diseases. Lupus. 2008;17(8):727-32.
156. Harvey GR, Butts S, Rands AL, Patel Y, McHugh NJ. Clinical and serological associations with anti-RNA polymerase antibodies in systemic sclerosis. Clinical and experimental immunology. 1999;117(2):395-402.
157. Bardoni A, Rossi P, Salvini R, Bobbio-Pallavicini F, Caporali R, Montecucco C. Autoantibodies to RNA-polymerases in Italian patients with systemic sclerosis. Clinical and experimental rheumatology. 2003;21(3):301-6.
158. Chartrand S, Swigris JJ, Peykova L, Chung J, Fischer A. A Multidisciplinary Evaluation Helps Identify the Antisynthetase Syndrome in Patients Presenting as Idiopathic Interstitial Pneumonia. The journal of rheumatology. 2016;43(5):887-92.
159. ATCC. "MRC5 Cell Line". ATCC in partnership with LGC standards, 2017. Web, 01 August 2017. Available from: http://www.lgcstandards-atcc.org/products/all/CCL-171.aspx?geo_country=gb#generalinformation.
160. ATCC. "A549 Cell Line". ATCC in partnership with LGC standards, 2017. Web, 01 August 2017. Available from: http://www.lgcstandards-atcc.org/Products/All/CCL-185.aspx?geo_country=gb.
161. US National Library of Medicine. "Basic Local Alignment Search Tool". National Centre for Biotechnology Information, 2016. Web, 10 July 2016. Available from: https://blast.ncbi.nlm.nih.gov/Blast.cgi
162. Liu D, Gong L, Zhu H, Pu S, Wu Y, Zhang W, et al. Curcumin Inhibits Transforming Growth Factor beta Induced Differentiation of Mouse Lung Fibroblasts to Myofibroblasts. Frontiers in pharmacology. 2016;7:419.
163. Pirkmajer S, Chibalin AV. Serum starvation: caveat emptor. American journal of physiology cell physiology. 2011;301(2):C272-9.
164. Schamberger CJ, Gerner C, Cerni C. Caspase-9 plays a marginal role in serum starvation-induced apoptosis. Experimental cell research. 2005;302(1):115-28.
165. MP Biomedicals. "Website for TCH Defined Serum Replacement". MP Biomedicals, 2016. Web, 10 November 2016. Available from: https://www.mpbio.com/product.php?pid=0920200&country=222.
166. Cohen PY, Breuer R, Zisman P, Wallach-Dayan SB. Bleomycin-Treated Chimeric Thy1-Deficient Mice with Thy1-Deficient Myofibroblasts and Thy-Positive Lymphocytes Resolve Inflammation without Affecting the Fibrotic Response. Mediators of inflammation. 2015;2015:942179.
167. Wynn TA, Ramalingam TR. Mechanisms of fibrosis: therapeutic translation for fibrotic disease. Nature medicine. 2012;18(7):1028-40.

168. Yu Z, Kastenmuller G, He Y, Belcredi P, Moller G, Prehn C, et al. Differences between human plasma and serum metabolite profiles. PloS one. 2011;6(7):e21230.
169. Desai SR, Veeraraghavan S, Hansell DM, Nikolakopolou A, Goh NS, Nicholson AG, et al. CT features of lung disease in patients with systemic sclerosis: comparison with idiopathic pulmonary fibrosis and nonspecific interstitial pneumonia. Radiology. 2004;232(2):560-7.
170. Crosby LM, Luellen C, Zhang Z, Tague LL, Sinclair SE, Waters CM. Balance of life and death in alveolar epithelial type II cells: proliferation, apoptosis, and the effects of cyclic stretch on wound healing. American journal of physiology lung cell molecular physiology. 2011;301(4):L536-46.
171. Balestrini JL, Billiar KL. Equibiaxial cyclic stretch stimulates fibroblasts to rapidly remodel fibrin. Journal of biomechanics. 2006;39(16):2983-90.
172. Htwe SS, Cha BH, Yue K, Khademhosseini A, Knox AJ, Ghaemmaghami AM. Role of Rho-Associated Coiled-Coil Forming Kinase Isoforms in Regulation of Stiffness-Induced Myofibroblast Differentiation in Lung Fibrosis. American journal of respiratory cell molecular biology. 2017;56(6):772-83.
173. Mantella LE, Quan A, Verma S. Variability in vascular smooth muscle cell stretch-induced responses in 2D culture. Vascular cell. 2015;7:7.
174. Rantapaa-Dahlqvist S, de Jong BA, Berglin E, Hallmans G, Wadell G, Stenlund H, et al. Antibodies against cyclic citrullinated peptide and IgA rheumatoid factor predict the development of rheumatoid arthritis. Arthritis and rheumatism. 2003;48(10):2741-9.
175. Fischer A, Swigris JJ, du Bois RM, Lynch DA, Downey GP, Cosgrove GP, et al. Anti-synthetase syndrome in ANA and anti-Jo-1 negative patients presenting with idiopathic interstitial pneumonia. Respiratory medicine. 2009;103(11):1719-24.
176. Fine A, Goldstein RH. The effect of transforming growth factor-beta on cell proliferation and collagen formation by lung fibroblasts. Journal of biological chemistry. 1987;262(8):3897-902.
177. Kurokowa M, Lynch K, Podolsky DK. Effects of growth factors on an intestinal epithelial cell line: transforming growth factor beta inhibits proliferation and stimulates differentiation. Biochemical and biophysical research communications. 1987;142(3):775-82.
178. Muller G, Behrens J, Nussbaumer U, Bohlen P, Birchmeier W. Inhibitory action of transforming growth factor beta on endothelial cells. Proceedings of the National Academy of Sciences of the United States of America. 1987;84(16):5600-4.
179. Varga J, Rosenbloom J, Jimenez SA. Transforming growth factor beta (TGF beta) causes a persistent increase in steady-state amounts of type I and type III collagen and fibronectin mRNAs in normal human dermal fibroblasts. Biochemical journal. 1987;247(3):597-604.
180. Raghu G, Masta S, Meyers D, Narayanan AS. Collagen synthesis by normal and fibrotic human lung fibroblasts and the effect of transforming growth factor-beta. American review of respiratory diseases. 1989;140(1):95-100.
181. Lasky JA, Ortiz LA, Tonthat B, Hoyle GW, Corti M, Athas G, et al. Connective tissue growth factor mRNA expression is upregulated in bleomycin-induced lung fibrosis. American journal of physiology. 1998;275(2 Pt 1):L365-71.
182. Wang Q, Usinger W, Nichols B, Gray J, Xu L, Seeley TW, et al. Cooperative interaction of CTGF and TGF-beta in animal models of fibrotic disease. Fibrogenesis tissue repair. 2011;4(1):4.

183. Liu HF, Liu H, Lv LL, Ma KL, Wen Y, Chen L, et al. CCN3 suppresses TGF-beta1-induced extracellular matrix accumulation in human mesangial cells in vitro. Acta Pharmacologica Sinica. 2018;39(2):222-9.
184. Crider BJ, Risinger GM, Jr., Haaksma CJ, Howard EW, Tomasek JJ. Myocardin-related transcription factors A and B are key regulators of TGF-beta1-induced fibroblast to myofibroblast differentiation. Journal of investigatie dermatology. 2011;131(12):2378-85.
185. Bonner JC, Badgett A, Lindroos PM, Osornio-Vargas AR. Transforming growth factor beta 1 downregulates the platelet-derived growth factor alpha-receptor subtype on human lung fibroblasts in vitro. American journal of respiratory cell moleular biology. 1995;13(4):496-505.
186. Singh V, Barbosa FL, Torricelli AA, Santhiago MR, Wilson SE. Transforming growth factor beta and platelet-derived growth factor modulation of myofibroblast development from corneal fibroblasts in vitro. Experimental eye research. 2014;120:152-60.
187. King TE, Jr., Pardo A, Selman M. Idiopathic pulmonary fibrosis. Lancet. 2011;378(9807):1949-61.
188. Coward WR, Saini G, Jenkins G. The pathogenesis of idiopathic pulmonary fibrosis. Therapeutic advances in respiratory disease. 2010;4(6):367-88.
189. Shipley GD, Tucker RF, Moses HL. Type beta transforming growth factor/growth inhibitor stimulates entry of monolayer cultures of AKR-2B cells into S phase after a prolonged prereplicative interval. Proceedings of the National Academy of Sciences of the United States of America. 1985;82(12):4147-51.
190. Jayachandran A, Konigshoff M, Yu H, Rupniewska E, Hecker M, Klepetko W, et al. SNAI transcription factors mediate epithelial-mesenchymal transition in lung fibrosis. Thorax. 2009;64(12):1053-61.
191. Kim KK, Kugler MC, Wolters PJ, Robillard L, Galvez MG, Brumwell AN, et al. Alveolar epithelial cell mesenchymal transition develops in vivo during pulmonary fibrosis and is regulated by the extracellular matrix. Proceedings of the National Academy of Sciences of the United States of America. 2006;103(35):13180-5.
192. Dantas AT, Goncalves SM, de Almeida AR, Goncalves RS, Sampaio MC, Vilar KM, et al. Reassessing the Role of the Active TGF-beta1 as a Biomarker in Systemic Sclerosis: Association of Serum Levels with Clinical Manifestations. Disease markers. 2016;2016:6064830.
193. Alhamad EH, Cal JG, Shakoor Z, Almogren A, AlBoukai AA. Cytokine gene polymorphisms and serum cytokine levels in patients with idiopathic pulmonary fibrosis. BMC medical genetics. 2013;14:66.
194. Blaauboer ME, Smit TH, Hanemaaijer R, Stoop R, Everts V. Cyclic mechanical stretch reduces myofibroblast differentiation of primary lung fibroblasts. Biochemical and biophysical research communications. 2011;404(1):23-7.
195. Heise RL, Stober V, Cheluvaraju C, Hollingsworth JW, Garantziotis S. Mechanical stretch induces epithelial-mesenchymal transition in alveolar epithelia via hyaluronan activation of innate immunity. Journal of biological chemistry. 2011;286(20):17435-44.
196. Cabrera-Benitez NE, Parotto M, Post M, Han B, Spieth PM, Cheng WE, et al. Mechanical stress induces lung fibrosis by epithelial-mesenchymal transition. Critical care medicine. 2012;40(2):510-7.
197. Froese AR, Shimbori C, Bellaye PS, Inman M, Obex S, Fatima S, et al. Stretch-induced Activation of Transforming Growth Factor-beta1 in Pulmonary

Fibrosis. American journal of respiratory and critical care medicine. 2016;194(1):84-96.

Appendix 1

38 Recruitment Centres for the UK-BILD Study

Aintree University Hospitals NHS Foundation Trust
Basildon and Thurrock University Hospital NHS Trust
Blackpool Teaching Hospitals NHS Foundation Trust
Calderdale & Huddersfield NHS Foundation Trust (Calderdale Royal Hospital)
Calderdale & Huddersfield NHS Foundation Trust (Huddersfield Royal Infirmary)
City Hospital Sunderland NHS Foundation Trust
Croydon Health Services NHS Trust
East Sussex Healthcare NHS Trust
Gateshead Health NHS Foundation Trust
Harrogate and District NHS Foundation Trust
King's College Hospital NHS Foundation Trust
Medway NHS Foundation Trust
Mid Yorkshire Hospitals NHS Trust
NHS Fourth Valley
North Bristol Trust
Northern Devon Healthcare NHS Trust
Pennine Acute Hospital NHS Trust (Fairfield General Hospital)
Pennine Acute Hospital NHS Trust (North Manchester General)
Pennine Acute Hospital NHS Trust (Royal Oldham)
Plymouth Hospitals NHS Trust
Royal Cornwall Hospital
Royal Derby NHS Foundation Trust
Royal Devon and Exeter Hospitals NHS Trust
Royal Wolverhampton Hospitals NHS Trust
Salford Royal NHS Foundation Trust
Sandwells and West Birmingham Hospitals NHS Trust
Sheffield Teaching Hospitals NHS Foundation Trust
Sherwood Forest NHS Foundation Trust
Shrewsbury and Telford Hospital NHS Trust
St George's University Hospitals NHS Foundation Trust
Staffordshire and Stoke on Trent Partnership NHS Trust
Surrey and Sussex Healthcare NHS Trust
Taunton and Somerset NHS Foundation Trust
University Hospital South Manchester
West Middlesex University Hospital NHS Trust
Western Sussex Hospitals Trust
Worcestershire Acute Hospitals NHS Trust

Appendix 2

Data Collection Sheet for the UK-BILD Study and Patient Consent Form

Assign study ID SITE _ _ _

UNIVERSITY OF LIVERPOOL

Athena SWAN

UK BIOMARKERS IN INTERSTITIAL LUNG DISEASE (BILD) STUDY

CLINICAL AND DEMOGRAPHIC PROFORMA

PATIENT'S DETAILS: (Complete patient's details / attach hospital sticker)

Patient's name _____

NHS No _____

Hospital No _____

Date of birth DD / MM / YYYY _____

ATTACH HOSPITAL STICKER

Gender (ring) Male / Female

Ethnicity (ring) Caucasian / Afro-Carribean / African / Asian / Mixed (specify) _____

Others (specify) _____

Date of ILD diagnosis MM / YYYY _____ (For date of diagnosis please use date of first CT scan showing fibrosis)

Smoking history (ring) Ex / never / current Number of pack years (ring) <20 >20 but <40 >40

Number of packs smoked per day X No of years smoking

ILD DIAGNOSTIC GROUP: (Select the correct diagnostic group from a to k and tick the most appropriate box within that group)

a) Connective Tissue Disease (CTD) - ILD

- Rheumatoid Arthritis (RA) ☐
- Systemic Lupus Erythematosus (SLE) ☐
- Sjogren's Syndrome ☐
- Mixed Connective Tissue Disorder (MCTD) ☐
- Undifferentiated Connective Tissue Disorder (UCTD) ☐
- Systemic Scleroderma (SSc) Limited ☐
- Systemic Scleroderma (SSc) Diffuse ☐
- Dermatomyositis (DM) ☐
- Amyopathic Dermatomyositis ☐
- Polymyositis (PM) ☐
- Inclusion Body Myositis (IBM) ☐
- CTD - Subtype not yet known ☐
- Other (specify) ☐ _____

Month / year of CTD diagnosis MM / YYYY _____

b) Idiopathic Pulmonary Fibrosis (IPF) History etc must be consistent with ATS / ERS guidelines

- Definite ☐ UIP on HRCT, no LBx
- Definite ☐ Fib NSIP on HRCT and LBx with UIP
- Probable ☐ Fib NSIP on HRCT , no LBx, >65 yrs old and MDT diagnosis IPF

c) Sarcoid

- Lofgrens syndrome ☐
- Lymph node disease alone ☐
- Parenchymal disease + / - LN but confined only to chest ☐
- Extra pulmonary disease / multisystem disease ☐

VERSION 3.0 DATED 03/11/2014 (PN / LS / RGC)

d) Known Hypersensitivity Pneumonitis ☐ Specify identified antigen _____
(Formerly Extrinsic Allergic Alveolitis - EAA)

e) Chronic Hypersensitivity Pneumonitis ☐ CT with mosaism and fibrosis affecting many zones (not just basal)
(Antigen unknown)

f) Asbestosis
Definite ☐ Exposure clearly enough to cause disease
Could be IPF vs. Asbestosis ☐

g) Idiopathic fibrotic NSIP ☐ fibrosis present mainly mid and basal, no signifcant mosacism, not UIP pattern, not MDT diagnosable as IPF, likely < 65 yrs old, no CTD features
(Non Specific Interstitial Pneumonia - NSIP)
HRCT diagnosis alone (ring) Yes / No
If yes is probable Fib NSIP only

h) Idiopathic COP ☐
(Cryptogenic Organising Pneumonia - COP)

i) Respiratory Bronchiolitis - ILD ☐

j) Less Common ILD
Lymphangioleiomyomatosis (LAM) ☐
Langerhans Cell Histiocytosis (LCH) ☐
Desquamative Interstitial Pneumonia (DIP) ☐
Acute Interstitial Pneumonia (AIP) ☐

k) Other ILD ☐ ILD not covered by the above, including differential diagnosis, specify _____

CTD SIGNS / SYMPTOMS / TEST RESULTS: (tick box if signs / symptoms present

Raynaud's ☐
Arthralgias/arthritis ☐
Sclerodactyly ☐
Calcinosis ☐
Raised CK ☐

Mechanics hands ☐
Myalgias ☐
Periungal erythema ☐
Telangiectasia ☐

PULMONARY SIGNS / SYMPTOMS: (tick box if sign/symptom present and whether Pulmonary HT based on RHC or ECG)

Clubbing ☐
End inspiratory crackles ☐
Pulmonary hypertension ☐ BASED ON:- RHC >25mmHg mPAP ☐
ECHO >40mmHg PAP ☐
(excluding Right AP)

MALIGNANCY: (ring if cancer present and if so add malignancy site / tissue type and the date of diagnosis)

Malignancy (ring) Yes / No
Month/ year of diagnosis MM / YYYY _____
Malignancy site / tissue type _____

RECRUITING CENTRE (complete the date the sample was collected)

Name of recruiting centre:
Name of Principal Investigator:
Date blood sample collected: DD / MM / YYYY _____

INSET

TRUST LOGO

Patient Information Sheet

Identification of disease susceptibility genes and antibodies associated with development and clinical characteristics of Interstitial Lung Disease (ILD).

We would like to invite you to take part in a research study examining the underlying causes of interstitial lung disease (ILD). Before deciding whether or not you want to participate, you will need to understand why the research is being done and what it will involve for you. Please take time to read the following information carefully and if there is anything you are unclear about or if you would like more information, please do not hesitate to ask.

What is the purpose of this study?
The purpose of this study is to gain a better understanding of what causes ILD, so that we can use this information to help design more effective drug treatments in the future. This is important because ILD causes progressive scarring of the lung tissue with a subsequent reduction in lung function. This can lead to symptoms such as shortness of breath and fatigue, and in more serious cases pulmonary hypertension (- high blood pressure within the vessels supplying the lung with blood) and right heart failure (- the inability of the right hand side of the heart to pump sufficient blood around the body to meet its needs). Current treatments are not always as effective as we would like and their usefulness can be limited by potentially damaging side effects. In order to try and understand what causes ILD, we would like to take a blood sample from you to carry out genetic and immunological testing (examining your DNA and antibody status). By comparing the test results obtained from patients with ILD against 'healthy controls' (people who do not have ILD), we hope to identify genetic and immunological differences between the two. This should indicate if there are any specific genes or antibodies involved in the development of ILD, and hopefully lead to better drug treatments in the future. We also wish to see if there are any substances in the blood (referred to as biomarkers) that could be used for the future diagnose ILD in the very early stages so that early treatment could be given.

Why have I been invited?
You have been invited to take part in this study because you have been diagnosed with interstitial lung disease. We want to examine this condition in more detail to determine whether or not there are any genetic or immunological factors involved in its development.

Do I have to take part?
It is up to you to decide whether or not you want to take part. You will be given a full explanation of the study, and what it would involve for you if you were to participate. You will also be given a copy of the patient information sheet to read and to keep, and the opportunity to ask any questions you may have. If having had sufficient time to consider your decision you want to take part, we would then ask you to sign a consent form to confirm you have agreed to take part. You would be free to withdraw from the study at any time, without giving a reason, and this would not affect your rights or the standard of care you receive.

What will happen to me if I take part?
If you decide to take part your consultant will fill in some basic details about yourself and your condition. The information requested is similar to the questions he/she would ask you at a normal consultation. A single sample of blood (20mls or 4 tea spoons) will be taken for genetic (DNA) and immunological (antibody) testing. This research blood sample will be taken at the same time as your usual routine blood samples, and therefore no additional needle insertion or clinic visits would be required. Additionally, we would like to ask your

permission to flag your details with the Medical Research Information Service (MRIS) so that we can eventually determine whether ILD patients are at a slightly increased risk of developing cancer as a result of their condition. If it is established that there is no increased risk, we could potentially avoid future unnecessary and unpleasant investigations to look for cancers in such patients. Please be aware that the increased risk of cancer is likely only very slight, if at all. This is something your consultant will be checking for, and will be happy to discuss with you, so don't be alarmed. In order to match up information we receive from the MRIS with your correct blood sample and clinical details, it is necessary for us to record and store some 'personal identifiers. Therefore we also ask your permission to store your name, hospital number, NHS number and date of birth in a centralised database. This database will be maintained on a password protected, NHS Trust Network computer, with limited access. This database will be kept in compliance with the Data Protection Act 1998 and NHS code of confidentiality.

What are the possible disadvantages and risks of taking part?
The only risk associated with this study is the needle insertion into a vein in your arm or wrist, in order to get a blood sample. This might cause you some slight discomfort and you might be bruised for a few days around the area of the needle insertion.

What are the possible benefits of taking part?
We cannot promise the study will directly benefit you, but the information we get from it will help improve the treatment of people with ILD in the future.

What will happen if I don't want to carry on with the study?
You can withdraw from the study at any time, without giving a reason, and this will not affect the quality of care you receive. If your stored blood sample or clinical details have not yet been used for research purposes, they can be destroyed if you wish.

Will my taking part in the study be kept confidential?
Clinical details about your condition will be stored in a centralised database, along will some 'patient identifiers' including your name, hospital number, NHS number and date of birth. This database will be maintained on a password protected, NHS computer at Salford Royal in compliance with the Data Protection Act 1998. Our procedures for handling, processing, storage and destruction of data are also fully compliant. If you join the study, your clinical details may be looked at by the doctors and researchers performing the genetic and immunological studies. Representatives of the sponsor, regulatory authorities and the NHS Trust will have access to your medical and research records for monitoring and auditing purposes. Data collected during the study could be sent to collaborating researchers in other countries including Europe and the USA where the laws may not protect your privacy to the same extent as the Data Protection Act in the UK. However, the results of your genetic and antibody testing, along with your clinical details would be sent in anonymised form, with no patient identifiers leaving the UK.

What will happen to any samples I give?
The blood samples will be sent to the Centre for Integrated Genomic Medical Research (CIGMR), within The University of Manchester, where they will be securely stored. Samples will be kept for future analyses as outlined above (genetic / immunological). Any details that directly identify you to your blood sample or clinical data (eg name, date of birth, hospital number) will be securely stored on the password protected NHS computer at Salford Royal. You are making a donation of your blood sample for use in research and we will assume formal responsibility for custodianship of your donated sample, as per the Nuffield Council on Bioethics Report 'Human Tissue: Ethical and Legal Issues' (1995).

What will happen to the results of the research study?
Broad scientific results will be published in peer reviewed medical journals. You will not be personally identifiable by any details given in any report or publication thus generated. Results with relevance to the individual will include the antibody result which your consultant may otherwise not have access to in your own hospital. This antibody result may provide some useful information about the clinical progression of your ILD.

Who is organising and funding the research?
The research is being organised by Professor Robert G Cooper (University of Liverpool) and Professor William Ollier (University of Manchester).

Who has reviewed the study?
All research in the NHS is looked at by independent group of people, called a Research Ethics Committee to protect your safety, rights, wellbeing and dignity. This study has been reviewed and given a favourable opinion by the North West Research Ethics Committee. It has also been reviewed by the study sponsor University of Liverpool. You will be given a copy of the patient information sheet and a signed consent form to keep.

Further information and contact details

INSERT LOCAL CONTACT DETAILS

INSERT TRUST LOGO

CONSENT FORM

(TO BE RETAINED AT SITE)

Title of project: **Identification of disease susceptibility genes and antibodies associated with development and clinical characteristics of Interstitial Lung Disease.**

Name of Researchers: Prof R. G. Cooper & Prof W. Ollier.

Please initial box

1. I confirm that I have read and understand the patient information sheet dated 29/05/2014 version 4.0 for the above study. I have had the opportunity to consider the information, ask questions and have had these answered satisfactorily. ☐

2. I understand that my participation is voluntary and that I am free to withdraw at any time, without any reason, without my medical care or legal rights being affected. ☐

3. I understand that sections of any of my medical notes may be looked at by the ILD research group or from regulatory authorities, the study sponsor and NHS trusts where it is relevant to my taking part in research. I give permission for these individuals to have access to my records. ☐

4. I agree to have my details flagged with the Medical Research Information Service and to have my name, hospital number, NHS number and DOB recorded on a centralised database and stored on a password protected. NHS computer ☐

5. I agree that my blood sample and clinical & laboratory data can be used in future ILD research projects. All samples and data provided to other researcher, either in the UK or Europe, will be done so in anonymised form ☐

6. I agree to take part in the above study ☐

_____	_____	_____
Name of Patient	Date	Signature
_____	_____	_____
Name of Person taking consent.	Date	Signature

Appendix 3

REC Approval Form

NHS
National Research Ethics Service
North West 5 Research Ethics Committee – Haydock Park
North West Centre for Research Ethics Committees
3rd Floor - Barlow House
4 Minshull Street
Manchester
M1 3DZ

Telephone: 0161 625 7819/7832
Facsimile: 0161 237 9427

11 March 2011

Dr Robert Cooper
Salford Royal NHS Foundation Trust
Clinical Science Building
Stott Lane, Salford,
Manchester M6 8HD

Dear Dr Cooper

Study Title:	**Identifying disease susceptibility genes and autoantibodies associated with the development and clinical characteristics of interstitial lung disease (ILD) in patients with and without proven connective tissue diseases (CTDs). Version 1.0 18/12/2010**
REC reference number:	**11/H1010/4**

Thank you for your letter, responding to the Committee's request for further information on the above research and submitting revised documentation.

The further information has been considered on behalf of the Committee by the Chair (Professor Ravi Gulati - Consultant Physician).

Confirmation of ethical opinion

On behalf of the Committee, I am pleased to confirm a favourable ethical opinion for the above research on the basis described in the application form, protocol and supporting documentation as revised, subject to the conditions specified below.

Ethical review of research sites

The favourable opinion applies to all NHS sites taking part in the study, subject to management permission being obtained from the NHS/HSC R&D office prior to the start of the study (see "Conditions of the favourable opinion" below).

Conditions of the favourable opinion

The favourable opinion is subject to the following conditions being met prior to the start of the study.

Management permission or approval must be obtained from each host organisation prior to the start of the study at the site concerned.

For NHS research sites only, management permission for research ("R&D approval") should be obtained from the relevant care organisation(s) in accordance with NHS research

governance arrangements. Guidance on applying for NHS permission for research is available in the Integrated Research Application System or at http://www.rdforum.nhs.uk.

Where the only involvement of the NHS organisation is as a Participant Identification Centre (PIC), management permission for research is not required but the R&D office should be notified of the study and agree to the organisation's involvement. Guidance on procedures for PICs is available in IRAS. Further advice should be sought from the R&D office where necessary.

Sponsors are not required to notify the Committee of approvals from host organisations.

It is the responsibility of the sponsor to ensure that all the conditions are complied with before the start of the study or its initiation at a particular site (as applicable).

Approved documents

The final list of documents reviewed and approved by the Committee is as follows:

Document	*Version*	*Date*
Covering Letter: From Paul New, Salford Royal NHS Foundation Trust		14 January 2011
REC application	2.2	14 January 2011
Protocol	1.0	18 December 2010
Investigator CV: Robert G Cooper		14 January 2011
Referees or other scientific critique report: Critique by Dr Ronan O'Driscoll, Consultant Respiratory Physician, Salford Royal NHS Foundation Trust		13 January 2011
Good Clinical Practice Training Certificate		22 March 2010
Clinical and Laboratory Proforma	1.0	18 December 2010
Response to Request for Further Information: From Paul New, Salford Royal NHS Foundation Trust		
Participant Information Sheet	2.0	18 February 2011
Participant Consent Form: To be retained at site	2.0	18 February 2011
Participant Consent Form: To be given to the patient	2.0	18 February 2011
Participant Consent Form: To be kept in medical notes	2.0	18 February 2011
Letter of invitation to participant	2.0	18 February 2011

Statement of compliance

The Committee is constituted in accordance with the Governance Arrangements for Research Ethics Committees (July 2001) and complies fully with the Standard Operating Procedures for Research Ethics Committees in the UK.

After ethical review

Now that you have completed the application process please visit the National Research Ethics Service website > After Review

You are invited to give your view of the service that you have received from the National Research Ethics Service and the application procedure. If you wish to make your views known please use the feedback form available on the website.

The attached document *"After ethical review – guidance for researchers"* gives detailed

guidance on reporting requirements for studies with a favourable opinion, including:

- Notifying substantial amendments
- Adding new sites and investigators
- Progress and safety reports
- Notifying the end of the study

The NRES website also provides guidance on these topics, which is updated in the light of changes in reporting requirements or procedures.

We would also like to inform you that we consult regularly with stakeholders to improve our service. If you would like to join our Reference Group please email:

referencegroup@nres.npsa.nhs.uk.

11/H1010/4	**Please quote this number on all correspondence**

With the Committee's best wishes for the success of this project

Yours sincerely

Professor Ravi S Gulati
Chair

Email: noel.graham@northwest.nhs.uk

Enclosures: "After ethical review – guidance for researchers"

Copy to:

Mr Paul New
Room C223
Clinical Science building
Salford Royal NHS Foundation Trust
Stott Lane
Salford
Manchester M6 8HD

R&D office for NHS care organisation at lead site –

Mrs Rachel Georgiou
Salford Royal NHS Foundation Trust
Sommerfield House
Eccles New Road
Salford
M6 8HD

Appendix 4

Buffers and Reagents Used in Experiments

Phosphate Buffered Saline (PBS) Solution for immunocytochemistry

PBS tablet (Sigma-Aldrich, Dorset, UK) dissolved in 200ml deionized water

0.01% Phosphate Buffered Saline with Tween for immunocytochemistry

10ml PBS solution as described above, 1ul Tween 20 solution (Sigma-Aldrich, Dorset, UK)

Tris-Acetate-EDTA (TAE) Buffer

A 50 x TAE buffer solution was produced consisting of;

242g Tris base (Sigma-Aldrich, Dorset, UK)

57.1ml glacial acetic acid (Sigma-Aldrich, Dorset, UK)

100ml 0.5M EDTA (pH 8.0)

Made up to 1L with distilled water

Once produced the solution was diluted to 1x using distilled water

2% Agarose Gel

100ml TAE, made according to protocol described above

2 gram agarose (Sigma-Aldrich, Dorset, UK)

2-3ul Safe View Nucleic Acid Stain (NBS Biologicals, Cambridgeshire, UK)

Solution mixed in a flask and heated in a microwave until fully dissolved. Poured into a gel casing and allowed to set.

Urea-Lysis Buffer

Solution prepared by mixing;

40.08g Urea (Sigma-Aldrich, Dorset, UK)

1M Tris / HCl (pH 6.8) - 1ml – *Prepared using 121.1g Tris base, adjusted to pH 6.8 using HCl, and made to a volume of 1L using distilled water*

10ml Glycerol

5ml, 20% sodium dodecyl sulphate (SDS)

0.01g Bromophenol blue

Transfer Buffer for Western Blot

10 x Transfer buffer (stock)

This was prepared by mixing;

30.28g Tris (Sigma-Aldrich, Dorset, UK)

144.1g glycine (Sigma-Aldrich, Dorset, UK)

Solution was made up to 1L with water and ensured pH was 6.05

1 x Transfer buffer

This was prepared by mixing;

100ml 10 x transfer buffer (as described above)

200ml analytical reagent grade methanol (Fisher Chemical, Fisher Scientific, Leicestershire, UK)

690ml distilled water

10ml Sodium Dodecyl Sulphate (SDS) 10x solution (Sigma-Aldrich, Dorset, UK)

Tris Buffered Saline (TBS) 10%

This solution was prepared using;

24.23g Trizma HCl (Sigma-Aldrich, Dorset, UK)

80.06g NaCl (Sigma-Aldrich, Dorset, UK)

Solution was mixed with 800ml distilled water and the pH adjusted to 7.6 with pure HCl, it was then made up to 1L with distilled water

Tris Buffered Saline with Tween, 0.1% Tween 20 (TBST)

100ml 10x TBS (prepared as described above)

890 ml distilled water

250ul tween 20 (Sigma Aldrich, Dorset, UK)

Solution was prepared by mixing the reagents above

3% milk blocking solution

1.2g Marvel dried skimmed milk powder (Premier Foods, St Albans, UK)

40ml TBST (prepared as described above)

Solution was prepared by mixing the reagents described above

Appendix 5

Papers and Abstracts Published From this Work

Review Article

RHEUMATOLOGY

Rheumatology 2017;56:1264–1271
doi:10.1093/rheumatology/kew320
Advance Access publication 20 October 2016

Review

The utility of comprehensive autoantibody testing to differentiate connective tissue disease associated and idiopathic interstitial lung disease subgroup cases

Caroline V. Cotton[1,2], Lisa G. Spencer[3], Robert P. New[1] and Robert G. Cooper[1,2]

Abstracts

Cotton CV, Betteridge ZE, Spencer LG, New RP, Lamb J, McHugh NJ, Cooper RG, UK-BILD Collaboration. Low level detection of CTD-associated autoantibodies in patients with idiopathic pulmonary fibrosis confirms this as a robust phenotype when diagnosed on clinical grounds alone. Rheumatology 2018, 57 (suppl_3), https://doi.org/10.1093/rheumatology/key075.206

Cotton CV, Spencer LG, New RP, Cooper RG. Comprehensive connective tissue disease serology could prevent unnecessary lung biopsies in amyopathic interstitial lung disease patients with anti-synthetases other than anti-Jo-1: An illustrative case series. Rheumatology 2017,56 (suppl 2), https://doi.org/10.1093/rheumatology/kex062.277

Cotton CV, Spencer LG, New RP, Cooper RG. When interstitial lung disease represents the major clinical feature in antisynthetase syndrome cases which are clearly amyopathic, is it justifiable to still regard detected antisynthetases as myositis-specific antibodies? Rheumatology 2016; 55 (suppl_1), Pages i133, https://doi.org/10.1093/rheumatology/kew135.003